

**AN INVESTIGATION INTO NEUROENDOCRINE REGULATORS OF EXCRETORY  
ORGANS IN THE ADULT DISEASE-VECTOR MOSQUITO, *Aedes Aegypti***

Farwa Sajadi

A DISSERTATION SUBMITTED TO THE FACULTY OF GRADUATE STUDIES IN  
PARTIAL FULFILMENT OF THE REQUIREMENTS FOR THE DEGREE OF  
DOCTOR OF PHILOSOPHY

GRADUATE PROGRAM IN BIOLOGY

YORK UNIVERSITY

TORONTO, ONTARIO, CANADA

MAY 2023

© Farwa Sajadi, 2023

## Abstract

Maintenance of ionic and osmotic homeostasis in insects allows them to succeed in many ecological and environmental niches, while utilizing a variety of feeding strategies. When faced with extreme and variable conditions, most insects regulate the composition of their blood within narrow limits. Haematophagous insects, such as the female yellow fever mosquito, *Aedes aegypti*, ingest bloodmeals comparable to twice their body volume, resulting in considerable amounts of salts and water in excess, threatening the osmotic and ionic balance of their haemolymph. Like other insects, mosquitoes achieve strict regulation of their hydromineral balance through the neuroendocrine control of their excretory system, consisting of the Malpighian ‘renal’ tubules (MTs), which are responsible for formation of the primary urine, along with the hindgut, which functions as a primarily reabsorptive organ. While extensive studies have examined this process of hydromineral balance in *A. aegypti* focusing on diuretic regulation, the roles of anti-diuretic hormones remained largely elusive. This research sought to advance our understanding of the hormonal regulation of the excretory system in *A. aegypti* by (1) investigating the role of CAPA neuropeptides as anti-diuretic hormones in adult MTs; (2) identifying the signalling components leading to CAPA-induced inhibition of fluid secretion; and (3) elucidating the expression and putative functional roles of ITP and ITP-L neuropeptides. In adult MTs, *Aedae*CAPA-1 peptides elicit a selective anti-diuretic role, inhibiting DH<sub>31</sub>- and 5HT-stimulated secretion through the NOS/cGMP/PKG pathway. CAPA-mediated inhibition promotes V-type H<sup>+</sup>-ATPase (VA) disassembly, reducing the driving force of DH<sub>31</sub>-stimulated secretion. Post-blood feeding, DH<sub>31</sub> peptides are immediately released into the female haemolymph to promote natriuresis and diuresis while CAPA peptides are released shortly after, hindering the effects of DH<sub>31</sub>. Lastly, examination of ITP and ITP-L neuropeptides in *A. aegypti* indicated enrichment of ITP in the

brain and ITP-L in the abdominal ganglia. Novel observations of *AedaeITP* and *AedaeITP-L* in feeding/starvation, ionoregulation, and reproductive behaviour and success suggest a vital pleiotropic role for these neuropeptides. Together, these studies highlight the complexity of neuroendocrine control of excretory organs in adult *A. aegypti* mosquitoes, furthering our understanding of various diuretic and anti-diuretic signalling systems in this important human disease vector.

## Acknowledgments

To the best supervisor I could have asked for, Dr. Jean-Paul Paluzzi - your unwavering support and encouragement is the biggest reason I am here today. To say it has been an honour to be in your lab and to be your second PhD student is an understatement. Every success, accomplishment, and milestone I have received during these last couple years and in the future is all owed to you. For every single opportunity you have presented me, for every reference letter you have written me, for every time you pushed me to do better, for every time you told me I had to increase my sample size (not that you do not trust me right?), and for every time you made me step outside my comfort zone to face new challenges, I want to thank you. You have set a ridiculously high standard for a PI, redefining what it means to be an amazing mentor and a leader. No matter what career path I choose, I hope to become even a fraction of what you stand for. Jean-Paul, I am *eternally* grateful for your kindness and faith in me, and I hope you will always have your door open for me in case I need your wise advice in life, and how to save money for a future mortgage as you like to keep reminding me! This truly has been the most rewarding experience of my life. Thank you, Jean-Paul.

To my supervisory committee, Dr. Andrew Donini and Dr. Raymond Kwong, thank you for your support and advice throughout these last many years. Andrew, thank you for your continuous guidance, and for always allowing me to use your lab and equipment whenever I needed. Raymond, thank you for all your advice, encouragement and feedback during the last couple years. I am forever grateful for both of you and for your never-ending support and kindness! A *special* thank you to Dr. Robert Tsushima for your generosity, advice, and for writing me *countless* reference letters!

To the first generation of the Paluzzi lab, thank you for keeping me sane and entertained throughout the first half of my PhD. Dave, you were Jean-Paul's first PhD student and my role model of what a PhD student should be like. Thank you for the countless hours of laughing, singing, all the advice (most of them appropriate), and support – you will always be like a big brother. Aryan, I will forever cherish the memories we shared in those four walls of the lab, staying till midnight stressing about deadlines and laughing through every failure and success - thank you for everything! To Azizia, Hiva, Massima, Andreea, Fidan, Alireza, Basma, and everyone else, I am forever grateful for all your help! To Hiva (my free therapist) thank you for letting me sit on your couch drinking tea and ranting for hours about everything, I am so grateful for our friendship!

Britney, there are not enough words to express how lucky I am to have experienced this journey with you. You were my bestie throughout this second half of my PhD, living this rich broke life with me and never hesitating to buy expensive coffees we cannot afford and souvenirs from our trips (Jean-Paul definitely judging us for our matching sweaters). Your kindness, love, and support were constant. Thank you for your daily 8:30am phone calls, for never judging me about

my visa bills, for us sharing the same guilty pleasures (no shame in watching the entire twilight series on our way to science conferences) and for being the best traveling partner. In short, you are stuck with me for life now, sorry!

To all my other lab mates, thank you to each and every one of you! Special thanks to Marishia and Zeynab for your help and delightful company! To my undergraduate helpers; Lulia, Chiara, and Fernanda, I will forever be grateful for all your amazing help and dedication into making my long lists of experiments possible! To Dr. Scott Kelly, the Donini lab, and the Kelly lab (Andrea, Gil, Lidiya, Ana, Sima, Chun, and Elia), thank you for all your help and always letting me take over your lab for whatever new experiment I had to do. Andrea, you inspired me to push through my boundaries, and was always there to provide me with your sage advice, and a good laugh! Fahad, you will always be a role model for what a hard-working scientist should look like, and while I may never live up to your standards, I will always be grateful for your continuous support, friendship, and the Office references! To all my friends, thank you for everything!

There will never be enough words to express the gratitude towards my family and loved ones. You have always pushed me to chase my dreams and follow whatever I set my mind to, encouraging and supporting me every step of the way. Even though I know you do not entirely understand what my research is (just something to do with mosquitoes and hopefully ridding them from this world of course) I know you are proud of me. Thank you for believing in me and being my biggest supporters and cheerleaders through life!!

## Contents

<b>Abstract</b> .....	<b>ii</b>
<b>Acknowledgments</b> .....	<b>iv</b>
<b>Table of Contents</b> .....	<b>vi</b>
<b>Table of Figures</b> .....	<b>ix</b>
<b>Table of Tables</b> .....	<b>xiii</b>
<b>List of Abbreviations</b> .....	<b>xiv</b>
<b>Statement of Contributions</b> .....	<b>xix</b>
<b>Chapter One: Overview</b> .....	<b>1</b>
1.1 The mosquito, <i>Aedes aegypti</i> .....	2
1.1.1 <i>A. aegypti</i> as a disease vector.....	2
1.1.2 <i>A. aegypti</i> lifecycle and distribution .....	3
1.1.3 <i>A. aegypti</i> reproductive system .....	6
1.1.4 <i>A. aegypti</i> excretory system .....	7
1.2 The role of MTs and hindgut .....	8
1.2.1 The cellular composition of MTs in <i>A. aegypti</i> .....	8
1.2.2 Ion transport in stimulated <i>A. aegypti</i> MTs .....	10
1.3 Neuroendocrine regulation of the MTs.....	14
1.3.1 The neuroendocrine system of <i>A. aegypti</i> .....	14
1.3.2 Hormonal regulation of MTs and hindgut .....	18
1.4 Research aims and objectives .....	26
1.4.1 Aim 1: Elucidate the role and signalling cascade of the CAPA neuropeptide in the MTs of the female <i>A. aegypti</i> mosquito.....	27
1.4.2 Aim 2: Characterize the expression and immunolocalization, and examine a potential role of ITP and ITP-L neuropeptides in the <i>A. aegypti</i> mosquito .....	28
1.6 References.....	30
<b>Chapter Two: Anti-diuretic action of a CAPA neuropeptide against a subset of diuretic hormones in the disease vector, <i>Aedes aegypti</i></b> .....	<b>48</b>
2.1 Summary .....	49
2.2 Introduction.....	51
2.3 Materials and Methods.....	55
2.4 Results.....	60
2.5 Discussion.....	68
2.6 References.....	78
2.7 Supplementary Figures .....	88

<b>Chapter Three: CAPA neuropeptides and their receptor form an anti-diuretic signalling system in the human disease vector, <i>Aedes aegypti</i></b> .....	<b>89</b>
3.1 Summary .....	90
3.2 Introduction.....	91
3.3 Materials and Methods.....	93
3.4 Results.....	102
3.5 Discussion.....	113
3.6 References.....	121
3.7 Supplementary Tables and Figures.....	133
<b>Chapter Four: The V-type H<sup>+</sup>-ATPase is targeted in anti-diuretic hormone control of the Malpighian ‘renal’ tubules</b> .....	<b>137</b>
4.1 Summary .....	138
4.2 Introduction.....	139
4.3 Materials and Methods.....	142
4.4 Results.....	153
4.5 Discussion.....	170
4.6 References.....	180
4.7 Supplementary Figures .....	191
<b>Chapter Five: Dynamics of DH<sub>31</sub> and CAPA neuropeptide release and activity post-bloodmeal in the female mosquito, <i>A. aegypti</i></b> .....	<b>197</b>
5.1 Summary .....	198
5.2 Introduction.....	200
5.3 Materials and Methods.....	203
5.4 Results.....	207
5.5 Discussion.....	217
5.6 References.....	227
<b>Chapter Six: Molecular characterization, localization, and physiological roles of ITP and ITP-L in the mosquito, <i>Aedes aegypti</i></b> .....	<b>236</b>
6.1 Summary .....	237
6.2 Introduction.....	238
6.3 Materials and Methods.....	240
6.4 Results.....	251
6.5 Discussion.....	272
6.6 References.....	281

6.7 Supplementary Tables and Figures .....	289
<b>Chapter Seven: Conclusions and future directions .....</b>	<b>297</b>
7.1 Summary .....	298
7.1.1 An anti-diuretic role for CAPA neuropeptides against select diuretic factors.....	299
7.1.2 Diuretic and anti-diuretic signalling systems: importance of neuropeptides and their cognate receptors .....	301
7.1.3 Characterization and novel roles for ITP and ITP-L neuropeptides in <i>A. aegypti</i> .....	302
7.2 Future Directions .....	304
7.3 References.....	309

## Table of Figures

<b>Figure 1-1.</b> Life cycle of the <i>A. aegypti</i> from egg hatching to emergence of the adult flying mosquito.....	5
<b>Figure 1-2.</b> Ion and water transport through principal and stellate cells of <i>A. aegypti</i> MTs.....	11
<b>Figure 1-3.</b> <i>Aedes aegypti</i> neuroendocrine system.....	17
<b>Figure 1-4.</b> Schematic diagram summarizing diuretic and anti-diuretic control of <i>A. aegypti</i> adult MTs .....	20
<b>Figure 2-1.</b> Effect of <i>Aedae</i> CAPA-1 on <i>in vitro</i> fluid secretion rate, cation (Na <sup>+</sup> and K <sup>+</sup> ) concentration and transport rate by adult female <i>A. aegypti</i> MTs stimulated with a variety of diuretic hormones.....	61
<b>Figure 2-2.</b> Effect of different concentrations of cGMP on <i>in vitro</i> fluid secretion rate, cation (Na <sup>+</sup> and K <sup>+</sup> ) concentration and transport rate by unstimulated MTs of adult female <i>A. aegypti</i> . .....	65
<b>Figure 2-3.</b> Effect of cGMP on <i>in vitro</i> fluid secretion rate, cation (Na <sup>+</sup> and K <sup>+</sup> ) concentration and transport rate by adult female <i>A. aegypti</i> MTs stimulated with a variety of diuretic hormones.....	67
<b>Figure 2-4.</b> Schematic diagram summarizing diuretic and anti-diuretic control of <i>A. aegypti</i> adult MTs.....	71
<b>Figure 2-S1.</b> Effects of <i>Aedae</i> CAPA-1, <i>Aedae</i> CAPA-2, and <i>Aedae</i> PK-1 on DH <sub>31</sub> -stimulated MTs of adult <i>A. aegypti</i> .....	88
<b>Figure 3-1.</b> CAPA neuropeptides (anti-diuretic hormone) receptor (CAPAr) functional deorphanization using a heterologous assay.....	103
<b>Figure 3-2.</b> Expression analysis of <i>CAPAr</i> transcript in the mosquito, <i>A. aegypti</i> .....	105
<b>Figure 3-3.</b> Mapping of anti-diuretic hormone in the abdominal ganglia of the central nervous system in adult <i>A. aegypti</i> .....	107
<b>Figure 3-4.</b> RNA interference (RNAi) of <i>CAPAr</i> abolishes anti-diuretic activity of CAPA neuropeptide on adult female <i>A. aegypti</i> MTs.....	109
<b>Figure 3-5.</b> Effect of a nitric oxide synthase (NOS) inhibitor (L-NAME) on the anti-diuretic activity of <i>Aedae</i> CAPA-1 and cGMP in <i>Drome</i> DH <sub>31</sub> - and 5HT-stimulated <i>A. aegypti</i> MTs.....	111
<b>Figure 3-6.</b> Effect of a protein kinase G (PKG) inhibitor (KT5823) on the anti-diuretic activity of <i>Aedae</i> CAPA-1 and cGMP in <i>Drome</i> DH <sub>31</sub> - and 5HT-stimulated <i>A. aegypti</i> MTs.....	112

<b>Figure 3-S1.</b> CAPA immunoreactivity observed in regions of the nervous system aside from the strongly-staining pair of neurosecretory cells in each of the abdominal ganglia.....	135
<b>Figure 3-S2.</b> Expression analysis of CAPA neuropeptide (anti-diuretic hormone) transcript in different regions of the nervous system relative to whole adult (A) male and (B) female <i>A. aegypti</i> mosquitoes.....	136
<b>Figure 4-1.</b> Effect of bafilomycin on fluid secretion rates and pH along with cyclic nucleotide second messengers on adult <i>A. aegypti</i> MTs.....	155
<b>Figure 4-2.</b> Effect of <i>Aedae</i> CAPA-1 and NOS/PKG inhibitors on VA and NKA activity in diuretic stimulated <i>A. aegypti</i> MTs.....	162
<b>Figure 4-3.</b> Membrane and cytosolic protein abundance of the V <sub>1</sub> complex in MTs of <i>A. aegypti</i> . .....	165
<b>Figure 4-4.</b> Immunolocalization of the V <sub>0</sub> and V <sub>1</sub> complexes in transverse sections of stimulated <i>A. aegypti</i> MTs.....	167
<b>Figure 4-5.</b> Immunolocalization of the V <sub>0</sub> and V <sub>1</sub> complexes in blood-fed <i>A. aegypti</i> females.....	169
<b>Figure 4-6.</b> Schematic diagram summarizing the signalling pathway of diuretic and anti-diuretic control of adult <i>A. aegypti</i> MTs.....	178
<b>Figure 4-S1.</b> Dose response of bafilomycin on fluid secretion rates of DH <sub>31</sub> -stimulated MTs <i>in vitro</i> isolated from adult female <i>A. aegypti</i> .....	191
<b>Figure 4-S2.</b> Effect of bafilomycin and <i>Aedae</i> CAPA-1 on the secretion rate and pH of the secreted fluid by unstimulated MTs <i>in vitro</i> from adult female <i>A. aegypti</i> .....	192
<b>Figure 4-S3.</b> Intracellular levels of cAMP in DH <sub>44</sub> -treated <i>A. aegypti</i> MTs.....	193
<b>Figure 4-S4.</b> Representative western blot of membrane and cytosolic protein fraction isolation validated using established membrane (aquaporin-1 in <i>A. aegypti</i> MTs) and cytosolic (beta-tubulin) protein markers.....	194
<b>Figure 4-S5.</b> Representative western blot image of membrane and cytosolic protein abundance of the V <sub>1</sub> complex in <i>A. aegypti</i> MTs.....	195
<b>Figure 4-S6.</b> Immunolocalization of the V <sub>0</sub> and V <sub>1</sub> complexes in cross sections of stimulated <i>A. aegypti</i> MTs.....	196
<b>Figure 5-1.</b> Functional heterologous receptor assay of CHO-K1 cells expressing the <i>A. aegypti</i> DH <sub>31</sub> receptor.....	210

<b>Figure 5-2.</b> <i>AedaeDH</i> <sub>31</sub> titres in blood-fed haemolymphs of female <i>A. aegypti</i> .....	212
<b>Figure 5-3.</b> Fluid secretion rates of <i>AedaeDH</i> <sub>31</sub> and collected blood fed haemolymphs in MTs of adult female <i>A. aegypti</i> .....	214
<b>Figure 5-4.</b> <i>AedaeCAPA</i> -1 titres in blood fed haemolymphs of female <i>A. aegypti</i> .....	216
<b>Figure 6-1.</b> Developmental and spatial transcript expression profile of <i>AedaeItp</i> and <i>AedaeItp-l</i> in <i>A. aegypti</i> .....	252
<b>Figure 6-2.</b> Immunolocalization of <i>AedaeItp</i> and <i>AedaeItp-L</i> in the central nervous system of the <i>A. aegypti</i> mosquito.....	255
<b>Figure 6-3.</b> Distribution of <i>AedaeItp</i> and <i>AedaeItp-l</i> transcript in the central nervous system of the <i>A. aegypti</i> mosquito.....	256
<b>Figure 6-4.</b> Effect of feeding and starvation on transcript expression levels of <i>AedaeItp</i> and <i>AedaeItp-l</i> in adult <i>A. aegypti</i> .....	258
<b>Figure 6-5.</b> <i>AedaeItp</i> and <i>AedaeItp-l</i> knockdown efficiency in adult <i>A. aegypti</i> .....	260
<b>Figure 6-6.</b> Immunolocalization of <i>AedaeItp</i> and <i>AedaeItp-L</i> in the central nervous system of adult <i>A. aegypti</i> mosquitoes following ds <i>AedaeItp</i> and ds <i>AedaeItp-l</i> injection .....	262
<b>Figure 6-7.</b> Distribution of <i>AedaeItp</i> and <i>AedaeItp-l</i> transcript in the central nervous system of adult <i>A. aegypti</i> mosquitoes after ds <i>AedaeItp</i> and ds <i>AedaeItp-l</i> injection.....	263
<b>Figure 6-8.</b> Effect of <i>AedaeItp</i> and <i>AedaeItp-l</i> knockdown on urine excretion in adult female <i>A. aegypti</i> .....	265
<b>Figure 6-9.</b> Effect of <i>AedaeItp</i> and <i>AedaeItp-l</i> knockdown on blood-feeding, egg laying, and larval hatching (egg viability) in adult <i>A. aegypti</i> .....	268
<b>Figure 6-10.</b> Total number of spermatozoa in the male seminal vesicle and female spermathecae of adult <i>A. aegypti</i> following RNAi (dsRNA)-mediated knockdown of <i>AedaeItp</i> or <i>AedaeItp-l</i> .....	271
<b>Figure 6-S1.</b> Primer sets mapped to <i>A. aegypti Itp</i> and <i>Itp-l</i> transcripts, and sequence alignment of <i>AedaeItp</i> and <i>AedaeItp-L</i> deduced peptides .....	290
<b>Figure 6-S2.</b> <i>AedaeItp</i> and <i>AedaeItp-L</i> preabsorbed controls and no primary controls.....	291
<b>Figure 6-S3.</b> Immunolocalization and distribution of both <i>AedaeItp</i> and <i>AedaeItp-L</i> peptide and transcript in the central nervous system of adult dsEgfp <i>A. aegypti</i> mosquitoes. ....	292

**Figure 6-S4.** Effect of control ds*Egfp* on blood-feeding, egg laying, and larval hatching (egg viability) in comparison to non-injected adult *A. aegypti*.....293

**Figure 6-S5.** Representative images of immunofluorescent nuclei of total spermatozoa in the male seminal vesicle and female spermathecae of adult *A. aegypti* following RNAi (dsRNA)-mediated knockdown of *AedaeItp* or *AedaeItp-l*.....294

**Figure 6-S7.** Total spermatozoa in the testes of adult male *A. aegypti* following RNAi (dsRNA)-mediated knockdown of *AedaeItp* or *AedaeItp-l*.....295

**Figure 6-S8.** Total spermatozoa in the male testes and seminal vesicle and female spermathecae of adult *A. aegypti* following ds*Egfp* injection.....296

**Figure 7-1.** Summary of research findings and overall impact to global society.....308

## Table of Tables

<b>Table 3-S1.</b> List and primary structure of several insect neuropeptides tested for functional activation of the mosquito anti-diuretic hormone (CAPA) receptor using heterologous bioassay.....	133
<b>Table 3-S2.</b> Oligonucleotides used for generation of fluorescent <i>in situ</i> hybridization probes, templates for <i>in vitro</i> dsRNA synthesis and gene-specific primers for quantitative PCR of the <i>Aedes aegypti</i> anti-diuretic hormone (CAPA) receptor. ....	134
<b>Table 5-1.</b> List and structure of insect neuropeptides used in the heterologous functional assay and summary of activity in eliciting a luminescent response.....	209
<b>Table 6-S1:</b> Gene-specific primer information used for amplification of <i>A. aegypti</i> <i>Itp</i> and <i>Itp-1</i> for RT-qPCR analysis, FISH probe synthesis and dsRNA synthesis. ....	289

## List of Abbreviations

- ADB — antibody dilution buffer
- ADH — anti-diuretic hormone
- ADP — adenosine diphosphate
- Aeq — aequorin
- AG — abdominal ganglia
- AeKCC1* — KCl cotransporter
- AeKir* — inwardly rectifying K<sup>+</sup> channel
- ANOVA — analysis of variance
- ATP — adenosine triphosphate
- AQP — aquaporin
- BF — brightfield
- BSA — bovine serum albumin
- cAMP — cyclic adenosine monophosphate
- CC — corpora cardiaca
- cDNA — complementary deoxyribonucleic acid
- CDP — *Culex* depolarizing peptide
- cGMP — cyclic guanosine monophosphate
- CHH — crustacean hyperglycemic hormone
- CHO-K1 — Chinese hamster ovary-K1 cell line
- CLB — cell lysis buffer
- CNS — central nervous system
- CRF — corticotropin-releasing factor-like hormone

DAPI — 4',6-diamidino-2-phenylindole

ddH<sub>2</sub>O — double distilled water

DH — diuretic hormone

DH<sub>31</sub> — calcitonin-related diuretic hormone 31

DH<sub>44</sub> — CRF-related diuretic peptide 44

DIG — digoxigenin

DMEM:F12 — Dulbecco's modified eagles medium:nutrient F12

DMSO — dimethyl sulfoxide

DNA — deoxyribonucleic acid

dNTP — deoxynucleotide triphosphate

DPBS — nuclease-free Dulbecco's phosphate-buffered saline

dsRNA — double stranded RNA

EDTA — ethylenediaminetetraacetic acid

EGFP — enhanced green fluorescent protein

FISH — fluorescence *in-situ* hybridization

GPCR — G protein-coupled receptor

HEIR — heat-induced epitope retrieval

HEPES — N-2-hydroxyethylpiperazine-N'-2-ethanesulfuronic acid

HRP — horseradish peroxidase

IP<sub>3</sub> — 1,4,5, tri-phosphate

ITP — ion transport peptide

ITP-L — ion transport peptide-like/long

5HT — 5-hydroxytryptamine

ISME — ion-selective microelectrode

kDa — kilodalton

KT5823 — protein kinase G (PKG) inhibitor

LDH — lactate dehydrogenase

LK — leukokinin

L-NAME — N $\omega$ -nitro-L-arginine methyl ester hydrochloride

MNP — mosquito natriuretic peptide

mRNA — messenger RNA

MT — Malpighian tubules

MW — molecular weight

NADH — reduced nicotinamide adenine dinucleotide

nBF — non-blood fed

NDAE — Na<sup>+</sup> driven anion exchanger

NHA — cation/H<sup>+</sup> antiporter

NHE — Na<sup>+</sup>/H<sup>+</sup> exchanger 2

NKA — Na<sup>+</sup>-K<sup>+</sup>-ATPase

NKCC — Na<sup>+</sup>-K<sup>+</sup>-2Cl<sup>-</sup> cotransporter

NO — nitric oxide

NOS — nitric oxide synthase

NSC — neurosecretory cell

NSS — normal sheep serum

NTC — no template control

ORF — open reading frame

OV— ovary

PBS — phosphate-buffered saline

PCR — polymerase chain reaction

PI — pars intercerebralis

PL — pars lateralis

PMSF — phenylmethylsulfonyl fluoride

PK — pyruvate kinase

PKA — protein kinase A

PKG — protein kinase G

PVO — perivisceral organs

PK1 — pyrokinin-1

PVDF — polyvinylidene difluoride

qRT-PCR or qPCR — quantitative real-time PCR

RNA — ribonucleic acid

RNAi — RNA interference

RpL429 — ribosomal protein L49

RpS18— ribosomal protein S18

RT — room temperature

RT-PCR — reverse transcriptase PCR

SDS-PAGE — sodium dodecyl sulfate polyacrylamide gel electrophoresis

SEG — suboesophageal ganglia

SEI — homogenization buffer containing sucrose, EDTA and imidazole

SEID — SEI with sodium deoxycholate

SEM — standard error of the mean

TBS-T — TBS with Tween-20

TG — thoracic ganglia

TMB — 3,3',5,5'-tetramethylbenzidine

VA — V-type H<sup>+</sup>-ATPase

VNC — ventral nerve cord

## **Statement of Contributions**

### **Chapter One**

This chapter was written by F. Sajadi with valuable guidance and editorial support from Dr. J. P. Paluzzi.

### **Chapter Two**

This chapter was written by F. Sajadi with valuable guidance and significant editorial support from Dr. J. P. Paluzzi. Data collection and formal analyses was executed by F. Sajadi with valuable assistance from Carmela Curcuruto.

### **Chapter Three**

This chapter was written by F. Sajadi with valuable guidance and significant editorial support from Dr. J. P. Paluzzi. Data collection and formal analyses was executed by F. Sajadi, with valuable assistance by Dr. J. P. Paluzzi, C. Papuptis, A. Wahedi, L. T. Ber, and A. Matei.

### **Chapter Four**

This chapter was written by F. Sajadi with valuable guidance and editorial support from Dr. J. P. Paluzzi. Data collection and formal analyses was executed by F. Sajadi, with valuable assistance from M. Vergara-Martínez from Universidad Nacional Autónoma de México, Mexico City, Mexico (MITACs student).

### **Chapter Five**

This chapter was written by F. Sajadi with valuable guidance and editorial support from Dr. J. P. Paluzzi. Data collection and formal analyses was executed by F. Sajadi, with valuable assistance from undergraduate students, Lulia Snan and Chiara Di Scipio.

### **Chapter Six**

This chapter was written by F. Sajadi with valuable guidance and significant editorial support from Dr. J. P. Paluzzi. Data collection and formal analyses was executed by F. Sajadi.

## **Chapter One**

### **Overview**

Part of this chapter has been published and reproduced with permission:

Sajadi, F., Paluzzi, J.P. (2021) Hormonal regulation and functional role of the 'renal' tubules in the disease vector, *Aedes aegypti*. *Vitamins and Hormones* Academic Press, 189–225.

## 1.1 The mosquito, *Aedes aegypti*

### 1.1.1 *A. aegypti* as a disease vector

The mosquito, *Aedes aegypti*, is a vector of several globally important arboviruses, which are viruses transmitted by arthropod vectors and include yellow fever virus (Jentes et al., 2011), dengue virus (Simmons et al., 2012), chikungunya virus (Leparc-Goffart et al., 2014) and the Zika virus (Oehler et al., 2014). Over the last 50 years, the global health impact of dengue and chikungunya virus has increased dramatically, with both diseases spreading across new geographic locations and increasing in incidence within their range (Weaver, 2014). Dengue virus is the most prevalent human arboviral infection causing approximately 100 million apparent annual infections world-wide, with almost half of the global population at risk of infection (Hasan et al., 2016; Jing and Wang, 2019; Otu et al., 2019). Dengue fever is principally transmitted through *A. aegypti*, which thrives despite urbanization by humans (Rigau-Pérez et al., 1998). Chikungunya virus has received significant public health attention due to outbreaks in Europe (Borgherini et al., 2007; la Ruche et al., 2010; Rezza et al., 2007), as well as more recent invasion into the Americas, with over a million cases recorded to date (Cauchemez et al., 2014; Johansson et al., 2014; Morens and Fauci, 2014). Increases in the distribution of transmission is due to lack of commercially available vaccines or antivirals for dengue and chikungunya viruses (Roy et al., 2014; Simmons et al., 2012). While yellow fever infections have been declining over the years due to extensive vector control and a vaccine developed more than 70 years ago (Chen and Wilson, 2020; Chippaux and Chippaux, 2018), the virus still infects a considerable amount of people in Africa and South America (Garske et al., 2014). Given the rapid global spread and public health impact of these viruses, comprehensively understanding the biology of *A. aegypti* will enable more efficient strategies for disease control.

### 1.1.2 *A. aegypti* lifecycle and distribution

After their domestication, *A. aegypti* mosquitoes became closely associated with human habitation (Powell and Tabachnick, 2013; Powell et al., 2018). Female *A. aegypti* mosquitoes prefer blood feeding on humans, with other vertebrates comprising only a small proportion of their bloodmeals (Jansen and Beebe, 2010). Unlike other mosquitoes, *A. aegypti* is a day-biting mosquito, taking a single or multiple bloodmeals (potentially from multiple hosts) during a single gonotrophic cycle, which starts at the time of the first bloodmeal and ends with egg-laying (Borgherini et al., 2007). In this way, female mosquitoes obtain vitamins, nutrients, proteins, and minerals essential for egg development (Beyenbach, 2003a). Female adult *A. aegypti* preferentially lay their eggs in artificial human-made containers such as water tanks, flowerpots, or other containers in and around the house. The eggs remain dormant until flooded with water and can withstand desiccation for up to one year (Clemons et al., 2010). Upon egg hatching, the mosquito goes through four larval stages and the pupal stage, all of which are aquatic (Figure 1-1). During the larval stages, which lasts at least four days, the instar spends the majority of time at the water surface due to the absence of gills. Larvae have a respiratory siphon located at the posterior of their body, allowing for tracheal breathing. As a result, they must remain close to the water surface to permit gas exchange, swimming under the water surface only to feed on organic matter such as algae and other microorganisms. Following the fourth instar, larvae enter the mobile, non-feeding aquatic pupal stage, which lasts about two days. Depending on the environmental conditions, the lifespan of the adult mosquito can range from two weeks to a month (Clemons et al., 2010). Although morphologically similar, female and male *A. aegypti* mosquitoes have notable distinguishing features including males having bushy antennae, which act as sensory organs to locate females (Christophers, 1960), compared to the slender antennae in

females. Males are also noticeably smaller in size relative to females, but the maxillary palps in males are as long as the proboscis whereas the palps in females are significantly shorter in length. Adults of both sexes feed on plant nectar, however females possess specialized mouthparts adapted to obtain bloodmeals from their vertebrate hosts (Clemons et al., 2010).

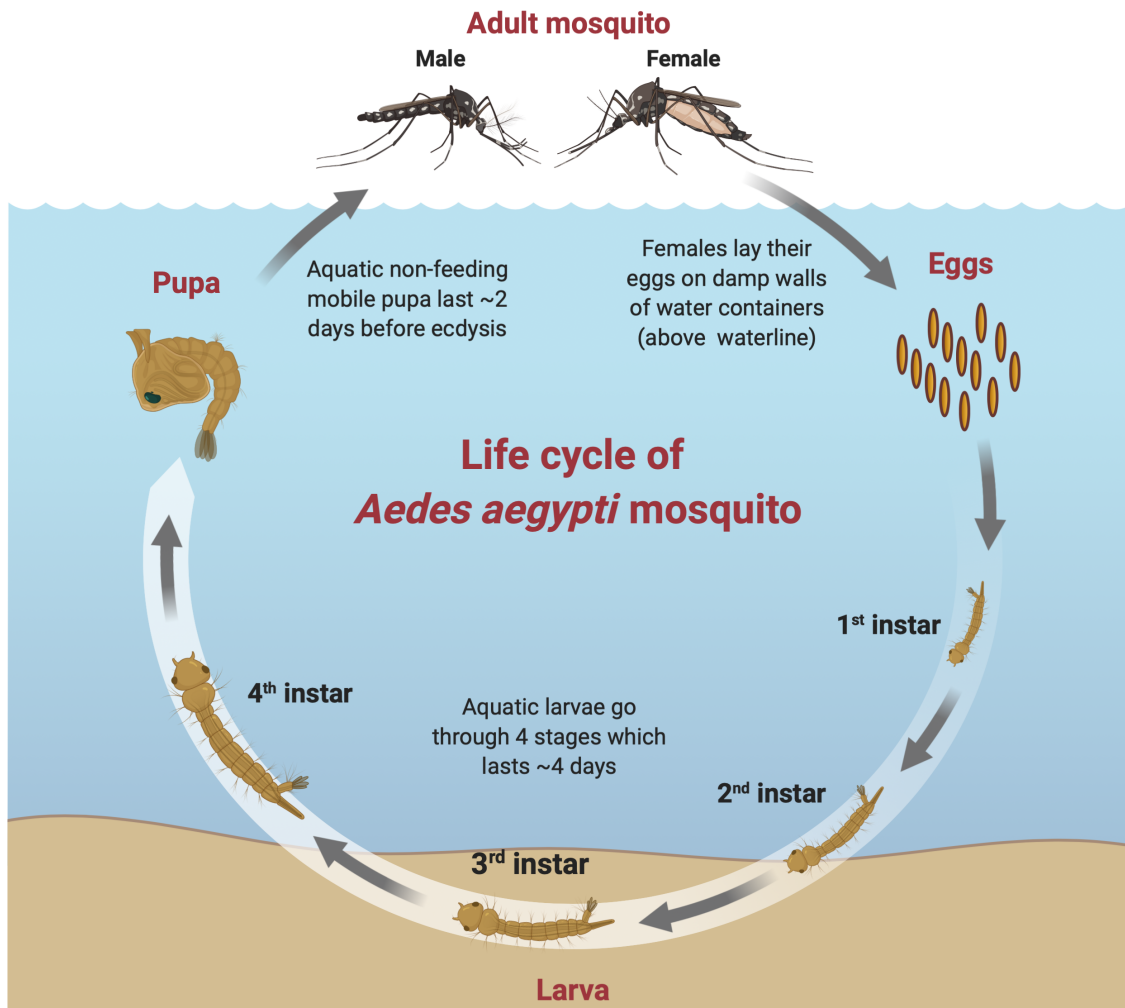


**Figure 1-1. Life cycle of the *A. aegypti* from egg hatching to emergence of the adult flying mosquito.** Female *Aedes* mosquitoes lay their eggs in human-made water containers, above the water surface. Upon egg hatching, the mosquito goes through four larval stages (lasting ~four days) before entering the non-feeding, mobile pupal stage. After ~two days, the pupa undergoes ecdysis into the adult terrestrial mosquito, with a lifespan ranging between two weeks to a month although this can vary greatly depending upon ambient temperature and humidity levels.

### 1.1.3 *A. aegypti* reproductive system

Mosquito reproduction is dependent on the coordination of behavioural and physiological processes that occur in mated females, which may include increased host-seeking and blood-feeding behaviours, rates of egg development, and sperm storage (Avila et al., 2011; Meuti and Short, 2019). Within 2-3 days after emergence, both sexes mate, and female mosquitoes must ingest a bloodmeal to acquire nutrients for egg development (Lehane, 1991). In male mosquitoes, spermatogenesis occurs in the paired testes, where spermatogonia (immature sperm cells) proliferate and mature into spermatocytes, spermatids, and finally into mature sperm cells, spermatozoa (Rocco et al., 2017; Rocco et al., 2019). Once matured, spermatozoa from each testis are transported via the vas deferens to the seminal vesicles, which act as storage units (Clements, 2000; Oliva et al., 2014; Rocco and Paluzzi, 2016). During copulation, male *A. aegypti* deposit sperm from the seminal vesicle into the bursa of the female reproductive tract, whereafter they rapidly concentrate at the spermathecal vestibule and migrate to the sperm storage organs, spermathecae, where they are stored long-term (Camargo et al., 2020; Degner and Harrington, 2016). Female *A. aegypti* usually mate once as a single insemination event allows sufficient sperm to be stored within the spermathecae to allow fertilization of all the eggs that a female will develop during her lifetime (Degner and Harrington, 2016; Oliva et al., 2013; Shaw et al.; Styer et al., 2007). As such, the storage and maintenance of sperm in the female are fundamental processes that maximize reproductive output and fitness (Orr and Zuk, 2012). To initiate fertilization, sperm is released from the spermathecae and travels down the spermathecal duct towards the paired ovaries to allow sperm penetration into the egg (Degner and Harrington, 2016).

While the bloodmeal serves to provide the female with essential proteins and nutrients required for egg production, it also contains large amounts of unwanted salts and water which poses a threat to the haemolymph homeostasis (Beyenbach, 2003a). To maintain hydromineral balance against the osmoregulatory stress from the bloodmeal, female mosquitoes have a specialized excretory system to help cope with this insult to their haemolymph balance.

#### **1.1.4 *A. aegypti* excretory system**

Insect haemolymph, analogous to vertebrate blood, is a fluid that circulates within the interior of the arthropod, remaining in direct contact with the tissues and organs of the insect. Similar to other insects in both aquatic and terrestrial habitats, *Aedes* mosquitoes face different osmoregulatory challenges, as their haemolymph homeostasis is continuously challenged in relation to feeding and environmental conditions. Larval *A. aegypti* normally reside in fresh water and face the osmoregulatory challenges of gaining water from drinking and through osmotic flux across their body surface, thus potentially causing dilution of the haemolymph (Bradley, 1987; O'Donnell, 2010; Patrick et al., 2006). Additionally, larvae are subject to constant diffusional loss of haemolymph ions into external media (Patrick et al., 2006). Post-eclosion, adult *A. aegypti* are subject to disparate osmoregulatory challenges and must switch from excretion of water to its preservation. During non-feeding conditions, terrestrial *A. aegypti* are tasked with conserving body water to preserve the concentration of haemolymph ions and avoid reduction in body volume (Beyenbach, 2003a; Coast, 2009; Patrick et al., 2006). However, upon taking a bloodmeal, adult females face the challenge of haemolymph ion dilution, as they take on a significant water load (Coast, 2009). To maintain hydromineral balance against osmoregulatory stress, insects like *A. aegypti* utilize a specialized excretory system, comprised of

the Malpighian ‘renal’ tubules (MTs) and the hindgut (Coast, 2007), which function to counter disturbances to their haemolymph balance. The MTs are responsible for primary urine formation, usually rich in NaCl and/or KCl, which is further modified through secretory and reabsorptive processes as the primary urine travels downstream of the MTs towards the hindgut (Coast, 2007). The final excreta can be hypo- or hyperosmotic to the insect haemolymph, depending on the environmental conditions or feeding status, and is enriched in nitrogenous and toxic wastes (Beyenbach, 2003a).

The insect alimentary canal organs, including the MTs, are essential organs responsible for alleviating osmoregulatory challenges. Various active and passive transepithelial transporters line the excretory system, such as ion exchangers, co-transporters, pumps, and ion and water channels, and the activity of these excretory organs are under neurochemical and hormonal control by various neuropeptides and biogenic amines (Beyenbach, 2003a; Coast, 2007; Coast, 2009; Phillips, 1981). The release of these hormones or neurochemicals along with the subsequent activation of their cognate receptors localized on target cells in tissues and organs of the excretory system, induces signal transduction pathways that trigger diuretic or anti-diuretic processes, allowing the insect to fine-tune hydromineral balance.

## **1.2 The role of MTs and hindgut**

### **1.2.1 The cellular composition of MTs in *A. aegypti***

In terrestrial insects, the main osmoregulatory and excretory organ are the MTs while the hindgut also plays an important role in reabsorptive processes (Coast et al., 2002). The change from an aquatic environment to a primarily terrestrial habitat results in functional reversal of the excretory system, from a process geared towards elimination of water to one critical for its

conservation (Beyenbach, 2003a). In addition to water, this system must control levels of the main electrolytes ( $\text{Na}^+$ ,  $\text{K}^+$  and  $\text{Cl}^-$ ), a function shared with the vertebrate kidney (Coast, 2007). The yellow fever mosquito has five MTs, connected at the junction between the midgut and hindgut. Female mosquitoes have considerably larger MTs than do males and results in the higher secretion rate of salt and water. This sexual dimorphism in the MTs reflects the female's capacity to secrete larger loads of salt and water following a bloodmeal, whereby *in vitro* studies have noted that female MTs secrete salt and water six times the rate of male MTs (Beyenbach, 2003a). In *A. aegypti* mosquitoes, MTs are made of a single layer of epithelial cells consisting of two types; mitochondrial-rich principal cells located in both the distal and proximal segment of the MTs, and smaller stellate cells, dispersed only in the distal two thirds of each tubule (Patrick et al., 2006). The principal cells facilitate active transport of  $\text{Na}^+$  and  $\text{K}^+$  from the haemolymph into the tubule lumen, while stellate cells aid in the transepithelial secretion of  $\text{Cl}^-$  (Beyenbach, 2003a; Patrick et al., 2006). The apical membrane of the principal cells contains a border of microvilli, rich in mitochondria and endoplasmic reticulum, which increases the surface area available for water and salt transport (Beyenbach, 2003a). Mitochondria residing in the brush border membrane fuel the ATP-consuming proton pump, the V-type  $\text{H}^+$ -ATPase (VA), that resides in the apical membrane (Patrick et al., 2006). Due to the higher transfer of  $\text{Na}^+$  and  $\text{K}^+$  between the haemolymph and MTs, the number and sizes of principal cells are much greater than stellate cells (ratio of approximately 5:1); the stellate cells constituting only between 16-26% of the total cell number of the MTs (Beyenbach, 2003a; Patrick et al., 2006). In contrast, the stellate cells have elongated, slender, cellular extensions, sharing contact with up to four adjacent principal cells (Patrick et al., 2006), lending support for a greater functional role than previously assumed.

### **1.2.2 Ion transport in stimulated *A. aegypti* MTs**

Primary urine production is driven by secondary active transport of Na<sup>+</sup> and K<sup>+</sup> cations into the tubule lumen, which establishes a transepithelial voltage, allowing passive entry of the counter ion, Cl<sup>-</sup> (Beyenbach, 2003a; O'Connor and Beyenbach, 2001). Water follows into the lumen through selective channels called aquaporins, driven by the osmotic gradient created by the net secretion of NaCl/KCl. Transepithelial transport from the haemolymph into the lumen of the MTs is achieved by co-transporters and channels lining the principal and stellate cells allowing transcellular transport, and through a paracellular pathway found between cells (Beyenbach, 2003a; Beyenbach and Piermarini, 2011; Piermarini and Calkins, 2014) (Figure 1-2).

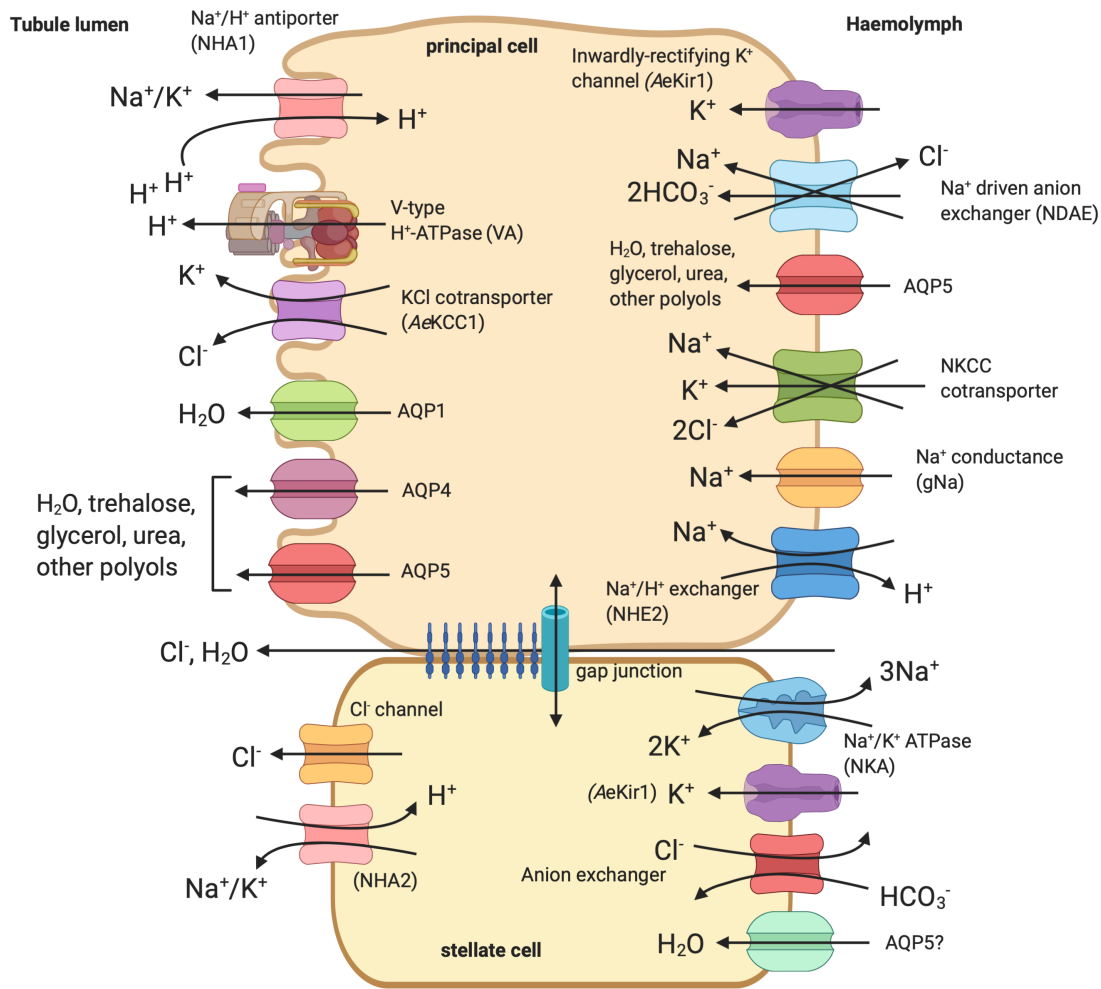


**Figure 1-2. Ion and water transport through principal and stellate cells of *A. aegypti* MTs.** The principal cells are responsible for transport of Na<sup>+</sup> and K<sup>+</sup> via secondary active transport. A V-type H<sup>+</sup>-ATPase (VA), localized in the brush border of the apical membrane, produces a H<sup>+</sup> gradient that drives the transport of Na<sup>+</sup> and K<sup>+</sup> across the apical membrane through cation/H<sup>+</sup> antiporter (NHA1) and a KCl cotransporter (AeKCC1). Ions are secreted from the haemolymph through a Na<sup>+</sup>/H<sup>+</sup> exchanger (NHE2) channel, a NKCC cotransporter, Na<sup>+</sup> driven anion exchanger (NDAE), and an inwardly-rectifying K<sup>+</sup> channel (AeKir1) localized on the basolateral membrane. Connected by septate junctions, stellate cells are responsible for the transcellular transport of Cl<sup>-</sup> through a Cl<sup>-</sup>/HCO<sub>3</sub><sup>-</sup> exchanger on the basolateral membrane and a Cl<sup>-</sup> channel on the apical membrane. Cations (Na<sup>+</sup> and K<sup>+</sup>) are secreted from the haemolymph through a Na<sup>+</sup>/K<sup>+</sup>-ATPase (NKA) and AeKir1, into the lumen through NHA2. Ion transport between the stellate and principal cells may connect through gap junctions localized between the cells. Water eventually follows the ions into the tubule lumen through aquaporins, AQP 1, 4, 5 localized in the apical membrane and AQP 5 in basolateral membrane of the principal cell. Adapted from (Beyenbach and Piermarini, 2011; Beyenbach et al., 2010; Piermarini et al., 2010; Piermarini et al., 2015). Proposed location of AQPs are based on findings from both larval and adult *Aedes* MTs (Drake et al., 2015; Misyura et al., 2020) and adult *Anopheles gambiae* MTs (Liu et al., 2011).

The active driving force responsible for ion transport is the bafilomycin-sensitive V-type H<sup>+</sup>-ATPase (VA) (Wieczorek et al., 1989; Wieczorek et al., 2009), which is expressed in the apical brush border membrane of the principal cells (Weng et al., 2003). The movement of protons into the lumen of the MTs creates a proton gradient, which energizes the exchange of Na<sup>+</sup> and K<sup>+</sup> ions (via Na<sup>+</sup>/H<sup>+</sup> and/or K<sup>+</sup>/H<sup>+</sup> antiporters) across the apical membrane. A basolaterally-localized bumetanide-sensitive Na<sup>+</sup>:K<sup>+</sup>:2Cl<sup>-</sup> (NKCC) cotransporter has also been identified in insect MTs, driven by the electrochemical gradient for Na<sup>+</sup> entry (Coast, 2007; Ianowski and O'Donnell, 2004). This cotransporter allows for transporting Na<sup>+</sup>, K<sup>+</sup>, and Cl<sup>-</sup> from the haemolymph into the principal cells (Hegarty et al., 1991). In addition to the NKCC cotransporter, K<sup>+</sup> is secreted across the basolateral membrane in principal cells through an inwardly rectifying K<sup>+</sup> (Kir) channel, such as *AeKir1* and across the apical membrane through the KCl cotransporter (*AeKCC1*), both recently cloned in *Aedes* MTs (Piermarini et al., 2013; Piermarini et al., 2015; Piermarini et al., 2011). The Na<sup>+</sup> gradient is maintained by a P-type Na<sup>+</sup>/K<sup>+</sup> ATPase (NKA), found on the basolateral membrane, with varying sensitivities to ouabain (Coast, 2007; Patrick et al., 2006; Weng et al., 2003).

The electrochemical gradient set up by active transport through the VA allow for the passive transport of other small haemolymph solutes into the lumen, such as Cl<sup>-</sup>. Currently, there are two proposed routes of transepithelial Cl<sup>-</sup> transport in *Aedes* MTs: a transcellular pathway through stellate cells and a paracellular route between the epithelial cells of the MTs (Beyenbach, 2003a; Beyenbach and Piermarini, 2011; Coast et al., 2005; Massaro et al., 2004; Weng et al., 2003). Transcellular secretion of Cl<sup>-</sup> into the tubule lumen occurs via a basolaterally localized Cl<sup>-</sup>/HCO<sub>3</sub><sup>-</sup> (anion) exchanger, whereby production of HCO<sub>3</sub><sup>-</sup> occurs in the principal cells and enters stellate cells through gap junctions (Calkins and Piermarini, 2017; Calkins et al.,

2015; Weng et al., 2008). After uptake of  $\text{Cl}^-$  into the cell,  $\text{Cl}^-$  channels on the apical membrane mediate the passive diffusion of the ions from the cell into the tubule lumen (Beyenbach and Piermarini, 2011). Eventually, during urine production, water follows into the lumen of the MTs through selective channels called aquaporins (AQP), driven by the osmotic gradient (Klowden, 2013).

### **1.2.2 The reabsorptive role of the hindgut**

The iono- and osmoregulatory mechanisms in the MTs have been extensively studied; however, not much research has been devoted towards understanding the mechanisms for ion and water transepithelial transport in the hindgut. The MTs generate a variable load of primary urine that is delivered to the hindgut to be modified prior to being voided as urine (Beyenbach, 2003a). After the primary urine is emptied into the hindgut, the bulk of water, ion, and metabolite reabsorption occurs in the rectum. Ultimately, the hindgut plays a dominant role in determining the composition of the final excreted waste (Coast, 2009).

The hindgut, composed of the anterior ileum and posterior rectum, is an excretory organ that functions in selectively reabsorbing substances back into the haemolymph (Patrick et al., 2006). In the locust, *Schistocerca gregaria*, the ileum is the major site for isosmotic fluid reabsorption and active  $\text{Na}^+$  and  $\text{Cl}^-$  reabsorption (Phillips et al., 1988; Phillips et al., 1994). Passive reabsorption of  $\text{K}^+$  occurs by electrical coupling with electrogenic  $\text{Cl}^-$  transport (Hanrahan and Phillips, 1983). Additionally, the ileum plays a major role in acid-base balance by reabsorbing  $\text{HCO}_3^-$  and secreting  $\text{H}^+$  protons into the lumen (Phillips et al., 1994). The final site of excretion is controlled by the rectum, which has a cuticle lining with greater permeability than the cuticle lining of the foregut (Phillips et al., 1994). The epithelial cells of the hindgut are

specialized for both active secretion and reabsorption, allowing for modification of the fluid by reabsorbing the useful solutes and water while eliminating compounds in excess (Hopkins 1967).

### **1.3 Neuroendocrine regulation of the MTs**

#### **1.3.1 The neuroendocrine system of *A. aegypti***

Similar to other animals such as vertebrates and other insects, *A. aegypti* elicit hormonal regulation of peripheral organs such as the alimentary canal through coordination of the nervous and endocrine systems. The neuroendocrine system is composed of neurohormones derived from the nervous system (as well as some peripheral endocrine glands and neurons) and these signalling molecules include neuropeptides and biogenic amines. The neurohormones are deposited within neurohaemal structures where the neurosecretory material is stored until release into circulation (Hartenstein, 2006). Neurons that produce neurohormones are called neurosecretory cells (NSCs) (Hartenstein, 2006; Scharrer, 1987). Thus, the NSCs and neurohaemal organs together form the neuroendocrine system (Raabe, 1989). An important class of signalling molecules are the neuropeptides, which are oligopeptides containing between 5-50 amino acid residues, and are the most structurally and functionally diverse class of neuroactive substances (Hartenstein, 2006; Mercier et al., 2007; Nässel, 2002; Schoofs et al., 2017). Neuropeptides are generated from prepropeptides, which are larger precursor proteins, and cell-specific gene transcription allows for limiting expression of different neuropeptides in specific sets of neurons in the nervous system (Benveniste and Taghert, 1999; Taghert, 1999). After translation, the peptide precursor can be further processed through post-translational modifications including (but not limited to) enzymatic cleavage and carboxy terminus amidation (Kumar and Bachhawat, 2012; Taghert, 1999; Veenstra, 2000; Zupanc, 1996). Once processed,

the neuropeptides are released from the nervous system and bind to their cognate receptors in order to exert their effects, acting as neuromodulators, neurohormones, and/or neurotransmitters. Neuromodulators regulate extrinsic signals, affecting groups of neurons at various synapses or effector cells at further distances (Mercier et al., 2007; Nässel, 2002). Neuropeptides can also act as neurohormones, which involves secretion into the circulatory system, to exert its effects on distal peripheral organs (Nässel, 2002). As such, the neurohormonal signal transmission is slower. Lastly, neurotransmitters can transmit electrical signals from one axon to another, by binding to receptors on a post-synaptic neuronal, or other effector cell, producing a rapid and transient response (Mercier et al., 2007; Nässel, 2002).

The insect central nervous system consists of several sets of NSCs located within the brain and ventral nerve cord (VNC), with the majority in the brain found in the dorso-medial protocerebrum, or the pars intercerebralis (PI) and pars lateralis (PL) (Hartenstein, 2006; Pipa, 1978; Raabe, 1989; Siegmund and Korge, 2001; Veelaert et al., 1998) (Figure 1-3). NSCs are also found in the suboesophageal ganglion (SEG), which is fused together with the brain in adult *A. aegypti* (Brown and Cao, 2001; Hartenstein, 2006). These NSCs project their axons, innervating neurohaemal organs, including the corpora cardiaca (CC) and abdominal perivisceral organs (PVOs) to release neurosecretory products into the haemolymph (Bräunig, 1987; Hartenstein, 2006; Strand et al., 2016). Once released, mature neuropeptides bind to their cognate receptors in target organs, tissues, and cells, triggering intracellular signalling cascades leading to specific physiological and behavioural responses. Majority of neuropeptides bind to G protein-coupled receptors (GPCRs), which contain a characteristic seven transmembrane domain architecture with an intracellular C-terminus and extracellular N-terminus (Mercier et al., 2007). As their name implies, the heterotrimeric G proteins that associate with GPCRs are composed of

three subunits ( $G\alpha$ ,  $G\beta$  and  $G\gamma$ ) and interact with the cytoplasmic face of the receptor (Mercier et al., 2007). Upon activation of the receptor by an appropriate ligand, a conformational change is initiated, and the GDP bound to the  $G\alpha$  subunit is replaced with a GTP molecule (Mahoney and Sunahara, 2016). The heterotrimeric complex then dissociates as a  $\beta\gamma$  dimer and  $\alpha$  subunit (Mercier et al., 2007), both of which can target other signalling proteins to initiate an intracellular cascade.

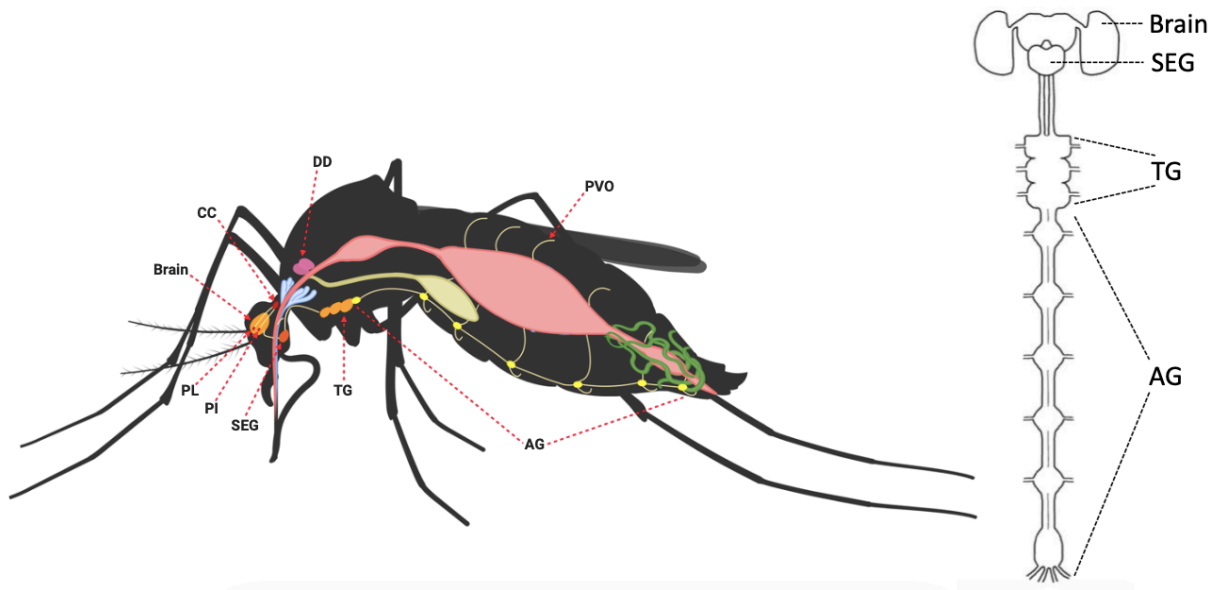


**Figure 1-3. *Aedes aegypti* neuroendocrine system.** Central NSCs are located in the pars intercerebralis (PI) and pars lateralis (PL), and ventral nerve cord (VNC), including the suboesophageal ganglia (SEG), thoracic ganglia (TG) and abdominal ganglia (AG). The NSCs cells project axons innervating neurohaemal organs, including the corpora cardiaca (CC) and abdominal perivisceral organs (PVOs), which release the neurosecretory products into the haemolymph.

### 1.3.2 Hormonal regulation of MTs and hindgut

The high rates of primary urine formation by the MTs immediately upon adult eclosion and post-bloodmeal require a precisely regulated hormone-mediated signalling pathway that coordinates downstream target proteins for ion and water transport (Jagge and Pietrantonio, 2008). The process of maintaining ionic homeostasis within the organism is primarily governed by the MTs and the hindgut. Notably, the MTs are not innervated, thus regulation of epithelial transport and fluid secretion in this organ occurs via circulating messengers in the haemolymph (Beyenbach, 2003a). The endocrine messengers are characterized by their effect on the rate of secretion and absorption by the MTs and gut, respectively. Diuretic hormones (DH) and anti-diuretic hormones (ADH) are endocrine factors that affect rates of fluid secretion and excretion by the chief iono- and osmoregulatory organs. As mentioned earlier, these hormones consist of a variety of neuropeptides and neurochemicals produced by NSCs in the brain and VNC ganglia (Beyenbach, 2003a; Coast, 2009). Research has shown that a variety of peptides and biogenic amines regulate diuresis and anti-diuresis in insects including: calcitonin (CT)-like DH, corticotropin-releasing factor (CRF)-like DH, kinin-like peptides, serotonin and other biogenic amines, and anti-diuretic factors (ADFs) such as the CAPA peptide and ion transport peptide (ITP) (Clark et al., 1998a; Coast et al., 2002; Coast et al., 2005; Eigenheer et al., 2002; Eigenheer et al., 2003; Ionescu and Donini, 2012; Phillips and Audsley, 1995). The ion transport processes and signalling mechanisms that are targeted vary with the different diuretic and anti-diuretic hormones and depends on the insect species. Stimulation of these hormonal receptors activate various signalling pathways acting through multiple second messenger systems including cyclic AMP (cAMP), cyclic GMP (cGMP), and  $\text{Ca}^{2+}$  (Beyenbach, 2012; Gioino et al., 2014; Ionescu and Donini, 2012; Quinlan and O'Donnell, 1998). The subsequent section will briefly highlight

some of the most well-studied regulators of the excretory system with particular emphasis on factors either well known or expected to control the adult mosquito excretory organs.

### *Diuretic hormone 31 (DH<sub>31</sub>)*

Although the midgut and hindgut impact the composition and volume of urine, the MTs serve the dominant role in haemolymph homeostasis, under control by neurohormones (Coast, 2009). In *A. aegypti*, mosquito natriuretic peptide (MNP) is an important diuretic hormone triggering diuresis after a bloodmeal (Beyenbach and Petzel, 1987), which is derived from the brain (Petzel et al., 1985). The calcitonin-like diuretic hormone 31 (DH<sub>31</sub>) was identified as the MNP in the mosquitoes *A. gambiae* and *A. aegypti* (Coast et al., 2005), selectively activating transepithelial secretion of Na<sup>+</sup> in the MTs, using cAMP as second messenger (Beyenbach, 2003a) (Figure 1-4). Released from NSCs, DH<sub>31</sub> binds to a GPCR expressed in select principal cells in a distal-proximal gradient, found alongside high expression of VA and cation/H<sup>+</sup> exchangers (Kwon et al., 2012). Upon receptor activation, there is an increase in cAMP production, which activates select Na<sup>+</sup> channels and the NKCC cotransporter (Beyenbach and Petzel, 1987), upregulating activity of the VA to increase fluid secretion (Karas et al., 2005). In both *A. aegypti* and the fruit fly, *Drosophila melanogaster*, a single gene coding for DH<sub>31</sub> has been found in the genome; with a single peptide isolated in the *Aedes* mosquito (Predel et al., 2010). While haemolymph concentrations of DH<sub>31</sub> have yet to be determined, Coast (2005) suggests DH<sub>31</sub> peptide is immediately released into circulation, stimulating rapid excretion of Na<sup>+</sup> and excess water.

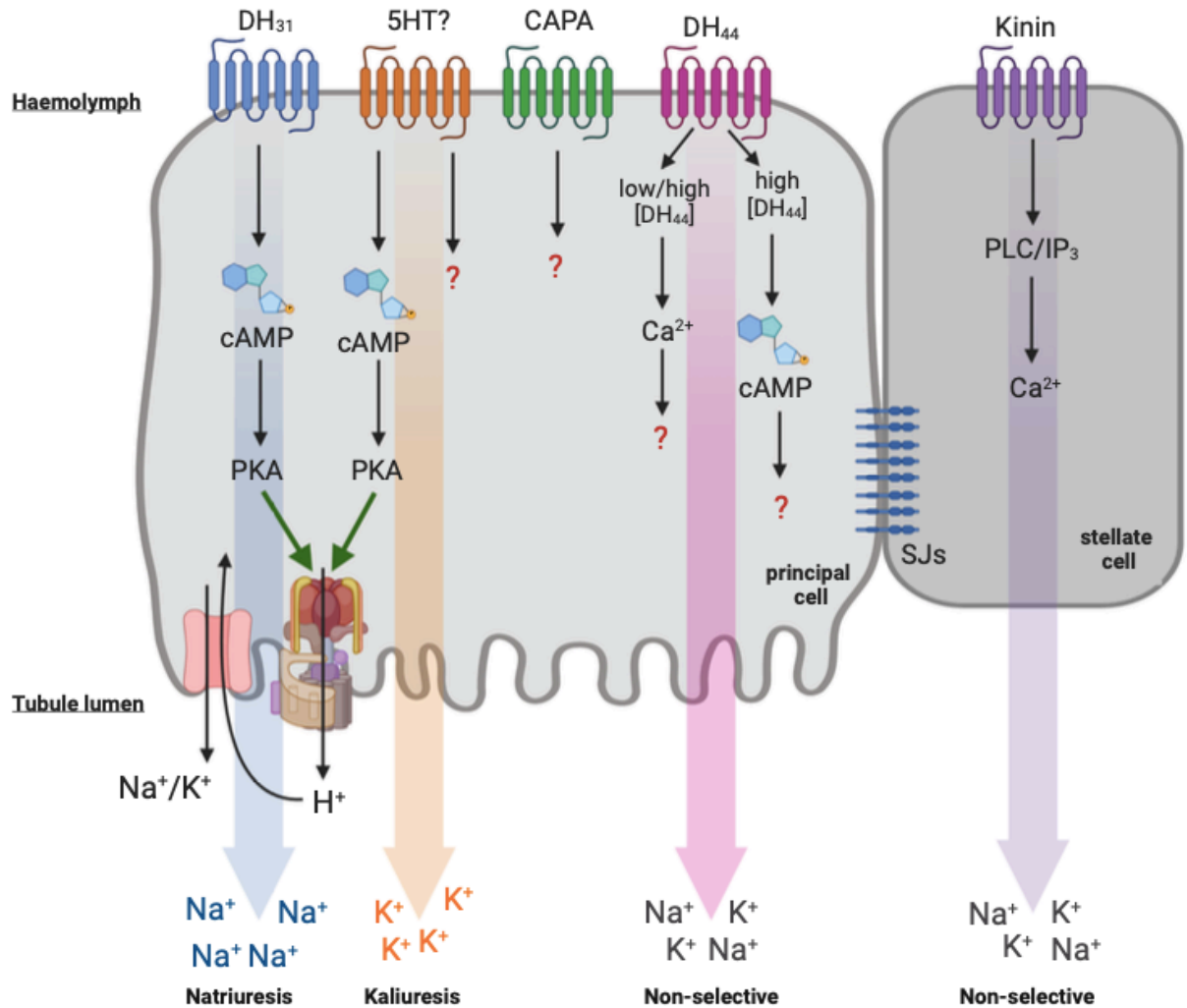


**Figure 1-4. Schematic diagram summarizing diuretic and anti-diuretic control of *A. aegypti* adult MTs.** Neurohormone receptors, including those for 5HT, and the peptides DH<sub>31</sub>, DH<sub>44</sub>, and CAPA, are localized to the basolateral membrane of principal cells, while the kinin receptor is localized exclusively to stellate cells. Stimulation of MTs with 5HT and DH<sub>31</sub> through their cognate receptors increases levels of the second messenger cAMP, with pronounced kaliuretic and natriuretic activity, respectively. DH<sub>44</sub>-related peptide receptor activation increases Ca<sup>2+</sup> and cAMP depending on the dose of peptide applied while kinin receptor signalling involves exclusively increases in intracellular levels of Ca<sup>2+</sup>. Both DH<sub>44</sub> and kinin non-selectively transports cations across the cell membrane. Abbreviations: protein kinase A (PKA), phospholipase C (PLC), 1,4,5, tri-phosphate (IP<sub>3</sub>), and septate junctions (SJs).

### *Diuretic hormone 44 (DH<sub>44</sub>)*

In dipteran MTs, both DH<sub>31</sub> and the corticotropin-releasing factor (CRF)-like diuretic hormone 44 (DH<sub>44</sub>), stimulate secretion through cAMP, increasing transepithelial cation (Na<sup>+</sup> and/or K<sup>+</sup>) transport, and subsequently, movement of osmotically obliged water into the lumen (Cabrero et al., 2002; Coast, 2001; Coast et al., 2005). While DH<sub>31</sub> selectively stimulates transepithelial Na<sup>+</sup> transport in mosquitoes (Coast et al., 2005; Petzel et al., 1985), DH<sub>44</sub> stimulates non-specific transport of both Na<sup>+</sup> and K<sup>+</sup> cations across the tubule membrane (Beyenbach, 2003a; Cabrero et al., 2002; Coast et al., 2005) (Figure 1-4). In *Aedes* MTs, DH<sub>44</sub>, which is related to the vertebrate CRF/urotensin/sauvagine family of peptides (Cabrero et al., 2002; Lovejoy and Jahan, 2006), has been shown to initiate diuresis via both paracellular and transcellular pathways, suggesting multiple receptors and second messenger systems might be involved. Specifically, low nanomolar concentrations of DH<sub>44</sub> stimulates weak secretion, acting through the paracellular pathway only (Clark et al., 1998b), and mediating this action by utilizing intracellular Ca<sup>2+</sup> as a second messenger (Clark et al., 1998a). At higher nanomolar concentrations, DH<sub>44</sub> elicits a stronger secretion response, influencing both paracellular and transcellular transport, increasing levels of cAMP and intracellular Ca<sup>2+</sup> (Clark et al., 1998b). While the DH<sub>44</sub> receptor has yet to be immunolocalized in the mosquito MTs, an indirect determination of cell-specific expression was achieved through an *ex vivo* receptor binding assay using fluorescently-conjugated DH<sub>44</sub>. Specifically, the DH<sub>44</sub> receptor was localized to principal cells of the MTs in both larval and adult *A. gambiae* MTs, with significantly higher fluorescent intensities in the former, which correlates with the greater transcript abundance of the DH<sub>44</sub> receptor reported in larval MTs relative to adults (Overend et al., 2015).

## *Kinin*

In *Aedes* female MTs, there are two routes for ion transport towards the tubule lumen; the paracellular path through septate junctions between cells, and the transcellular route through either principal or stellate cells (Beyenbach, 2003a; Beyenbach, 2003b). While  $\text{Na}^+$  and  $\text{K}^+$  cations are transported transcellularly through principal cells (Beyenbach and Masia, 2002; O'Connor and Beyenbach, 2001; Petzel et al., 1999), secretion of  $\text{Cl}^-$  occurs through both the paracellular and transcellular routes. Chloride transport in dipterans, such as *A. aegypti*, is stimulated by the endogenous insect kinins (Veenstra et al., 1997). The insect kinin family are a group of multifunctional neuropeptide hormones with diuretic and myotropic activity in insects (Nachman et al., 2009). First isolated from the cockroach *Leucophaea maderae* head extracts, kinins were originally believed to act as gut smooth muscle agonists (Holman et al., 1987). Leucokinin diuretic activity was first investigated in *A. aegypti* MTs, increasing transepithelial  $\text{Cl}^-$  conductance, thus depolarizing the transepithelial voltage (Schepel et al., 2010). There are three endogenous *A. aegypti* kinin peptides encoded by a single cDNA, functioning to increase fluid secretion by the MTs and induce hindgut contractions (Cady and Hagedorn, 1999a; Veenstra et al., 1997). Upon receptor activation, *Aedes* kinins increase intracellular 1,4,5, triphosphate ( $\text{IP}_3$ ) in isolated *Aedes* MTs, suggesting kinins act by increasing levels of intracellular  $\text{Ca}^{2+}$  from  $\text{IP}_3$ -sensitive calcium stores (Cady and Hagedorn, 1999b). Consistent with the established expression in stellate cells of the MTs in the fruit fly *D. melanogaster* (Radford et al., 2002) and another mosquito, *Anopheles stephensi* (Radford et al., 2004), the kinin receptor in *A. aegypti* was similarly localized within stellate cells verifying they are the main target of *Aedes* kinin peptides (Lu et al., 2011) (Figure 1-4).

### *5-hydroxytryptamine, 5HT*

The last family member of diuretic hormones thus far known to act on *Aedes* MTs is serotonin (5-hydroxytryptamine, 5HT), an endogenous neurohormone found in *A. aegypti*. Specifically, 5HT has been found to hold a variety of functions within the mosquito, particularly in the excretory and gas exchange systems (Ionescu and Donini, 2012; Pietrantonio et al., 2001). Notably, 5HT is known to control diuresis in diverse insect species, demonstrating a dose-dependent diuretic effect on MTs, acting to increase fluid secretion rate in both larval and adult *A. aegypti* MTs (Clark and Bradley, 1996; Clark and Bradley, 1997; Donini et al., 2006; Ionescu and Donini, 2012) as well as increasing the amount of fluid delivered to the hindgut (Messer and Brown, 1995; Veenstra, 1988). In the kissing bug, *Rhodnius prolixus*, among its many roles including cuticle plasticization necessary for blood meal engorgement (Orchard, 2006), 5HT is released into the haemolymph post-bloodmeal to induce diuresis (Lange et al., 1989), binding to a 5HT type-2b receptor, which was characterized in *R. prolixus* (Paluzzi et al., 2015). However, no receptor of this type has yet been shown to be enriched in MTs in *A. aegypti*. A 5HT7 type receptor in *A. aegypti* has been localized to the tracheolar cells associated with the MTs, but not to the tubule epithelium (Pietrantonio et al., 2001) suggesting another isoform may be present and mediates the activity of 5HT directly on the MTs. More recently, another 5HT receptor, a putative type 1 receptor family member that the authors referred to as AaSeR-1, has been immunolocalized in larval stage of *A. aegypti* to different regions of the alimentary canal, including the gastric caeca, midgut, and hindgut, as well as the MTs (Petrova and Moffett, 2016) (Figure 1-4).

## CAPA

While considerable studies have examined diuretic factors and their effects on secretion rate, limited studies have investigated the role of anti-diuretic hormones. One of first identified factors shown to act on the MTs to inhibit fluid secretion (Quinlan et al., 1997) was a cardioacceleratory peptide (CAP2b) originally sequenced in the hawkmoth *Manduca sexta* (Huesmann et al., 1995), part of the CAPA family of peptides (Paluzzi, 2012). This discovery revealed that like the hindgut, the MTs could also be hormonally regulated to inhibit diuresis or counter the actions of diuretic hormones. It was previously assumed that diuresis was terminated by simply reducing the concentration of diuretic hormones circulating in the haemolymph (Maddrell, 1964). Later, research studies established that this termination of diuresis (at least in a subset of insects) is also a result of the release of another peptide, CAPA, acting as an anti-diuretic hormone to decrease urine production (Paluzzi and Orchard, 2006; Quinlan and O'Donnell, 1998; Quinlan et al., 1997; Paluzzi et al., 2008). Genes encoding for the CAPA peptides are named *capability*, and the first such gene was identified in *D. melanogaster* (Kean et al., 2002). The 151 amino acid *D. melanogaster* CAPA precursor is cleaved by prohormone convertases at arginine-monobasic (R) and/or arginine/lysine-dibasic (RR, KR) sites giving rise to the bioactive CAPA peptides (Predel and Wegener, 2006). The cleavage sequence pattern has been seen to be evolutionarily conserved within most insect species, including *A. aegypti* (Predel and Wegener, 2006). The first two peptides, CAPA-1 (or CAPA-PVK-1) and CAPA-2 (or CAPA-PVK-2), characteristically contain the consensus carboxyl terminal sequence, FPRV-NH<sub>2</sub>. CAPA peptides have been shown to exhibit species-specific and dose-dependent effects, displaying both diuretic and anti-diuretic activity (Ionescu and Donini, 2012; MacMillan et al., 2018; Pollock et al., 2004; Terhzaz et al., 2012) (Figure 1-4).

### *Ion transport peptide (ITP) and ITP-like (ITP-L)*

Once the secreted fluid passes from the MTs into the hindgut, anti-diuretic hormones can act upon the hindgut to promote water reabsorption, amongst other processes (Phillips, 1981). In the desert locust *S. gregaria*, anti-diuretic hormones play an important role in maintaining reabsorptive processes of the hindgut. This regulation is achieved through alteration of the primary fluid entering the hindgut, changing the rate of water and ion transport across the epithelium (Phillips, 1981). The first identified anti-diuretic hormone shown to act on the locust hindgut was the ion transport peptide (ITP) (Phillips and Audsley, 1995), which belongs to the family of crustacean hyperglycemic hormones (CHH) (Nagai et al., 2014). Meredith *et al.* identified the complete amino acid sequence of *SchgrITP*, with a 72-residue sequence comprising the mature peptide and six cysteine residues, proposed to participate in disulphide bridge formation (Meredith et al., 1996). An ITP-long or ITP-like (ITP-L) isoform was also discovered, which contained a 121 base pair insert at amino acid position 40 of ITP, with the resultant mature ITP-L peptide only 4 amino acids longer than ITP (Meredith et al., 1996). The locust homolog of ITP promotes water reabsorption by acting on the electrogenic Cl<sup>-</sup> pump, exerting its effect through a cAMP pathway to increase Na<sup>+</sup>, K<sup>+</sup>, and Cl<sup>-</sup> reabsorption (Audsley et al., 2013; Phillips et al., 1996). In a recent study in *D. melanogaster*, transcript levels of ITP were shown to increase under desiccation stress believed to protect the fly from water loss by reducing excretion rate (through the hindgut), increasing thirst, and promoting ingestion of water *in lieu* of food, consequently establishing a role as an anti-diuretic hormone (Gáliková et al., 2018). However, to date, the functions of *A. aegypti* ITP and/or ITP-L have not been investigated so far.

#### 1.4 Research aims and objectives

Insects are faced with various osmoregulatory challenges during feeding and when transitioning between habitats or facing challenges related to their environmental conditions, which causes disruption of haemolymph homeostasis. Terrestrial insects have evolved a specialized excretory system to help them mitigate these challenges related to feeding and desiccating environmental conditions (Beyenbach, 2003a). Haematophagous insects such as the *A. aegypti* mosquito ingest large bloodmeals, whereby diuretic hormones are released to act on the MTs to drive secretion of copious amounts of urine to maintain osmotic balance. Multiple studies have examined the effects of diuretic factors on *Aedes* mosquitoes (Clark and Bradley, 1998; Coast et al., 2005; Ionescu and Donini, 2012; Lu et al., 2011; Veenstra, 1988), with only limited attention on anti-diuretic factors, such as CAPA peptides (Ionescu and Donini, 2012; Paluzzi and Orchard, 2006; Paluzzi et al., 2012). Investigating hormonal regulation of anti-diuresis is important in terrestrial insects, since this is the predominant physiological state, interrupted only briefly during post-prandial diuresis in insects engorging on a liquid meal, whether plant nectar or vertebrate blood. Although extensive studies have examined the process of hydromineral balance in terrestrial insects, many factors are needed for the precise control of haemolymph homeostasis in the face of varied ionic and osmotic challenges. Many terrestrial insects are recognized as disease vectors or agricultural pests, and therefore, further understanding this meticulous regulation can aid in lessening the burden of these insects through development of novel pest management strategies that are based on or that can interfere with endogenous hormones regulating hydromineral balance.

#### **1.4.1 Aim 1: Elucidate the role and signalling cascade of the CAPA neuropeptide in the MTs of the female *A. aegypti* mosquito**

While extensive studies have investigated the effects of CAPA neuropeptides on diuresis, the role of *Aedae*CAPA-1 in adult *A. aegypti* remains unclear. A previous study demonstrated an anti-diuretic role for CAPA neuropeptides in larval *A. aegypti*, with low concentrations inhibiting the diuretic response of 5HT-stimulated secretion (Ionescu and Donini, 2012). Low levels of CAPA were proposed to activate the NOS/PKG pathway to inhibit stimulated secretion (Ionescu and Donini, 2012), which is further corroborated with established immunoreactivity and expression of NOS in female MTs (Pollock et al., 2004). These findings provide a framework for the first anti-diuretic signalling system established in the *Aedes* mosquito, which provides further insight into the complex neuropeptidergic regulation of the MTs. Based on these findings, and previous established anti-diuretic roles of CAPA neuropeptides in other insects (Paluzzi and Orchard, 2006), it was hypothesized that in *A. aegypti* MTs, CAPA acts as an anti-diuretic hormone, activating the NOS/cGMP/PKG pathway to inhibit diuretic-stimulated secretion, and ultimately reduce excessive water loss in the mosquito. The objectives of this research aim were four-fold:

- (1) Explore the role of CAPA neuropeptides against extensively studied diuretics including DH<sub>31</sub>, 5HT, DH<sub>44</sub>, and kinin in the female MTs;
- (2) Characterize the cellular localization of the CAPA receptor (CAPA-R), and identify cellular targets involved in the signalling cascade of CAPA-mediated inhibition;
- (3) Identify the role and regulation of the V-type H<sup>+</sup>-ATPase in CAPA-mediated inhibition of fluid secretion;

- (4) Determine hormonal titres of diuretic (specifically DH<sub>31</sub>) and anti-diuretic (specifically CAPA) neuropeptides in the haemolymph of females prior to and post-blood feeding to elucidate the timing of release of diuretic and anti-diuretic peptides.

#### **1.4.2 Aim 2: Characterize the expression and immunolocalization, and examine a potential role of ITP and ITP-L neuropeptides in the *A. aegypti* mosquito**

Several critical processes in an insect's life require the actions of a coordinated endocrine control system through the release of various neuropeptides (Raabe, 1989). In insects, neuropeptides play a fundamental role in orchestrating various physiological processes including development, osmoregulation, reproduction, and behaviour and feeding (Nässel and Zandawala, 2019). The insect ion transport peptide (ITP) and its alternatively spliced variant, ITP-like or ITP-long (ITP-L) belong to the crustacean hyperglycemic hormone (CHH) family of peptides and are widely conserved among insect species (Dai et al., 2007). While limited information about ITP and ITP-L is available, studies have localized ITP to the central nervous system in insects including larval and adult stages of *M. sexta*, *B. mori*, *D. melanogaster*, and *S. gregaria* (Begum et al., 2009; Dai et al., 2007; Dirksen, 2009; Dirksen et al., 2008) whereas ITP-L has been localized to the central nervous system, specifically the abdominal ganglia and peripheral tissues such as the midgut in *T. castaneum* (Begum et al., 2009) and MTs and hindgut in *S. gregaria* (Meredith et al., 1996). Suggested functions of both peptides has been linked to: anti-diuretic and drinking-promoting hormones in *D. melanogaster* and *S. gregaria* (Gáliková et al., 2018; Phillips and Audsley, 1995), regulating ovarian maturation in *T. castaneum* (Begum et al., 2009), ecdysis in *M. sexta* (Drexler et al., 2007), and clock neuron modulation in *D. melanogaster* (Johard et al., 2009). However, nothing is known on the expression pattern, tissue distribution and localization, or putative physiological roles of ITP and/or ITP-L in *A. aegypti*.

Therefore, considering these advancements made with respect to ITP/ITP-L in other insect species, it was hypothesized that *AedaeITP* and *AedaeITP-L* transcript and peptide i) is localized to the central nervous system (brain and ventral nerve cord) of the mosquito and ii) function as pleiotropic factors similar to the CHH family of hormones, specifically as an anti-diuretic hormone. The objective of this research included:

- (1) Investigate the expression, spatial distribution and localization of *AedaeITP* and *AedaeITP-L* at both the transcript and protein level, and elucidate potential physiological functions for these neuropeptides including roles in starvation, iono-regulation, and reproductive behaviour.

## 1.6 References

- Audsley, N., Jensen, D., and Schooley, D. A.** (2013). Signal transduction for *Schistocerca gregaria* ion transport peptide is mediated via both cyclic AMP and cyclic GMP. *Peptides* **41**, 74–80.
- Avila, F. W., Sirot, L. K., LaFlamme, B. A., Rubinstein, C. D., and Wolfner, M. F.** (2011). Insect seminal fluid proteins: identification and function. *Annu. Rev. Entomol.* **56**, 21–40.
- Begum, K., Li, B., Beeman, R. W., and Park, Y.** (2009). Functions of ion transport peptide and ion transport peptide-like in the red flour beetle *Tribolium castaneum*. *Insect Biochem. Mol. Biol.* **39**, 717–725.
- Benveniste, R. J., and Taghert, P. H.** (1999). Cell type-specific regulatory sequences control expression of the *Drosophila* FMRF-NH2 neuropeptide gene. *J. Neurobiol.* **38**, 507–520.
- Beyenbach, K. W.** (2003a). Transport mechanisms of diuresis in Malpighian tubules of insects. *J. Exp. Biol.* **206**, 3845–3856.
- Beyenbach, K. W.** (2003b). Regulation of tight junction permeability with switch-like speed. *Curr. Opin. Nephrol. Hypertens.* **12**, 543–550.
- Beyenbach, K. W.** (2012). A dynamic paracellular pathway serves diuresis in mosquito Malpighian tubules. *Ann. NY Acad. Sci.* **1258**, 166–176.
- Beyenbach, K. W., and Masia, R.** (2002). Membrane conductances of principal cells in Malpighian tubules of *Aedes aegypti*. *J. Insect. Physiol.* **48**, 375–386.
- Beyenbach, K., and Petzel, D.** (1987). Diuresis in mosquitoes: role of a natriuretic factor. *Physiol.* **2**, 171–175.

- Beyenbach, K. W., and Piermarini, P. M.** (2011). Transcellular and paracellular pathways of transepithelial fluid secretion in Malpighian (renal) tubules of the yellow fever mosquito *Aedes aegypti*. *Acta. Physiol.* **202**, 387–407.
- Borgherini, G., Poubeau, P., Staikowsky, F., Lory, M., le Moullec, N., Becquart, J. P., Wengling, C., Michault, A., and Paganin, F.** (2007). Outbreak of chikungunya on reunion island: early clinical and laboratory features in 157 adult patients. *Clin. Infect. Dis.* **44**, 1401–1407.
- Bradley, T. J.** (1987). Physiology of osmoregulation in mosquitoes. *Ann. Rev. Entomol.* **32**, 439–462.
- Bräunig, P.** (1987). The satellite nervous system - an extensive neurohemal network in the locust head. *J. Comp. Physiol.* **160**, 69–77.
- Brown, M. R., and Cao, C.** (2001). Distribution of ovary ecdysteroidogenic hormone I in the nervous system and gut of mosquitoes. *J. Insect Sci.* **1**, 1–11.
- Cabrero, P., Radford, J. C., Broderick, K. E., Costes, L., Veenstra, J. A., Spana, E. P., Davies, S. A., and Dow, J. A. T.** (2002). The Dh gene of *Drosophila melanogaster* encodes a diuretic peptide that acts through cyclic AMP. *J. Exp. Biol.* **205**, 3799–3807.
- Cady, C., and Hagedorn, H. H.** (1999a). The effect of putative diuretic factors on in vivo urine production in the mosquito, *Aedes aegypti*. *J. Insect Physiol.* **45**, 317–325.
- Cady, C., and Hagedorn, H. H.** (1999b). Effects of putative diuretic factors on intracellular second messenger levels in the Malpighian tubules of *Aedes aegypti*. *J. Insect Physiol.* **45**, 327–337

- Calkins, T. L., and Piermarini, P. M.** (2017). A blood meal enhances innexin mRNA expression in the midgut, Malpighian tubules, and ovaries of the yellow fever mosquito *Aedes aegypti*. *Insects* **8**, 124.
- Calkins, T. L., Woods-Acevedo, M. A., Hildebrandt, O., and Piermarini, P. M.** (2015). The molecular and immunochemical expression of innexins in the yellow fever mosquito, *Aedes aegypti*: insights into putative life stage- and tissue-specific functions of gap junctions. *Comp. Biochem. Physiol. B. Biochem. Mol. Biol.* **183**, 11–21.
- Camargo, C., Ahmed-Braimah, Y. H., Amaro, I. A., Harrington, L. C., Wolfner, M. F., and Avila, F. W.** (2020). Mating and blood-feeding induce transcriptome changes in the spermathecae of the yellow fever mosquito *Aedes aegypti*. *Sci. Rep.* **10**, 14899.
- Cauchemez, S., Ledrans, M., Poletto, C., Quenel, P., de Valk, H., Colizza, V., and Boëlle, P. Y.** (2014). Local and regional spread of chikungunya fever in the Americas. *Eurosurveillance* **19**, 20854.
- Chen, L. H., and Wilson, M. E.** (2020). Yellow fever control: current epidemiology and vaccination strategies. *Trop. Dis. Travel. Med. Vaccines.* **6**, 1.
- Chippaux, J. P., and Chippaux, A.** (2018). Yellow fever in Africa and the Americas: a historical and epidemiological perspective. *J. Ven. Anim. Tox. Trop. Dis.* **24**, 20.
- Christophers, S. R.** (1960). *Aedes aegypti* (L), the yellow fever mosquito: its life history, bionomics and structure. London: Cambridge University Press. **739**.
- Clark, T. M., and Bradley, T. J.** (1996). Stimulation of Malpighian tubules from larval *Aedes aegypti* by secretagogues. *J. Insect Physiol.* **42**, 593–602.

- Clark, T. M., and Bradley, T. J.** (1997). Malpighian tubules of larval *Aedes aegypti* are hormonally stimulated by 5-hydroxytryptamine in response to increased salinity. *Arch. Insect Biochem. Physiol.* **34**, 123–141.
- Clark, T. M., and Bradley, T. J.** (1998). Additive effects of 5-HT and diuretic peptide on *Aedes* Malpighian tubule fluid secretion. *Comp. Biochem. Physiol. - A Mol. Integr. Physiol.* **119**, 599–605.
- Clark, T. M., Hayes, T. K., Holman, G. M., and Beyenbach, K. W.** (1998a). The concentration-dependence of CRF-like diuretic peptide: mechanisms of action. *J. Exp. Biol.* **201**, 1753–1762.
- Clark, T. M., Hayes, T. K., and Beyenbach, K. W.** (1998b). Dose-dependent effects of CRF like diuretic peptide on transcellular and paracellular transport pathways. *Am. J. Physiol.* **274**, F834-40.
- Clemons, A., Haugen, M., Flannery, E., Tomchaney, M., Kast, K., Jacowski, C., Le, C., Mori, A., Holland, W. S., Sarro, J., et al.** (2010). *Aedes aegypti*: an emerging model for vector mosquito development. *Cold Spr. Harb. Protoc.* **5**, <https://doi.org/10.1101/pdb.emo141>.
- Coast, G. M., Webster, S. G., Schegg, K. M., Tobe, S. S., and Schooley, D. A.** (2001). The *Drosophila melanogaster* homologue of an insect calcitonin-like diuretic peptide stimulates V-ATPase activity in fruit fly Malpighian tubules. *J. Exp. Biol.* **204**, 1795–1804.
- Coast, G.** (2007). The endocrine control of salt balance in insects. *Gen. Comp. Endocrinol.* **152**, 332–338.
- Coast, G. M.** (2009). Neuroendocrine control of ionic homeostasis in blood-sucking insects. *J. Exp. Biol.* **212**, 378–386.

- Coast, G. M., Orchard, I., Phillips, J. E., and Schooley, D. A.** (2002). Insect diuretic and antidiuretic hormones. *Adv. Insect Phys.* **29**, 279–409.
- Coast, G. M., Garside, C. S., Webster, S. G., Schegg, K. M., and Schooley, D. A.** (2005). Mosquito natriuretic peptide identified as a calcitonin-like diuretic hormone in *Anopheles gambiae* (Giles). *J. Exp. Biol.* **208**, 3281–3291.
- Dai, L., Zitnan, D., and Adams, M. E.** (2007). Strategic expression of ion transport peptide gene products in central and peripheral neurons of insects. *J. Comp. Neurol.* **500**, 353–367.
- Degner, E. C., and Harrington, L. C.** (2016). A mosquito sperm's journey from male ejaculate to egg: mechanisms, molecules, and methods for exploration. *Mol. Reprod. Dev.* **83**, 897–911.
- Dircksen, H.** (2009). Insect ion transport peptides are derived from alternatively spliced genes and differentially expressed in the central and peripheral nervous system. *J. Exp. Biol.* **212**, 401–412.
- Drake, L. L., Rodriguez, S. D., and Hansen, I. A.** (2015). Functional characterization of aquaporins and aquaglyceroporins of the yellow fever mosquito, *Aedes aegypti*. *Sci. Rep.* **5**, 7795.
- Donini, A., Patrick, M. L., Bijelic, G., Christensen, R. J., Ianowski, J. P., Rheault, M. R., and O'Donnell, M. J.** (2006). Secretion of water and ions by Malpighian tubules of larval mosquitoes: effects of diuretic factors, second messengers, and salinity. *Physiol. Biochem. Zool.* **79**, 645–655.
- Drexler, A. L., Harris, C. C., de LaPena, M. G., Asuncion-Uchi, M., Chung, S., Webster, S., and Fuse, M.** (2007). Molecular characterization and cell-specific expression of an ion transport peptide in the tobacco hornworm, *Manduca sexta*. *Cell Tissue Res.* **329**, 391–408.

- Eigenheer, R. A., Nicolson, S. W., Schegg, K. M., Hul, J. J., and Schooley, D. A. (2002).** Identification of a potent antidiuretic factor acting on beetle Malpighian tubules. *Proc. Natl. Acad. Sci. USA* **99**, 84–89.
- Eigenheer, R. A., Wiehart, U. M., Nicolson, S. W., Schoofs, L., Schegg, K. M., Hull, J. J., and Schooley, D. A. (2003).** Isolation, identification and localization of a second beetle antidiuretic peptide. *Peptides* **24**, 27–34.
- Gáliková, M., Dircksen, H., and Nässel, D. R. (2018).** The thirsty fly: ion transport peptide (ITP) is a novel endocrine regulator of water homeostasis in *Drosophila*. *PLoS Genet.* **14**, e1007618.
- Garske, T., van Kerkhove, M. D., Yactayo, S., Ronveaux, O., Lewis, R. F., Staples, J. E., Perea W., Ferguson, N. M., Burke, D., de La Hoz, F., et al. (2014).** Yellow fever in Africa: estimating the burden of disease and impact of mass vaccination from outbreak and serological data. *PLoS Med.* **11**, e1001638.
- Gioino, P., Murray, B. G., and Ianowski, J. P. (2014).** Serotonin triggers cAMP and PKA-mediated intracellular calcium waves in Malpighian tubules of *Rhodnius prolixus*. *Am. J. Physiol. Regul. Integr. Comp. Physiol.* **307**, R828–R836.
- Hanrahan, J. W., and Phillips, J. E. (1983).** Cellular mechanisms and control of KCl absorption in insect hindgut. *J. Exp. Biol.* **106**, 71–89.
- Hartenstein, V. (2006).** The neuroendocrine system of invertebrates: a developmental and evolutionary perspective. *J. Endocrinol.* **190**, 555–570.
- Hasan, S., Jamdar, S. F., Alalowi, M., and al Ageel Al Beaiji, S. M. (2016).** Dengue virus: a global human threat: review of literature. *J. Int. Soc. Prev. Comm. Dent.* **6**, 1–6.

- Hegarty, J. L., Zhang, B., Pannabecker, T. L., Petzel, D. H., Baustian, M. D., and Beyenbach, K. W.** (1991). Dibutyryl cAMP activates bumetanide-sensitive electrolyte transport in Malpighian tubules. *Am. J. Physiol.* **261**, C521–C529.
- Holman, G. M., Cook, B. J., and Nachman, R. J.** (1987). Isolation, primary structure and synthesis of leucokinins VII and VIII: the final members of this new family of cephalomyotropic peptides isolated from head extracts of *Leucophaea maderae*. *Comp. Biochem. Physiol. Comp.* **88**, 31–34.
- Hopkins, C. R.** (1967). The fine-structural changes observed in the rectal papillae of the mosquito *Aedes aegypti*, L. and their relation to the epithelial transport of water and inorganic ions. *J. R. Microsc. Soc.* **86**, 235–252.
- Huesmann, G. R., Cheung, C. C., Loi, P. K., Lee, T. D., Swiderek, K. M., and Tublitz, N. J.** (1995). Amino acid sequence of CAP2b, an insect cardioacceleratory peptide from the tobacco hawkmoth *Manduca sexta*. *FEBS Lett.* **371**, 311–314.
- Ianowski, J. P., and O'Donnell, M. J.** (2004). Basolateral ion transport mechanisms during fluid secretion by *Drosophila* Malpighian tubules: Na<sup>+</sup> recycling, Na<sup>+</sup>:K<sup>+</sup>:2Cl<sup>-</sup> cotransport and Cl<sup>-</sup> conductance. *J. Exp. Biol.* **207**, 2599–2609.
- Ionescu, A., and Donini, A.** (2012). *Aedes* CAPA-PVK-1 displays diuretic and dose dependent antidiuretic potential in the larval mosquito *Aedes aegypti* (Liverpool). *J. Insect Physiol.* **58**, 1299–1306.
- Jagge, C. L., and Pietrantonio, P. v.** (2008). Diuretic hormone 44 receptor in Malpighian tubules of the mosquito *Aedes aegypti*: evidence for transcriptional regulation paralleling urination. *Insect Mol. Biol.* **17**, 413–426.

- Jansen, C. C., and Beebe, N. W.** (2010). The dengue vector *Aedes aegypti*: what comes next. *Microbes Infect.* **12**, 272–279.
- Jentes, E. S., Pomeroy, G., Gershman, M. D., Hill, D. R., Lemarchand, J., Lewis, R. F., Staples, J. E., Tomori, O., Wilder-Smith, A., and Monath, T. P.** (2011). The revised global yellow fever risk map and recommendations for vaccination, 2010: consensus of the informal WHO working group on geographic risk for Yellow fever. *Lancet Infect. Dis.* **11**, 622–632.
- Jing, Q., and Wang, M.** (2019). Dengue epidemiology. *J. Glob. Health* **3**, 37–45.
- Johansson, M. A., Powers, A. M., Pesik, N., Cohen, N. J., and Erin Staples, J.** (2014). Nowcasting the spread of chikungunya virus in the Americas. *PLoS One* **9**, e104915.
- Johard, H. A. D., Yoishii, T., Dirksen, H., Cusumano, P., Rouyer, F., Helfrich-Förster, C., and Nässel, D. R.** (2009). Peptidergic clock neurons in *Drosophila*: ion transport peptide and short neuropeptide F in subsets of dorsal and ventral lateral neurons. *J. Comp. Neurol.* **516**, 59–73.
- Karas, K., Brauer, P., and Petzel, D.** (2005). Actin redistribution in mosquito Malpighian tubules after a blood meal and cyclic AMP stimulation. *J. Insect Physiol.* **51**, 1041–1054.
- Kean, L., Cazenave, W., Costes, L., Broderick, K. E., Graham, S., Pollock, V. P., Davies, S. A., Veenstra, J. A., and Dow, J. A. T.** (2002). Two nitridergic peptides are encoded by the gene capability in *Drosophila melanogaster*. *Am. J. Physiol. Regul. Integr. Comp. Physiol.* **282**, R1297–R1307.
- Klowden, M. J.** (2013). *Physiological Systems in Insects: Third Edition*. Amsterdam: Elsevier.
- Kumar, A., and Bachhawat, A. K.** (2012). Pyroglutamic acid: throwing light on a lightly studied metabolite. *Curr. Sci.* **102**, 288–297.

- Kwon, H., Lu, H. L., Longnecker, M. T., and Pietrantonio, P. V.** (2012). Role in diuresis of a calcitonin receptor (GPCRAL1) expressed in a distal-proximal gradient in renal organs of the mosquito *Aedes aegypti* (L.). *PLoS One* **7**, e50374.
- La Ruche, G., Souarès, Y., Armengaud, A., Peloux-Petiot, F., Delaunay, P., Desprès, P., Lenglet, A., Jourdain, F., Leparç-Goffart, I., Charlet, F., et al.** (2010). First two autochthonous dengue virus infections in metropolitan France. *Eurosurveillance* **15**, 1–5.
- Lange, A. B., Orchard, I., and Michael Barrett, F.** (1989). Changes in haemolymph serotonin levels associated with feeding in the blood-sucking bug, *Rhodnius prolixus*. *J. Insect Physiol.* **35**, 393–399.
- Leparç-Goffart, I., Nougairède, A., Cassadou, S., Prat, C., and de Lamballerie, X.** (2014). Chikungunya in the Americas. *Lancet* **383**, 514.
- Lovejoy, D. A., and Jahan, S.** (2006). Phylogeny of the corticotropin-releasing factor family of peptides in the metazoa. *Gen. Comp. Endocrinol.* **146**, 1–8.
- Lu, H. L., Kersch, C., and Pietrantonio, P. V.** (2011). The kinin receptor is expressed in the Malpighian tubule stellate cells in the mosquito *Aedes aegypti* (L.): a new model needed to explain ion transport? *Insect Biochem. Mol. Biol.* **41**, 135–140.
- MacMillan, H. A., Nazal, B., Wali, S., Yerushalm, G. Y., Misyura, L., Donini, A., and Paluzzi, J. P.** (2018). Anti-diuretic activity of a CAPA neuropeptide can compromise *Drosophila* chill tolerance. *J. Exp. Biol.* **221**, doi: 10.1242/jeb.185884.
- Maddrell, S. H. P.** (1964). Excretion in the blood-sucking bug, *Rhodnius prolixus* Stål: II. the normal course of diuresis and the effect of temperature. *J. Exp. Biol.* **41**, 163–176.
- Mahoney, J. P., and Sunahara, R. K.** (2016). Mechanistic insights into GPCR–G protein interactions. *Curr. Opin. Struct. Biol.* **41**, 247–254.

- Massaro, R. C., Lee, L. W., Patel, A. B., Wu, D. S., Yu, M. J., Scott, B. N., Schooley, D. A., Schegg, K. M., and Beyenbach, K. W.** (2004). The mechanism of action of the antidiuretic peptide Tenmo ADFa in Malpighian tubules of *Aedes aegypti*. *J. Exp. Biol.* **207**, 2877–2888.
- Mercier, J., Doucet, D., and Retnakaran, A.** (2007). Molecular physiology of crustacean and insect neuropeptides. *J. Pestic. Sci.* **32**, 345–359.
- Meredith, J., Ring, M., Macins, A., Marschall, J., Cheng, N. N., Theilmann, D., Brock, H. W., and Phillips, J. E.** (1996). Locust ion transport peptide (ITP): primary structure, cDNA and expression in a baculovirus system. *J. Exp. Biol.* **199**, 1053–1061.
- Messer, A. C., and Brown, M. R.** (1995). Non-linear dynamics of neurochemical modulation of mosquito oviduct and hindgut contractions. *J. Exp. Biol.* **198**, 2325–2336.
- Meuti, M. E., and Short, S. M.** (2019). Physiological and environmental factors affecting the composition of the ejaculate in mosquitoes and other insects. *Insects* **10**, 74.
- Misyura, L., Guardian, E. G., Durant, A. C., and Donini, A.** (2020). A comparison of aquaporin expression in mosquito larvae (*Aedes aegypti*) that develop in hypo-osmotic freshwater and iso-osmotic brackish water. *PLoS One* **15**, e0234892.
- Morens, D. M., and Fauci, A. S.** (2014). Chikungunya at the door — déjà vu all over again? *N. Engl. J. Med.* **371**, 885–887.
- Nachman, R. J., Pietrantonio, P. V., and Coast, G. M.** (2009). Toward the development of novel pest management agents based upon insect kinin neuropeptide analogues. *Ann. N. Y. Acad. Sci.* John Wiley & Sons, Ltd. 251–261.

- Nagai, C., Mabashi-Asazuma, H., Nagasawa, H., and Nagata, S.** (2014). Identification and characterization of receptors for ion transport peptide (ITP) and ITP-like (ITPL) in the silkworm *Bombyx mori*. *J. Biol. Chem.* **289**, 32166–32177.
- Nässel, D. R.** (2002). Neuropeptides in the nervous system of *Drosophila* and other insects: multiple roles as neuromodulators and neurohormones. *Prog. Neurobiol.* **68**, 1–84.
- Nässel, D. R., and Zandawala, M.** (2002). Recent advances in neuropeptide signaling in *Drosophila*, from genes to physiology and behaviour. *Prog. Neurobiol.* **179**.
- O'Connor, K. R., and Beyenbach, K. W.** (2001). Chloride channels in apical membrane patches of stellate cells of Malpighian tubules of *Aedes aegypti*. *J. Exp. Biol.* **204**, 367–378.
- O'Donnell, M. J.** (2010). Mechanisms of excretion and ion transport in invertebrates. *Compr. Physiol.* <https://doi.org/10.1002/cphy.cp130217>.
- Oehler, E., Watrin, L., Larre, P., Leparç-Goffart, I., Lastère, S., Valour, F., Baudouin, L., Mallet, H. P., Musso, D., and Ghawche, F.** (2014). Zika virus infection complicated by guillain-barré syndrome case report, French Polynesia. *Eurosurveillance* **19**, 51–58.
- Oliva, C. F., Damiens, D., Vreysen, M. J. B., Lemperière, G., and Gilles, J.** (2013). Reproductive strategies of *Aedes albopictus* (Diptera: Culicidae) and implications for the sterile insect technique. *PLoS One* **8**, e78884.
- Oliva, C. F., Damiens, D., and Benedict, M. Q.** (2014). Male reproductive biology of *Aedes* mosquitoes. *Acta. Trop.* **132**, S12–S19.
- Orchard, I.** (2006). Serotonin: a coordinator of feeding-related physiological events in the blood-gorging bug, *Rhodnius prolixus*. *Comp. Biochem. Physiol. - A Mol. Integr. Physiol.* **144**, 316–324.
- Orr, T. J., and Zuk, M.** (2012). Sperm storage. *Curr. Biol.* **22**, R8–R10.

- Otu, A., Ebenso, B., Etokidem, A., and Chukwuekezie, O.** (2019). Dengue fever – an update review and implications for Nigeria, and similar countries. *Afr. Health Sci.* **19**, 2000–2007.
- Overend, G., Cabrero, P., Halberg, K. A., Ranford-Cartwright, L. C., Woods, D. J., Davies, S. A., and Dow, J. A. T.** (2015). A comprehensive transcriptomic view of renal function in the malaria vector, *Anopheles gambiae*. *Insect Biochem. Mol. Biol.* **67**, 47–58.
- Paluzzi, J. P.** (2012). Anti-diuretic factors in insects: the role of CAPA peptides. *Gen. Comp. Endocrinol.* **176**, 300–308.
- Paluzzi, J. P., and Orchard, I.** (2006). Distribution, activity and evidence for the release of an anti-diuretic peptide in the kissing bug *Rhodnius prolixus*. *J. Exp. Biol.* **209**, 907–915.
- Paluzzi, J. P., Naikhwah, W., and O'Donnell, M. J.** (2012). Natriuresis and diuretic hormone synergism in *R. prolixus* upper Malpighian tubules is inhibited by the anti-diuretic hormone, *RhoprCAPA-α2*. *J. Insect Physiol.* **58**, 534–542.
- Paluzzi, J. P., Bhatt, G., Wang, C. H. J., Zandawala, M., Lange, A. B., and Orchard, I.** (2015). Identification, functional characterization and pharmacological profile of a serotonin type-2b receptor in the medically important insect, *Rhodnius prolixus*. *Front. Neurosci.* **9**, 175.
- Patrick, M. L., Aimanova, K., Sanders, H. R., and Gill, S. S.** (2006). P-type Na<sup>+</sup>/K<sup>+</sup>-ATPase and V-type H<sup>+</sup>-ATPase expression patterns in the osmoregulatory organs of larval and adult mosquito *Aedes aegypti*. *J. Exp. Biol.* **209**, 4638–4651.
- Petrova, A., and Moffett, D. F.** (2016). Comprehensive immunolocalization studies of a putative serotonin receptor from the alimentary canal of *Aedes aegypti* larvae suggest its diverse roles in digestion and homeostasis. *PLoS One* **11**, e0146587.

- Petzel, D. H., Hagedorn, H. H., and Beyenbach, K. W.** (1985). Preliminary isolation of mosquito natriuretic factor. *Am. J. Physiol. Regul. Integr. Comp. Physiol.* **249**, R379–R386.
- Petzel, D. H., Pirotte, P. T., and van Kerkhove, E.** (1999). Intracellular and luminal pH measurements of Malpighian tubules of the mosquito *Aedes aegypti*: the effects of cAMP. *J. Insect Physiol.* **45**, 973–982.
- Phillips, J.** (1981). Comparative physiology of insect renal function. *Am. J. Physiol.* **241**, R24157.
- Phillips, J. E., and Audsley, N.** (1995). Neuropeptide control of ion and fluid transport across locust hindgut. *Integr. Comp. Biol.* **35**, 503–514.
- Phillips, J. E., Audsley, N., Lechleitner, R., Thomson, B., Meredith, J., and Chamberlin, M.** (1988). Some major transport mechanisms of insect absorptive epithelia. *Comp. Biochem. Physiol. A. Physiol.* **90**, 643–650.
- Phillips, J. E., Thomson, R. B., Audsley, N., Peach, J. L., and Stagg, A. P.** (1994). Mechanisms of acid-base transport and control in locust excretory system. *Physiol. Zool.* **67**, 95–119.
- Phillips, J. E., Wiens, C., Audsley, N., Jeffs, L., Bilgen, T., and Meredith, J.** (1996). Nature and control of chloride transport in insect absorptive epithelia. *J. Exp. Zool.* 292–299.
- Piermarini, P. M., and Calkins, T. L.** (2014). Evidence for intercellular communication in mosquito renal tubules: a putative role of gap junctions in coordinating and regulating the rapid diuretic effects of neuropeptides. *Gen. Comp. Endocrinol.* **203**, 43–48.
- Pietrantonio, P. V., Jagge, C., and McDowell, C.** (2001). Cloning and expression analysis of a 5HT7-like serotonin receptor cDNA from mosquito *Aedes aegypti* female excretory and respiratory systems. *Insect Mol. Biol.* **10**, 357–369.

- Pipa, R. L.** (1978). Locations and central projections of neurons associated with the retrocerebral neuroendocrine complex of the cockroach *Periplaneta americana* (L.). *Cell Tissue Res.* **193**, 443–455.
- Pollock, V. P., McGettigan, J., Cabrero, P., Maudlin, I. M., Dow, J. A. T., and Davies, S. A.** (2004). Conservation of capa peptide-induced nitric oxide signalling in Diptera. *J. Exp. Biol.* **207**, 4135–4145.
- Predel, R., and Wegener, C.** (2006). Biology of the CAPA peptides in insects. *Cell. Mol. Life Sci.* **63**, 2477–2490.
- Predel, R., Neupert, S., Garczynski, S. F., Crim, J. W., Brown, M. R., Russell, W. K., Kahnt, J., Russell, D. H., and Nachman, R. J.** (2010). Neuropeptidomics of the mosquito *Aedes aegypti*. *J. Proteome Res.* **9**, 2006–2015.
- Quinlan, M. C., and O'Donnell, M. J.** (1998). Anti-diuresis in the blood-feeding insect *Rhodnius prolixus* Stål: antagonistic actions of cAMP and cGMP and the role of organic acid transport. *J. Insect Physiol.* **44**, 561–568.
- Quinlan, M. C., Tublitz, N. J., and O'Donnell, M. J.** (1997). Anti-diuresis in the blood-feeding insect *Rhodnius prolixus* Stål: the peptide CAP(2b) and cyclic GMP inhibit Malpighian tubule fluid secretion. *J. Exp. Biol.* **200**, 2363–2367.
- Raabe, M.** (1989). Synthesis and release sites of neurohormones. *Rec. Dev. Insect Neur.* Boston, MA: Springer US. 1–68.
- Radford, J. C., Davies, S. A., and Dow, J. A. T.** (2002). Systematic G-protein-coupled receptor analysis in *Drosophila melanogaster* identifies a leucokinin receptor with novel roles. *J. Biol. Chem.* **277**, 38810–38817.

- Radford, J. C., Terhzaz, S., Cabrero, P., Davies, S. A., and Dow, J. A. T.** (2004). Functional characterisation of the *Anopheles* leucokinins and their cognate G-protein coupled receptor. *J. Exp. Biol.* **207**, 4573–4586.
- Rezza, G., Nicoletti, L., Angelini, R., Romi, R., Finarelli, A., Panning, M., Cordioli, P., Fortuna, C., Boros, S., Magurano, F., et al.** (2007). Infection with chikungunya virus in Italy: an outbreak in a temperate region. *Lancet* **370**, 1840–1846.
- Rigau-Pérez, J. G., Clark, G. G., Gubler, D. J., Reiter, P., Sanders, E. J., and Vorndam, A. V.** (1998). Dengue and dengue haemorrhagic fever. *Lancet* **352**, 971–977.
- Rocco, D. A., and Paluzzi, J. P.** (2016). Functional role of the heterodimeric glycoprotein hormone, GPA2/GPB5, and its receptor, LGR1: an invertebrate perspective. *Gen. Comp. Endocrinol.* **234**, 20–27.
- Rocco, D. A., Kim, D. H., and Paluzzi, J. P.** (2017). Immunohistochemical mapping and transcript expression of the GPA2/GPB5 receptor in tissues of the adult mosquito, *Aedes aegypti*. *Cell Tissue Res.* **369**, 313–330.
- Rocco, D. A., Garcia, A. S. G., Scudeler, E. L., dos Santos, D. C., Nóbrega, R. H. and Paluzzi, J. P.** (2019). Glycoprotein hormone receptor knockdown leads to reduced reproductive success in male *Aedes aegypti*. *Front. Physiol.* **10**, 266.
- Paluzzi, J. P., Russell, W. K., Nachman, R. J., and Orchard, I.** (2008). Isolation, cloning, and expression mapping of a gene encoding an antidiuretic hormone and other CAPA-related peptides in the disease vector, *Rhodnius prolixus*. *Endocrin.* **9**, 4638–4646.
- Piermarini, P. M., Dunemann, S. M., Rouhier, M. F., Calkins, T. L., Raphemot, R., Denton, J. S., Hine, R. M., and Beyenbach, K. W.** (2015). Localization and role of inward rectifier

- K<sup>+</sup> channels in Malpighian tubules of the yellow fever mosquito *Aedes aegypti*. *Insect Biochem. Mol. Biol.* **67**, 59–73.
- Piermarini, P. M., Hine, R. M., Schepel, M., Miyauchi, J., and Beyenbach, K. W.** (2011). Role of an apical K, Cl cotransporter in urine formation by renal tubules of the yellow fever mosquito (*Aedes aegypti*). *Am. J. Physiol. Regul. Integr. Comp. Physiol.* **5**, R1318–R1337.
- Piermarini, P. M., Rouhier, M. F., Schepel, M., Kosse, C., and Beyenbach K. W.** (2012). Cloning and functional characterization of inward-rectifying potassium (Kir) channels from Malpighian tubules of the mosquito *Aedes aegypti*. *Insect Biochem. Mol. Biol.* **1**, 75–90.
- Powell, J. R., Gloria-Soria, A., and Kotsakiozi, P.** (2018). Recent history of *Aedes aegypti*: vector genomics and epidemiology records. *Bioscience* **11**, 854–860.
- Powell, J. R., and Tabachnick, W.** (2013). History of domestication and spread of *Aedes aegypti* – a review. *Mem. Inst. Oswaldo Cruz.* **108**, 11-17.
- Roy, C. J., Adams, A. P., Wang, E., Plante, K., Gorchakov, R., Seymour, R. L., Vinet-Oliphant, H., Weaver, S. C.** (2014). Chikungunya vaccine candidate is highly attenuated and protects nonhuman primates against telemetrically monitored disease following a single dose. *J. Infect. Dis.* **209**, 1891–1899.
- Scharrer, B.** (1987). Insects as models in neuroendocrine research. *Annu. Rev. Entomol.* **32**, 1–16.
- Schepel, S. A., Fox, A. J., Miyauchi, J. T., Sou, T., Yang, J. D., Lau, K., Blum, A. W., Nicholson, L. K., Tiburcy, F., Nachman, R. J., et al.** (2010). The single kinin receptor signals to separate and independent physiological pathways in Malpighian tubules of the yellow fever mosquito. *Am. J. Physiol. Regul. Integr. Comp. Physiol.* **299**, R612–R622.

- Schoofs, L., De Loof, A., and van Hiel, M. B.** (2017). Neuropeptides as regulators of behavior in insects. *Annu. Rev. Entomol.* **62**, 35–52.
- Shaw, W. R., Teodori, E., Mitchell, S. N., Baldini, F., Gabrieli, P., Rogers, D. W., and Catteruccia, F.** (2014). Mating activates the heme peroxidase HPX15 in the sperm storage organ to ensure fertility in *Anopheles gambiae*. *Proc. Natl. Acad. Sci. USA* **111**, 5854–5859.
- Siegmund, T., and Korge, G.** (2001). Innervation of the ring gland of *Drosophila melanogaster*. *J. Comp. Neurol.* **431**, 481–491.
- Simmons, C. P., Farrar, J. J., van Vinh Chau, N., and Wills, B.** (2012). Current concepts: dengue. *N. Engl. J. Med.* **366**, 1423–1432.
- Strand, M. R., Brown, M. R., and Vogel, K. J.** (2016). Mosquito peptide hormones: diversity, production, and function. *Adv. Insect Physiol.* **55**, 145–188.
- Styer, L. M., Minnick, S. L., Sun, A. K., and Scott, T. W.** (2007). Mortality and reproductive dynamics of *Aedes aegypti* (Diptera: Culicidae) fed human blood. *Vec.-Bor. Zoon. Dis.* **7**, 86–98.
- Taghert, P. H.** (1999). FMRFamide neuropeptides and neuropeptide-associated enzymes in *Drosophila*. *Microsc. Res. Tech.* **45**, 80–95.
- Terhzaz, S., Cabrero, P., Robben, J. H., Radford, J. C., Hudson, B. D., Milligan, G., Dow, J. A. T., and Davies, S. A.** (2012). Mechanism and function of *Drosophila* capa GPCR: a desiccation stress-responsive receptor with functional homology to human neuromedinu receptor. *PLoS One* **7**, e29897.
- Veelaert, D., Schoofs, L., and De Loof, A.** (1998). Peptidergic control of the corpus cardiacum-corpora allata complex of locusts. *Int. Rev. Cytol.* **182**, 249–302.

- Veenstra, J. A.** (1988). Effects of 5-hydroxytryptamine on the Malpighian tubules of *Aedes aegypti*. *J. Insect Physiol.* **34**, 299–304.
- Veenstra, J. A.** (2000). Mono- and dibasic proteolytic cleavage sites in insect neuroendocrine peptide precursors. *Arch. Insect Biochem. Physiol.* **43**, 49–63.
- Veenstra, J. A., Pattillo, J. M., and Petzel, D. H.** (1997). A single cDNA encodes all three *Aedes* leucokinins, which stimulate both fluid secretion by the Malpighian tubules and hindgut contractions. *J. Biol. Chem.* **272**, 10402–10407.
- Weaver, S. C.** (2014). Arrival of chikungunya virus in the new world: prospects for spread and impact on public health. *PLoS Negl. Trop. Dis.* **8**, e2921.
- Weng, X. H., Huss, M., Wiczorek, H., and Beyenbach, K. W.** (2003). The V-type H<sup>+</sup>-ATPase in Malpighian tubules of *Aedes aegypti*: localization and activity. *J. Exp. Biol.* **206**, 2211–2219.
- Weng, X. H., Piermarini, P. M., Yamahiro, A., Yu, M. J., Aneshansley, D. J., and Beyenbach, K. W.** (2008). Gap junctions in Malpighian tubules of *Aedes aegypti*. *J. Exp. Biol.* **211**, 409–422.
- Wiczorek, H., Weerth, S., Schindlbeck, M., and Klein, U.** (1989). A vacuolar-type proton pump in a vesicle fraction enriched with potassium transporting plasma membranes from tobacco hornworm midgut. *J. Biol. Chem.* **264**, 11143–11148.
- Wiczorek, H., Beyenbach, K. W., Huss, M., and Vitavska, O.** (2009). Vacuolar-type proton pumps in insect epithelia. *J. Exp. Biol.* **212**, 1611–1619.
- Zupanc, G. K. H.** (1996). Peptidergic transmission: From morphological correlates to functional implications. *Micron.* **27**, 35–91.

## Chapter Two

### **Anti-diuretic action of a CAPA neuropeptide against a subset of diuretic hormones in the disease vector, *Aedes aegypti***

A modified version of this chapter has been published and reproduced with permission:

Sajadi, F., Curcuruto, C., Al Dhaheri, A., Paluzzi, J.P.V (2018). Anti-diuretic action of a CAPA neuropeptide against a subset of diuretic hormones in the disease vector, *Aedes aegypti*. *Journal of Experimental Biology* 221(7). <https://doi.org/10.1242/jeb.177089>

Curcuruto, C and Al Dhaheri, A. collected larval *A. aegypti* fluid secretion rates, shown as Figure 1-1 (not included in this chapter) in manuscript Sajadi et al., 2018.

## 2.1 Summary

The mosquito *Aedes aegypti* is a vector responsible for transmitting various pathogens to humans, and their prominence as chief vectors of human disease is largely due to their anthropophilic blood feeding behaviour. Larval stage mosquitoes must deal with the potential dilution of their haemolymph in freshwater, whereas the haematophagus *A. aegypti* female faces the challenge of excess ion and water intake after a blood meal. The excretory system, composed of the Malpighian tubules (MTs) and hindgut, is strictly controlled by neuroendocrine factors, responsible for the regulation of diuresis across all developmental stages. The highly studied insect MTs are influenced by a variety of diuretic hormones and, in some insects, anti-diuretic factors. In the present study, we investigated the effects of the *Aedae*CAPA-1 neuropeptide on adult female *A. aegypti* MTs stimulated with various diuretic factors including serotonin (5HT), a corticotropin-related factor (CRF) diuretic peptide (DH<sub>44</sub>), a calcitonin-related diuretic hormone (DH<sub>31</sub>) and a kinin-related diuretic peptide. Overall, our findings establish that *Aedae*CAPA-1 specifically inhibits secretion of adult MTs stimulated by 5HT and DH<sub>31</sub>, whilst having no activity on MTs stimulated by other diuretic factors. Furthermore, although *Aedae*CAPA-1 acts as an anti-diuretic, it does not influence the relative proportions of cations transported by adult MTs, thus maintaining the kaliuretic activity of 5HT and natriuretic activity of DH<sub>31</sub>. In addition, we tested the effects of the second messenger cGMP in adult MTs. We established that cGMP has similar effects to *Aedae*CAPA-1, strongly inhibiting 5HT- and DH<sub>31</sub>-stimulated fluid secretion, but with only minor effects on CRF-stimulated diuresis. Interestingly, although *Aedae*CAPA-1 has no inhibitory activity on kinin-stimulated fluid secretion, cGMP strongly inhibited fluid secretion by this diuretic hormone, which targets stellate cells specifically. Collectively, these results support that *Aedae*CAPA-1 inhibits select diuretic factors

acting on the principal cells and this probably involves cGMP as a second messenger. Kinin-stimulated diuresis, which targets stellate cells, is also inhibited by cGMP, suggesting that another anti-diuretic factor in addition to *Aedae*CAPA-1 may exist and utilize cGMP as a second messenger.

## 2.2 Introduction

The mosquito *Aedes aegypti* functions as the primary vector for several viruses; most notably dengue, chikungunya, yellow-fever, and Zika (Laurence et al., 2005; Murray et al., 2013; Ng and Ojcius, 2009). Like other blood feeding arthropods, female *A. aegypti* transmit these pathogenic species during the secretion of saliva into the host during a bloodmeal (Ribeiro et al., 1984).

Adult *A. aegypti* exclusively oviposit in freshwater, which is hypotonic to larval haemolymph. Thus, larvae are susceptible to the continual gain of freshwater from drinking and by osmotic flux of fluid from the external environment across the body surface (Bradley, 1987; Patrick et al., 2006). Concurrently, larvae are subject to the constant diffusional loss of predominant haemolymph ions to the external media (Patrick et al., 2006). As such, larvae possess distinct osmoregulatory mechanisms, allowing them to achieve and maintain ionic homeostasis by excreting a dilute urine and maximizing the active uptake of ions into the haemolymph from the external media (Bradley, 1987).

Post-eclosion, adult *A. aegypti* are subject to disparate osmoregulatory challenges. Under non-feeding circumstances, *A. aegypti* must conserve haemolymph volume to prevent desiccation and the concentration of their haemolymph ions (Patrick et al., 2006). Initially upon blood feeding by adult females, there is a significant water and NaCl load from the blood plasma, and a subsequent  $K^+$  load during erythrocyte lysis (Coast, 2009). Therefore, a carefully controlled mechanism must exist which can selectively regulate the absorption and secretion of ions to maintain homeostasis following a bloodmeal.

A number of specialized organs are responsible for ionoregulation and osmoregulation in *A. aegypti*, including the midgut, Malpighian tubules (MTs), and the hindgut, as well as the anal

papillae in larval stages (Bradley, 1987). The five functionally and structurally homologous MTs are responsible for the formation of primary urine (Beyenbach et al., 1993). The MTs are comprised of two cell types that form a simple epithelium; large principal cells, and thin stellate cells (Beyenbach et al., 2010). The principal cells facilitate active transport of  $\text{Na}^+$  and  $\text{K}^+$  into the lumen of the MTs from the haemolymph, while stellate cells aid in transepithelial secretion of  $\text{Cl}^-$  (O'Connor and Beyenbach, 2001). The active driving force responsible for ion transport is the V-type  $\text{H}^+$ -ATPase (proton pump) (Wieczorek et al., 1989; Wieczorek et al., 2009), which is localized on the brush-border membrane of principal cells (Weng et al., 2003). The movement of protons into the MT lumen creates a proton gradient, which energizes exchange of alkali cations (via  $\text{Na}^+/\text{H}^+$  and/or  $\text{K}^+/\text{H}^+$  antiporters) across the apical membrane (Wieczorek, 1992; Wieczorek et al., 1991). A basolaterally localized bumetanide-sensitive  $\text{Na}^+:\text{K}^+:2\text{Cl}^-$  cotransporter has been identified in the MTs of *A. aegypti*, transporting  $\text{Na}^+$ ,  $\text{K}^+$ , and  $\text{Cl}^-$  from the haemolymph into the principal cells (Hegarty et al., 1991). Transport of  $\text{KCl}$  and  $\text{NaCl}$  provide the osmotic gradient that drives water movement into the tubules via aquaporins (Klowden, 2013). The fluid secreted by the MTs is received by the hindgut and is further modified via the selective reabsorption of solutes and water (Larsen et al., 2014).

The MTs do not receive nervous system innervation; thus, regulation of epithelial ion transport and fluid secretion occurs via circulating messengers in the haemolymph (Beyenbach, 2003). Diuretic hormone regulation of the MTs has been extensively studied in *A. aegypti*. One of the factors known to influence fluid secretion by MTs is the biogenic amine serotonin (5-hydroxytryptamine, 5HT). In larval *A. aegypti*, 5HT titre in the haemolymph increases in response to salinity and this hormone increases fluid and ion secretion by MTs (Clark and Bradley, 1996; Clark and Bradley, 1997). In adult *A. aegypti*, 5HT is also known to increase ion

and fluid secretion rates, albeit without eliciting pronounced natriuretic activity (Veenstra, 1988). Upon bloodmeal engorgement by adult females, mosquito natriuretic peptide (MNP) is released into the haemolymph and stimulates diuresis and natriuresis (Beyenbach and Petzel, 1987; Petzel et al., 1986; Wheelock et al., 1988). MNP acts via cAMP to stimulate the secretion of Na<sup>+</sup>-rich primary urine by the MTs (Beyenbach, 2003; Petzel et al., 1987), which has been identified as a calcitonin-like diuretic hormone 31 (DH<sub>31</sub>) in both mosquitoes *Anopheles gambiae* and *A. aegypti* (Coast et al., 2005). In comparison, the CRF-related diuretic peptide (DH<sub>44</sub>) stimulates nonspecific transport of both cations (Coast et al., 2005), and increases levels of cAMP in MTs (Cady and Hagedorn, 1999). Kinin-like diuretic peptides have been shown to influence the activity of insect MTs by increasing fluid secretion and Cl<sup>-</sup> conductance into the lumen of the MTs through signalling via inositol 1,4,5-triphosphate and elevating intracellular calcium levels through mobilization of IP<sub>3</sub>-sensitive calcium stores (Cady and Hagedorn, 1999; O'Donnell et al., 1996). Members of the CAPA peptide family are also known to elicit control over the MTs, whereby either diuretic or anti-diuretic actions have been established in different insects (Ionescu and Donini, 2012; Paluzzi et al., 2008; Pollock et al., 2004; Quinlan et al., 1997). CAPA peptides, which are also referred to as periviscerokinins, are linked to the neurohaemal system of the abdominal ganglia (Predel and Wegener, 2006), and evidence from the Triatomine bug *Rhodnius prolixus* indicates these peptides are released as hormones to coordinate the cessation of diuresis in this insect (Paluzzi and Orchard, 2006).

Although there has been extensive research investigating the neuroendocrine control of *A. aegypti* MTs, most studies have focused on diuretic hormones (Cady and Hagedorn, 1999; Clark and Bradley, 1996; Clark et al., 1998b; Clark et al., 1998a; Coast et al., 2005; Donini et al., 2006; Veenstra, 1988). Limited studies examining anti-diuretic control of the mosquito MTs include an

exogenous anti-diuretic factor from the beetle, *Tenebrio molitor*, which was shown to decrease fluid secretion by adult MTs through the intracellular second messenger cGMP (Massaro et al., 2004). In addition, low concentrations of an endogenous CAPA peptide were shown to inhibit fluid secretion also through a cGMP signalling mechanism, although supraphysiological concentrations of either CAPA or cGMP showed diuretic activity (Ionescu and Donini, 2012).

In the current study, we investigated the anti-diuretic activity of *Aedae*CAPA-1 on MTs from adult female *A. aegypti* stimulated by different diuretic factors. Specifically, we utilized concentrations of *Aedae*CAPA-1 similar to those that were previously found to have anti-diuretic activity on unstimulated MTs in larval *A. aegypti* (Ionescu and Donini, 2012). We examined the activity of *Aedae*CAPA-1 on transepithelial fluid transport in adult females and determined the concentration and transport rate of the primary cations ( $\text{Na}^+$  and  $\text{K}^+$ ) present in the secreted fluid of MTs isolated from adult female *A. aegypti*. Our results reveal that CAPA peptides are selectively anti-diuretic against a subset of diuretic factors in adult stage mosquitoes, but do not perturb the proportions of ions transported under the stimulation of each specific diuretic hormone. The proposed second messenger, cGMP, mimics the selective anti-diuretic actions of *Aedae*CAPA-1 against diuretic hormones known to target the principal cells. Furthermore, cGMP is also capable of inhibiting kinin-stimulated diuresis, which is intriguing as this diuretic hormone targets the stellate cells. These findings indicate that both principal and stellate cell-mediated diuresis is reduced through signalling mechanisms involving cGMP, but only the CAPA anti-diuretic hormone acting on principal cells is currently known while the stellate-cell directed anti-diuretic hormone remains elusive.

## 2.3 Materials and Methods

### Insect rearing

Eggs of *Aedes aegypti* (Liverpool strain) were collected from an established laboratory colony maintained in the Department of Biology at York University, Toronto, Ontario and hatched in double-distilled water in an environmental chamber (26°C, 12h:12h light:dark cycle). Larvae were fed daily with several drops of a solution comprised of 2% (w/v) Argentine beef liver powder (NOW foods, Bloomingdale, IL, USA) and 2% (w/v) brewer's yeast. Adult female *A. aegypti* were routinely fed on sheep's blood in Alsevers solution (Cedarlane Laboratories, Burlington, ON, Canada) using an artificial feeding system described previously (Rocco et al., 2017). All adults were fed 10% sucrose solution *ad libitum*.

### Neurochemicals and peptide dosages

Serotonin hydrochloride (5-hydroxytryptamine, 5HT) was purchased from a local supplier (Sigma-Aldrich, Oakville, ON, Canada), dissolved in ultrapure water to make a 1 mmol l<sup>-1</sup> stock solution. *Aedae*CAPA-1 (GPTVGLFAFPRV-NH<sub>2</sub>) was commercially synthesized (Genscript, Piscataway, NJ, USA) at a purity of >98% and 1 mmol l<sup>-1</sup> stock solutions were prepared in cell culture-grade ultrapure water (Wisent Corporation, St. Bruno, QC, Canada). We utilized peptide orthologs from other species for the three families of mosquito diuretic peptides tested: *Drosophila melanogaster* calcitonin-related peptide (*Drome*DH<sub>31</sub>) was used *in lieu* of mosquito natriuretic peptide (MNP), and was a generous gift from Michael J. O'Donnell (McMaster University, Hamilton, ON, Canada); *Rhodnius prolixus* corticotropin releasing factor-related (CRF-related, DH<sub>44</sub>) diuretic peptide (*Rhopr*DH<sub>44</sub>) was used *in lieu* of the mosquito CRF-related diuretic peptide, and was a generous gift from Ian Orchard (University of Toronto,

Mississauga, ON, Canada); *Culex* depolarizing peptide (CDP) was used as a representative mosquito kinin-related peptide (Hayes et al., 1994) and was obtained from a commercial supplier (Bachem, Bubendorf, Switzerland).

Dosages of diuretic hormones were adapted from previous studies and selected based on their half maximal effective concentration ( $EC_{50}$ ) on isolated MTs. Specifically, following preliminary experimentation, a dose of  $10 \text{ nmol l}^{-1}$  *Rhopr*DH<sub>44</sub> in adult tubules was found to produce an intermediate level of stimulation, which is similar to concentrations of a mosquito CRF-related diuretic peptide previously used on *A. aegypti* MTs (Clark et al., 1998b). A dose of  $25 \text{ nmol l}^{-1}$  *Drome*DH<sub>31</sub> peptide was used based on the dose-response determinations for *A. gambiae* MNP (Coast et al., 2005). A  $50 \text{ nmol l}^{-1}$  dosage of CDP was selected as an intermediate titre, as previous research determined a kinin-related peptide with an  $EC_{50}$  of  $15 \text{ nmol l}^{-1}$  in stimulating fluid secretion by isolated *A. aegypti* MTs (Schepel et al., 2010). Following preliminary examination and referring to previous investigations on the dose-dependency of 5HT secretory activity on *A. aegypti* MTs (Clark and Bradley, 1998; Veenstra, 1988), an intermediate dose of  $100 \text{ nmol l}^{-1}$  5HT was selected to stimulate fluid secretion by the MTs. Finally, a concentration of  $1 \text{ fmol l}^{-1}$  ( $10^{-15} \text{ mol l}^{-1}$ ) was selected for *Aedae*CAPA-1 based on a dose-response curve of *Aedae*CAPA-1 against DH<sub>31</sub>-stimulated tubules (Figure 2-S1A) and was previously found to have significant anti-diuretic activity in larval *A. aegypti* (Ionescu and Donini, 2012). Similar dose-response studies were conducted to test activity of *Aedae*CAPA-2 and *Aedes* pyrokinin-1 (*Aedae*PK-1) against DH<sub>31</sub>-stimulated tubules (Figure 2-S1B,C).

### MT fluid secretion assay

In order to determine secretion rates, a modified Ramsay secretion assay (Ramsay, 1954) was performed on isolated MTs in 3–6-day old non-blood fed female adults. Dissections were performed under physiological saline adapted from Petzel et al., (1987) that contained (in mmol l<sup>-1</sup>): 150 NaCl, 25 N-2-hydroxyethylpiperazine-N'-2-ethanesulfuronic acid (HEPES), 3.4 KCl, 7.5 NaOH, 1.8 NaHCO<sub>3</sub>, 1 MgSO<sub>4</sub>, 1.7 CaCl<sub>2</sub> and 5 glucose, and titrated to pH 7.1. Immediately before use, the physiological saline was diluted 1:1 with Schneider's Insect Medium (Sigma-Aldrich). MTs were transferred to a Sylgard-lined petri dish containing 20 µL saline bathing droplets submerged beneath hydrated mineral oil to prevent evaporation. The proximal ends of the MTs were removed from the bathing saline and suspended in the mineral oil by looping around a Minutien pin to allow for secretion measurements.

In the interest of determining whether *Aedae*CAPA-1 antagonizes the effects of the known diuretic factors (5HT, *Rhopr*DH<sub>44</sub>, CDP, and *Drome*DH<sub>31</sub>), secretion rates were monitored over 60 min treatments. Following the incubation, the size of the secreted droplets was measured via the use of a microscope eyepiece micrometer and fluid secretion rates (FSR) were calculated as described previously (Donini et al., 2008). For experimental treatments, the MTs were either treated with the diuretic factor alone or in combination with *Aedae*CAPA-1 at a final concentration of 1 fmol l<sup>-1</sup>. Basal (unstimulated) secretion rates were measured for 120 mins in adult MTs treated with saline to determine control rates of secretion and confirm the activity of the diuretic hormones used in this study.

Dose-response activity of a membrane-permeable analog of cyclic guanosine monophosphate (Sigma-Aldrich Canada Ltd, Oakville, ON, Canada), 8-bromo-cGMP (henceforth referred to as cGMP), was determined on basal fluid secretion rates of adult MTs

using concentrations ranging from 10 nmol l<sup>-1</sup> to 10 μmol l<sup>-1</sup>. Maximal inhibition of MT fluid secretion by cGMP was observed at 100 nmol l<sup>-1</sup>, and consequently, this concentration of cGMP was used against diuretic hormone-stimulated MTs from adult female *A. aegypti*.

### **Ion-selective microelectrodes (ISME)**

The concentrations of Na<sup>+</sup> and K<sup>+</sup> were measured using ion-selective microelectrodes (ISME). Microelectrodes were pulled from glass capillaries (TW-150-4, World Precision Instruments, Sarasota, FL, USA) using a Sutter P-97 Flaming Brown pipette puller (Sutter Instruments, San Raffael, CA, USA). Next, the microelectrodes were silanized with *N,N*-dimethyltrimethylsilylamine (Fluka, Buchs, Switzerland). The Na<sup>+</sup> microelectrode was backfilled with 100 mmol l<sup>-1</sup> NaCl and the K<sup>+</sup> microelectrode with 100 mmol l<sup>-1</sup> KCl. The tip of the electrode was filled with Na<sup>+</sup> ionophore (Sodium ionophore II cocktail A; Fluka, Buchs, Switzerland) for Na<sup>+</sup> measurements and K<sup>+</sup> ionophore (potassium ionophore I cocktail B; Fluka) for K<sup>+</sup> measurements. The electrode tips were then coated with ~3.5% (w/v) polyvinyl chloride (PVC) dissolved in tetrahydrofuran, to avoid displacement of ionophore cocktail when submerged in paraffin oil (Rheault and O'Donnell, 2004). Reference electrodes (1B100F-4, World Precision Instruments, Sarasota, FL, USA) were backfilled with 500 mmol l<sup>-1</sup> KCl, which were used for recording both Na<sup>+</sup> and K<sup>+</sup> concentrations.

### **Measurement of [Na<sup>+</sup>] and [K<sup>+</sup>] in secreted droplets**

Microelectrodes and reference electrodes were connected to an electrometer through silver chloride wires where voltage signals were recorded through a data acquisition system (Picolog for Windows, version: 5.25.3). Both the reference electrode and ISME were placed into

the secreted droplet under the paraffin oil and Na<sup>+</sup> and K<sup>+</sup> concentrations were recorded as the voltage difference in comparison to the standard calibrations. Na<sup>+</sup> microelectrodes were calibrated in the standards, 200 mmol l<sup>-1</sup> NaCl and 20 mmol l<sup>-1</sup> NaCl + 180 mmol l<sup>-1</sup> LiCl, and K<sup>+</sup> microelectrodes were calibrated in the standards, 150 mmol l<sup>-1</sup> KCl + 50 mmol l<sup>-1</sup> LiCl and 15 mmol l<sup>-1</sup> KCl + 185 mmol l<sup>-1</sup> LiCl, as described previously (Donini et al., 2008). The concentration of the cations in the secreted fluid ([ion]<sub>sf</sub>) were calculated using the equation described previously (Donini et al., 2008; Paluzzi et al., 2012):

$$[\text{ion}]_{\text{sf}} = [\text{C}] \times 10^{\Delta V/m}$$

where [C] is the concentration in mmol l<sup>-1</sup> of the calibration solution used to calibrate the ISME,  $\Delta V$  is the difference between the voltage recorded from the secreted droplet and the voltage of the same calibration solution, and  $m$  is the voltage difference between the two standard calibrations, which is also the slope. The transport rate of Na<sup>+</sup> or K<sup>+</sup> (in pmol min<sup>-1</sup>) was calculated as the product of FSR and [ion]<sub>sf</sub> determined by ISME as previously described (Rheault and O'Donnell, 2004).

### **Statistical analyses**

Data was compiled using Microsoft Excel and transferred to Graphpad Prism software v.7 to create figures and conduct all statistical analyses. Data was analyzed accordingly using either unpaired t-tests or one-way ANOVA and Bonferroni post-test, with differences between treatments considered significant if  $p < 0.05$ .

## 2.4 Results

### Effect of *Aedae*CAPA-1 on transepithelial fluid and cation secretion in adult MTs

Application of 100 nmol l<sup>-1</sup> 5HT to adult female MTs resulted in an approximately 6-fold significant increase in fluid secretion compared with unstimulated MTs (Figure 2-1). In contrast, co-application of 1 fmol l<sup>-1</sup> *Aedae*CAPA-1 with 5HT in adult MTs resulted in a reduced fluid secretion rate, not different from that of unstimulated MTs (Figure 2-1A). Moreover, fluid secretion rates of MTs treated with *Aedae*CAPA-1 and 5HT were significantly lower than those treated with 5HT alone. To examine the influence of *Aedae*CAPA-1 on transepithelial cation transport, Na<sup>+</sup> and K<sup>+</sup> concentrations were measured using ISME. MTs treated with 5HT alone did not exhibit any difference in the concentration of Na<sup>+</sup> (Figure 2-1B) or K<sup>+</sup> (Figure 2-1C) in the secreted fluid compared to MTs treated with 5HT together with *Aedae*CAPA-1. However, relative to unstimulated MTs, both treatments led to a significant decrease in Na<sup>+</sup> concentration and, correspondingly, a significant increase in K<sup>+</sup> concentration. The transepithelial transport rate of both Na<sup>+</sup> (Figure 2-1D) and K<sup>+</sup> (Figure 2-1E) was approximately tripled in MTs treated with 5HT alone compared with unstimulated controls. Co-application of *Aedae*CAPA-1 led to a similar K<sup>+</sup> flux which was not different from that of MTs treated with 5HT alone; however, Na<sup>+</sup> transport rate was significantly reduced when *Aedae*CAPA-1 was co-applied compared with the effect of 5HT alone. Overall, *Aedae*CAPA-1 did not influence the relative proportions of cations transported (Figure 2-1F), with 5HT treatment leading to a similar transport ratio to that of unstimulated MTs.

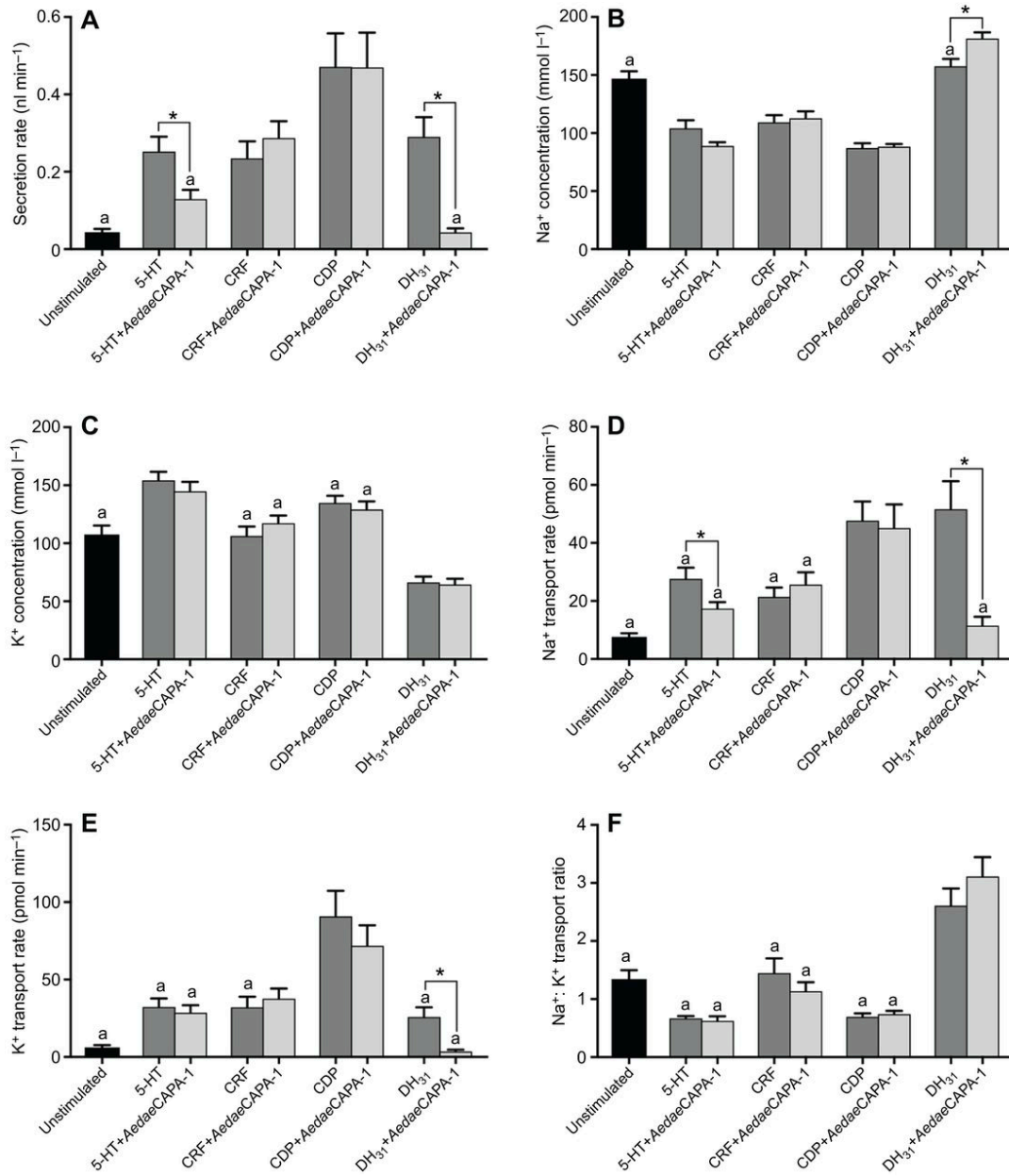


**Figure 2-1. Effect of *AedaeCAPA-1* on *in vitro* fluid secretion rate, cation (Na<sup>+</sup> and K<sup>+</sup>) concentration and transport rate by adult female *A. aegypti* MTs stimulated with a variety of diuretic hormones.** *AedaeCAPA-1* (1 fmol l<sup>-1</sup>) was applied to MTs stimulated with 100 nmol l<sup>-1</sup> 5HT, 10 nmol l<sup>-1</sup> *RhoprDH*<sub>44</sub> (CRF), 50 nmol l<sup>-1</sup> CDP or 25 nmol l<sup>-1</sup> *DromeDH*<sub>31</sub> (DH<sub>31</sub>). (A) The tubule secretion assay was performed over a 60 min incubation period for the diuretic and *AedaeCAPA-1*, and 120 min for unstimulated controls. (B) Na<sup>+</sup> and (C) K<sup>+</sup> concentrations in the secreted fluid were measured using ion-selective microelectrodes (ISME), and the values were used to calculate the cation transport rate and ratio (D–F). Values are presented as means±SEM, n=20–63. Bars that are not significantly different from unstimulated controls are denoted with the same letter, as determined by a one-way ANOVA and Bonferroni post-test. An asterisk denotes statistical significance between two experimental treatments involving a specific diuretic factor alone or in combination with *AedaeCAPA-1*, as determined by an unpaired t-test.

Adult female MTs treated with both 1 fmol l<sup>-1</sup> *Aedae*CAPA-1 and 10 nmol l<sup>-1</sup> *Rhopr*DH<sub>44</sub> did not exhibit changes to fluid secretion compared with MTs receiving *Rhopr*DH<sub>44</sub> alone (Figure 2-1A), with both experimental treatments resulting in secretion rates significantly greater than those of unstimulated controls. Similarly, MTs treated with *Rhopr*DH<sub>44</sub> alone did not have any difference in the concentration of Na<sup>+</sup> (Figure 2-1B) or K<sup>+</sup> (Figure 2-1C) in the secreted fluid compared to MTs treated with *Rhopr*DH<sub>44</sub> together with *Aedae*CAPA-1, although both treatments caused a decrease in the Na<sup>+</sup> concentration relative to unstimulated MTs. As expected, because of the lack of inhibition of *Aedae*CAPA-1 on *Rhopr*DH<sub>44</sub>-stimulated fluid secretion, transepithelial transport of Na<sup>+</sup> (Figure 2-1D) was indifferent between treatments involving *Rhopr*DH<sub>44</sub> alone or together with *Aedae*CAPA-1 or when compared with unstimulated controls. The transport rate of K<sup>+</sup> in *Rhopr*DH<sub>44</sub>-stimulated MTs was similar to that of unstimulated controls (Figure 2-1E) whereas a small but significant increase in K<sup>+</sup> flux was observed when *Aedae*CAPA-1 was co-applied with *Rhopr*DH<sub>44</sub> compared with unstimulated controls. Overall, *Aedae*CAPA-1 did not influence the ratio of cations transported (Figure 2-1F), with *Rhopr*DH<sub>44</sub> leading to a roughly equimolar transport rate of each cation comparable to that of unstimulated control MTs.

The secretion rates of adult MTs treated with a mosquito kinin-related peptide (CDP) alone or co-applied with 1 fmol l<sup>-1</sup> *Aedae*CAPA-1 were similar (Figure 2-1A), with both experimental treatments having secretion rates significantly greater (~12-fold) than those of unstimulated controls. Addition of 1 fmol l<sup>-1</sup> *Aedae*CAPA-1 to adult MTs treated with CDP had no influence on Na<sup>+</sup> (Figure 2-1B) and K<sup>+</sup> (Figure 2-1C) concentrations, although a decrease in the Na<sup>+</sup> concentration of the secreted fluid was observed compared with unstimulated controls. Similarly, *Aedae*CAPA-1 did not influence transepithelial cation transport in CDP-stimulated

MTs (Figure 2-1D,E) with both cations showing a significant increase in transport rate relative to unstimulated controls. As a result, *AedaeCAPA-1* had no effect on the ratio of cation transport in CDP-stimulated MTs (Figure 2-1F) and neither treatment differed from unstimulated controls.

Adult MTs treated with 25 nmol l<sup>-1</sup> *DromeDH<sub>31</sub>* and 1 fmol l<sup>-1</sup> *AedaeCAPA-1* had a significantly lower secretion rate by over 7-fold compared to MTs stimulated with *DromeDH<sub>31</sub>* alone (Figure 2-1A). Notably, MTs treated with *DromeDH<sub>31</sub>* alone had secretion rates significantly greater than those of unstimulated controls whereas MTs receiving *DromeDH<sub>31</sub>* combined with *AedaeCAPA-1* had rates of secretion that were not different from those of unstimulated controls. Fluid secreted by adult MTs receiving *DromeDH<sub>31</sub>* combined with *AedaeCAPA-1* (but not alone) had a significant increase in Na<sup>+</sup> concentration compared with unstimulated controls (Figure 2-1B). The two *DromeDH<sub>31</sub>* experimental treatments also had a significantly different Na<sup>+</sup> concentration in the secreted fluid, with higher Na<sup>+</sup> titre in the MTs co-treated with *AedaeCAPA-1*. Comparatively, K<sup>+</sup> concentrations in the secreted fluid was significantly reduced compared with unstimulated controls when *DromeDH<sub>31</sub>* was tested alone or together with *AedaeCAPA-1* (Figure 2-1C). As expected, considering the influence of *AedaeCAPA-1* on the *DromeDH<sub>31</sub>*-stimulated fluid secretion rate, the transepithelial transport rate of both cations was also affected. Specifically, compared with unstimulated MTs, *DromeDH<sub>31</sub>* led to significantly greater transport rate of Na<sup>+</sup> whereas *AedaeCAPA-1* abolished this increase (Figure 2-1D). In particular, the two experimental treatments were also significantly different, with *AedaeCAPA-1* reducing Na<sup>+</sup> transport rate compared to MTs treated with *DromeDH<sub>31</sub>* alone. Relative to unstimulated controls, no significant change was observed in the K<sup>+</sup> transport rate in MTs treated with *DromeDH<sub>31</sub>* alone or together with *AedaeCAPA-1* (Figure 2-1E), although these two experimental treatments were found to be significantly different such

that *Aedae*CAPA-1 significantly reduced  $K^+$  transport rate. Thus, although the ratio of cations was modified by treatment with *Drome*DH<sub>31</sub>, which led to an approximate 2-fold increase in  $Na^+$  transport compared with unstimulated controls, the elevated  $Na^+ : K^+$  transport ratio was sustained in *Drome*DH<sub>31</sub>-stimulated MTs challenged with *Aedae*CAPA-1 (Figure 2-1F).

### **Effect of cGMP on basal (unstimulated) fluid and cation secretion in adult MTs**

CAPA peptides have been shown to elicit their effects on insect MT fluid secretion through second messenger pathways that involve cGMP (Ionescu and Donini, 2012; Kean et al., 2002; Pollock et al., 2004; Quinlan et al., 1997). Thus, we investigated the activity of this prospective second messenger in adult *A. aegypti* MTs to determine its actions on basal and diuretic hormone-stimulated fluid and ion secretion. Application of 100 and 10  $nmol\ l^{-1}$  cGMP resulted in a significant inhibition of basal secretion rates, with maximal inhibition leading to a 10-fold decrease, observed with treatment of 100  $nmol\ l^{-1}$  cGMP (Figure 2-2A). cGMP did not influence the  $Na^+$  and  $K^+$  concentrations in the secreted fluid at any of the tested concentrations (Figure 2-2B,C); however, cation transport rate was reduced (Figure 2-2D,E), with a significant decrease in  $Na^+$  flux when 10-100  $nmol\ l^{-1}$  cGMP was used compared with unstimulated MTs. Overall, cGMP did not change the relative ratio of cation transport in the secreted fluid compared with unstimulated controls (Figure 2-2F).

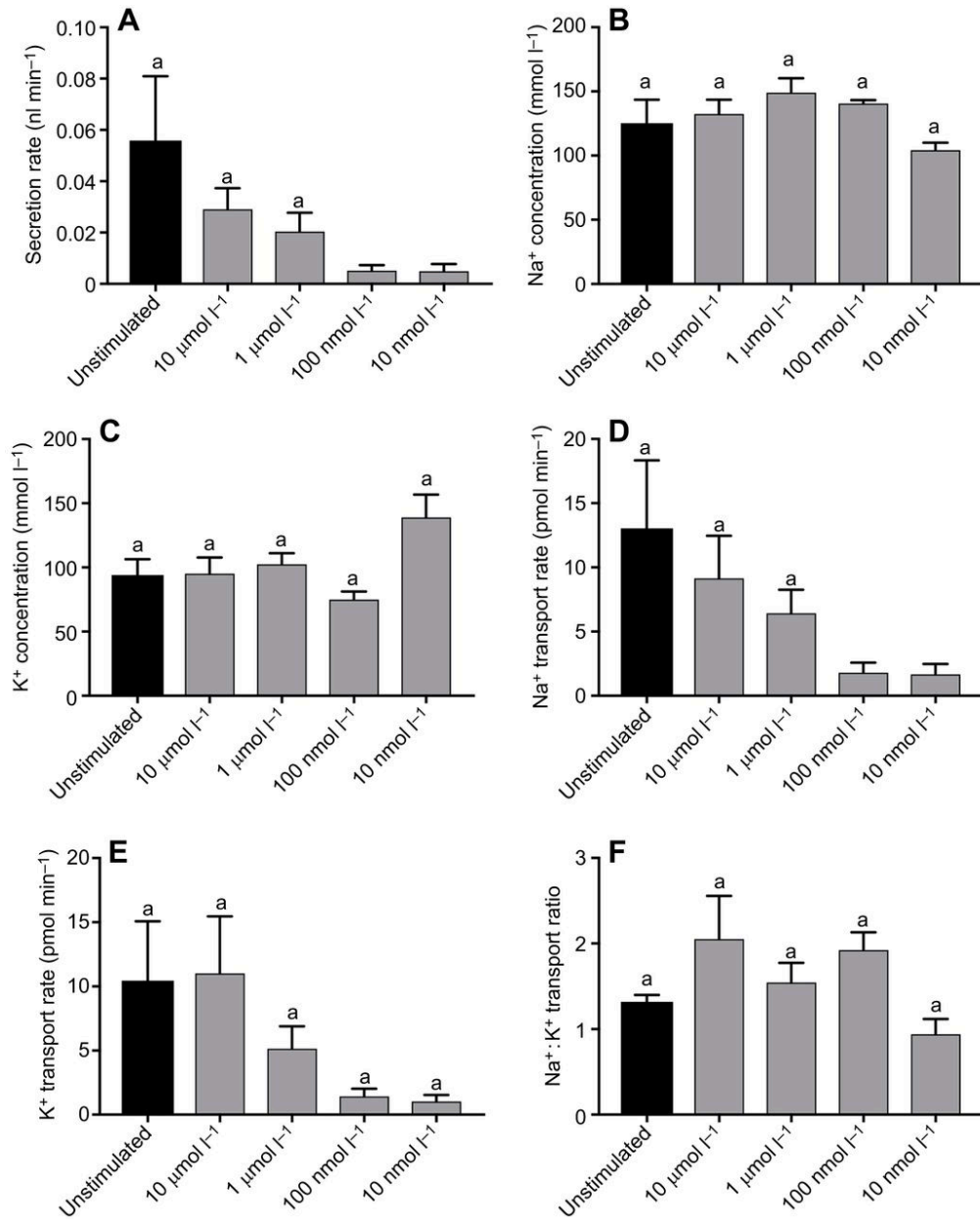


**Figure 2-2.** Effect of different concentrations of cGMP on *in vitro* fluid secretion rate, cation (Na<sup>+</sup> and K<sup>+</sup>) concentration and transport rate by unstimulated MTs of adult female *A. aegypti*. Doses of 10 nmol<sup>-1</sup> to 10 μmol<sup>-1</sup> cGMP were applied to adult MTs, and effects were compared against basal unstimulated MTs. (A) MT secretion rate; (B) Na<sup>+</sup> and (C) K<sup>+</sup> concentrations in the secreted fluid; (D) Na<sup>+</sup> and (E) K<sup>+</sup> transport rate; and (F) cation transport ratio. Values are presented as means±SEM, n=6–12. Bars that are not significantly different from unstimulated controls are denoted with the same letter, as determined by a one-way ANOVA and Bonferroni post-test.

## Effect of cGMP on transepithelial fluid and cation secretion against diuretic-stimulated adult MTs

In order to determine whether cGMP is involved in the anti-diuretic function of CAPA peptides in adult MTs, we investigated the effects of 100 nmol l<sup>-1</sup> cGMP, which we determined was a maximally inhibitory concentration on basal secretion rates. Similar to the effects of *Aedae*CAPA-1, 100 nmol l<sup>-1</sup> cGMP significantly decreased the fluid secretion rate of 5HT- and *Drome*DH<sub>31</sub>-stimulated MTs, whilst having a small inhibitory effect on *Rhopr*DH<sub>44</sub>-stimulated MTs (Figure 2-3). While all diuretic factors elicited significantly greater secretion rates relative to unstimulated MTs, a significant decrease in fluid secretion was observed in 5HT-stimulated MTs and *Drome*DH<sub>31</sub>-stimulated MTs when co-applied with cGMP, but not when MTs were stimulated with *Rhopr*DH<sub>44</sub>. Interestingly, and rather unexpectedly, cGMP also resulted in a substantial (~9-fold) decrease in fluid secretion rate in CDP-stimulated MTs. Although the cation concentrations in most treatments were not influenced by cGMP (Figure 2-3B,C) being similar to unstimulated controls, CDP-stimulated MTs had a significantly higher Na<sup>+</sup> concentration in the secreted fluid when cGMP was co-applied compared with unstimulated MTs and those treated with CDP alone. The transepithelial transport rate of both Na<sup>+</sup> and K<sup>+</sup> decreased in *Drome*DH<sub>31</sub>-stimulated and CDP-stimulated MTs when they were treated with cGMP (Figure 2-3D,E), while no change in cation transport was observed when *Rhopr*DH<sub>44</sub>-stimulated MTs were treated with cGMP. In 5HT-stimulated MTs, only the Na<sup>+</sup> transport rate was significantly reduced when cGMP was co-applied. Consistent with the effect of application of *Aedae*CAPA-1 to MTs stimulated with the various diuretics, cGMP had no overall effect on the relative proportions of the two primary cations in the secreted fluid (Figure 2-3F).

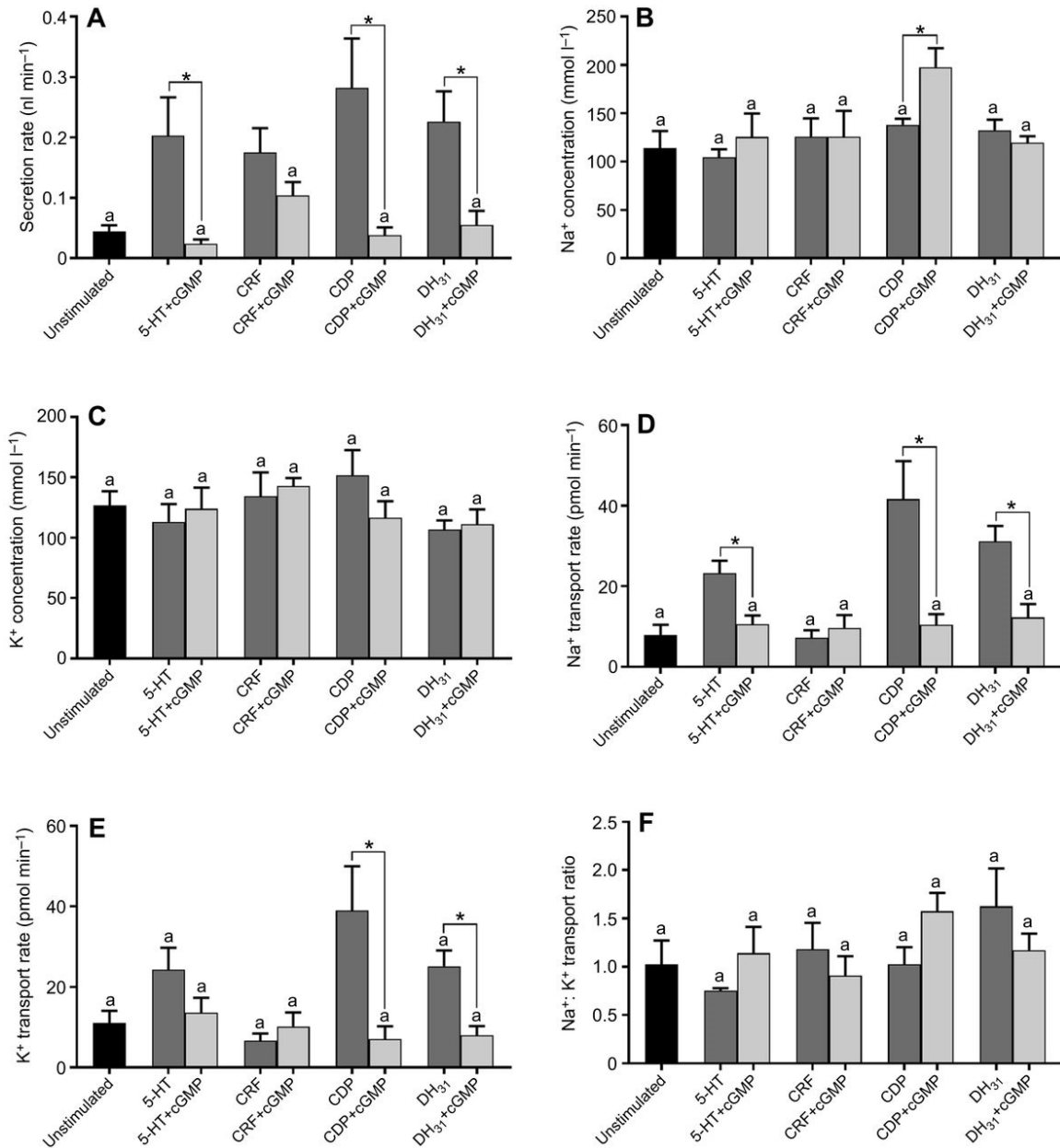


**Figure 2-3. Effect of cGMP on *in vitro* fluid secretion rate, cation (Na<sup>+</sup> and K<sup>+</sup>) concentration and transport rate by adult female *A. aegypti* MTs stimulated with a variety of diuretic hormones.** cGMP (100 nmol l<sup>-1</sup>) was applied to adult MTs stimulated with 100 nmol l<sup>-1</sup> 5HT, 10 nmol l<sup>-1</sup> *Rhopr*DH<sub>44</sub> (CRF), 50 nmol l<sup>-1</sup> CDP or 25 nmol l<sup>-1</sup> *Drome*DH<sub>31</sub> (DH<sub>31</sub>). (A) The tubule secretion assay was performed over a 60 min incubation period for the diuretic and cGMP, and 120 min for unstimulated controls. (B) Na<sup>+</sup> and (C) K<sup>+</sup> concentrations in the secreted fluid were measured using ion-selective microelectrodes (ISME), and the values were used to calculate the cation transport rate and ratio (D–F). Values are presented as means±SEM, n=7–18. Bars that are not significantly different from unstimulated controls are denoted with the same letter, as determined by a one-way ANOVA and Bonferroni post-test. Statistical significance between the two experimental treatments involving a specific diuretic factor alone or in combination with cGMP is denoted by an asterisk, as determined by an unpaired t-test.

## 2.5 Discussion

Transepithelial transport of ions and osmotically obliged water by insect MTs is regulated by at least five types of hormones derived from the nervous system. These include: (i) biogenic amines, such as 5HT, (ii) CRF-related peptides (DH<sub>44</sub>), (iii) CDPs, or kinin-related peptides, (iv) cardioacceleratory peptides (CAPA) and (v) calcitonin-like (DH<sub>31</sub>) peptides (Clark and Bradley, 1998; Schepel et al., 2010). These hormones, along with 5HT, all have been reported to elicit diuretic activity in *A. aegypti* MTs, whereas only CAPA peptides have been shown to function additionally as an anti-diuretic in larval *A. aegypti* MTs. Specifically, CAPA peptides elicit a diuretic function in larval *A. aegypti* at high concentrations, while functioning as an anti-diuretic at low concentrations (Ionescu and Donini, 2012). Similarly, the diuretic activity of CAPA peptides has been shown to be conserved for a variety of Dipteran species but is lacking in non-dipteran insects (Pollock et al., 2004). Interestingly, a few studies have also reported CAPA peptides elicit anti-diuretic actions in the fruit fly, *D. melanogaster* (Macmillan et al., 2018; Rodan et al., 2012).

The present study examined the effect of *Aedae*CAPA-1 on fluid secretion and ion transport by *A. aegypti* MTs stimulated with various diuretic factors. Considering these diuretics target unique receptors, involving distinct signalling cascades and, in some cases, have dissimilar cellular targets (i.e. principal versus stellate cells), we predicted *Aedae*CAPA-1 would not have a ubiquitous inhibitory action against all diuretic factors. Given its high structural similarity to the endogenous calcitonin-like mosquito natriuretic peptide, *Drome*DH<sub>31</sub> was expected to have both diuretic and natriuretic activities, functioning to stimulate fluid secretion whilst favouring transepithelial Na<sup>+</sup> transport (Coast et al., 2005). Previous studies have shown mosquito DH<sub>31</sub> to be the main hormone eliciting natriuresis in *A. aegypti* and *A. gambiae* (Coast et al., 2005). Here,

we found that *Aedae*CAPA-1 inhibits fluid secretion by MTs stimulated by *Drome*DH<sub>31</sub> and, moreover, inhibits transport of both primary cations without influencing the natriuretic activity of *Drome*DH<sub>31</sub> on adult MTs. Anti-diuretic activity of *Aedae*CAPA-1 has been reported previously on larval *A. aegypti* MTs, with low doses of CAPA being effective against 5HT-stimulated secretion (Ionescu and Donini, 2012; Sajadi et al., 2018) as well as DH<sub>31</sub>-stimulated secretion (Sajadi et al., 2018). Data in the current study demonstrates *Aedae*CAPA-1 inhibits fluid secretion stimulated by 5HT in adult stage mosquitoes. In addition, the kaliuretic action of 5HT measured in adults was not influenced, as transport of both cations was inhibited, and the secreted fluid remained K<sup>+</sup> rich compared with that for unstimulated MTs. Studies performed on the kissing bug, *Rhodnius prolixus*, established a dose-dependent inhibitory (i.e. anti-diuretic) action of native and structurally related CAPA peptides (Paluzzi and Orchard, 2006; Paluzzi et al., 2008). *Rhopr*CAPA- $\alpha$ 2 reduces the natriuresis stimulated by both endogenous diuretic hormones, namely 5HT and the CRF-related *Rhopr*DH<sub>44</sub>, which revealed that natriuretic activity could be hindered without influencing *Rhopr*DH<sub>44</sub>-stimulated diuresis (Paluzzi et al., 2012). Thus, inhibitory activity of CAPA peptides in these distinct blood feeding insects may be driven by two unique mechanisms as natriuretic activity of *Drome*DH<sub>31</sub> was unchanged. The *capa* gene gives rise to two CAPA peptides, CAPA-1 (or CAPA-PVK-1) and CAPA-2 (or CAPA-PVK-2), containing the consensus carboxyl terminal sequence, FRPV-NH<sub>2</sub>. In adult female *A. aegypti* MTs, CAPA peptides (both CAPA-1 and CAPA-2) were found to elicit an anti-diuretic role against DH<sub>31</sub>-stimulated MTs (Figure 2-S1B). Additionally, the *capa* gene encodes the pyrokinin-1 (PK1 or tryptopyrokinin) peptide, suggested to influence hindgut physiology in insects (Nassel and Winther, 2010). Despite the anti-diuretic role of both CAPA peptides in *Aedes* MTs, PK1 has no effect on DH<sub>31</sub>-stimulated secretion, with further studies showing its

receptor (PK1-R) to be highly enriched in the rectum of the *Aedes* mosquitoes, with no expression found in the MTs (Lajevardi and Paluzzi, 2020).

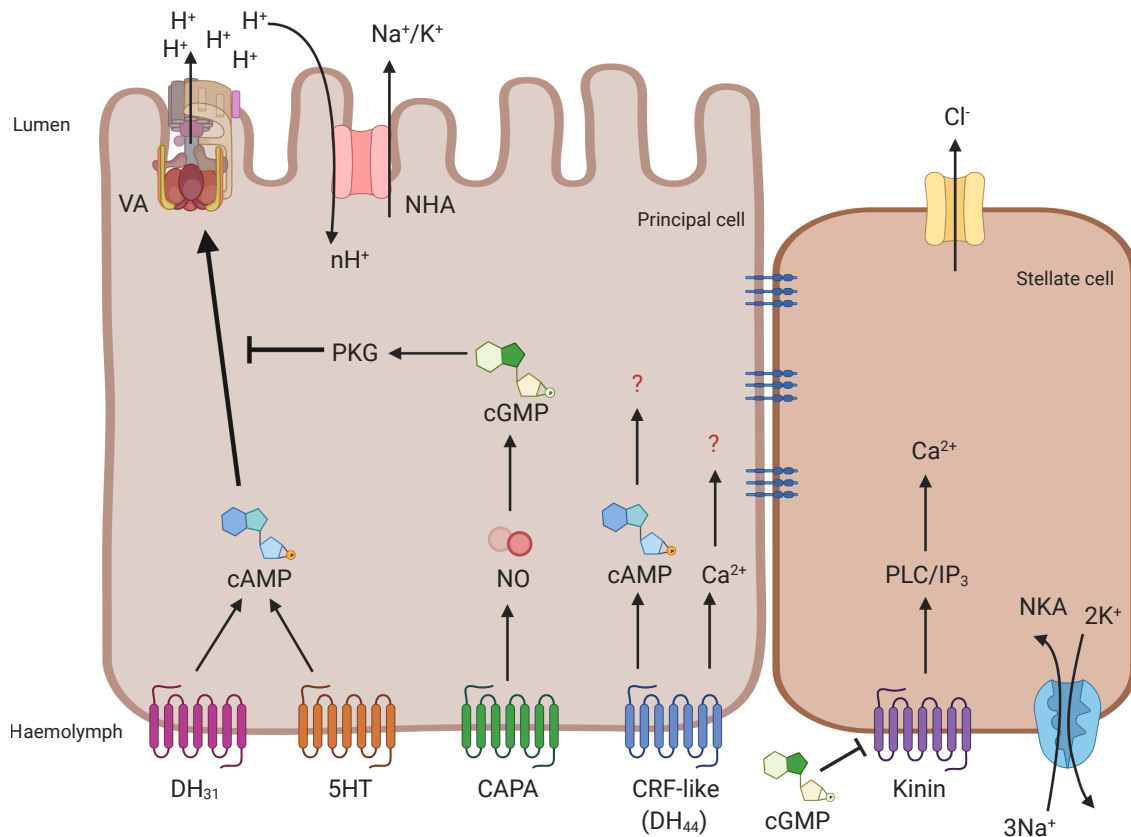


**Figure 2-4. Schematic diagram summarizing diuretic and anti-diuretic control of *A. aegypti* adult MTs.** The principal cells are responsible for transport of  $\text{Na}^+$  and  $\text{K}^+$  via secondary active transport. The V-type  $\text{H}^+$ -ATPase, localized in the brush border of the apical membrane, produces a  $\text{H}^+$  gradient that drives the exchange of  $\text{Na}^+$  and  $\text{K}^+$  across the apical membrane through cation/ $\text{H}^+$  antiporters. Ions are secreted from the haemolymph through a  $\text{Na}^+:\text{K}^+:2\text{Cl}^-$  cotransporter localized on the basolateral membrane. Neurohormone receptors, including those for 5HT and the peptides  $\text{DH}_{31}$ , CRF ( $\text{DH}_{44}$ ) and CAPA, are localized to the basolateral membrane of principal cells, while the kinin receptor is localized exclusively to stellate cells. Stimulation of MTs with 5HT and  $\text{DH}_{31}$  through their cognate receptors increases levels of the second messenger cAMP. CRF-related peptide ( $\text{DH}_{44}$ ) receptor activation increases  $\text{Ca}^{2+}$  and cAMP depending on the dose of peptide applied, while kinin receptor signalling involves exclusively increases in intracellular levels of  $\text{Ca}^{2+}$ . Our data indicate an anti-diuretic effect of *Aedae*CAPA-1 in 5HT- and  $\text{DH}_{31}$ -stimulated MTs, inhibiting non-selective cation transport and fluid secretion through an undetermined pathway but, in contrast, having only minor and no inhibitory activity on CRF ( $\text{DH}_{44}$ )- and kinin-stimulated diuresis, respectively. This anti-diuretic activity may involve the second messenger cGMP, which duplicates the strong inhibitory effects observed on 5HT- and  $\text{DH}_{31}$ -stimulated diuresis acting on principal cells. Lastly, cGMP is also capable of strongly inhibiting kinin-stimulated diuresis that is facilitated via stellate cells, which suggests an additional anti-diuretic factor may exist in mosquitoes.

Notably, the present study examined the effect of *Aedae*CAPA-1 against DH<sub>31</sub>-stimulated secretion for the first time in insects. Based on previous studies, the DH<sub>31</sub>-like MNP acts via its second messenger, cAMP, activating the V-type H<sup>+</sup>-ATPase and selectively driving an increase in Na<sup>+</sup> secretion into the lumen (Coast et al., 2005). The additional Na<sup>+</sup>, as well as Cl<sup>-</sup> as a counter-ion, is secreted with osmotically obliged water, increasing secretion ~7-fold and the Na<sup>+</sup>:K<sup>+</sup> concentration ratio ~10-fold (Coast et al., 2005). Our data indicate lumen-directed secretion of Na<sup>+</sup> ions is maintained in the presence of *Aedae*CAPA-1, albeit at a significantly lower transport rate. Similar to the actions of the DH<sub>31</sub>-related peptide, 5HT induces diuresis via the activation of adenylate cyclase to increase intracellular concentrations of cAMP (Cady and Hagedorn, 1999; Clark and Bradley, 1998). It is believed that cAMP promotes the assembly of the V-type H<sup>+</sup>-ATPase in the apical membrane to initiate proton and cation secretion into the MT lumen (Baumann and Walz, 2012; Rein et al., 2008).

Comparable to the effects observed with *Aedae*CAPA-1, this study revealed that cGMP strongly inhibited fluid secretion and cation transport in both 5HT- and DH<sub>31</sub>-stimulated adult MTs. In *Tenebrio molitor*, two structurally unrelated anti-diuretic peptides were identified (*Tenmo*-ADFa and *Tenmo*-ADFb) that are potent inhibitors effective in the femtomolar and picomolar range (Eigenheer et al., 2002; Eigenheer et al., 2003), which is similar to the femtomolar concentrations used in the present study. Both ADFa and ADFb exert their effects on MTs through cGMP, reducing cAMP to inhibit fluid secretion by *T. molitor* MTs (Eigenheer et al., 2002; Eigenheer et al., 2003). Similarly, studies have shown that cGMP inhibits fluid secretion in *R. prolixus* and probably does so by reducing intracellular levels of cAMP (Quinlan et al., 1997), which is elevated after stimulation with 5HT and the CRF-related peptidergic diuretic hormone (Gioino et al., 2014; Te Brugge et al., 2002). This was further supported when

the addition of cAMP, at high concentrations, reversed the inhibitory effects of cGMP (Quinlan and O'Donnell, 1998). Similarly, previous research on *A. aegypti* revealed that cGMP is probably the second messenger, leading to the anti-diuretic action of CAPA peptides in larvae (Ionescu and Donini, 2012) and adult mosquitoes (see Chapters 3 & 4) as well as an exogenous factor, *T. molitor* ADFa (Massaro et al., 2004), with similar inhibitory actions on adult MTs.

In contrast to the anti-diuretic activity on fluid secretion stimulated by 5HT and the DH<sub>31</sub>-related peptide, diuresis stimulated by a CRF-related peptide (*Rhopr*DH<sub>44</sub>) was not affected by *Aedae*CAPA-1 treatment in adult MTs. In addition, cation concentrations and transport rates remained unchanged by *Aedae*CAPA-1 in adult MTs stimulated by *Rhopr*DH<sub>44</sub>. Similarly, application of cGMP had only a minor effect on secretion rate and did not influence cation transport in *Rhopr*DH<sub>44</sub>-stimulated MTs, suggesting cGMP may play a role in the anti-diuretic function of CAPA peptides. In mosquitoes, the DH<sub>31</sub>-related peptide is natriuretic whereas the CRF-related diuretic peptide (DH<sub>44</sub>) elicits non-selective transport of cations (Coast et al., 2005), and the current observations are consistent with these findings (for example, see Figure 2-1). In insects, CRF-like peptides have been shown to initiate diuresis in MTs via the transcellular and paracellular pathways, suggesting that multiple receptors and second messenger systems may be involved. Specifically, low nanomolar concentrations of a CRF-related peptide were linked to the stimulation of the paracellular pathway only (Clark et al., 1998b), mediating this action through intracellular Ca<sup>2+</sup> as a second messenger (Clark et al., 1998a). In contrast, high nanomolar concentrations of a CRF-related peptide were shown to influence both paracellular and transcellular transport, increasing intracellular Ca<sup>2+</sup> and cAMP second messengers (Clark et al., 1998b). Thus, this suggests the mild inhibitory action of cGMP against *Rhopr*DH<sub>44</sub>-stimulated

fluid secretion may be linked to signalling via cAMP as a result of the mid-nanomolar concentration of *RhoprDH*<sub>44</sub> utilized in this study.

Insect kinin-related peptides, including the CDP utilized herein, are known to activate a Cl<sup>-</sup> conductance pathway independently of cAMP, utilizing inositol 1,4,5-trisphosphate (IP<sub>3</sub>) as a second messenger to stimulate the release of intracellular Ca<sup>2+</sup> (Hayes et al., 1994; Quinlan and O'Donnell, 1998; Yu and Beyenbach, 2002) following activation of the kinin receptor (Lu et al., 2011; Radford et al., 2002). Thus, there is probably no direct interaction between CAPA and CDP signalling pathways. Additionally, the CAPA receptors are localized to the principal cells in *D. melanogaster* (Terhzaz et al., 2012) and *A. aegypti* (see Chapter 3; Sajadi et al., 2020), whereas the kinin receptor has been immunolocalized to the stellate cells of the MTs, and functions to regulate anion permeability of the epithelium (Lu et al., 2011; Radford et al., 2002). Interestingly, our results found that application of cGMP resulted in an inhibition of CDP-stimulated fluid secretion and cation transport, similar to inhibitory effects on diuresis stimulated by 5HT and *DromeDH*<sub>31</sub>. In *D. melanogaster*, cGMP was shown to inhibit depolarization induced in kinin-stimulated MTs, suggesting an anti-diuretic effect (Ruka et al., 2013) as fluid secretion rates were not directly measured. Thus, in agreement with observations made in another dipteran insect, our results support the presence of an additional anti-diuretic hormone that signals through cGMP and reduces the activity of diuretic factors targeting stellate cells (Ruka et al., 2013).

Synthesized by neurosecretory cells in the central nervous system, CAPA peptides in *D. melanogaster* act on the principal cells in the MTs by activating L-type voltage-gated Ca<sup>2+</sup> channels, increasing intracellular Ca<sup>2+</sup> levels (Kean et al., 2002). The rise in Ca<sup>2+</sup> levels activate nitric oxide synthase (NOS) to initiate production of nitric oxide (NO). Finally, NO activates a

soluble guanylate cyclase, resulting in the production of cGMP, and consequent effects on secretion (Dow and Davies, 2003). In *A. aegypti*, it has been proposed that low levels of CAPA peptides lead to activation of protein kinase G, via elevated levels of cGMP (Ionescu and Donini, 2012), and resulting in its anti-diuretic activity in larval *A. aegypti*. When tested on *D. melanogaster* MTs, CAPA peptides stimulated fluid secretion in the 1 mmol l<sup>-1</sup> to 10 nmol l<sup>-1</sup> range (Pollock et al., 2004). However, CAPA peptides tested using lower concentrations that are anti-diuretic in mosquitoes do not activate calcium signalling in *D. melanogaster* MTs expressing an aequorin transgene (Davies et al., 2012), indicating species-specific activities of this neuropeptide family, which is reasonable considering their highly different diets and lifestyles.

Similar to effects seen in larval *A. aegypti* (Ionescu and Donini, 2012), our results suggest *Aedae*CAPA-1 increases cGMP levels in principal cells, as this second messenger mimicked the anti-diuretic actions in 5HT- and *Drome*DH<sub>31</sub>-stimulated MTs in adult females. Antagonistic effects between cGMP and cAMP, the latter being the second messenger of DH<sub>31</sub> and 5HT, were illustrated previously in *R. prolixus*, whereby cGMP was proposed to activate a cAMP-specific phosphodiesterase, reducing levels of the second messenger activating diuresis (Quinlan and O'Donnell, 1998). Similar antagonistic effects of cAMP and cGMP are emerging in *A. aegypti* MTs, given the present and previous accounts of cGMP being an inhibitory second messenger (Ionescu and Donini, 2012; Massaro et al., 2004). Notably, however, both these second messengers have been shown to lead to stimulation of diuresis in *D. melanogaster* principal cells (Davies et al., 1995; Kean et al., 2002; Kerr et al., 2004). Interestingly, cGMP signalling was shown to stimulate diuresis following activation of the mammalian atrial natriuretic peptide receptor ectopically expressed specifically in stellate cells (Kerr et al., 2004), while it was

inferred to have an anti-diuretic effect on kinin-stimulated MTs (Ruka et al., 2013). Nonetheless, as the natriuretic activity of *Drome*DH<sub>31</sub> is unaffected in response to *Aedae*CAPA-1, it is possible that the inhibitory mechanism differs somewhat to that in *R. prolixus*, where diuretic hormone-induced natriuresis is attenuated by the endogenous CAPA peptide (Paluzzi et al., 2012). Taken together, the inhibition of fluid secretion by MTs stimulated by a subset of diuretic hormones (i.e. DH<sub>31</sub>-related peptide and 5HT) and, the absence of any modulation of the relative proportions of the primary cations transported, highlights the importance of *Aedae*CAPA-1 solely as an anti-diuretic hormone in *A. aegypti*. Thus, natriuretic and kaliuretic activity, elicited by the DH<sub>31</sub>-related peptide and 5HT, respectively, is maintained while the rate of diuresis is slowed, which could have implications for downstream processes such as reabsorption in the hindgut.

Receptors for some of these regulators of the MTs have been identified in *A. aegypti*, including a kinin receptor expressed in stellate cells (Lu et al., 2011; Pietrantonio et al., 2005) and a DH<sub>31</sub>-related peptide receptor that shows a peculiar distal to proximal gradient of expression in principal cells of the MTs (Kwon and Pietrantonio, 2013), as well as two CRF-related peptide receptors, one of which is highly enriched in the renal MTs (Jagge and Pietrantonio, 2008). Other receptors, such as the endogenous 5HT receptor expressed within the *A. aegypti* MTs, remain elusive, as a 5HT<sub>7</sub> receptor isoform transcript was localized to the tracheolar cells associated with the MTs but was not localized to tubule epithelium, suggesting that another receptor variant must be present (Pietrantonio et al., 2001). Similarly, expression of the CAPA receptor in *A. aegypti* has been recently identified and characterized (see Chapter 3; Sajadi et al., 2020), and orthologues have been described in other Dipteran species and found to be enriched in the MTs (Iversen et al., 2002; Olsen et al., 2007; Park et al., 2002), with

localization to the principal cells (Terhzaz et al., 2012). Thus, it is apparent that more research is required to fully understand the complex interaction and cross-talk between all the hormonal regulators of *A. aegypti* MTs as well as those found in other insects. Further understanding the role of each specific hormone family, including both diuretic and anti-diuretic factors, will help resolve this complex regulatory network. Given the central importance of the MTs in insect biology, these insights will be useful considering the need for novel strategies or compounds which can more specifically and efficiently reduce the burden of disease vector species as well as insect pests of agriculture.

## 2.6 References

- Baumann, O., and Walz, B.** (2012). The blowfly salivary gland - a model system for analyzing the regulation of plasma membrane V-ATPase. *J. Insect Physiol.* **58**, 450–458.
- Beyenbach, K. W.** (2003). Transport mechanisms of diuresis in Malpighian tubules of insects. *J. Exp. Biol.* **206**, 3845–3856.
- Beyenbach, K., and Petzel, D. H.** (1987). Diuresis in mosquitoes: role of a natriuretic factor. *Physiology* **2**, 171–175.
- Beyenbach, K. W., Oviedo, A., and Aneshansley, D. J.** (1993). Malpighian tubules of *Aedes aegypti*: five tubules, one function. *J. Insect Physiol.* **39**, 639–648.
- Beyenbach, K. W., Skaer, H., and Dow, J. A. T.** (2010). The developmental, molecular, and transport biology of Malpighian tubules. *Annu. Rev. Entomol.* **55**, 351–374.
- Bradley, T. J.** (1987). Physiology of osmoregulation in mosquitoes. *Annu. Rev. Entomol.* **32**, 439–462.
- Cady, C., and Hagedorn, H. H.** (1999). Effects of putative diuretic factors on intracellular second messenger levels in the Malpighian tubules of *Aedes aegypti*. *J. Insect Physiol.* **45**, 327–337.
- Clark, T. M., and Bradley, T. J.** (1996). Stimulation of Malpighian tubules from larval *Aedes aegypti* by secretagogues. *J. Insect Physiol.* **42**, 593–602.
- Clark, T. M., and Bradley, T. J.** (1997). Malpighian tubules of larval *Aedes aegypti* are hormonally stimulated by 5-hydroxytryptamine in response to increased salinity. *Arch. Insect Biochem. Physiol.* **34**, 123–141.

- Clark, T. M., and Bradley, T. J.** (1998). Additive effects of 5-HT and diuretic peptide on *Aedes* Malpighian tubule fluid secretion. *Comp. Biochem. Physiol. – A Mol. Integr. Physiol.* **119**, 599–605.
- Clark, T. M., Hayes, T. K., Holman, G. M., and Beyenbach, K. W.** (1998a). The concentration-dependence of CRF-like diuretic peptide: mechanisms of action. *J. Exp. Biol.* **201**, 1753–1762.
- Clark, T. M., Hayes, T. K., and Beyenbach, K. W.** (1998b). Dose-dependent effects of CRF-like diuretic peptide on transcellular and paracellular transport pathways. *Am. J. Physiol.* **274**, F834–F840.
- Coast, G. M.** (2009). Neuroendocrine control of ionic homeostasis in blood-sucking insects. *J. Exp. Biol.* **212**, 378–386.
- Coast, G. M., Garside, C. S., Webster, S. G., Schegg, K. M., and Schooley, D. A.** (2005). Mosquito natriuretic peptide identified as a calcitonin-like diuretic hormone in *Anopheles gambiae* (Giles). *J. Exp. Biol.* **208**, 3281–3291.
- Davies, S. A., Huesmann, G. R., Maddrell, S. H. P., O'Donnell, M. J., Skaer, N. J. V., Dow, J. A. T., and Tublitz, N. J.** (1995). CAP(2b), a cardioacceleratory peptide, is present in *Drosophila* and stimulates tubule fluid secretion via cGMP. *Am. J. Physiol.* **269**, R1321–R1326.
- Davies, S. A., Cabrero, P., Povsic, M., Johnston, N. R., Terhzaz, S., and Dow, J. A. T.** (2012). Signaling by *Drosophila* capa neuropeptides. *Gen. Comp. Endocrinol.* **188**, 60–66.
- Donini, A., Patrick, M. L., Bijelic, G., Christensen, R. J., Ianowski, J. P., Rheault, M. R., and O'Donnell, M. J.** (2006). Secretion of water and ions by Malpighian tubules of larval

mosquitoes: effects of diuretic factors, second messengers, and salinity. *Physiol. Biochem. Zool.* **79**, 645–655.

**Donini, A., O'Donnell, M. J., and Orchard, I.** (2008). Differential actions of diuretic factors on the Malpighian tubules of *Rhodnius prolixus*. *J. Exp. Biol.* **211**, 42–48.

**Dow, J. A. T., and Davies, S. A.** (2003). Integrative physiology and functional genomics of epithelial function in a genetic model organism. *Physiol. Rev.* **83**, 687–729.

**Eigenheer, R. A., Nicolson, S. W., Schegg, K. M., Hul, J. J., and Schooley, D. A.** (2002). Identification of a potent antidiuretic factor acting on beetle Malpighian tubules. *Proc. Natl. Acad. Sci. USA* **99**, 84–89.

**Eigenheer, R. A., Wiehart, U. M., Nicolson, S. W., Schoofs, L., Schegg, K. M., Hull, J. J., and Schooley, D. A.** (2003). Isolation, identification and localization of a second beetle antidiuretic peptide. *Peptides* **24**, 27–34.

**Gioino, P., Murray, B. G., and Ianowski, J. P.** (2014). Serotonin triggers cAMP and PKA-mediated intracellular calcium waves in Malpighian tubules of *Rhodnius prolixus*. *Am. J. Physiol. Regul. Integr. Comp. Physiol.* **307**, R828–R836.

**Hayes, T. K., Mark Holman, G., Pannabecker, T. L., Wright, M. S., Strey, A. A., Nachman, R. J., Hoel, D. F., Olson, J. K., and Beyenbach, K. W.** (1994). Culekinin depolarizing peptide: a mosquito leucokinin-like peptide that influences insect Malpighian tubule ion transport. *Regul. Pept.* **52**, 235–248.

**Hegarty, J. L., Zhang, B., Pannabecker, T. L., Petzel, D. H., Baustian, M. D., and Beyenbach, K. W.** (1991). Dibutyryl cAMP activates bumetanide-sensitive electrolyte transport in Malpighian tubules. *Am. J. Physiol.* **261**, C521–C529.

- Ionescu, A., and Donini, A.** (2012). *Aedes*CAPA-PVK-1 displays diuretic and dose dependent antidiuretic potential in the larval mosquito *Aedes aegypti* (Liverpool). *J. Insect Physiol.* **58**, 1299–1306.
- Iversen, A., Cazzamali, G., Williamson, M., Hauser, F., and Grimmelikhuijzen, C. J. P.** (2002). Molecular cloning and functional expression of a *Drosophila* receptor for the neuropeptides capa-1 and -2. *Biochem. Biophys. Res. Commun.* **299**, 628–633.
- Jagge, C. L., and Pietrantonio, P. V.** (2008). Diuretic hormone 44 receptor in Malpighian tubules of the mosquito *Aedes aegypti*: evidence for transcriptional regulation paralleling urination. *Insect Mol. Biol.* **17**, 413–426.
- Kean, L., Cazenave, W., Costes, L., Broderick, K. E., Graham, S., Pollock, V. P., Davies, S. A., Veenstra, J. A., and Dow, J. A. T.** (2002). Two nitridergic peptides are encoded by the gene capability in *Drosophila melanogaster*. *Am. J. Physiol. Regul. Integr. Comp. Physiol.* **282**, R1297–R1307.
- Kerr, M., Davies, S. A., and Dow, J. A. T.** (2004). Cell-specific manipulation of second messengers; a toolbox for integrative physiology in *Drosophila*. *Curr. Biol.* **14**, 1468–74.
- Klowden, M. J.** (2013). *Physiological Systems in Insects: Third Edition*. Amsterdam: Elsevier.
- Kwon, H., and Pietrantonio, P. V.** (2013). Calcitonin receptor 1 (*AedaeGPCRCAL1*) hindgut expression and direct role in myotropic action in females of the mosquito *Aedes aegypti* (L.). *Insect Biochem. Mol. Biol.* **43**, 588–593.
- Lajevardi, A., and Paluzzi, J. P.** (2020). Receptor characterization and functional activity of pyrokinins on the hindgut in the adult mosquito, *Aedes aegypti*. *Front. Physiol.* **11**, 490.
- Larsen, E. H., Deaton, L. E., Onken, H., O'Donnell, M., Grosell, M., Dantzler, W. H., and Weihrauch, D.** (2014). Osmoregulation and excretion. *Compr. Physiol.* **4**, 405–573.

- Laurence, M., Dauga, C., Garrigues, T., Schaffner, F., Failloux, M., and Vazeille, A.-B.** (2005). Phylogeography of *Aedes* (Stegomyia) *aegypti* (L.) and *Aedes* (Stegomyia) *albopictus* (Skuse) (Diptera: Culicidae) based on mitochondrial DNA variations. *Genet. Res.* **86**, 1–11.
- Lu, H. L., Kersch, C., and Pietrantonio, P. V.** (2011). The kinin receptor is expressed in the Malpighian tubule stellate cells in the mosquito *Aedes aegypti* (L.): a new model needed to explain ion transport? *Insect Biochem. Mol. Biol.* **41**, 135–140.
- Massaro, R. C., Lee, L. W., Patel, A. B., Wu, D. S., Yu, M. J., Scott, B. N., Schooley, D. A., Schegg, K. M., and Beyenbach, K. W.** (2004). The mechanism of action of the antidiuretic peptide Tenmo ADFa in Malpighian tubules of *Aedes aegypti*. *J. Exp. Biol.* **207**, 2877–2888.
- Murray, N. E. A., Quam, M. B., and Wilder-Smith, A.** (2013). Epidemiology of dengue: past, present and future prospects. *Clin. Epidemiol.* **5**, 299–309.
- Nassel, D. R., and Winther, A. M. E.** (2010). *Drosophila* neuropeptides in regulation of physiology and behaviour. *Prog. Neurobiol.* **92**, 42–104.
- Ng, L. F. P., and Ojcius, D. M.** (2009). Chikungunya fever - re-emergence of an old disease. *Microbes Infect.* **11**, 1163–11644.
- O'Connor, K. R., and Beyenbach, K. W.** (2001). Chloride channels in apical membrane patches of stellate cells of Malpighian tubules of *Aedes aegypti*. *J. Exp. Biol.* **204**, 367–378.
- O'Donnell, M. J., Dow, J. A. T., Huesmann, G. R., Tublitz, N. J., and Maddrell, S. H. P.** (1996). Separate control of anion and cation transport in Malpighian tubules of *Drosophila melanogaster*. *J. Exp. Biol.* **199**, 1163–1175.

- Olsen, S. S., Cazzamali, G., Williamson, M., Grimmelikhuijzen, C. J. P., and Hauser, F.** (2007). Identification of one capa and two pyrokinin receptors from the malaria mosquito *Anopheles gambiae*. *Biochem. Biophys. Res. Commun.* **362**, 245–251.
- Paluzzi, J. P., and Orchard, I.** (2006). Distribution, activity and evidence for the release of an anti-diuretic peptide in the kissing bug *Rhodnius prolixus*. *J. Exp. Biol.* **209**, 907–915.
- Paluzzi, J. P., Russell, W. K., Nachman, R. J., and Orchard, I.** (2008). Isolation, cloning, and expression mapping of a gene encoding an antidiuretic hormone and other CAPA-related peptides in the disease vector, *Rhodnius prolixus*. *Endocrinology* **149**, 4638–4646.
- Paluzzi, J. P., Naikhwah, W., and O'Donnell, M. J.** (2012). Natriuresis and diuretic hormone synergism in *R. prolixus* upper Malpighian tubules is inhibited by the anti-diuretic hormone, *RhoprCAPA-α2*. *J. Insect Physiol.* **58**, 534–542.
- Park, Y., Kim, Y. J., and Adams, M. E.** (2002). Identification of G protein-coupled receptors for *Drosophila* PRXamide peptides, CCAP, corazonin, and AKH supports a theory of ligand-receptor coevolution. *Proc. Natl. Acad. Sci. USA* **99**, 11423–11428.
- Patrick, M. L., Aimanova, K., Sanders, H. R., and Gill, S. S.** (2006). P-type Na<sup>+</sup>/K<sup>+</sup>-ATPase and V-type H<sup>+</sup>-ATPase expression patterns in the osmoregulatory organs of larval and adult mosquito *Aedes aegypti*. *J. Exp. Biol.* **209**, 4638–4651.
- Petzel, D. H., Hagedorn, H. H., and Beyenbach, K. W.** (1986). Peptide nature of two mosquito natriuretic factors. *Am. J. Physiol.* **250**, R328-32.
- Petzel, D. H., Berg, M. M., and Beyenbach, K. W.** (1987). Hormone-controlled cAMP-mediated fluid secretion in yellow-fever mosquito. *Am. J. Physiol. Regul. Integr. Comp. Physiol.* **253**, R701–R711.

- Pietrantonio, P. V., Jagge, C., and McDowell, C.** (2001). Cloning and expression analysis of a 5HT7-like serotonin receptor cDNA from mosquito *Aedes aegypti* female excretory and respiratory systems. *Insect Mol. Biol.* **10**, 357–369.
- Pietrantonio, P. V., Jagge, C., Taneja-Bageshwar, S., Nachman, R. J., and Barhoumi, R.** (2005). The mosquito *Aedes aegypti* (L.) leucokinin receptor is a multiligand receptor for the three *Aedes* kinins. *Insect Mol. Biol.* **14**, 55–67.
- Pollock, V. P., McGettigan, J., Cabrero, P., Maudlin, I. M., Dow, J. A. T., and Davies, S. A.** (2004). Conservation of capa peptide-induced nitric oxide signalling in Diptera. *J. Exp. Biol.* **207**, 4135–4145.
- Predel, R., and Wegener, C.** (2006). Biology of the CAPA peptides in insects. *Cell. Mol. Life Sci.* **63**, 2477–2490.
- Quinlan, M. C., and O'Donnell, M. J.** (1998). Anti-diuresis in the blood-feeding insect *Rhodnius prolixus* Stål: antagonistic actions of cAMP and cGMP and the role of organic acid transport. *J. Insect Physiol.* **44**, 561–568.
- Quinlan, M. C., Tublitz, N. J., and O'Donnell, M. J.** (1997). Anti-diuresis in the blood-feeding insect *Rhodnius prolixus* Stål: the peptide CAP(2b) and cyclic GMP inhibit Malpighian tubule fluid secretion. *J. Exp. Biol.* **200**, 2363–2367.
- Radford, J. C., Davies, S. A., and Dow, J. A. T.** (2002). Systematic G-protein-coupled receptor analysis in *Drosophila melanogaster* identifies a leucokinin receptor with novel roles. *J. Biol. Chem.* **277**, 38810–38817.
- Ramsay, J. A.** (1954). Active transport of water by the Malpighian tubules of the stick insect, *Dixippus morosus* (Orthoptera, Phasmidae). *J. Exp. Biol.* **31**, 104–113.

- Rein, J., Voss, M., Blenau, W., Walz, B., and Baumann, O.** (2008). Hormone-induced assembly and activation of V-ATPase in blowfly salivary glands is mediated by protein kinase A. *Am. J. Physiol. Cell Physiol.* **294**, C56–C65.
- Rheault, M. R., and O'Donnell, M. J.** (2004). Organic cation transport by Malpighian tubules of *Drosophila melanogaster*: application of two novel electrophysiological methods. *J. Exp. Biol.* **207**, 2173–2184.
- Ribeiro, J., Rossignol, P., and Spielman, A.** (1984). Role of mosquito saliva in blood vessel location. *J. Exp. Biol.* **108**, 1–7.
- Rocco, D. A., Kim, D. H., and Paluzzi, J. P.** (2017). Immunohistochemical mapping and transcript expression of the GPA2/GPB5 receptor in tissues of the adult mosquito, *Aedes aegypti*. *Cell Tissue Res.* **369**, 313–330.
- Ruka, K. A., Miller, A. P., and Blumenthal, E. M.** (2013). Inhibition of diuretic stimulation of an insect secretory epithelium by a cGMP-dependent protein kinase. *Am. J. Physiol. Renal. Physiol.* **304**, F1210–F1216.
- Sajadi, F., Curcuruto, C., Al Dhaheeri, A., Paluzzi, J. P.** (2018). Anti-diuretic action of a CAPA neuropeptide against a subset of diuretic hormones in the disease vector, *Aedes aegypti*. *J. Exp. Biol.* **7**. <https://doi.org/10.1242/jeb.177089>.
- Sajadi, F., Uyklu, A., Paputsis, C., Lajevardi, A., Wahedi, A., Ber, L. T., Matei, A., Paluzzi, J. P.** (2020). CAPA neuropeptides and their receptor form an anti-diuretic hormone signaling system in the human disease vector, *Aedes aegypti*. *Sci. Rep.* **10**. <https://doi.org/10.1038/s41598-020-58731-y>.
- Schepel, S. A., Fox, A. J., Miyauchi, J. T., Sou, T., Yang, J. D., Lau, K., Blum, A. W., Nicholson, L. K., Tiburcy, F., Nachman, R. J., et al.** (2010). The single kinin receptor

- signals to separate and independent physiological pathways in Malpighian tubules of the yellow fever mosquito. *Am. J. Physiol. – Regul. Integr. Comp. Physiol.* **299**, R612–R622.
- Te Brugge, V. A., Schooley, D. A., and Orchard, I.** (2002). The biological activity of diuretic factors in *Rhodnius prolixus*. *Peptides* **23**, 671–681.
- Terhzaz, S., Cabrero, P., Robben, J. H., Radford, J. C., Hudson, B. D., Milligan, G., Dow, J. A. T., and Davies, S. A.** (2012). Mechanism and function of *Drosophila* capa GPCR: a desiccation stress-responsive receptor with functional homology to human neuromedinU receptor. *PLoS One* **7**, e29897.
- Veenstra, J. A.** (1988). Effects of 5-hydroxytryptamine on the Malpighian tubules of *Aedes aegypti*. *J. Insect Physiol.* **34**, 299–304.
- Weng, X. H., Huss, M., Wieczorek, H., and Beyenbach, K. W.** (2003). The V-type H<sup>+</sup>-ATPase in Malpighian tubules of *Aedes aegypti*: localization and activity. *J. Exp. Biol.* **206**, 2211–2219.
- Wheelock, G. D., Petzel, D. H., Gillett, J. D., Beyenbach, K. W., and Hagedorn, H. H.** (1988). Evidence for hormonal control of diuresis after a blood meal in the mosquito *Aedes aegypti*. *Arch. Insect Biochem. Physiol.* **7**, 75–89.
- Wieczorek, H.** (1992). The insect V-ATPase, a plasma membrane proton pump energizing secondary active transport: molecular analysis of electrogenic potassium transport in the tobacco hornworm midgut. *J. Exp. Biol.* **172**, 335–343.
- Wieczorek, H., Weerth, S., Schindlbeck, M., and Klein, U.** (1989). A vacuolar-type proton pump in a vesicle fraction enriched with potassium transporting plasma membranes from tobacco hornworm midgut. *J. Biol. Chem.* **264**, 11143–11148.

**Wieczorek, H., Putzenlechner, M., Zeiske, W., and Klein, U.** (1991). A vacuolar-type proton pump energizes  $K^+/H^+$  antiport in an animal plasma membrane. *J. Biol. Chem.* **266**, 15340–15347.

**Wieczorek, H., Beyenbach, K. W., Huss, M., and Vitavska, O.** (2009). Vacuolar-type proton pumps in insect epithelia. *J. Exp. Biol.* **212**, 1611–1619.

**Yu, M. J., and Beyenbach, K. W.** (2002). Leucokinin activates  $Ca^{2+}$ -dependent signal pathway in principal cells of *Aedes aegypti* Malpighian tubules. *Am. J. Physiol. Renal Physiol.* **283**, F499–F508.

## 2.7 Supplementary Figures

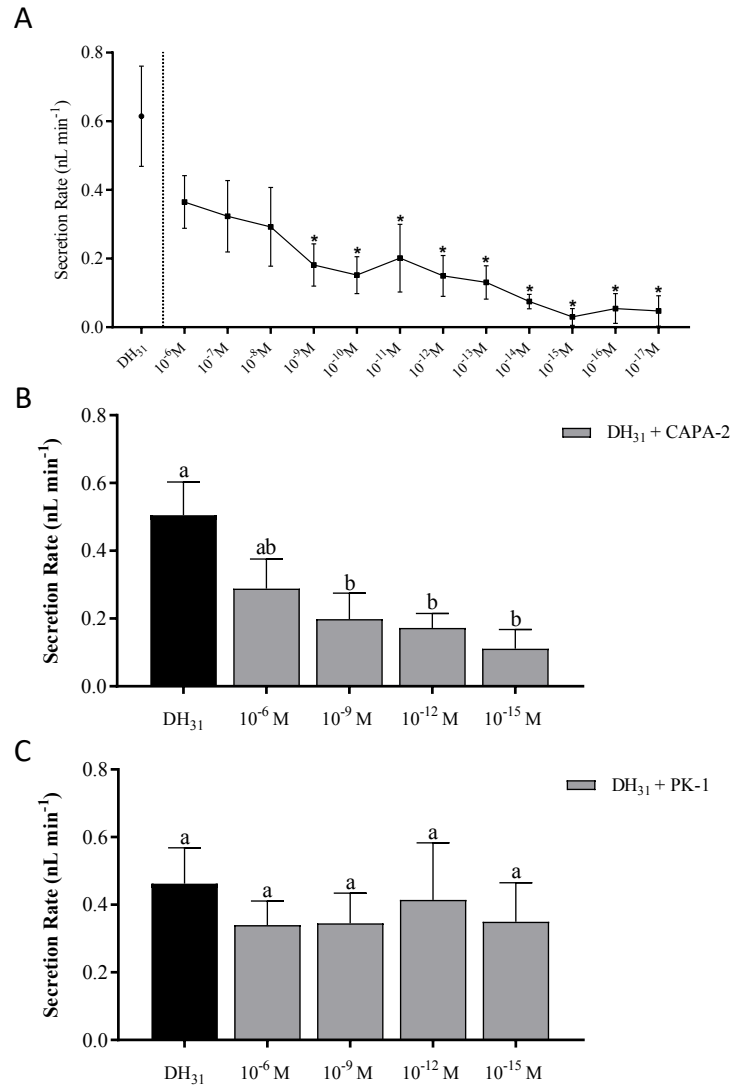


**Figure 2-S1. Effects of *AedaeCAPA-1*, *AedaeCAPA-2*, and *AedaePK-1* on DH<sub>31</sub>-stimulated MTs of adult *A. aegypti*.** Doses of (A) *AedaeCAPA-1* (B) *AedaeCAPA-2* and (C) *AedaePK-1* were applied to adult tubules for 60 min, n=15–16. (A) Doses that are significantly different from DH<sub>31</sub>-stimulated controls are denoted with an asterisk and (B,C) columns that are not significantly different from DH<sub>31</sub>-stimulated controls are denoted with the same letter, as determined by a one-way ANOVA and Bonferroni post-test.

## Chapter Three

### **CAPA neuropeptides and their receptor form an anti-diuretic hormone signalling system in the human disease vector, *Aedes aegypti***

A modified version of this chapter has been published and reproduced with permission:

Sajadi, F., Uyuklu, A., Paputis, C., Lajevardi, A., Wahedi, A., Ber, L.T., Matei, A., Paluzzi, J.P. (2020). CAPA neuropeptides and their receptor form an anti-diuretic hormone signalling system in the human disease vector, *Aedes aegypti*. *Scientific Reports* 10. <https://doi.org/10.1038/s41598-020-58731-y>

### 3.1 Summary

Insect CAPA neuropeptides are homologs of mammalian neuromedin U and are known to influence ion and water balance by regulating the activity of the Malpighian ‘renal’ tubules (MTs). Several diuretic hormones are known to increase primary fluid and ion secretion by insect MTs, and in adult female mosquitoes, a calcitonin-related peptide (DH<sub>31</sub>) called mosquito natriuretic peptide, increases sodium secretion to compensate for the excess salt load acquired during blood feeding. An endogenous mosquito anti-diuretic hormone was recently described, having potent inhibitory activity against select diuretic hormones, including DH<sub>31</sub>. Herein, we functionally deorphanized, both *in vitro* and *in vivo*, a mosquito anti-diuretic hormone receptor (*AedaeADHr*) with expression analysis indicating localization within principal cells in the MTs. Characterization using a heterologous *in vitro* system demonstrated the receptor was highly sensitive to mosquito CAPA neuropeptides while *in vivo*, *AedaeADHr* knockdown abolished CAPA-induced anti-diuretic control of DH<sub>31</sub>-stimulated MTs. CAPA neuropeptides are produced within a pair of neurosecretory cells in each of the abdominal ganglia, whose axonal projections innervate the abdominal neurohaemal organs, where these neurohormones are released into circulation. Lastly, pharmacological inhibition of nitric oxide synthase (NOS) and protein kinase G (PKG) signalling eliminated anti-diuretic activity of CAPA, highlighting the role of the second messenger cGMP and NOS/PKG in this anti-diuretic signalling pathway.

### 3.2 Introduction

Neuropeptides are central regulators of behaviours and control a plethora of physiological processes in all eukaryotic organisms. Insects, like many other animals, contain a comprehensive repertoire of neuropeptides along with their cognate receptors, which are essential for controlling complex biological phenomena including circadian rhythms, diapause, development, reproduction, pheromone biosynthesis, metabolism, circulation, stress, as well as hydromineral balance (Coast et al., 2002; Gäde, 2004; He et al., 2017; Hillyer, 2018; Nässel and Winther, 2010; Rafaeli, 2009; Raikhel et al., 2005; Schoofs et al., 2017; Terhzaz et al., 2015; Van Wielendaele et al., 2012). Insects have a high surface area to volume ratio, which has implications for their ability to maintain levels of water and ions within a normal homeostatic range. In order to ensure their survival, most insects have a relatively ‘simple’ excretory system comprised of the Malpighian ‘renal’ tubules (MTs) and hindgut (ileum and rectum). The MTs produce the primary urine acting to clear the haemolymph of excess ions, metabolites, and toxins while the hindgut generally functions in reabsorptive processes eliminating any unintentional loss of essential ions and amino acids (Phillips et al., 1987; Phillips et al., 1988). The insect excretory system is under complex control, which may include direct innervation and regulation by neurotransmitters such as proctolin, as observed in the hindgut of many insects (Cantera and Nässel, 1991; Steele et al., 1997). The excretory system in insects is also under the control by various circulating hormones (Coast, 2007; O’Donnell and Spring, 2000), which is the sole mechanism of extrinsic control in the non-innervated MTs, while endocrine factors may also influence the hindgut (Coast et al., 2002).

The overwhelming majority of studies investigating regulators of the insect excretory system have focused on diuretic regulators of the MTs (Baldwin et al., 2001; Cabrero et al.,

2002; Coast et al., 2005; Davies et al., 2012; Donini et al., 2008; Furuya et al., 2000; Lehmborg et al., 1991; Maddrell et al., 1991; Te Brugge et al., 2011), with only a few studies characterizing factors responsible for controlling reabsorptive processes across hindgut epithelia (Audsley and Phillips, 1990; Audsley et al., 1992; Audsley et al., 2006; Audsley et al., 2013; Paluzzi et al., 2014; Phillips et al., 1987). In addition, a few anti-diuretic factors that inhibit primary urine secretion by the insect MTs have also been reported (Eigenheer et al., 2002; Ionescu and Donini, 2012; Laenen et al., 2001; Lavigne et al., 2001; Massaro et al., 2004; Paluzzi and Orchard, 2006), acting to counter the activity of the diuretic hormones that increase ion and water secretion rates. An endogenous anti-diuretic hormone was recently identified in the disease-vector mosquito, *Aedes aegypti*, that strongly inhibits select diuretic factors including the mosquito natriuretic peptide (a calcitonin-related diuretic hormone) (Chapter 2; Sajadi et al., 2018), which is critical for the post-prandial sodium-rich diuresis that follows blood gorging by adult females (Coast et al., 2005). Similarly, anti-diuretic activity of CAPA neuropeptides has been reported earlier in larval *A. aegypti* (Ionescu and Donini, 2012) as well as in other insects (Coast et al., 2010; Coast et al., 2011; Paluzzi and Orchard, 2006; Quinlan et al., 1997; Rodan et al., 2012; Wiehart et al., 2002), with signalling involving cGMP as a second messenger (Paluzzi and Orchard, 2006; Quinlan and O'Donnell, 1998; Rodan et al., 2012; Wiehart et al., 2002; Sajadi et al., 2018; see Chapter 2). In addition to their clear anti-diuretic roles, CAPA peptides have also been linked to desiccation, where desiccation stress in the fruit fly, *Drosophila melanogaster*, leads to upregulation of *capa* mRNA, which is suggested to elevate CAPA levels in the CNS (Terhzaz et al., 2012). In many insects, CAPA peptides act through a conserved nitridergic signalling pathway leading to increased fluid secretion by MTs (Davies et al., 2012; Terhzaz et al., 2012). The mosquito anti-diuretic hormone is a member of the CAPA peptide

family, which along with other insect PRXamide peptides, share homology to the vertebrate neuromedin U peptides (Jurenka, 2015). CAPA neuropeptides are most abundant in specialized neurosecretory ventral abdominal (Va) neurons (Gabilondo et al., 2011; Gabilondo et al., 2018; Santos et al., 2006; Suska et al., 2011) of the abdominal ganglia (or in the analogous neuromeres in insects with fused abdominal ganglia) (Predel and Wegener, 2006; Predel et al., 2010) and stored within abdominal perivisceral organs (Eckert et al., 2002; Pollák et al., 2005; Tublitz and Truman, 1985; Wegener et al., 2001), which are major neurohaemal organs facilitating neurohormone release into circulation for delivery to target organs expressing receptors.

In the present study, I utilized a combination of molecular tools, heterologous functional assays, physiological bioassays, and reverse genetics techniques to identify and unravel the functional role of an anti-diuretic hormone receptor in the disease-vector mosquito, *A. aegypti*. This current data provides further evidence that mosquito CAPA neuropeptides, together with their cognate receptor (*AedaeADHr* or *CAPAr*) identified herein, function in a neuroendocrine system halting the stimulatory activity of diuretic hormones that, if left unregulated, may compromise ion and water homeostasis in this important anthropophilic mosquito.

### **3.3 Materials and Methods**

#### **Animals and dissections**

Various stages of *A. aegypti* (Liverpool strain) were obtained from a laboratory colony maintained as described previously (Rocco et al., 2017). All mosquitoes were raised under a 12h:12h light-dark cycle regime. Whole insects at each post-embryonic stage were used for examining developmental expression profiles and dissected tissues and organs were isolated from adults of each sex that were four-days post-eclosion. Adults were immobilized with brief

exposure to carbon dioxide and then dissected to isolate individual organs using fine forceps (Fine Science Tools, North Vancouver, BC, Canada) under nuclease-free Dulbecco's phosphate-buffered saline (DPBS) at room temperature (RT).

### **Heterologous receptor functional activation bioluminescence assay**

The complete CAPA receptor in *A. aegypti* was identified and found to be 3461 base pairs (bp) with an open reading frame of 2139 bp encoding a receptor protein of 712 residues (Sajadi et al., 2020). The open reading frame of the cloned *A. aegypti* CAPAr was inserted into pcDNA3.1+ mammalian expression vector following procedures described previously (Wahedi and Paluzzi, 2018; Gondalia et al., 2016; Oryan et al., 2018). Using a recombinant CHO-K1 cell line stably expressing aequorin (Paluzzi et al., 2012), *A. aegypti* CAPAr was transiently expressed following growth and transfection conditions as reported recently (Wahedi and Paluzzi, 2018). Cells were harvested for the functional assay at 48 h post-transfection by detaching cells from the culture flask using 5 mM EDTA in DPBS and later cells were resuspended at a concentration of  $10^6$ – $10^7$  cells/mL in assay media and incubated with coelenterazine *h*, as described previously (Oryan et al., 2018). Prior to running the functional assay, cells were diluted 10-fold in assay media and left to incubate for one additional hour. Several endogenous as well as other insect neuropeptides representing a variety of neuropeptide families (see Table 3-S1) were tested by preparing serial dilutions of each peptide in assay media. All peptides were commercially synthesized at a purity of >90% (Genscript, Piscataway, NJ, USA) and 1 mM stock solutions were prepared by dissolving 1 mg of each peptide in water or DMSO as appropriate based on specific peptide characteristics. Recombinant CHO-K1 cells expressing the *A. aegypti* CAPAr were loaded into each well of a multi-well plate using an

automated injector module linked to a Synergy 2 Multi Mode Microplate Reader (BioTek, Winooski, VT, USA) which measured kinetic luminescent response from each well for 20 sec immediately following cell loading onto the different peptides at various doses.

### **Immunohistochemistry**

The dissected tissues/organs were fixed overnight at 4°C with 4% paraformaldehyde prepared in DPBS and were then washed several times with DPBS to remove fixative. The tissues were subsequently permeabilized in 4% Triton X-100, 10% normal sheep serum (NSS) and 2% bovine serum albumin (BSA) prepared in DPBS and incubated for 1 h at RT on a rocking platform and then washed several times with DPBS to remove any traces of the permeabilization solution. The primary antibody was prepared using a custom affinity-purified rabbit polyclonal antibody (Genscript, Piscataway, NJ, USA) produced against *Rhodnius prolixus RhoprCAPA-2* (EGGFISFPRV-NH<sub>2</sub>; a kind gift from Prof. Ian Orchard, University of Toronto), which was diluted 1:1000 in 0.4% Triton X-100 containing 2% NSS and 2% BSA in DPBS. Tissues were incubated in the primary antibody solution for 48 h at 4°C on a rocking platform, and no primary controls were incubated in the same solution of 0.4% Triton X-100 containing 2% BSA and 2% NSS in DPBS but lacking primary antibody. After the primary antibody incubation, tissues were washed three times for 1 h, each with DPBS at RT. The secondary antibody solution was prepared using Alexa Fluor 488-conjugated cross-adsorbed goat anti-rabbit immunoglobulin G (Life Technologies, Burlington, ON, Canada) diluted 1:200 in DPBS containing 10% NSS. The tissues were incubated in the secondary antibody solution overnight at 4°C on a rocking platform and then washed with DPBS several times at RT. Tissues were mounted in ProLong Diamond Antifade Mountant containing DAPI (Molecular Probes,

Eugene, OR, USA) onto microscope slides and analyzed using a Lumen Dynamics XCite™ 120Q Nikon fluorescence microscope (Nikon, Mississauga, ON, Canada) or EVOS FL Auto Live-Cell Imaging System (Life Technologies, Burlington, ON, Canada).

### **RNA probe template preparation**

To obtain a template for synthesizing DIG-labelled probes for use in fluorescence *in situ* hybridization (FISH), a 373 bp fragment of the *A. aegypti* CAPA partial mRNA (GenBank Accession: XM\_001650839) previously described (Predel et al., 2010), and a 743 bp product of the anti-diuretic hormone receptor identified herein with primers designed (Table 3-S2) using the Primer3 plugin in Geneious® 6.1.8 (Biomatters Ltd., Auckland, New Zealand) were amplified using standard Taq DNA Polymerase (New England Biolabs, Whitby, ON, Canada) following manufacturer-recommended conditions. PCR products were column-purified with PureLink Quick PCR Purification Kit (Life Technologies, Burlington, ON, Canada) and amplified in a subsequent PCR reaction to generate cDNA products with incorporated T7 promoter sequences (Table 3-S2) to facilitate *in vitro* RNA synthesis of anti-sense or sense probes. The final purified PCR products for use as templates for RNA probe synthesis were quantified on a Synergy 2 Multi Mode Microplate Reader.

### **Digoxigenin (DIG)-labelled RNA probe synthesis**

PCR templates generated as described above (Table 3-S2) were used for *in vitro* transcription reactions using the HiScribe T7 RNA Synthesis Kit (New England Biolabs, Whitby, ON, Canada) following the recommended conditions when using modified nucleotides. Digoxigenin-labelled UTP was supplemented in a 35:65 ratio (DIG-UTP to standard UTP) either

as a separate analog (digoxigenin-11-UTP) or in a pre-mixed 10X DIG-RNA labelling mix (Sigma-Aldrich, Oakville, ON, Canada). Template DNA was removed following treatment with RNase-free DNase I (New England Biolabs, Whitby, ON, Canada) and an aliquot of the synthesized RNA probes were then visually assessed using standard agarose gel electrophoresis and quantified on a Synergy 2 Multi Mode Microplate Reader.

### **Fluorescence *in situ* hybridization (FISH)**

An optimized FISH procedure based on a protocol described previously for *R. prolixus* (Paluzzi et al., 2008; Paluzzi and Orchard, 2010) was utilized involving peroxidase-mediated tyramide signal amplification to localize cells expressing either the CAPA peptide mRNA or the anti-diuretic hormone receptor (*CAPAr*) mRNA. Tissues/organs were dissected under nuclease-free DPBS and were immediately placed in microcentrifuge tubes containing freshly-prepared fixation solution (4% paraformaldehyde prepared in DPBS) and fixed for 1 h at RT on a rocker. Tissues/organs were subsequently washed five times with 0.1% Tween-20 in DPBS (PBT) and treated with 1% H<sub>2</sub>O<sub>2</sub> (diluted in DPBS) for 20 min at RT to quench endogenous peroxidase activity. Tissues/organs were then incubated in 4% Triton X-100 (Sigma Aldrich, Oakville, ON, Canada) in PBT for 1 h at RT to permeabilize the tissues and then washed with copious PBT. A secondary fixation of the tissues/organs was performed for 20 min in 4% paraformaldehyde in DPBS and then washed using PBT to remove all traces of fixative. The tissues/organs were then rinsed in a 1:1 mixture of PBT-RNA hybridization solution (50% formamide, 5X SSC, 0.1 mg/mL heparin, 0.1 mg/mL sonicated salmon sperm DNA and 0.1% Tween-20) which was then replaced with RT RNA hybridization that had been prepared earlier by denaturing in a boiling water bath for 5 min and subsequently cooled on ice for 5 min. The samples were then incubated

at 56°C for 1 h, which served as the pre-hybridization treatment. During the pre-hybridization incubation, labelled RNA probe (anti-sense for experimental or sense for control) was added to pre-boiled RNA hybridization solution (2–4 ng/μL final concentration) and this mixture was heated at 80°C for 3 min to denature the single-stranded RNA probes and then cooled on ice for 5 min. The samples were then incubated overnight in this hybridization solution containing the DIG-labelled RNA probe at 56°C. The following day, samples were washed twice with fresh hybridization solution (minus probe) and subsequently with 3:1, 1:1 and 1:3 (vol/vol) mixtures of hybridization solution-PBT (all pre-warmed to 56°C). The tissues were subsequently washed with PBT pre-warmed to 56°C and in the final wash step were left to equilibrate to RT. Next, to reduce non-specific staining, samples were blocked with PBTB (DPBS, 0.1% Tween-20, 1% Molecular Probes block reagent; Invitrogen, Carlsbad, CA, USA) for 1 h. Tissues/organs were then incubated with a mouse anti-DIG biotin-conjugated antibody (Jackson ImmunoResearch Laboratories, West Grove, PA, USA) diluted 1:400 and incubated for 1.5 h at RT on a rocker in the dark. The antibody solution was subsequently removed, and tissues were subjected to several washes in PBTB over the course of 1 h. Tissues/organs were then incubated with horseradish peroxidase-streptavidin conjugate (Molecular Probes, Eugene, OR, USA) diluted 1:100 in PBTB for 1 h and the tissues were once again washed with PBTB several times over the course of an hour. Finally, prior to treatment with tyramide solution for the signal amplification of the target mRNA transcripts, samples were washed twice with PBT and once with DPBS. Afterwards, a tyramide solution was prepared consisting of Alexa Fluor 568 tyramide dye in amplification buffer containing 0.015% H<sub>2</sub>O<sub>2</sub>. After experimenting with various dilutions of the labeled tyramide, a 1:100 and 1:500 dilution of tyramide dye gave optimal results with minimal background staining for the ganglia and MTs, respectively. After the last DPBS wash was

removed from the tissues/organs, the tyramide solution was added and the tissues were incubated in the dark for 1 h on a rocker at RT. The tyramide solution was then removed and the samples were washed with DPBS several times over the course of an hour. The tissues/organs were stored in DPBS overnight at 4°C and then mounted on cover slips with mounting media comprised of DPBS with 50% glycerol containing 4 µg/mL 4',6- diamidino-2-phenylindole dihydrochloride (DAPI). Tissues/organs were analyzed using a Lumen Dynamics XCite™ 120Q fluorescence microscope or EVOS FL Auto Live-Cell Imaging System.

### **Synthesis of dsRNA for RNA interference and RT-qPCR**

Double-stranded RNA (dsRNA) was synthesized and column-purified using the MEGAscript® RNAi Kit (Invitrogen, Carlsbad, CA, USA) following the recommended protocol using primers for ds*CAPAr* synthesis (Table 3-S2) and primers as reported previously for ds*ARG* (Durant et al., 2017), which is an ampicillin resistance gene cloned from standard sequencing plasmid (pGEM T-Easy) that served as a negative control. A Nanoject Nanoliter Injector (Drummond Scientific, Broomall, PA, USA) was used to inject one-day old female mosquitoes with 1 µg (in ~140 nL) of either ds*CAPAr* or ds*ARG*. After injection, mosquitoes were recovered in a photo period-, temperature- and humidity-controlled incubator. Total RNA was then isolated from four-day old whole female mosquitoes injected with ds*CAPAr* or ds*ARG* using the Monarch Total RNA Miniprep Kit (New England Biolabs, Whitby, ON, Canada) and used as template (500 ng) for cDNA synthesis using the iScript™ Reverse Transcription Supermix (Bio-Rad, Mississauga, ON, Canada) following recommended guidelines, diluting cDNA ten-fold prior to quantitative RT-PCR. *AedaeCAPAr* and *AedaeCAPA* transcript levels were quantified using gene-specific primers that were positioned on different exons (Table 3-S2) and

PowerUP™ SYBR® Green Master Mix (Applied Biosystems, Carlsbad, CA, USA) and measured on a StepOnePlus Real-Time PCR System (Applied Biosystems, Carlsbad, CA, USA) following conditions described previously (Gondalia et al., 2016). A similar procedure for cDNA synthesis and transcript quantification as outline above was followed for total RNA isolated from each post-embryonic developmental stage and tissues/organs dissected from adult stage mosquitoes. Relative expression levels were determined using the  $\Delta\Delta C_T$  method and were normalized to the geometric mean of *rp49* and *rps18* reference genes, which were previously characterized and determined as optimal endogenous controls (Paluzzi et al., 2014). Measurements were taken from three biological replicates, all of which included three technical replicates per reaction and a no-template negative control.

### **Malpighian tubule fluid secretion assay**

In order to determine fluid secretion rates, a modified Ramsay secretion assay (Ramsay, 1954) was performed on isolated MTs of 3–6-day old adult female *A. aegypti*, as reported recently (Chapter 2; Sajadi et al., 2018). Tissue dissections were performed under physiological saline prepared as described previously (Petzel et al., 1987; Chapter 2; Sajadi et al., 2018) diluted 1:1 with Schneider's Insect Medium (Sigma-Aldrich, Oakville, ON, Canada). Individual MTs were removed and transferred to a Sylgard-lined Petri dish containing 20  $\mu$ l saline bathing droplets immersed in hydrated mineral oil to prevent evaporation. The proximal end of the MT was removed from the bathing saline and wrapped around a Minutien pin to allow for secretion measurements. Dosages of 25 nmol l<sup>-1</sup> *DromeDH*<sub>31</sub> (Coast et al., 2005) or 100 nmol l<sup>-1</sup> 5HT (Clark and Bradley, 1998; Veenstra, 1988) alone or in combination with 1 fmol l<sup>-1</sup> *AedaeCAPA*-1 (see Chapter 2; Sajadi et al., 2018) were applied to the isolated MTs as previously described

(Chapter 2; Sajadi et al., 2018). Dosage of *Aedae*CAPA-1 was based on a dose-response curve of *Aedae*CAPA-1 against DH<sub>31</sub>-stimulated tubules (Chapter 2; Sajadi et al., 2018), and the selected dose used to assess pharmacological blockade of prospective signalling partners was within the range of effective titres of *Aedae*CAPA-1. To investigate the effects of the pharmacological blockers, a nitric oxide synthase (NOS) inhibitor, N $\omega$ -Nitro-L-arginine methyl ester hydrochloride (L-NAME), and protein kinase G (PKG) inhibitor, KT5823, (Sigma-Aldrich Canada Ltd, Oakville, ON, Canada) were used against 5HT- and DH<sub>31</sub>-stimulated MTs. Dosages of 2  $\mu\text{mol l}^{-1}$  L-NAME (manufacturer's recommended dose) and 5  $\mu\text{mol l}^{-1}$  KT5823 (Ionescu and Donini, 2012) were applied to the MTs. The inhibitors were treated in conjunction with 1  $\text{fmol l}^{-1}$  *Aedae*CAPA-1 and/or 100  $\text{nmol l}^{-1}$  cyclic guanosine monophosphate, 8 bromo-cGMP (cGMP) (see Chapter 2; Sajadi et al., 2018) (Sigma-Aldrich, Oakville, ON, Canada). Unstimulated controls consisted of tubules bathed in physiological saline with no diuretic application. Following a 60-minute incubation period, the size of the secreted droplet was measured using a calibrated eyepiece micrometer and fluid secretion rate (FSR) was calculated as described previously (Donini et al., 2008).

### **Statistical analyses**

Data was compiled using Microsoft Excel and transferred to Graphpad Prism software v.8 (Graphpad Software, San Diego, CA, USA) to create figures and conduct all statistical analyses. Data was analyzed accordingly using either unpaired t-tests or one-way ANOVA and appropriate post-hoc test as reported in the figure captions, with differences between treatments considered significant if  $p < 0.05$ .

### 3.4 Results

#### Functional ligand-receptor interaction heterologous assay

The endogenous peptidergic ligands for the cloned anti-diuretic hormone receptor were identified using a heterologous functional assay using CHO-K1 cells stably expressing a bioluminescent calcium sensor, aequorin (Paluzzi et al., 2012; Wahedi and Paluzzi, 2018). The receptor was activated by all endogenously expressed peptides encoded by the CAPA gene in *A. aegypti* (Figure 3-1A), including two CAPA peptides (periviscerokinins) and pyrokinin 1-related peptide. Notably however, the pyrokinin 1-related peptide displayed very poor activity compared to the two CAPA peptides, which were the most potent ligands with half maximal effective concentrations in the low nanomolar range ( $EC_{50} = 5.62\text{--}6.76$  nM), whereas a significantly higher concentration of pyrokinin-1 was needed to achieve even low level CAPAR activation. Several other endogenous mosquito peptides as well as additional insect peptides belonging to distinct peptide families were tested and displayed no detectable activity over background levels of luminescence (Figure 3-1B). Controls where the CHO-K1 aequorin cells were transfected with empty pcDNA3.1<sup>+</sup> vector showed no detectable luminescence response (data not shown) to any of the peptides used in this study, confirming the calcium-based luminescence signal was a result of CAPA neuropeptide ligands activating the transiently expressed *A. aegypti* CAPA receptor.

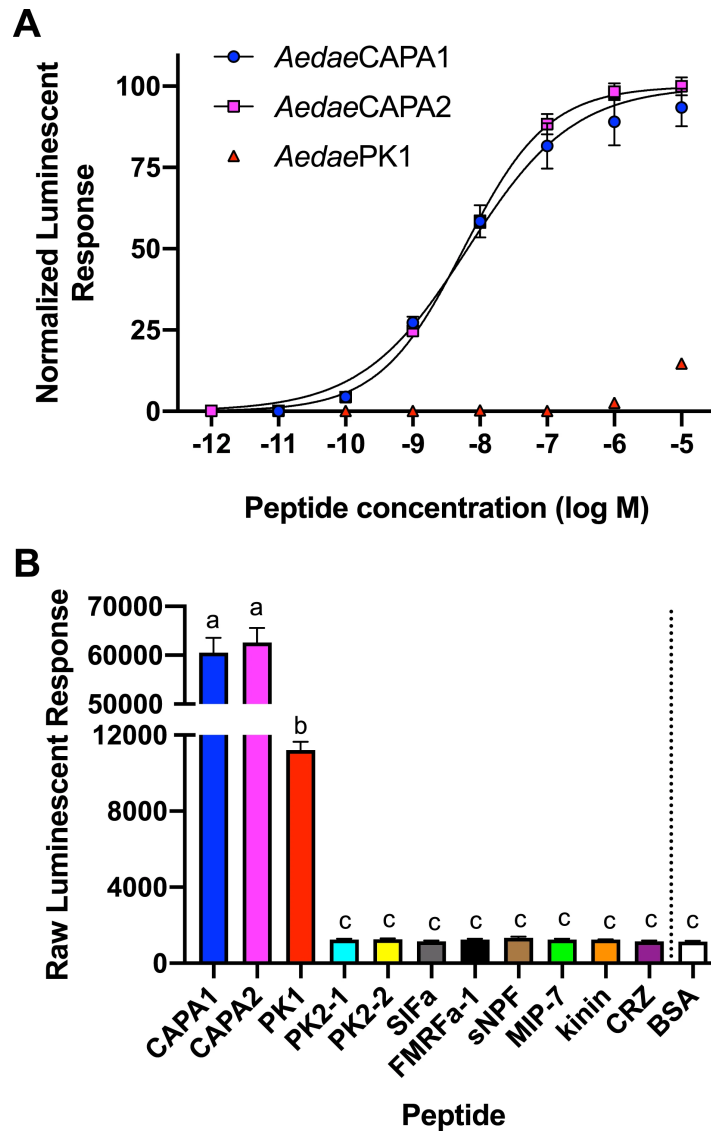


**Figure 3-1. CAPA neuropeptides (anti-diuretic hormone) receptor (CAPAR) functional deorphanization using a heterologous assay.** (A) Normalized dose-response curve demonstrating specificity of CAPAR functional activation by CAPA gene-derived neuropeptides. (B) Raw luminescent response following application of each CAPA gene-derived neuropeptide and representative neuropeptides belonging to several insect families, each tested at 10  $\mu$ M. For peptide sequence information and species origin, see (Table 3-S1). Only CAPA gene-derived neuropeptides resulted in a significant luminescent response relative to BSA control (vehicle). At this saturating dose, no difference in response was observed between the two endogenous CAPA neuropeptides, *Aedae*CAPA-1 and *Aedae*CAPA-2; *Aedae*PK-1 demonstrated a significantly lower luminescent response (only ~20% activity compared to either CAPA peptide), but nonetheless this response was significantly higher compared to all other tested peptides that were identical to background luminescent responses obtained with vehicle control (BSA). Different letters denote bars that are significantly different from one another as determined by a one-way ANOVA and Tukey's multiple comparison post-hoc test ( $p < 0.01$ ). Data represent the mean  $\pm$  SEM ( $n = 3$ ).

### ***CAPAr* transcript profile and cell-specific localization**

We determined the developmental expression profile of the *A. aegypti* CAPA receptor (*CAPAr*) transcript in each post-embryonic developmental stage of the mosquito. Over the four larval stages and pupal stage of development, the *CAPAr* transcript level remained unchanged (Figure 3-2A); however, in adults, *CAPAr* transcript levels were significantly higher in adult male mosquitoes compared to adult female, pupal stage and first instar larval mosquitoes (Figure 3-2A). To confirm site of biological action of the anti-diuretic hormones *in vivo*, we determined the *CAPAr* expression profile in adult *A. aegypti*, examining several tissues/organs in adult male and female mosquitoes. In males, *CAPAr* transcript was detected in reproductive tissues, head, carcass (i.e. the headless mosquito excluding the alimentary canal and reproductive tissues), and midgut while low background levels were found in the hindgut (Figure 3-2B). Notably, *CAPAr* transcript was observed in the Malpighian ‘renal’ tubules (MTs) where expression was significantly enriched by ~150-fold compared to all other tissues/organs examined (Figure 3-2B). A similar expression profile was observed in female mosquitoes with *CAPAr* transcript present in head, carcass, and midgut, while low background levels were detected in hindgut and reproductive organs. Similar to males, *CAPAr* was significantly enriched in the MTs of females relative to all other examined tissues/organs by nearly 150-fold (Figure 3-2B). Using fluorescent *in situ* hybridization, the *CAPAr* transcript was localized using an anti-sense probe specifically to principal cells of the MTs (distinguished by their larger nuclei) and absent in stellate cells (smaller nuclei) (Figure 3-2C). Specificity of *CAPAr* transcript localization was confirmed using a sense control probe, with no signal detected in any cell type of the MTs (Figure 3-2D).

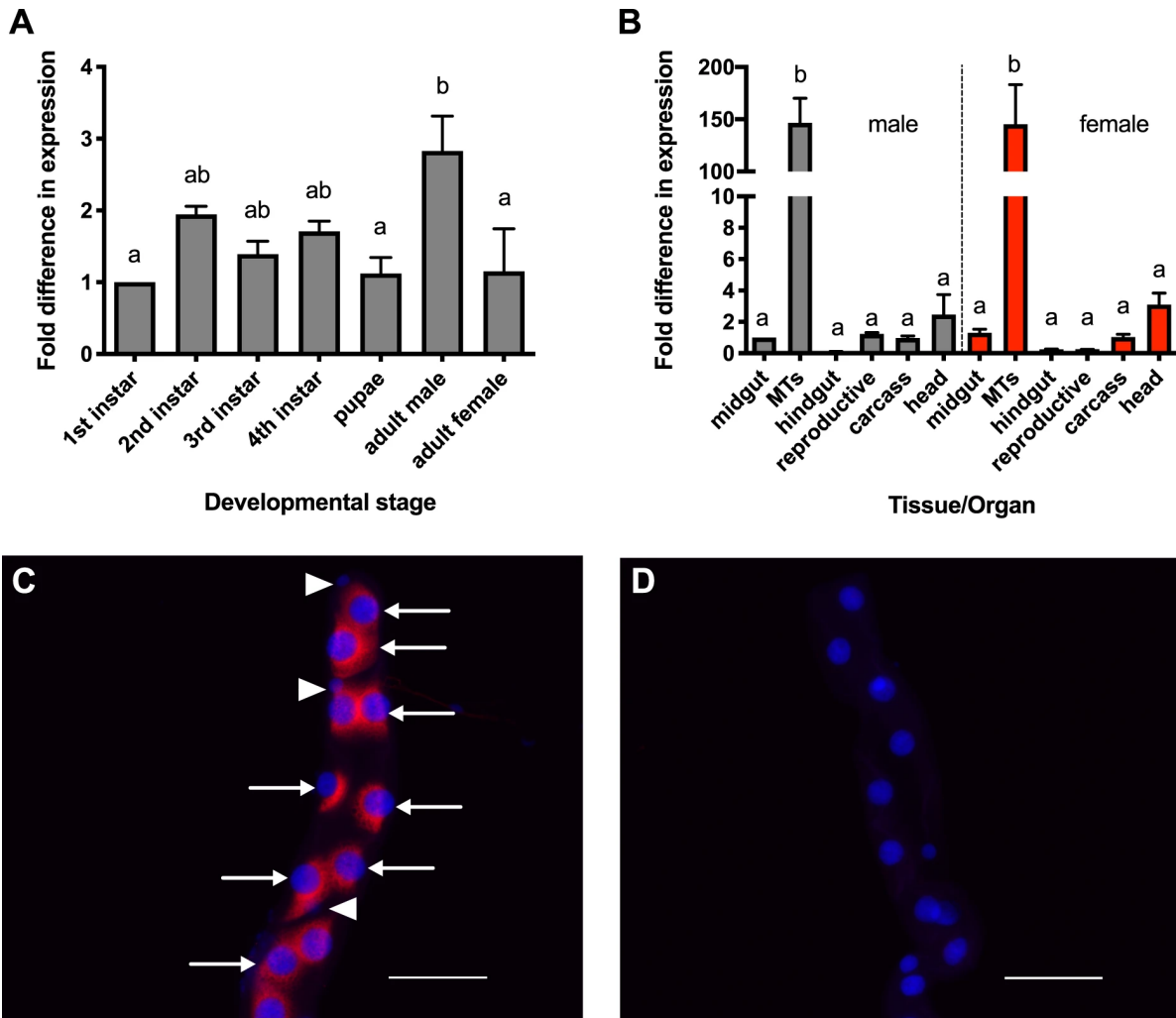


**Figure 3-2. Expression analysis of *CAPAr* transcript in the mosquito, *A. aegypti*.** (A) Ontogenic expression profile of *CAPAr* transcript over post-embryonic stages of the *A. aegypti* mosquito shown relative to transcript levels in 1<sup>st</sup> instar larvae. (B) Spatial expression is analyzed in various tissues/organs from four-day old adult females, with transcript abundance shown relative to levels in the male midgut. (C) Cell-specific expression of *CAPAr* mRNA in principal cells (arrows) of MTs from adult female *A. aegypti* detected using an anti-sense probe, with no detection in the stellate cells (arrowheads). (B) No signal was detected in preparations hybridized with control *CAPAr* sense probe. All images acquired using identical microscope settings; scale bars in (C,D) are 100  $\mu$ m.

### ***CAPA* transcript and mature neuropeptide immunolocalization within the abdominal ganglia**

*CAPA*-like immunoreactivity was localized within all six of the abdominal ganglia, including the terminal ganglion of the ventral nerve cord in the central nervous system. Specifically, each abdominal ganglion contains a pair of ventrally-localized strongly immunoreactive neurosecretory cells (Figure 3-3A-C). Axonal projections from these *CAPA*-like immunoreactive neurosecretory cells emanate dorsally and anteriorly within each ganglion, exiting via the median nerve (Figure 3-3C). Weakly staining *CAPA*-like immunoreactive cells were also observed in other regions of the central nervous system, including the brain, suboesophageal ganglion and thoracic ganglia (Figure 3-S1); however, *CAPA* transcript was significantly enriched (~140-fold) only within the abdominal ganglia but not in other regions of the nervous system (Figure 3-S2). Within the abdominal ganglia, *CAPA* transcript was localized within each pair of strongly staining *CAPA*-like immunoreactive neurosecretory cells (Figure 3-3D,E). Preparations treated with *CAPA* transcript sense probes did not detect any cells in the abdominal ganglia nor anywhere else in the central nervous system.

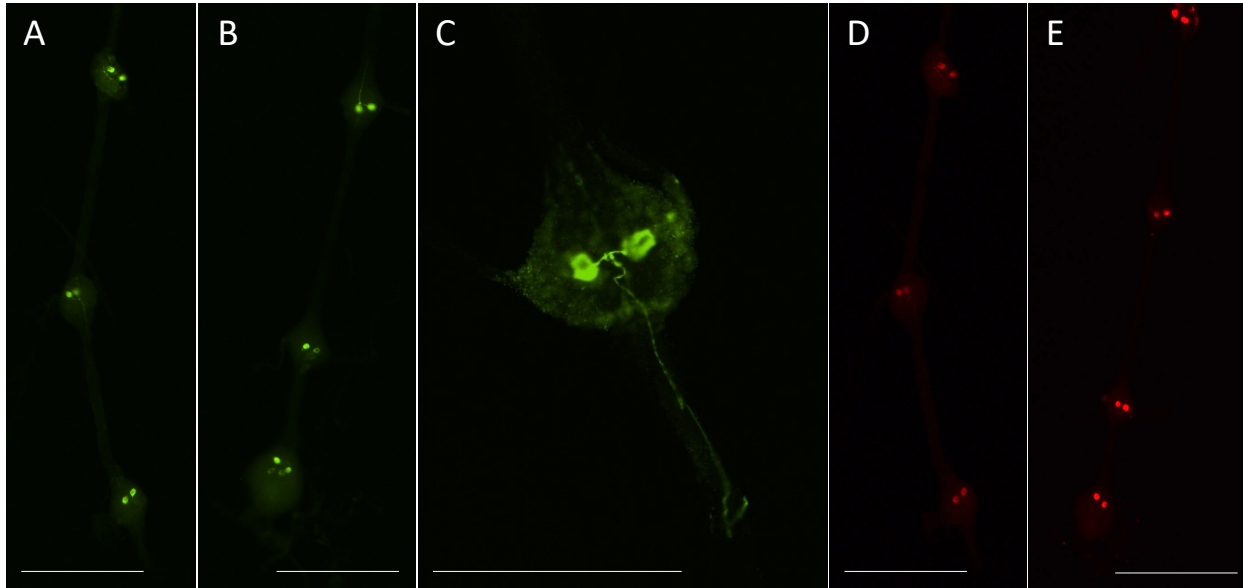


**Figure 3-3. Mapping of anti-diuretic hormone in the abdominal ganglia of the central nervous system in adult *A. aegypti*.** (A-C) Immunohistochemical distribution of CAPA neuropeptides in the abdominal ganglia (AG); specifically, a pair of highly immunoreactive neurosecretory cells within the (A,B) abdominal ganglia. Higher magnification of AG3 (C) demonstrating CAPA immunoreactivity within ventrally-positioned neurosecretory cells with axonal projections emanating dorsally within the ganglia and projecting anteriorly into the median nerve. (D,E) *CAPA* transcript localization by fluorescent *in situ* hybridization revealing pairs of neurons within each (D) AG1–3 (E) AG3–6. Scale bars: 200  $\mu\text{m}$  (A,B,D,E) and 100  $\mu\text{m}$  (C).

### ***CAPAr* knockdown abolishes anti-diuretic hormone activity**

To confirm that the anti-diuretic hormone action of the CAPA neuropeptides is mediated through this specific receptor expressed within the principal cells of the MTs, one day-old female *A. aegypti* were injected with ds*CAPAr* to knockdown *CAPAr* transcript levels. Relative to control mosquitoes injected with ds*ARG* (encoded ampicillin-resistance gene cloned from standard plasmid vector), *CAPAr* transcript was significantly reduced by ~75% in four-day old females (Figure 3-4A). With significant knockdown verified in four-day old adult mosquito samples from the same experimental cohort, a modified Ramsay assay was conducted as previously described (see Chapter 2; Sajadi et al., 2018) on dsRNA-treated females to examine whether the anti-diuretic hormone activity of a CAPA anti-diuretic hormone was compromised. The results confirmed that the CAPA neuropeptide, specifically *AedaeCAPA-1*, had no inhibitory activity against DH<sub>31</sub>-stimulated MTs in *CAPAr* knockdown females (Figure 3-4B). In contrast, *AedaeCAPA-1* potently inhibited DH<sub>31</sub>-stimulated fluid secretion by MTs in ds*ARG*-treated control female mosquitoes (Figure 3-4B).

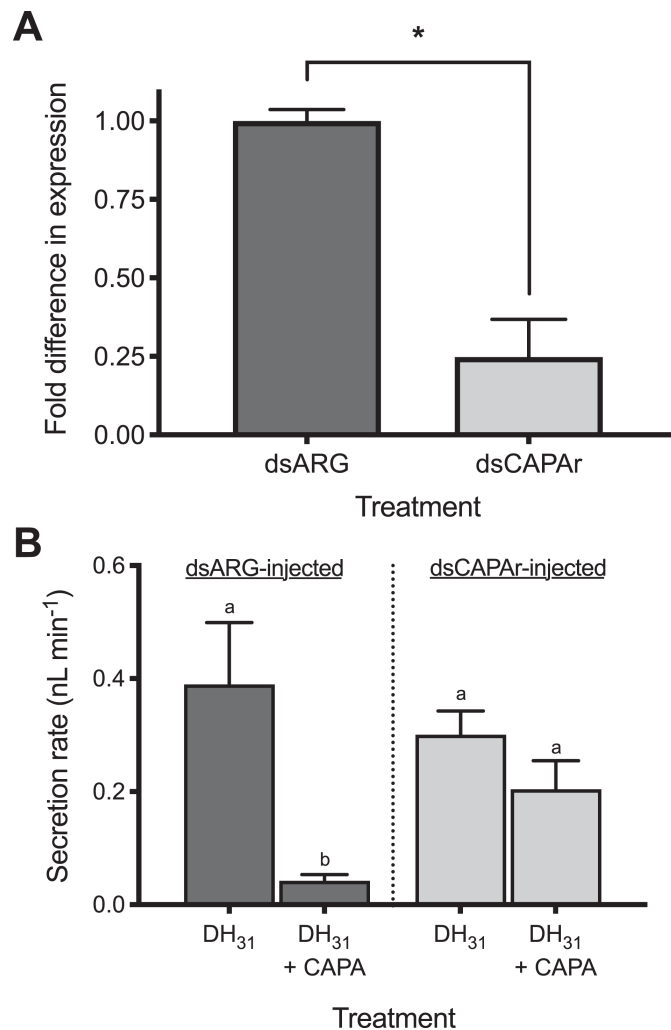


**Figure 3-4. RNA interference (RNAi) of *CAPAr* abolishes anti-diuretic activity of CAPA neuropeptide on adult female *A. aegypti* MTs.** (A) Verification of significant knockdown (>75%) of *CAPAr* transcript in MTs of four-day old adult female *A. aegypti* by RNAi achieved through injection of ds*CAPAr* on day one post-eclosion. (B) Functional consequences of *CAPAr* knockdown demonstrating loss of anti-diuretic hormone activity by *AedaeCAPA*-1 against *DromeDH*<sub>31</sub>-stimulated fluid secretion by MTs. In (A), knockdown of *CAPAr* transcript was analyzed by one-tailed t-test (\* denotes significant knockdown,  $p < 0.01$ ). In (B), fluid secretion rates by MTs presented as mean $\pm$ SEM and analyzed by one-way ANOVA and Tukey's multiple comparison post-test, where different letters denote treatments that are significantly different ( $p < 0.05$ ,  $n = 14-33$ ).

### **Effect of pharmacological blockade on the inhibition of fluid secretion**

To further understand the anti-diuretic signalling pathway involving the CAPA neuroendocrine system, pharmacological blockers, including inhibitors of NOS ( $L$ -NAME) and PKG (KT5823), were tested against diuretic hormone-stimulated MTs alone and together with either *Aedae*CAPA-1 or cGMP. In  $DH_{31}$ -stimulated MTs,  $L$ -NAME had no influence on the inhibitory effect of cGMP whereas the inhibitory effect of *Aedae*CAPA-1 was abolished (Figure 3-5A). In 5HT-stimulated MTs, the results indicate that neither *Aedae*CAPA-1 nor cGMP inhibition are influenced by  $L$ -NAME (Figure 3-5B). Application of KT5823 abolished the inhibitory effect of both cGMP and *Aedae*CAPA-1 in  $DH_{31}$ -stimulated MTs (Figure 3-6A). Similarly, the inhibitory activity of *Aedae*CAPA-1 and cGMP on 5HT-stimulated tubules was abolished when treated with KT5823 (Figure 3-6B). Collectively, these results indicate that *Aedae*CAPA-1 inhibits select diuretic factors acting on the principal cells and involves NO and cGMP as a second messenger in  $DH_{31}$ -stimulated tubules, whereas cGMP, but not NO, is critical in the anti-diuretic activity of *Aedae*CAPA-1 on 5HT-stimulated MTs.

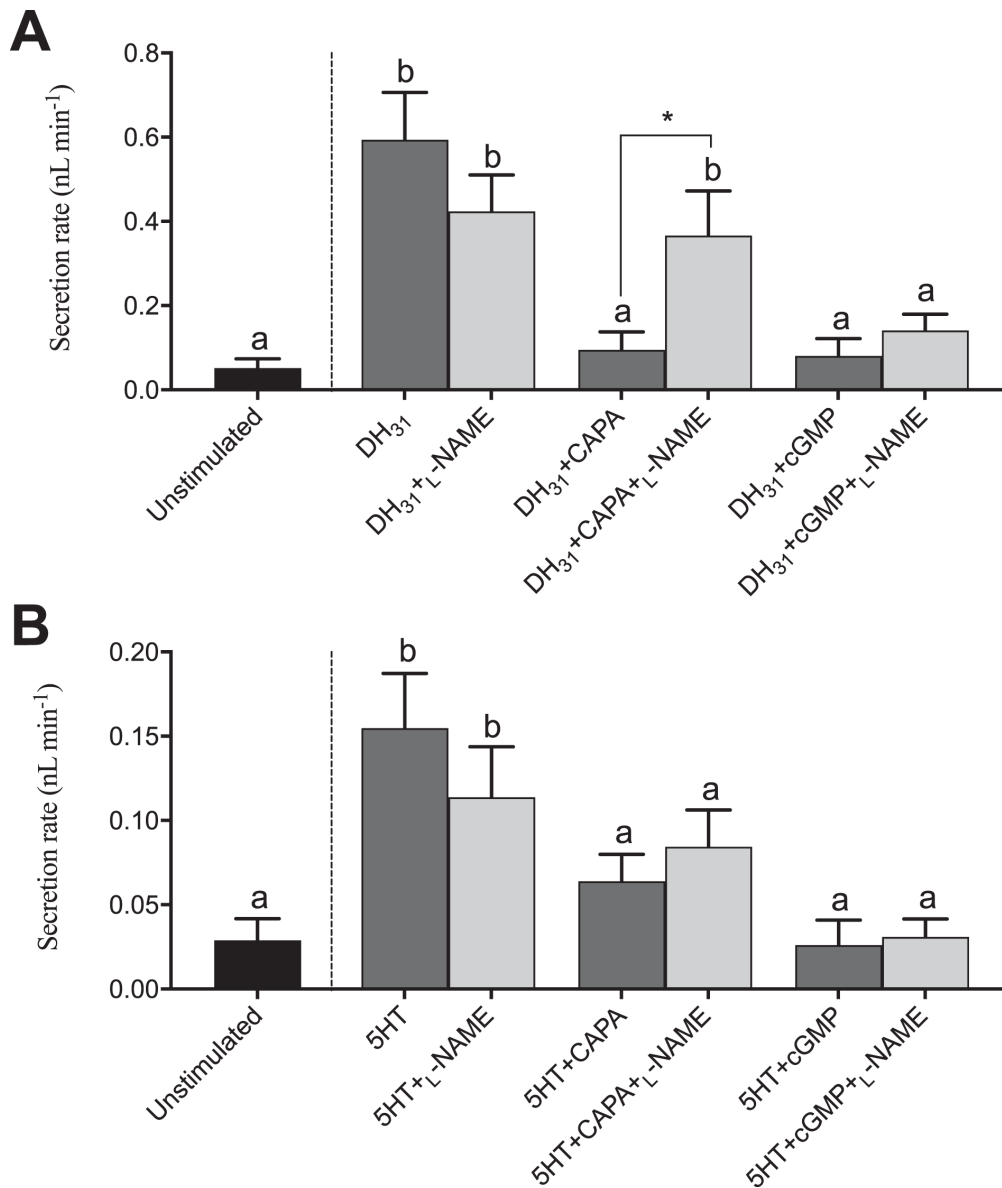


**Figure 3-5. Effect of a nitric oxide synthase (NOS) inhibitor ( $L$ -NAME) on the anti-diuretic activity of *Aedae*CAPA-1 and cGMP in *Drome*DH<sub>31</sub>- and 5HT-stimulated *A. aegypti* MTs.** The NOS inhibitor,  $L$ -NAME, was applied against (A) *Drome*DH<sub>31</sub>- and (B) 5HT-stimulated MTs alone or in the presence of either *Aedae*CAPA-1 or cGMP. Secretion rates are presented as mean $\pm$ SEM, n=17–22. Columns that are significantly different from unstimulated controls are denoted with a distinct letter, as determined by a one-way ANOVA and Bonferroni post-test ( $p < 0.05$ ).

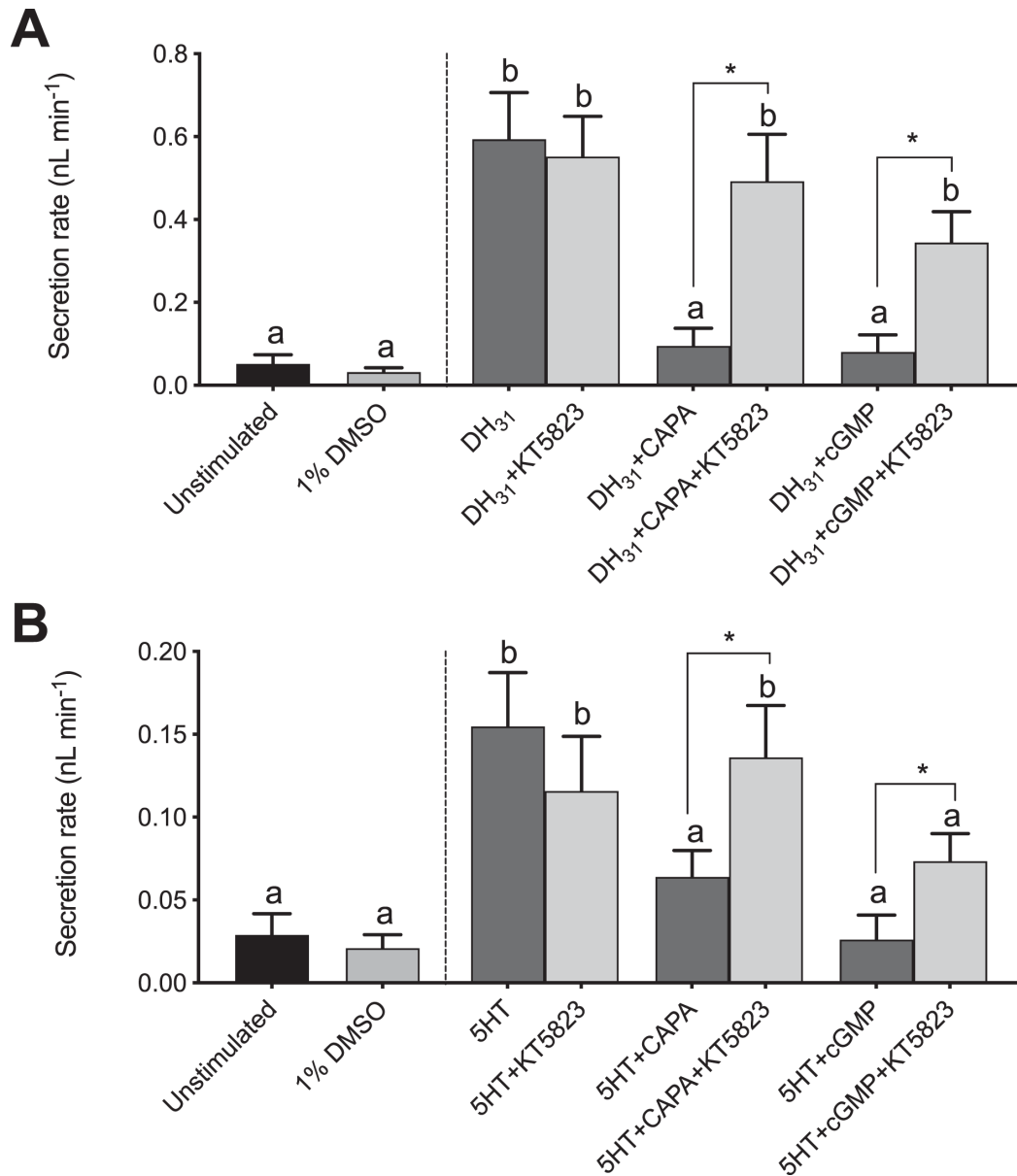


**Figure 3-6. Effect of a protein kinase G (PKG) inhibitor (KT5823) on the anti-diuretic activity of *Aedae*CAPA-1 and cGMP in *Drome*DH<sub>31</sub>- and 5HT-stimulated *A. aegypti* MTs.** The PKG inhibitor, KT5823, was applied against (A) *Drome*DH<sub>31</sub>- and (B) 5HT-stimulated MTs alone or in the presence of either *Aedae*CAPA-1 or cGMP. Secretion rates are presented as mean±SEM, n=16–25. Columns that are significantly different from unstimulated controls are denoted with a distinct letter, as determined by a one-way ANOVA and Bonferroni post-test (p<0.05).

### 3.5 Discussion

Like many animals, insects must regulate the ionic and osmotic levels of their internal environment to ensure homeostatic levels of water and electrolytes are maintained. This is critical not only for challenges linked to feeding, including the intake of too much or too little water and/or ions, but is also important for daily exchange of these elements with the environment through other routes such as waste elimination or water loss during respiration. The insect excretory system acts to maintain hydromineral balance of the haemolymph by either increasing the removal of water and/or ions in excess or the recycling of these same elements when in short supply. The insect Malpighian ‘renal’ tubules (MTs) play a key role as the organ responsible for primary urine production, which can then be modified by downstream elements of the excretory system such as the hindgut (Coast et al., 2002). The MTs are the chief iono- and osmoregulatory organ and are under rigorous control by neuroendocrine factors, including both diuretic hormones (DHs) and anti-diuretic hormones (ADHs), which regulate transepithelial movement of ions and osmotically obliged water. These hormones consist of a variety of peptides as well as other neurochemicals produced by neurosecretory cells in the brain and ventral nerve cord (Beyenbach, 2003; Coast, 2009). Classically, DHs stimulate primary urine secretion by the MTs, whereas ADHs increase fluid reabsorption from the hindgut (Coast, 2007; Phillips, 1981). However, countless studies in diverse insect species have established that ADHs can also act on the MTs to reduce primary urine secretion (Chapter 2; Sajadi et al., 2018 Eigenheer et al., 2003; Ionescu and Donini, 2012; Paluzzi and Orchard, 2006; Quinlan and O’Donnell, 1998; Rodan et al., 2012). CAPA neuropeptides have been demonstrated to display potent anti-diuretic effects in a variety of insects (Coast et al., 2011; Paluzzi et al., 2012; Quinlan and O’Donnell, 1998; Wiehart et al., 2002), including *A. aegypti* mosquitoes (Ionescu and

Donini, 2012; Chapter 2; Sajadi et al., 2018), while they have been shown to function as DHs and ADHs in *D. melanogaster* (Davies et al., 1997; Kean et al., 2002; MacMillan et al., 2018; Rodan et al., 2012).

The current study provides definitive evidence supporting the importance of this anti-diuretic hormone system in the disease vector mosquito, *A. aegypti*, by characterization and functional deorphanization of an anti-diuretic hormone receptor that is highly enriched in the MTs and demonstrates high selectivity for the mosquito CAPA neuropeptides. Previous studies have functionally deorphanized a number of CAPA receptor orthologs in other insects including dipterans (Terhzaz et al., 2012; Olsen et al., 2007; Iverson et al., 2002; Park et al., 2002), lepidopterans (Shen et al., 2017), coleopterans (Jiang et al., 2014), hemipterans (Paluzzi et al., 2010), as well as in the southern cattle tick (Yang et al., 2013). Here, we have functionally validated the specific ligands of the elusive *A. aegypti* CAPA receptor demonstrating that two of the peptides encoded by the mosquito CAPA gene (Predel et al., 2010), *Aedae*-CAPA-1 and -CAPA-2, potentially activate this receptor leading to calcium signalling that elicits a bioluminescent response. While none of the other tested ligands representing multiple insect peptide families were active on the mosquito CAPA receptor, the third peptide encoded by the CAPA gene, *Aedae*PK-1, had lower agonist activity with a potency of over five orders of magnitude lower compared to the canonical CAPA ligands. *Aedae*PK-1 is a member of the pyrokinin-1 family of peptides that contain the GXWFGPRL-NH<sub>2</sub> (where normally X = V, M or L) consensus C-terminal sequence and recently a revised tryptopyrokinin nomenclature has been adopted to differentiate these neuropeptides from distinct pyrokinin families (Veenstra, 2014). In agreement with our findings, a subset of previous studies on insect CAPA receptor orthologs have been shown minor responsiveness to tryptopyrokinin ligands, with high doses eliciting low

level CAPA receptor activation (Shen et al., 2017; Jiang et al., 2014; Paluzzi et al., 2010). Interestingly, this minor promiscuousness has not been observed for other dipteran CAPA receptors characterized previously (Olsen et al., 2017; Iverson et al., 2002; Park et al., 2002).

Members of the insect CAPA neuropeptide family are often also referred to as periviscerokinins due to their myotropic activity on visceral muscle and their source of release from the segmental abdominal neurohaemal organs known as perivisceral/perisymphatic organs (Paluzzi and Orchard, 2006; Predel and Wegener, 2006; Jiang et al., 2014). Herein, we have immunolocalized CAPA neuropeptides within a pair of ventral neurosecretory cells within each abdominal ganglia, whose axonal projections extend dorsally and anteriorly exiting each abdominal ganglion via the median nerve. CAPA immunoreactivity extends towards and is localized to the abdominal neurohaemal organs, the perivisceral organs, where these neuropeptides can be released into the haemolymph to elicit their neurohaemal actions on target sites expressing the CAPA receptor (Sajadi et al., 2020). The *CAPA* transcript was highly enriched within the abdominal ganglia of adult mosquitoes, confirming the transcript encoding the anti-diuretic hormone prepropeptide colocalized to these same neurosecretory cells. In support of these findings, peptidomic approaches using MALDI-TOF mass spectrometry have previously provided evidence for the presence of putative CAPA neuropeptides within isolated abdominal ganglia, including the terminal ganglion, from adult *A. aegypti* (Predel et al., 2010). Collectively, these findings establish that the transcript and the mature peptide are present within the adult mosquito abdominal ganglia with the neurohormones being released into the insect circulatory system to act upon target tissues. Lastly, considering the low level CAPA transcript and immunoreactivity detected in other regions of the nervous system indicates that the abdominal ganglia, and their associated neurohaemal organs, are the primary source of the anti-

diuretic hormone in adult *A. aegypti*. This also corroborates earlier peptidomic studies indicating the absence of CAPA peptides, or differential processing of the CAPA precursor, in other regions of the nervous system aside from the abdominal ganglia where these neuropeptides are highly abundant (Predel et al., 2010; Predel et al., 2004; Wegener et al., 2006).

Having established the origin of the CAPA neuropeptide anti-diuretic hormones and their potent activity on the heterologously expressed CAPA receptor, we next aimed to confirm the expression profile of the transcript encoding the CAPA receptor. Expression of *CAPAr* was observed in all post-embryonic ontogenic stages with significant enrichment in adult male mosquitoes, compared to females. Although the biological relevance of this differential expression remains unclear, this may relate to the sexual size dimorphism between adult male and female *A. aegypti* (Wormington and Juliano, 2014), with the smaller males being inherently more susceptible to desiccation stress due to their higher surface area to volume ratio. In other insects, *CAPAr* transcript expression has been observed throughout most post-embryonic developmental stages (Iverson et al., 2002; Jiang et al., 2014; Graveley et al., 2011). The MTs are composed of two cell types forming a simple epithelium; large principal cells and thin stellate cells (Beyenbach, 2003). Principal cells facilitate the active transport of cations ( $\text{Na}^+$  and  $\text{K}^+$ ) into the lumen of the MTs from the haemolymph, while the stellate cells facilitate the transepithelial secretion of  $\text{Cl}^-$ , the predominant inorganic anion (O'Donnell et al., 1996). In adult stages, expression analysis of *CAPAr* verified significant enrichment of this receptor in the MTs in both male and female mosquitoes. Furthermore, cell-specific expression mapping confirmed that the *CAPAr* transcript is restricted to the principal cells of the MTs and absent in the smaller stellate cells. In other insects, *CAPAr* transcript has been detected in various regions of the alimentary canal (Chintapalli et al., 2007; Jiang et al., 2014; Paluzzi et al., 2010),

including the principal cells of the MTs where this receptor is exclusively expressed in the fruit fly (Terhzaz et al., 2012). Interestingly, the *D. melanogaster* CAPA hormonal circuit has been recently reported to play a critical role in regulating metabolic homeostasis through actions on additional alimentary canal organs where its receptor is expressed including the brain, midgut enteroendocrine cells along with visceral muscle in the anterior and posterior midgut and the hindgut (Koyama et al., 2021). All in all, these observations are in line with well-known physiological roles established for CAPA neuropeptides, which have been shown to modulate rates of fluid secretion by MTs in various insects (Coast et al., 2010; Ionescu and Donini, 2012; Petzel et al., 1987; Raabe et al., 1966; Ramsay, 1954). In dipterans, these effects are mediated via action on the principal cells acting through a second messenger cascade involving calcium, nitric oxide, and cGMP signalling (Davies et al., 2012; Pollock et al., 2004).

We next examined whether normal anti-diuretic hormone signalling, which requires the neuronally-derived CAPA peptide hormones activating their receptor expressed in the principal cells of the MTs, could be impeded by using RNA interference against the *CAPAr* transcript. One-day old mosquitoes were injected with *CAPAr*-targeted dsRNA resulting in knockdown at four-day old, where *CAPAr* transcript was significantly reduced. We examined whether *CAPAr* knockdown females retained sensitivity to CAPA peptides, which have been shown to inhibit fluid secretion by MTs by select diuretic hormones (see Chapter 2; Sajadi et al., 2018). Indeed, *CAPAr* knockdown abolished the anti-diuretic activity of a CAPA neuropeptide against MTs stimulated with *DromeDH*<sub>31</sub>, an analog of mosquito natriuretic peptide. Collectively, through RNAi-mediated knockdown, these findings confirm that mosquito anti-diuretic hormones, which belong to the CAPA peptide family, are produced in pairs of neurosecretory cells in each of the abdominal ganglia whereby they are released through the neurohaemal organs and influence the

MTs by acting on their receptor expressed within the principal cells of this organ. Further, the results confirm that sustained anti-diuretic hormone signalling, which requires the steady state expression of ligand and receptor, is necessary for facilitating the anti-diuretic control of the MTs.

In *D. melanogaster* and other dipterans, CAPA peptides have been shown to stimulate the nitric oxide (NO)/cGMP signalling pathway to induce diuresis (Pollock et al., 2004). When released, CAPA peptides bind to GPCRs found in principal (type I) cells of MTs, increasing  $Ca^{2+}$  levels in the cell through activation of L-type voltage gated calcium channels (MacPherson et al., 2001). The influx of  $Ca^{2+}$  through these channels activates NOS, causing the production of NO, which subsequently activates guanylate cyclase to increase levels of cGMP in the MTs (Terhzaz et al., 2012). Ultimately, the activation of the NO/cGMP pathway stimulates the apical V-type  $H^+$ -ATPase (proton pump), to increase fluid secretion in *D. melanogaster*. In the mosquito *A. aegypti*, CAPA peptides lead to activation of PKG, via elevated levels of cGMP and exogenous cGMP considerably inhibits fluid secretion rate (see Chapter 2; Sajadi et al., 2018). Herein, this current study sought to establish the roles of NO, cGMP and PKG on the anti-diuretic effects of CAPA peptides on adult mosquito MTs. Inhibitory doses of cGMP and a CAPA neuropeptide, namely *Aedae*CAPA-1, were treated with a NOS inhibitor, L-NAME, and a PKG inhibitor, KT5823. These investigations established that L-NAME did not alter the inhibitory effects of exogenous cGMP since this drug inhibits NOS, which is upstream of cGMP and, as a result, inhibition of  $DH_{31}$ -stimulated secretion was unaffected. Contrastingly, *Aedae*CAPA-1 mediated inhibition of  $DH_{31}$ -stimulated MTs was mitigated in the presence of L-NAME, reducing the anti-diuretic effects observed with *Aedae*CAPA-1. Comparatively, these findings are similar but are not identical to the effects of the PKG inhibitor, KT5823, which abolished the anti-diuretic

activity of both *Aedae*CAPA-1 and cGMP, resulting in normal DH<sub>31</sub>-induced diuresis. Similar results were observed in 5HT-stimulated MTs with one exception; *Aedae*CAPA-1 inhibition appeared to be independent of NOS since L-NAME had no influence on the anti-diuretic activity of *Aedae*CAPA-1 in 5HT-stimulated MTs. Interestingly, the inhibition of both DH<sub>31</sub>- and 5HT-stimulated diuresis by *Aedae*CAPA-1 and cGMP were sensitive to the PKG inhibitor, KT5823, which indicates that while some differences in signalling associated with inhibition of different diuretic hormones may occur, these inhibitory pathways likely converge and involve cGMP activating protein kinase G. Taken together, the findings in this study provide definitive evidence that CAPA peptides are anti-diuretic hormones in the mosquito *A. aegypti*, which inhibit fluid secretion of adult mosquito MTs through a signalling cascade involving the NOS/cGMP/PKG pathway. Further studies are necessary in mosquitoes as well as other insects to elucidate the differential regulation by DHs and ADHs given ample data supporting that cGMP and related effectors can be both stimulatory (Davies et al., 1995; Davies et al., 1997; Davies et al., 2012; Ionescu and Donini, 2012; Terhzaz et al., 2012) and inhibitory (Ionescu and Donini, 2012; Massaro et al., 2004; Paluzzi and Orchard, 2006; Quinlan and O'Donnell, 1998; Ruka et al., 2013; Wormington and Juliano, 2014; MacMillan et al., 2018) in their control on insect MTs. In conclusion, this study has characterized an anti-diuretic hormone system in the adult mosquito *A. aegypti* providing evidence of a neural-renal axis whereby the neuropeptidergic anti-diuretic hormone is released by the abdominal segmental neurohaemal organs and subsequently targets its cognate receptor expressed within the principal cells of the MTs to counteract the activity of a subset of mosquito diuretic hormones. Fine-tuning of stimulatory and inhibitory hormones controlling the insect excretory system is of utmost importance to ensure overall organismal

homeostasis to combat variable environmental conditions or feeding-related states that could perturb hydromineral balance if left unregulated.

### 3.6 References

- Audsley, N., and Phillips, J. E.** (1990). Stimulants of ileal salt transport in neuroendocrine system of the desert locust. *Gen. Comp. Endocrinol.* **80**, 127–137.
- Audsley, N., McIntosh, C., and Phillips, J. E.** (1992). Actions of ion-transport peptide from locust corpus cardiacum on several hindgut transport processes. *J. Exp. Biol.* **173**, 275–288.
- Audsley, N., Meredith, J., and Phillips, J. E.** (2006). Haemolymph levels of *Schistocerca gregaria* ion transport peptide and ion transport-like peptide. *Physiol. Entomol.* **31**, 154–163.
- Audsley, N., Jensen, D., and Schooley, D. A.** (2013). Signal transduction for *Schistocerca gregaria* ion transport peptide is mediated via both cyclic AMP and cyclic GMP. *Peptides* **41**, 74–80.
- Baldwin, D. C., Schegg, K. M., Furuya, K., Lehmborg, E., and Schooley, D. A.** (2001). Isolation and identification of a diuretic hormone from *Zootermopsis nevadensis*. *Peptides* **22**, 147–152.
- Beyenbach, K. W.** (2003). Transport mechanisms of diuresis in Malpighian tubules of insects. *J. Exp. Biol.* **206**, 3845–3856.
- Cabrero, P., Radford, J. C., Broderick, K. E., Costes, L., Veenstra, J. A., Spana, E. P., Davies, S. A., and Dow, J. A. T.** (2002). The Dh gene of *Drosophila melanogaster* encodes a diuretic peptide that acts through cyclic AMP. *J. Exp. Biol.* **205**, 3799–3807.
- Cantera, R., and Nässel, D. R.** (1991). Dual peptidergic innervation of the blowfly hindgut: A light- and electron microscopic study of FMRFamide and proctolin immunoreactive fibers. *Comp. Biochem. and Physiol.* **99**, 517–525.
- Chintapalli, V. R., Wang, J., and Dow, J. A.** (2007). Using FlyAtlas to identify better *Drosophila melanogaster* models of human disease. *Nat. Genet.* **39**, 715–720.

- Clark, T. M., and Bradley, T. J.** (1998). Additive effects of 5-HT and diuretic peptide on *Aedes* Malpighian tubule fluid secretion. *Comp. Biochem. Physiol. - A Mol. Integr. Physiol.* **119**, 599–605.
- Coast, G.** (2007). The endocrine control of salt balance in insects. *Gen. Comp. Endocrinol.* **152**, 332–338.
- Coast, G. M.** (2009). Neuroendocrine control of ionic homeostasis in blood-sucking insects. *J. Exp. Biol.* **212**, 378–386.
- Coast, G. M., Orchard, I., Phillips, J. E., and Schooley, D. A.** (2002). Insect diuretic and antidiuretic hormones. *Adv. Insect Phys.* **29**, 279–409.
- Coast, G. M., Garside, C. S., Webster, S. G., Schegg, K. M., and Schooley, D. A.** (2005). Mosquito natriuretic peptide identified as a calcitonin-like diuretic hormone in *Anopheles gambiae* (Giles). *J. Exp. Biol.* **208**, 3281–3291.
- Coast, G. M., TeBrugge, V. A., Nachman, R. J., Lopez, J., Aldrich, J. R., Lange, A., and Orchard, I.** (2010). Neurohormones implicated in the control of Malpighian tubule secretion in plant sucking heteropterans: the stink bugs *Acrosternum hilare* and *Nezara viridula*. *Peptides* **31**, 468–473.
- Coast, G. M., Nachman, R. J., and Lopez, J.** (2011). The control of Malpighian tubule secretion in a predacious hemipteran insect, the spined soldier bug *Podisus maculiventris* (Heteroptera, Pentatomidae). *Peptides* **32** 493–499.
- Davies, S. A., Huesmann, G. R., Maddrell, S. H. P., O'Donnell, M. J., Skaer, N. J. V., Dow, J. A. T., and Tublitz, N. J.** (1995). CAP(2b), a cardioacceleratory peptide, is present in *Drosophila* and stimulates tubule fluid secretion via cGMP. *Am. J. Physiol.* **269**, R1321–R1236.

- Davies, S. A., Stewart, E. J., Huesmann, G. R., Skaer, N. J. V., Maddrell, S. H. P., Tublitz, N. J., and Dow, J. A. T.** (1997). Neuropeptide stimulation of the nitric oxide signaling pathway in *Drosophila melanogaster* Malpighian tubules. *Am. J. Physiol.* **273**, R823–R827.
- Davies, S. A., Cabrero, P., Povsic, M., Johnston, N. R., Terhzaz, S., and Dow, J. A. T.** (2012). Signaling by *Drosophila* capa neuropeptides. *Gen. Comp. Endocrinol.* **188**, 60–66.
- Donini, A., O'Donnell, M. J., and Orchard, I.** (2008). Differential actions of diuretic factors on the Malpighian tubules of *Rhodnius prolixus*. *J. Exp. Biol.* **211**, 42–48.
- Durant, A. C., Chasiotis, H., Misyura, L., and Donini, A.** (2017). *Aedes aegypti* Rhesus glycoproteins contribute to ammonia excretion by larval anal papillae. *J. Exp. Biol.* **220**, 588–596.
- Eckert, M., Herbert, Z., Pollák, E., Molnár, L., and Predel, R.** (2002). Identical cellular distribution of all abundant neuropeptides in the major abdominal neurohemal system of an insect (*Periplaneta americana*). *J. Comp. Neurol.* **452**, 264–275.
- Eigenheer, R. A., Nicolson, S. W., Schegg, K. M., Hul, J. J., and Schooley, D. A.** (2002). Identification of a potent antidiuretic factor acting on beetle Malpighian tubules. *Proc. Natl. Acad. Sci. USA* **99**, 84–89.
- Eigenheer, R. A., Wiehart, U. M., Nicolson, S. W., Schoofs, L., Schegg, K. M., Hull, J. J., and Schooley, D. A.** (2003). Isolation, identification and localization of a second beetle antidiuretic peptide. *Peptides* **24**, 27–34.
- Furuya, K., Milchak, R. J., Schegg, K. M., Zhang, J., Tobe, S. S., Coast, G. M., and Schooley, D. A.** (2000). Cockroach diuretic hormones: characterization of a calcitonin-like peptide in insects. *Proc. Natl. Acad. Sci. USA* **97**, 6469–6474.

- Gabilondo, H., Losada-Pérez, M., Del Saz, D., Molina, I., León, Y., Canal, I., Torroja, L., and Benito-Sipos, J.** (2011). A targeted genetic screen identifies crucial players in the specification of the *Drosophila* abdominal Capaergic neurons. *Mech. Dev.* **128**, 208–221.
- Gabilondo, H., Rubio-Ferrera, I., Losada-Pérez, M., Del Saz, D., León, Y., Molina, I., Torroja, L., Allan, D. W., and Benito-Sipos, J.** (2018). Segmentally homologous neurons acquire two different terminal neuropeptidergic fates in the *Drosophila* nervous system. *PLoS One* **13**, e0194281.
- Gäde, G.** (2004). Regulation of intermediary metabolism and water balance of insects by neuropeptides. *Annu. Rev. Entomol.* **49**, 93–113.
- Graveley, B. R., Brooks, A. N., Carlson, J. W., Duff, M. O., Landolin, J. M., Yang, L., Artieri, C. G., van Baren, M. J., Boley, N. Booth, B. W., et al.** (2011). The developmental transcriptome of *Drosophila melanogaster*. *Nat.* **471**, 473–479.
- Gondalia, K., Qudrat, A., Bruno, B., Fleites Medina, J., and Paluzzi J. P.** (2016). Identification and functional characterization of a pyrokinin neuropeptide receptor in the Lyme disease vector, *Ixodes scapularis*. *Peptides* **89**, 42–54.
- He, Q., Wu, B., Price, J. L., and Zhao, Z.** (2017). Circadian rhythm neuropeptides in *Drosophila*: signals for normal circadian function and circadian neurodegenerative disease. *Int. J. Mol. Sci.* **18**, 886.
- Hillyer, J. F.** (2018). Insect heart rhythmicity is modulated by evolutionarily conserved neuropeptides and neurotransmitters. *Curr. Opin. Insect Sci.* **29**, 41–48.
- Ionescu, A., and Donini, A.** (2012). *Aedes* CAPA-PVK-1 displays diuretic and dose dependent antidiuretic potential in the larval mosquito *Aedes aegypti* (Liverpool). *J. Insect Physiol.* **58**, 1299–1306.

- Iverson, A., Cazzamali, G., Williamson, M., Hauser, F., and Grimmelikhujzen, C. J.** (2002). Molecular cloning and functional expression of a *Drosophila* receptor for the neuropeptides capa-1 and -2. *Biochem. Biophys. Res. Commun.* **229**, 628–633.
- Jiang, H., Wei, Z., Nachman, R. J., Adams, M. E., and Park, Y.** (2014). Functional phylogenetics reveals contributions of pleiotropic peptide action to ligand-receptor coevolution. *Sci. Rep.* **4**, 6800.
- Jurenka, R.** (2015). The PRXamide neuropeptide signalling system, conserved in animals. *Adv. Insect Physiol.* **49**, 123–170.
- Kean, L., Cazenave, W., Costes, L., Broderick, K. E., Graham, S., Pollock, V. P., Davies, S. A., Veenstra, J. A., and Dow, J. A. T.** (2002). Two nitridergic peptides are encoded by the gene capability in *Drosophila melanogaster*. *Am. J. Physiol. Regul. Integr. Comp. Physiol.* **282**, R1297–R1307.
- Koyama, T., Terhzaz, S., Naseem, T., Nagy, S., Rewitz, K., Dow, J. A. T., Davies, S. A., and Halberg, K. V.** (2021). A nutrient-responsive hormonal circuit mediates an inter-tissue program regulating metabolic homeostasis in adult *Drosophila*. *Nat. Commun.* **12**.
- Laenen, B., de Decker, N., Steels, P., Van Kerkhove, E., and Nicolson, S.** (2001). An antidiuretic factor in the forest ant: purification and physiological effects on the Malpighian tubules. *J. Insect Physiol.* **47**, 185–193.
- Lavigne, C., Embleton, J., Audy, P., King, R. R., and Pelletier, Y.** (2001). Partial purification of a novel insect antidiuretic factor from the Colorado potato beetle, *Leptinotarsa decemlineata* (Say) (Coleoptera: Chrysomelidae), which acts on Malpighian tubules. *Insect Biochem. Mol. Biol.* **31**, 339–347.

- Lehmberg, E., Ota, R. B., Furuya, K., King, D. S., Applebaum, S. W., Ferenz, H. J., and Schooley, D. A.** (1991). Identification of a diuretic hormone of *Locusta migratoria*. *Biochem. Biophys. Res. Commun.* **179**, 1036–1041.
- MacMillan, H. A., Nazal, B., Wali, S., Yerushalm, G. Y., Misyura, L., Donini, A., and Paluzzi, J. P.** (2018). Anti-diuretic activity of a CAPA neuropeptide can compromise *Drosophila* chill tolerance. *J. Exp. Biol.* **221**, doi: 10.1242/jeb.185884.
- MacPherson, M. R., Pollock, V. P., Broderick, K. E., Kean, L., O’Connell, F. C., Dow, J. A. T., and Davies, S. A.** (2001). L-type calcium channels regulate epithelial fluid transport in *Drosophila melanogaster*. *Am. J. Physiol.* **280**, C394–C407.
- Maddrell, S. H. P., Herman, W. S., Mooney, R. L., and Overton, J. A.** (1991). 5-Hydroxytryptamine: a second diuretic hormone in *Rhodnius prolixus*. *J. Exp. Biol.* **156**, 557–566.
- Massaro, R. C., Lee, L. W., Patel, A. B., Wu, D. S., Yu, M. J., Scott, B. N., Schooley, D. A., Schegg, K. M., and Beyenbach, K. W.** (2004). The mechanism of action of the antidiuretic peptide Tenmo ADFa in Malpighian tubules of *Aedes aegypti*. *J. Exp. Biol.* **207**, 2877–2888.
- Nässel, D. R., and Winther, Å. M. E.** (2010). *Drosophila* neuropeptides in regulation of physiology and behavior. *Prog. Neurobiol.* **92**, 42–104.
- O’Donnell, M. J., and Spring, J. H.** (2000). Modes of control of insect Malpighian tubules: synergism, antagonism, cooperation and autonomous regulation. *J. Insect Physiol.* **46**, 107–117.
- Olsen, S. S., Cazzamali, G., Williamson, M., Grimmelikhuijzen, C. J. P., and Hauser, F.** (2007). Identification of one capa and two pyrokinin receptors from the malaria mosquito *Anopheles gambiae*. *Biochem. Biophys. Res. Commun.* **362**, 245–251.

- Oryan, A., Wahedi, A., and Paluzzi, J. P.** (2018). Functional characterization and quantitative expression analysis of two GnRH-related peptide receptors in the mosquito, *Aedes aegypti*. *Biochem. Biophys. Res. Commun.* **497**, 550–557.
- Paluzzi, J. P., and Orchard, I.** (2006). Distribution, activity and evidence for the release of an anti-diuretic peptide in the kissing bug *Rhodnius prolixus*. *J. Exp. Biol.* **209**, 907–915.
- Paluzzi, J. P., and Orchard, I.** (2010). A second gene encodes the anti-diuretic hormone in the insect, *Rhodnius prolixus*. *Mol. Cell Endocrinol.* **317**, 53–63.
- Paluzzi, J. P., Park, Y., Nachman, R. J., and Orchard, I.** (2010). Isolation, expression analysis, and functional characterization of the first antidiuretic hormone receptor in insects. *Proc. Natl. Acad. Sci. USA* **107**, 10290–10295.
- Paluzzi, J. P., Naikhwah, W., and O'Donnell, M. J.** (2012). Natriuresis and diuretic hormone synergism in *R. prolixus* upper Malpighian tubules is inhibited by the anti-diuretic hormone, *RhoprCAPA- $\alpha$ 2*. *J. Insect Physiol.* **58**, 534–542.
- Paluzzi, J. P., Vanderveken, M., and O'Donnell, M. J.** (2014). The heterodimeric glycoprotein hormone, GPA2/GPB5, regulates ion transport across the hindgut of the adult mosquito, *Aedes aegypti*. *PLoS One* **9**, e86386.
- Paluzzi, J. P., Young, P., Defferrari, M. S., Orchard, I., Carlini, C. R., and O'Donnell, M. J.** (2012). Investigation of the potential involvement of eicosanoid metabolites in anti-diuretic hormone signaling in *Rhodnius prolixus*. *Peptides* **34**, 127–134.
- Park, Y., Kim, Y.-J. J. Y.-J., and Adams, M. E.** (2002). Identification of G protein-coupled receptors for *Drosophila* PRXamide peptides, CCAP, corazonin, and AKH supports a theory of ligand-receptor coevolution. *Proc. Natl Acad. Sci. USA* **99**, 11423–11428.

- Petzel, D. H., Berg, M. M., and Beyenbach, K. W.** (1987). Hormone-controlled cAMP-mediated fluid secretion in yellow-fever mosquito. *Am. J. Physiol.* **253**, R701–R711.
- Phillips, J.** (1981). Comparative physiology of insect renal function. *Am. J. Physiol.* **241**, R241–R257.
- Phillips, J. E., Thomson, B., Hanrahan, J., and Chamberlin, M.** (1987). Mechanisms and control of reabsorption in insect hindgut. *Adv. In Insect Phys.* **19**, 329–422.
- Phillips, J. E., Audsley, N., Lechleitner, R., Thomson, B., Meredith, J., and Chamberlin, M.** (1988). Some major transport mechanisms of insect absorptive epithelia. *Comp. Biochem. Physiol. A Comp. Physiol.* **90**, 643–650.
- Pollák, E., Eckert, M., Molnár, L., and Predel, R.** (2005). Differential sorting and packaging of capa-gene related products in an insect. *J. Comp. Neurol.* **481**, 84–95.
- Pollock, V. P., McGettigan, J., Cabrero, P., Maudlin, I. M., Dow, J. A. T., and Davies, S. A.** (2004). Conservation of capa peptide-induced nitric oxide signalling in Diptera. *J. Exp. Biol.* **207**, 4135–4145.
- Predel, R., and Wegener, C.** (2006). Biology of the CAPA peptides in insects. *Cell. Mol. Life Sci.* **63**, 2477–2490.
- Predel, R., Neupert, S., Garczynski, S. F., Crim, J. W., Brown, M. R., Russell, W. K., Kahnt, J., Russell, D. H., and Nachman, R. J.** (2010). Neuropeptidomics of the mosquito *Aedes aegypti*. *J. Proteome Res.* **9**, 2006–2015.
- Predel, R., Wegener, C., Russell, W. K., Tichy, S. E., Russell, D. H., and Nachman, R. J.** (2004). Peptidomics of CNS-associated neurohaemal systems of adult *Drosophila melanogaster*: a mass spectrometric survey of peptides from individual flies. *J. Comp. Neurol.* **474**, 379–392.

- Quinlan, M. C., and O'Donnell, M. J.** (1998). Anti-diuresis in the blood-feeding insect *Rhodnius prolixus* Stål: antagonistic actions of cAMP and cGMP and the role of organic acid transport. *J. Insect Physiol.* **44**, 561–568.
- Quinlan, M. C., Tublitz, N. J., and O'Donnell, M. J.** (1997). Anti-diuresis in the blood-feeding insect *Rhodnius prolixus* Stål: the peptide CAP(2b) and cyclic GMP inhibit Malpighian tubule fluid secretion. *J. Exp. Biol.* **200**, 2363–2367.
- Raabe, M., Cazal, M., Chalaye, D., and de Bessé, N.** (1966). Action cardioaccélétratrice des organes neurohémaux périssymphatiques ventraux des quelques insectes. *C. R. Acad. Sci. Hebd. Seances Acad. Sci. D.* **263**, 2002–2005.
- Rafaeli, A.** (2009). Pheromone biosynthesis activating neuropeptide (PBAN): regulatory role and mode of action. *Gen. Comp. Endocrinol.* **162**, 69–78.
- Raikhel, A. S., Brown, M. R., and Belles, X.** (2005). Hormonal control of reproductive processes. *Compr. Mol. Insect Sci.* **3**, 433–491
- Ramsay, J. A.** (1954). Active transport of water by the Malpighian tubules of the stick insect, *Dixippus morosus* (Orthoptera, Phasmidae). *J. Exp. Biol.* **31**, 104–113.
- Rocco, D. A., Kim, D. H., and Paluzzi, J. P.** (2017). Immunohistochemical mapping and transcript expression of the GPA2/GPB5 receptor in tissues of the adult mosquito, *Aedes aegypti*. *Cell. Tissue. Res.* **369**, 313–330.
- Rodan, A. R., Baum, M., and Huang, C. L.** (2012). The *Drosophila* NKCC Ncc69 is required for normal renal tubule function. *Am. J. Physiol.* **303**, C883–C894.
- Ruka, K. A., Miller, A. P., and Blumenthal, E. M.** (2013). Inhibition of diuretic stimulation of an insect secretory epithelium by a cGMP-dependent protein kinase. *Am. J. Physiol. Renal Physiol.* **304**, F1210–F1216.

- Sajadi, F., Curcuruto, C., Al Dhaheri, A., and Paluzzi, J. P.** (2018). Anti-diuretic action of a CAPA neuropeptide against a subset of diuretic hormones in the disease vector, *Aedes aegypti*. *J. Exp. Biol.* **221**.
- Sajadi, F., Uyuklu, A., Paputsis, C., Lajevardi, A., Wahedi, A., Ber, L. T., Matei, A., and Paluzzi, J. P.** (2020). CAPA neuropeptides and their receptor form an anti-diuretic hormone signaling system in the human disease vector, *Aedes aegypti*. *Sci. Rep.* **1**. <https://doi.org/10.1038/s41598-020-58731-y>.
- Santos, J. G., Pollák, E., Rexer, K. H., Molnár, L., and Wegener, C.** (2006). Morphology and metamorphosis of the peptidergic Va neurons and the median nerve system of the fruit fly, *Drosophila melanogaster*. *Cell Tissue Res.* **326**, 187–199.
- Schoofs, L., De Loof, A., and Van Hiel, M. B.** (2017). Neuropeptides as regulators of behavior in insects. *Annu. Rev. Entomol.* **62**, 35–52.
- Shen, Z., Chen, Y., Hong, L., Cui, Z., Yang, H., He, X., Shi, Y., Shi, L., Han, F., and Zhou, N.** (2017). BNGR-A25L and -A27 are two functional G protein-coupled receptors for CAPA periviscerokinin neuropeptides in the silkworm *Bombyx mori*. *J. Biol. Chem.* **292**, 16554–16570.
- Steele, R. W., Lange, A. B., Orchard, I., and Starratt, A. N.** (1997). Comparison of the myotropic activity of position-2 modified analogues of proctolin on the hindgut of *Periplanta americana* and the oviduct of *Locusta migratoria*. *J. Insect Physiol.* **43**, 931–938.
- Suska, A., Miguel-Aliaga, I., and Thor, S.** (2011). Segment-specific generation of *Drosophila* Capability neuropeptide neurons by multi-faceted Hox cues. *Dev. Biol.* **353**, 72–80.

- Te Brugge, V., Paluzzi, J. P., Schooley, D. A., and Orchard, I.** (2011). Identification of the elusive peptidergic diuretic hormone in the blood-feeding bug *Rhodnius prolixus*: a CRF-related peptide. *J. Exp. Biol.* **214**, 371–381.
- Terhzaz, S., Cabrero, P., Robben, J. H., Radford, J. C., Hudson, B. D., Milligan, G., Dow, J. A. T., and Davies, S. A.** (2012). Mechanism and function of *Drosophila* capa GPCR: a desiccation stress-responsive receptor with functional homology to human neuromedinU receptor. *PLoS One* **7**, e29897.
- Terhzaz, S., Teets, N. M., Cabrero, P., Henderson, L., Ritchie, M. G., Nachman, R. J., Dow, J. A. T., Denlinger, D. L., and Davies, S. A.** (2015). Insect capa neuropeptides impact desiccation and cold tolerance. *Proc. Natl. Acad. Sci. USA* **112**, 2882–2887.
- Tublitz, N. J., and Truman, J. W.** (1985). Identification of neurons containing cardioacceleratory peptides (CAPs) in the ventral nerve cord of the tobacco hawkmoth, *Manduca sexta*. *J. Exp. Biol.* **116**, 395–410.
- Van Wielendaele, P., Badisco, L., and Vanden Broeck, J.** (2012). Neuropeptidergic regulation of reproduction in insects. *Gen. Comp. Endocrinol.* **188**, 23–34.
- Veenstra, J. A.** (1988). Effects of 5-Hydroxytryptamine on the Malpighian tubules of *Aedes aegypti*. *J. Insect Physiol.* **34**, 299–304.
- Veenstra, J. A.** (2014). The contribution of the genomes of a termite and a locust to our understanding of insect neuropeptides and neurohormones. *Front. Physiol.* **5**, 454.
- Wahedi, A., and Paluzzi, J. P.** (2018). Molecular identification, transcript expression, and functional deorphanization of the adipokinetic hormone/corazonin-related peptide receptor in the disease vector, *Aedes aegypti*. *Sci. Rep.* **8**, 2146.

- Wegener, C., Linde, D., and Eckert, M.** (2001). Periviscerokinins in cockroaches: release, localization, and taxon-specific action on the hyperneural muscle. *Gen. Comp. Endocrinol.* **121**, 1–12.
- Wegener, C., Reinl, T., Jansch, L., and Predel, R.** (2006). Direct mass spectrometric peptide profiling and fragmentation of larval peptide hormone release sites in *Drosophila melanogaster* reveals tagma-specific peptide expression and differential processing. *J. Neurochem.* **96**, 1362–1374.
- Wiehart, U. I. M., Nicolson, S. W., Eigenheer, R. A., and Schooley, D. A.** (2002). Antagonistic control of fluid secretion by the Malpighian tubules of *Tenebrio molitor*: effects of diuretic and antidiuretic peptides and their second messengers. *J. Exp. Biol.* **205**, 493–501.
- Wormington, J. D., and Juliano, S. A.** (2014). Sexually dimorphic body size and development time plasticity in *Aedes* mosquitoes (Diptera: Culicidae). *Evol. Ecol. Res.* **16**, 223–234.
- Yang, Y., Bajracharya, P., Castillo, P., Nachman, R. J., and Pietrantonio, P. V.** (2013). Molecular and functional characterization of the first tick CAP2b (periviscerokinins) receptor from *Rhipicephalus (Boophilus) microplus* (Acari: Ixodidae). *Gen. Comp. Endocrinol.* **194**.
- Zandawala, M., Marley, R., Davies, S. A., and Nassel, D. R.** (2018). Characterization of a set of abdominal neuroendocrine cells that regulate stress physiology using colocalized diuretic peptides in *Drosophila*. *Cell. Mol. Life Sci.* **6**, 1099–1115.

### 3.7 Supplementary Tables and Figures

**Table 3-S1. List and primary structure of several insect neuropeptides tested for functional activation of the mosquito anti-diuretic hormone (CAPA) receptor using heterologous bioassay.** NA denotes peptides with no detectable activity when tested up to 10  $\mu$ M.

Peptide Family (Name)	Sequence	EC <sub>50</sub> on CAPAr	Species (reference)
CAPA (CAPA1)	GPTVGLFAPRV-NH <sub>2</sub>	6.76 nM	<i>Aedes aegypti</i> (Predel et al., 2010)
CAPA (CAPA2)	pQGLVPFPRV-NH <sub>2</sub>	5.62 nM	<i>Aedes aegypti</i> (Predel et al., 2010)
Pyrokinin-1 (PK1)	AGNSGANSGMWFGPRL-NH <sub>2</sub>	>10 $\mu$ M	<i>Aedes aegypti</i> (Predel et al., 2010)
Pyrokinin-2 (PK2-1)	NTVNFSRRL-NH <sub>2</sub>	NA	<i>Rhodnius prolixus</i> (Paluzzi & O'Donnell, 2012)
Pyrokinin-2 (PK2-2)	SPPFAPRL-NH <sub>2</sub>	NA	<i>Rhodnius prolixus</i> (Paluzzi & O'Donnell, 2012)
SIFamide peptide (SIFa)	GYRKPPFNGSIF-NH <sub>2</sub>	NA	<i>Aedes aegypti</i> (Predel et al., 2010)
Extended FMRFamides (FMRFa-1)	SALDKNFMRF-NH <sub>2</sub>	NA	<i>Aedes aegypti</i> (Predel et al., 2010)
Short neuropeptide F (sNPF)	KAVRSPSLRLRF-NH <sub>2</sub>	NA	<i>Aedes aegypti</i> (Predel et al., 2010)
Myoinhibitory peptide (MIP-7)	AWNSLHGGW-NH <sub>2</sub>	NA	<i>Rhodnius prolixus</i> (Paluzzi et al., 2015)
Leucokinin (kinin)	NSVVLGKKQRFHSWG-NH <sub>2</sub>	NA	<i>Drosophila melanogaster</i> (Zandawala et al., 2018)
Corazonin (CRZ)	pQTFQYSRGWTN-NH <sub>2</sub>	NA	<i>Aedes aegypti</i> (Oryan et al., 2018)

**Table 3-S2. Oligonucleotides used for generation of fluorescent *in situ* hybridization probes, templates for *in vitro* dsRNA synthesis and gene-specific primers for quantitative PCR of the *Aedes aegypti* anti-diuretic hormone (CAPA) receptor.**

Oligo name	Oligo sequence (5'3')	Function	Accession (nucleotide position)
<i>Aedes</i> CAPAF fish	GACCTGGACAGCGTCAGC	FISH probe template	XM_001650839.1(28-45)
<i>Aedes</i> CAPAR fish	CAGTTCCTTTGATCTCGGTG	FISH probe template	XM_001650839.1(400-381)
<i>Aedes</i> CAPA F1-T7	<u>TAATACGACTCACTATAGG</u> GCGA... GACCTGGACAGCGTCAGC	FISH sense probe template	XM_001650839.1(28-45)
<i>Aedes</i> CAPA R1-T7	<u>TAATACGACTCACTATAGG</u> GCGA... CAGTTCCTTTGATCTCGGTG	FISH anti-sense probe template	XM_001650839.1(400-381)
<i>Aedes</i> CAPA-qPCRfor	<u>GCTGTTTGCCTTTCCAAG</u>	qPCR forward primer	XM_001650839.1(78-95)
<i>Aedes</i> CAPA-qPCRrev	<u>AACCACATGCCGCTGTTG</u>	qPCR reverse primer	XM_001650839.1(344-327)
<i>Aedes</i> CAPArRNAiF1	CCCACGGAAATCATGGACT	FISH probe and dsRNA template	MN433886 (275-293)
<i>Aedes</i> CAPArRNAiR1	GCGGATTTGCATTCCCATC	FISH probe and dsRNA template	MN433886 (1017-999)
<i>Aedes</i> CAPArRNAiF-T7	<u>TTTAATACGACTCACTATAG</u> <u>GGAGACCCACGGAAATCAT</u> GGACT	FISH sense probe and dsRNA template	MN433886 (275-293)
<i>Aedes</i> CAPArRNAiR-T7	<u>TTTAATACGACTCACTATAG</u> <u>GGAGAGCGGATTTGCATTC</u> CCATC	FISH anti-sense probe and dsRNA template	MN433886 (1017-999)
<i>Aedes</i> CAPAr-qPCRfor	GATGCTTAGCAATCCGGAA	qPCR forward primer	MN433886 (909-927)
<i>Aedes</i> CAPAr-qPCRrev	GACGGAAAACAGCCACGTA	qPCR reverse primer	MN433886 (1239-1221)

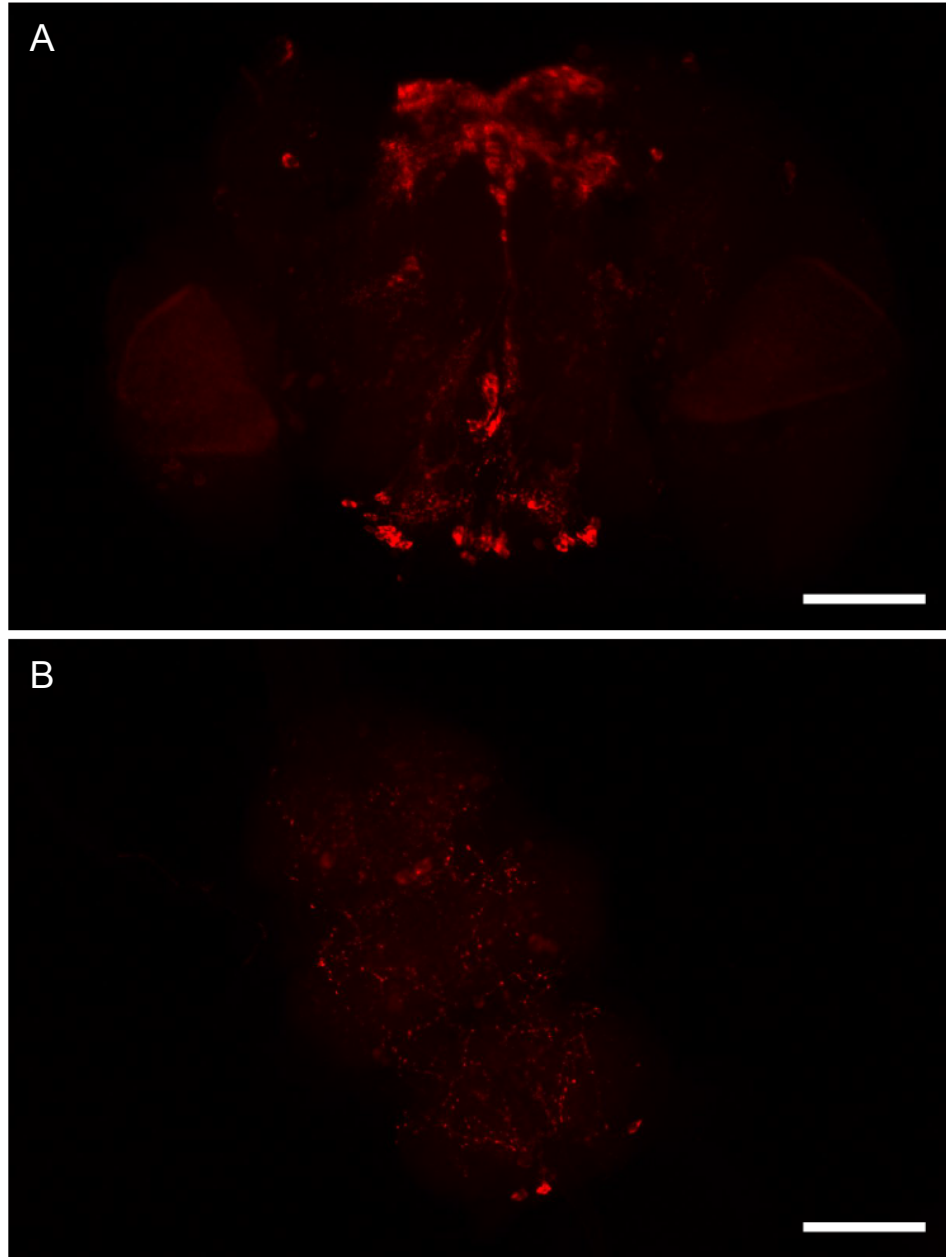


**Figure 3-S1. CAPA immunoreactivity observed in regions of the nervous system aside from the strongly-staining pair of neurosecretory cells in each of the abdominal ganglia.** (A) CAPA immunoreactive staining in the brain showing a bilateral pair of neurons in each hemisphere of the brain and immunoreactive processes in the central margin with unknown origin. In the posterior suboesophageal ganglion, a number of small bilaterally-paired neurons (20-30 cells total) were detected. (B) In the fused thoracic ganglia, CAPA immunoreactive processes were observed on the ventral surface, with no consistently detected immunoreactive neurons. Although a qualitative observation, CAPA immunoreactive staining was substantially weaker in the brain, SOG and thoracic ganglia since exposure and gain settings on the fluorescence microscope were adjusted substantially to enable detection of weak immunoreactive staining. Scale bars: 100 $\mu$ m.

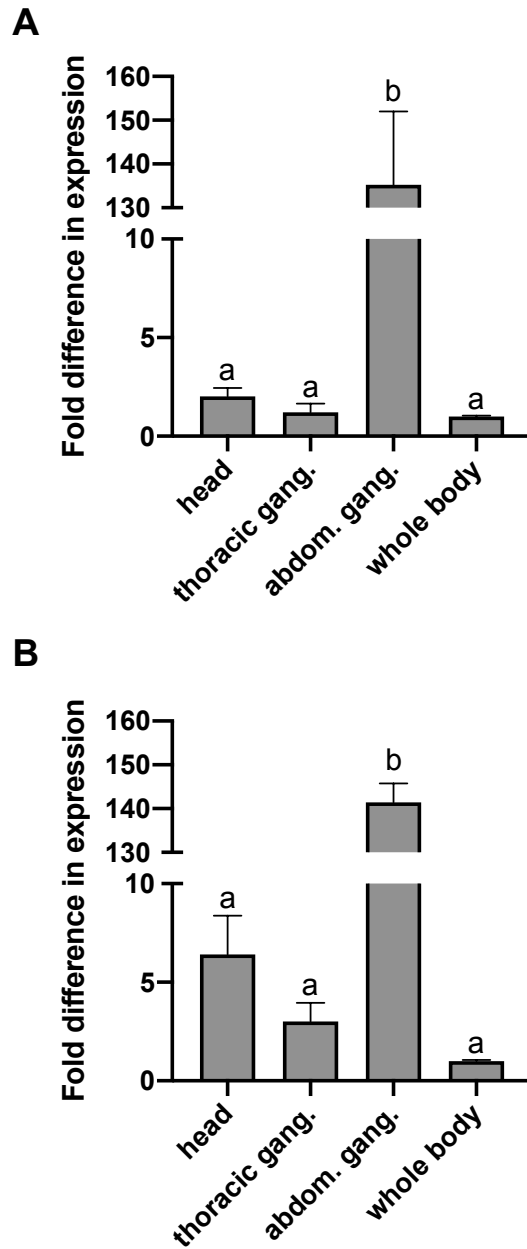


**Figure 3-S2. Expression analysis of CAPA neuropeptide (anti-diuretic hormone) transcript in different regions of the nervous system relative to whole adult (A) male and (B) female *A. aegypti* mosquitoes.** Different letters denote bars that are significantly different from one another as determined by a one-way ANOVA and Tukey's multiple comparison post-hoc test ( $p < 0.01$ ). Data represent the mean  $\pm$  SEM ( $n=3$ ).

## Chapter Four

### **The V-type H<sup>+</sup>-ATPase is targeted in anti-diuretic hormone control of the Malpighian ‘renal’ tubules**

This chapter has been submitted for publishing.

Sajadi, F., M. Vergara-Martínez., Paluzzi, J.P. (2023). The V-type H<sup>+</sup>-ATPase is targeted in anti-diuretic hormone control of the Malpighian ‘renal’ tubules in *Aedes aegypti*.  
*bioRxiv* doi: <https://doi.org/10.1101/2022.02.13.480270>

## 4.1 Summary

Like other insects, secretion by mosquito Malpighian tubules (MTs) is driven by the V-type H<sup>+</sup>-ATPase (VA) localized in the apical membrane of principal cells. The anti-diuretic neurohormone CAPA inhibits secretion by MTs stimulated by select diuretic hormones; however, the cellular effectors of this inhibitory signalling cascade remain unclear. Herein, we demonstrate that the VA inhibitor bafilomycin selectively inhibits serotonin (5HT)- and calcitonin-related diuretic hormone (DH<sub>31</sub>)-stimulated secretion. VA activity increases in DH<sub>31</sub>-treated MTs, whereas CAPA abolishes this increase through a NOS/cGMP/PKG signalling pathway. A critical feature of VA activation involves the reversible association of the cytosolic (V<sub>1</sub>) and membrane (V<sub>o</sub>) complexes. Indeed, higher V<sub>1</sub> protein abundance was found in membrane fractions of DH<sub>31</sub>-treated MTs whereas CAPA significantly decreased V<sub>1</sub> abundance in membrane fractions while increasing it in cytosolic fractions. Immunolocalization of V<sub>1</sub> was observed strictly in the apical membrane of MTs treated with DH<sub>31</sub> alone whereas immunoreactivity was dispersed following CAPA treatment. VA complexes colocalized apically in female MTs shortly after a bloodmeal consistent with the peak and post-peak phases of diuresis. Comparatively, V<sub>1</sub> immunoreactivity in MTs was more dispersed and did not colocalize with the V<sub>o</sub> complex in the apical membrane at 3 hours post-bloodmeal, representing a timepoint after the late phase of diuresis has concluded. Therefore, CAPA inhibition of MTs involves reducing VA activity and promotes complex dissociation hindering secretion. Collectively, these findings reveal a key target in hormone-mediated inhibition of MTs countering diuresis that provides a deeper understanding of this critical physiological process necessary for hydromineral balance.

## 4.2 Introduction

Insect post-prandial diuresis is under rigorous control by neuroendocrine factors acting on the Malpighian ‘renal’ tubules (MTs) to regulate primary urine production (Beyenbach, 2003). In the yellow fever mosquito, *Aedes aegypti*, several diuretics have been identified that regulate urine production including serotonin (5HT), calcitonin-related diuretic hormone (DH<sub>31</sub>), corticotropin-releasing factor-related diuretic hormone (DH<sub>44</sub>) and leucokinin-related (LK) diuretic hormone (Clark and Bradley, 1997; Coast and Garside, 2005; Lu et al., 2011; Chapter 2). An anti-diuretic peptidergic neurohormone, CAPA, selectively inhibits DH<sub>31</sub>- (Chapter 2; Sajadi et al., 2018) and 5HT-stimulated secretion of MTs (Ionescu and Donini, 2012; Chapter 2; Sajadi et al. 2018). Insect CAPA neuropeptides are produced in the central nervous system and are evolutionarily related to the vertebrate neuromedin U peptides (Jurenka, 2015). In *Drosophila melanogaster*, CAPA peptides have been shown to act through a conserved nitridergic signalling pathway to stimulate diuresis by MTs (Davies et al., 2012; Terhzaz et al., 2012); however, a few other studies have alluded to an anti-diuretic role (MacMillan et al., 2018; Rodan et al., 2012). In contrast, in both larval and adult *A. aegypti*, CAPA peptides inhibit fluid secretion through a signalling cascade involving the NOS/cGMP/PKG pathway (Ionescu and Donini, 2012; Chapter 3; Sajadi et al., 2020). Despite this, the anti-diuretic signalling mechanism and downstream cellular targets, such as the ion channels and transporters, remain elusive.

In insect MTs, including *A. aegypti*, the bafilomycin-sensitive V-type H<sup>+</sup>-ATPase (VA), also known as the proton pump, functions as an electrogenic pump allowing the transport of protons from the cytoplasm to the tubule lumen, thus generating a cell-negative membrane voltage (Weng et al., 2003; Wieczorek et al., 2009). This membrane voltage can then drive secondary transport processes such as the cation/H<sup>+</sup> exchanger or anion/H<sup>+</sup> cotransporter

(Wieczorek, 1992; Wieczoreks et al., 1991). Originally found in vacuolar membranes of animals and plants, the VA has since been found to be essential in cell function in both invertebrates and vertebrates (Harvey et al., 1998). In insects, the VA is densely located in the apical brush border membrane of tubule principal cells (Li et al., 2017; Weng et al., 2003), which is rich in mitochondria and endoplasmic reticula, fueling the ATP-consuming proton pump (Beyenbach, 2003; Patrick et al., 2006). Previous studies have shown VA localization within the apical membrane of principal cells along the entire length of the MTs (Patrick et al., 2006), but absent in stellate cells that express relatively higher levels of the P-type  $\text{Na}^+/\text{K}^+$ -ATPase (NKA) (Patrick et al., 2006). Due to stronger VA immunoreactivity observed in MTs (Patrick et al., 2006), and greater ATPase activity by electrophysiological assays (Weng et al., 2003; Wieczorek et al., 2009), the VA is categorized as serving mainly, but not exclusively (Beyenbach et al., 2000), stimulated transport mechanisms, whereas the NKA serves basic cell housekeeping functions when MTs are undergoing low unstimulated rates of secretion (Beyenbach et al., 2000; Hine et al., 2014; Weng et al., 2003).

Stimulation of distinct diuretic hormone receptors can activate various signalling pathways, including elevation of cyclic AMP (cAMP) levels which is known to increase VA activity and assembly in insects (Dames et al., 2006). In *A. aegypti*,  $\text{DH}_{31}$ , identified as the mosquito natriuretic peptide (Coast et al., 2005), selectively activates transepithelial secretion of  $\text{Na}^+$  in the MTs, using cAMP as a second messenger (Beyenbach, 2003), and upregulating the VA function to stimulate fluid secretion (Karas et al., 2005). Similarly, 5HT-stimulated diuresis is also thought to be mediated (at least in part) through the cAMP second messenger pathway (Cady and Hagedorn, 1999), activating protein kinase A (PKA) to increase the transepithelial voltage of the basolateral membrane in tubule principal cells (Beyenbach, 2003; Petzel et al.,

1999). In contrast, DH<sub>44</sub> has been shown to initiate diuresis via the paracellular and transcellular pathways, with higher nanomolar concentrations increasing cAMP and Ca<sup>2+</sup>, influencing both paracellular and transcellular transport, and lower nanomolar concentrations acting through the paracellular pathway only, via intracellular Ca<sup>2+</sup> (Clark et al., 1998). Thus, due to its predominant role in fluid secretion, the VA could be a likely target for both diuretic and anti-diuretic factors.

Eukaryotic V-ATPases are a multi-subunit protein composed of up to 14 different polypeptides, which form two major structural complexes. The peripheral V<sub>1</sub> complex (400-600 kDa), is invariably present in the cytoplasm and interacts with ATP, ADP, and inorganic phosphate (Beyenbach and Wiczorek, 2006). The cytosolic V<sub>1</sub> complex consists of eight different subunits (A-H): a globular headpiece with three alternating subunits A and B forming a hexamer with nucleotide binding sites located at their interface, a central rotor stalk with single copies of subunits D and F, and lastly, a peripheral stalk made up of subunits C, E, G, and H (Beyenbach and Wiczorek, 2006). The B subunit, shown to have high sequence similarity amongst several species from fungi to mammals (Novak et al., 1992; Pan et al., 1993), is a 56 kDa polypeptide, and is one of the two sites (along with subunit A) (Wiczorek et al., 1999b) in the V<sub>1</sub> complex that binds ATP. In contrast, the membrane-integrated V<sub>o</sub> complex (150-350 kDa) mediates the transport of H<sup>+</sup> across the membrane (Beyenbach and Wiczorek, 2006) and is composed of at least six different subunits, which collectively function in the proton translocation pathway (Beyenbach and Wiczorek, 2006; Weng et al., 2003). Although the proton channel of the VA can be blocked pharmacologically by the macrolide antibiotic, bafilomycin (Zhang et al., 1994), there are two known intrinsic mechanisms for VA regulation: firstly, through oxidation of the cystine residue on the A subunit of the V<sub>1</sub> complex, thus

preventing ATP hydrolysis; secondly, through reversible disassembly of the V<sub>1</sub> complex from the holoenzyme (Dschida and Bowman, 1995; Weng et al., 2003). While the role and regulation of the VA by diuretic hormones in insect MTs has been studied (Rein et al., 2008; Wiczorek et al., 1999a; Zimmermann et al., 2003), research examining anti-diuretic signalling mechanisms involving the VA remain in their infancy.

This study aimed to identify the cellular targets necessary for CAPA-mediated inhibition of fluid secretion by MTs stimulated by select diuretic factors in adult female *A. aegypti*. Our results provide evidence that CAPA neuropeptides inhibit diuretic-stimulated fluid secretion by VA complex dissociation, thus hindering VA function and activity.

### **4.3 Materials and Methods**

#### **Animal rearing**

Eggs of *Aedes aegypti* (Liverpool strain) were collected from an established laboratory colony described previously (Chapter 2; Sajadi et al., 2018; Rocco et al., 2017). All mosquitoes were raised under a 12h:12h light:dark cycle. Non-blood fed female insects (three-six days post-eclosion) were used for bioassays, dissected under physiological saline (*Aedes* saline) adapted from (Petzel et al., 1987) that contained (in mmol<sup>-1</sup>): 150 NaCl, 25 HEPES, 3.4 KCl, 7.5 NaOH, 1.8 NaHCO<sub>3</sub>, 1 MgSO<sub>4</sub>, 1.7 CaCl<sub>2</sub>, and 5 glucose, and titrated to pH 7.1.

#### **MT fluid secretion assay**

In order to determine fluid secretion rates, modified Ramsay assays were performed as described previously (Chapter 2; Sajadi et al., 2018; Sajadi et al., 2021). Female adults (3-6 day old) were dissected under physiological *Aedes* saline prepared as described above, and MTs were

removed and placed in a Sylgard-lined Petri dish containing 20  $\mu\text{L}$  bathing droplets (1:1 mixture of Schneider's Insect Medium (Sigma-Aldrich, Oakville, ON, Canada): *Aedes* saline, immersed in hydrated mineral oil to prevent evaporation. The proximal end of each tubule was wrapped around a Minutien pin to allow for fluid secretion measurements. To investigate the effects of second messengers, cAMP and cGMP, on fluid secretion rate,  $10^{-4}$  M 8 bromo-cAMP (cAMP) (Coast et al., 2005; Quinlan and O'Donnell, 1998) and  $10^{-8}$  M 8 bromo-cGMP (cGMP) (Chapter 2; Sajadi et al., 2018) (Sigma-Aldrich, Oakville, ON, Canada) were used against unstimulated MTs. To test the effects of the pharmacological blocker KT5720 (Ionescu and Donini, 2012) (protein kinase A (PKA) inhibitor), a dosage of  $5 \mu\text{mol l}^{-1}$  (manufacturer's recommended dose) was used against  $25 \text{ nmol l}^{-1}$   $\text{DH}_{31}$ - and  $10 \text{ nmol l}^{-1}$   $\text{DH}_{44}$ -stimulated MTs.

### **Time course inhibition of bafilomycin**

Dosage of bafilomycin  $\text{A}_1$  was based on a dose-response analysis of bafilomycin against  $\text{DH}_{31}$ -stimulated tubules (Figure 4-S1). In the interest of determining whether bafilomycin inhibits the effects of the diuretic factors, dosages of  $25 \text{ nmol l}^{-1}$  *Drome* $\text{DH}_{31}$  (~84% identical to *Aedae* $\text{DH}_{31}$ ) (Chapter 2; Sajadi et al., 2018; Coast et al., 2005; Vanderveken and O'Donnell, 2014),  $100 \text{ nmol l}^{-1}$  5HT (Chapter 2; Sajadi et al., 2018; Clark and Bradley, 1998; Veenstra, 1988), and  $10 \text{ nmol l}^{-1}$  *Rhopr* $\text{DH}$  (CRF-related diuretic peptide,  $\text{DH}_{44}$ ) (~48% overall identity; ~65% identity and ~92% similarity within the highly-conserved N-terminal region to *Aedae* $\text{DH}_{44}$ ) (Chapter 2; Sajadi et al., 2018; Clark et al., 1998; Lee et al., 2016; Te Brugge et al., 2011), were applied to the isolated MTs. Neurohormone receptors, including those for 5HT, and the peptides  $\text{DH}_{31}$ ,  $\text{DH}_{44}$ , and CAPA, are localized to the basolateral membrane of principal cells (Chapter 3; Sajadi et al., 2020; Kwon et al., 2012; Kwon and Pietrantonio, 2013; Overend et al.,

2015; Petrova and Moffett, 2016), while the LK receptor is localized exclusively to stellate cells (Lu et al., 2011). As a result, the effects of bafilomycin were tested on diuretics known to act on the principal cells of the MTs. After incubating with the individual diuretics for 30 min (using the modified Ramsay assay), diuretic peptide was added alone (controls) or in combination with bafilomycin (final concentration of  $10^{-5}$  M). The fluid secretion rate was recorded every 10 min for a total of 80 min. To determine whether inhibition of the VA was involved in the anti-diuretic activity of CAPA peptides on adult MTs, the effects of  $1 \text{ fmol l}^{-1}$  *Aedae*CAPA-1 (Chapter 2; Sajadi et al., 2018; Chapter 3; Sajadi et al., 2020) were investigated in combination with  $\text{DH}_{31}$  and bafilomycin.

### **Measurement of pH of secreted fluid**

The pH of secreted fluid was measured by using ion-selective microelectrodes (ISME) pulled from glass capillaries (TW-150-4, World Precision Instruments, Sarasota, FL, USA) using a Sutter P-97 Flaming Brown pipette puller (Sutter Instruments, San Rafael, CA, USA). Microelectrodes were silanized with *N,N*-dimethyltrimethylsilylamine (Fluka, Buchs, Switzerland) pipetted onto the interior of a glass dish inverted over the group of microelectrodes. A 1:2 ratio of number of microelectrodes to amount of silanization solution (in  $\mu\text{l}$ ) was used. The microelectrodes were left to silanize for 75 min at  $350^{\circ}\text{C}$  and left to cool before use. The microelectrodes were back-filled with a solution containing  $100 \text{ mmol l}^{-1}$  NaCl and  $100 \text{ mmol l}^{-1}$  sodium citrate that was titrated to pH 6.0 and front-filled using Hydrogen Ionophore I – cocktail B (Fluka, Buchs, Switzerland). The electrode tips were then coated with  $\sim 3.5\%$  (w/v) polyvinyl chloride (PVC) dissolved in tetrahydrofuran, to avoid displacement of the ionophore cocktail when submerged in the paraffin oil (Rheault and O'Donnell, 2004). The  $\text{H}^{+}$ -selective

microelectrodes were calibrated in *Aedes* saline titrated to either pH 7.0 or pH 8.0. Reference electrodes were prepared from glass capillaries (1B100F-4, World Precision Instruments, Sarasota, FL, USA) using a pipette puller described above and were backfilled with 500 mmol l<sup>-1</sup> KCl. Secreted droplet pH measurements were done immediately after collection to prevent alkalization of the droplet due to carbon dioxide diffusion into the paraffin oil. Microelectrodes and reference electrodes were connected to an electrometer through silver chloride wires where voltage signals were recorded through a data acquisition system (Picolog for Windows, version 5.25.3). In order to measure pH of the secreted fluid, tubules were set up using the Ramsay assay, and pH measurements were recorded every 10 min for a total of 60 min.

### **NKA and VA activities**

The NKA and VA activity in the MTs was determined using a modified 96-well microplate method (Jonusaite et al., 2011; McCormick, 1993), which relies on the enzymatic coupling of ouabain- or bafilomycin-sensitive hydrolysis of ATP to the oxidation of reduced nicotinamide adenine dinucleotide (NADH). The microplate spectrophotometer is therefore able to directly measure the disappearance of NADH. Adult female MTs (three to six day old) were dissected and incubated for 30 min in *Aedes* saline, diuretic (DH<sub>31</sub>, 5HT, or DH<sub>44</sub>) alone or combined with *Aedae*CAPA-1. Following the 30-min incubation, MTs were collected into 1.5 mL microcentrifuge tubes (40-50 sets of MTs per tube = 200-250 MTs per treatment), flash frozen in liquid nitrogen and stored at -80°C. To investigate the effects of the pharmacological blockers, a nitric oxide synthase (NOS) inhibitor, N<sub>ω</sub>-Nitro-L-arginine methyl ester hydrochloride (L-NAME), and protein kinase G (PKG) inhibitor, KT5823, were used against DH<sub>31</sub>-stimulated MTs treated with *Aedae*CAPA-1 or 10<sup>-8</sup> M cGMP. Dosages of 2 μmol l<sup>-1</sup> L-

NAME (manufacturer's recommended dose) and  $5 \mu\text{mol l}^{-1}$  KT582336 were applied to the MTs (Chapter 3; Sajadi et al., 2020; Ionescu and Donini, 2012; Sajadi et al., 2021). Tissues were thawed on ice and  $150 \mu\text{L}$  of homogenizing buffer (four parts of SEI with composition (in  $\text{mmol l}^{-1}$ ): 150 sucrose, 10 EDTA, and 50 imidazole; pH 7.3 and one part of SEID with composition: 0.5% of sodium deoxycholic acid in SEI) and MTs were then sonicated on ice for 10 sec (two pulses of 5 sec) and subsequently centrifuged at  $10,000 \times g$  for 10 min at  $4^\circ\text{C}$ . The supernatant was transferred into a fresh microcentrifuge tube and stored on ice.

Prior to the assay, three solutions were prepared (Solution A, B, and C) and all stored on ice. Solution A contained 4 units  $\text{mL}^{-1}$  lactate dehydrogenase (LDH), 5 units  $\text{mL}^{-1}$  pyruvate kinase (PK), 50  $\text{mmol l}^{-1}$  imidazole, 2.8  $\text{mmol l}^{-1}$  phosphoenolpyruvate (PEP), 0.22  $\text{mmol l}^{-1}$  ATP, and 50  $\text{mmol l}^{-1}$  NADH, pH 7.5. The solution was subsequently mixed with a salt solution in a 4:1 ratio (salt solution composition (in  $\text{mmol l}^{-1}$ ): 189 NaCl, 10.5  $\text{MgCl}_2$ , 42 KCl, and 50 imidazole, pH 7.5. Working solution B consisted of solution A with 5  $\text{mmol l}^{-1}$  ouabain and solution C consisted of solution A with 10  $\mu\text{mol l}^{-1}$  bafilomycin. The concentrations of ouabain and bafilomycin were based on previous studies (Jonusaite et al., 2011). To ensure the batch of assay mixture (Solution A) was effective, an adenosine diphosphate (ADP) standard curve was run. ADP standards were prepared as follows: 0  $\text{nmol l}^{-1}$  ( $200 \mu\text{L}$  of 50  $\text{mmol l}^{-1}$  imidazole buffer (IB), pH 7.5); 5  $\text{nmol l}^{-1}$  (25  $\mu\text{L}$  of 4  $\text{mmol l}^{-1}$  ADP stock and 175  $\mu\text{L}$  of IB); 10  $\text{nmol l}^{-1}$  (50  $\mu\text{L}$  of 4  $\text{mmol l}^{-1}$  ADP stock/ 150  $\mu\text{L}$  of IB); 20  $\text{nmol l}^{-1}$  (100  $\mu\text{L}$  of 4  $\text{mmol l}^{-1}$  ADP stock/100  $\mu\text{L}$  of IB); 40  $\text{nmol l}^{-1}$  (40  $\mu\text{L}$  of 4  $\text{mmol l}^{-1}$  ADP stock). The standards were added to a 96-well polystyrene microplate in duplicates of 10  $\mu\text{L}$  per well, followed by the addition of 200  $\mu\text{L}$  of solution A. The plate was placed in a Thermo Multiscan Spectrum microplate spectrophotometer (Thermo Electron Co., San Jose, USA) set at  $25^\circ\text{C}$  and a linear rate of NADH

disappearance was measured at 340 nm. The absorbance spectra were recorded and analyzed using the Multiscan Spectrum data acquisition system with SkanIt version 2.2 software. The ADP standards (0 to 40 nmoles well<sup>-1</sup>) should yield an optical density (OD) between 0.9 and 0.2 OD units, while the slope of the curve should result in -0.012 to -0.014 OD nmol ADP<sup>-1</sup>. Homogenized MT samples were thawed and added to the microplate (kept on ice) in six replicates of 10 µL per well. Next, two wells per sample were filled with 200 µL of working solution A, two wells with 200 µL of working solution B and two wells with 200 µL of working solution C. The microplate was quickly placed in the microplate spectrophotometer and the decrease in NADH absorbance was measured for 30 min at 340 nm. NKA and VA activity was calculated using the following equation:

$$\text{NKA or VA activity} = (((\Delta\text{ATPase}/S)/[P]) \times 60 \text{ (min)}),$$

where  $\Delta\text{ATPase}$  is the difference in ATP hydrolysis in the absence and presence of ouabain or bafilomycin,  $S$  is the slope of the ADP standard curve,  $[P]$  is the protein concentration of the sample. Protein was quantified using a Bradford assay (Sigma-Aldrich, Oakville, ON, Canada) according to manufacturer's guidelines with bovine serum albumin (Bioshop Canada Inc., Burlington, ON, Canada) as a standard. Final activity was expressed as micromoles of ADP per milligram of protein per hour.

### **Protein processing and western blot analyses**

MTs were isolated under physiological saline from 40-50 female *A. aegypti* for each biological replicate (defined as n=1) and incubated for 60 min in the following three treatments: *Aedes* saline, 25 nmol l<sup>-1</sup> DH<sub>31</sub>, or 25 nmol l<sup>-1</sup> DH<sub>31</sub> + 1 fmol l<sup>-1</sup> *Aedae*CAPA-1. Following the incubation, tissues were stored at -80°C until processing. To separate the membrane and

cytosolic proteins, a membrane protein extraction kit was used (ThermoFisher Scientific, Mississauga, ON, Canada) following recommended guidelines for soft tissue with minor modifications including 200  $\mu$ L of permeabilization and solubilization buffer and a 1:200 protease inhibitor cocktail (Sigma-Aldrich, Oakville, ON, Canada) in both buffers. Final protein concentrations were calculated by Bradford assay (Sigma-Aldrich, Oakville, ON, Canada) according to manufacturer's guidelines with bovine serum albumin (BioRad Laboratories, Mississauga, ON, Canada) as a standard and quantified using an A<sub>o</sub> Absorbance Microplate Reader (Azure Biosystems, CA, USA) at 595 nm.

Protein samples were denatured by heating for 5 min at 100°C with 6X loading buffer (225 mmol l<sup>-1</sup> Tris-HCl, pH 6.8, 3.5% (w/v) SDS, 35% glycerol, 12.5% (v/v)  $\beta$ -mercaptoethanol and 0.01% (w/v) Bromophenol blue). Into each lane, 5  $\mu$ g of protein was loaded onto a 4% stacking and 12% resolving sodium dodecyl sulphate polyacrylamide gel electrophoresis (SDS-PAGE) gel. Protein samples were migrated initially at 80 V for 30 min and subsequently at 110 V for 90 min before being transferred onto a polyvinylidene difluoride (PVDF) membrane using a wet transfer method at 100 V for 60 min in a cold transfer buffer. Following transfer, PVDF membranes were blocked with 5% skim milk powder in Tris-buffered saline (TBS-T; 9.9 mmol l<sup>-1</sup> Tris, 0.15 mmol l<sup>-1</sup> NaCl, 0.1 mmol l<sup>-1</sup> Tween-20, 0.1 mmol l<sup>-1</sup> NP-40 pH 7.4) for 60 min at RT, and incubated on a rocking platform overnight at 4°C with a guinea pig polyclonal anti-VA (Ab 353-2 against the V<sub>1</sub> complex of the VA (Weng et al., 2003), a kind gift from Profs. Wieczorek and Tiburcy, University of Osnabruck, Germany, used at a 1:2000 dilution in 5% skim milk in TBS-T. The next day, PVDF membranes were washed for 60 min in TBST-T, changing the wash buffer every 15 min. Immunoblots were then incubated with a goat anti-guinea pig HRP conjugated secondary antibody (1:2500 in 5% skim milk in TBS-T) (Life

Technologies, Burlington, ON, Canada) for 60 min at RT and subsequently washed three times for 15 min with TBS-T. Lastly, blots were incubated with the Clarity Western ECL substrate and images were acquired using a ChemiDoc MP Imaging System (BioRad Laboratories, Mississauga, ON, Canada). Molecular weight measurements were performed using Image Lab 5.0 software (BioRad Laboratories, Mississauga, ON, Canada). PVDF membranes were then probed with Coomassie brilliant blue, since total protein normalization is now considered the benchmark method for quantitative analysis of western blot data (Butler et al., 2019; Fosang and Colbran, 2015) and has been used in studies involving *A. aegypti* protein normalization (Durant and Donini, 2020). ImageJ software (NIH, USA) was used to quantify protein abundance. (Figure S4-3 and Figure S4-5) show a saturated blot of the 56kDa band to ensure visualization of the 74kDa and 32kDa band, however protein quantification was measured using a pre-saturated blot).

To confirm successful separation of membranes from cytosol using the membrane protein extraction kit, saline-incubated MTs were incubated in either anti-beta-tubulin (cytosolic marker, 1:5000) or -AaAQP1 affinity purified rabbit polyclonal antibody (generous gift from Dr. Andrew Donini, York University, Canada) (Misyura et al., 2020) (membrane marker, 1:1000). Blots were then incubated with a goat anti-mouse (for beta-tubulin) or goat anti-rabbit (for AQP1) HRP-conjugated secondary antibody (1:5000 in 5% skim milk in TBS-T) (Life Technologies, Burlington, ON, Canada) for 60 min at RT.

### **Immunolocalization of VA complexes in MTs**

Immunohistochemistry of the MTs localizing the VA complexes was conducted following a previously published protocol (Chasiotis and Kelly, 2008). Adult female MTs (three

to six day old) were dissected out in *Aedes* saline and incubated following similar conditions described in the western blot section above. After the incubation, the MTs were immersed in Bouin's solution and fixed for 2 h in small glass vials. To test *in vivo* changes of the VA complexes, five to six day old females were allowed to blood feed for 20 min (Rocco et al., 2017), after which female mosquitoes were isolated at 10 min, 30 min, and 3 hr post bloodmeal. Similarly aged, non-blood fed (sucrose-fed) females were isolated as controls. Following the bloodmeal, whole body females were immersed in Bouin's solution and fixed for 3 h in small glass vials. Tissues/whole body females were then rinsed three times and stored in 70% ethanol at 4°C until further processing. Fixed samples were dehydrated through a series of ethanol washes: 70% ethanol for 30 min, 95% ethanol for 30 min, and 100% ethanol three times for 30 min. The samples were cleared with xylene (ethanol:xylene for 30 min then 100% xylene three times for 30 min), and infiltrated in Paraplast Plus Tissue Embedding Medium (Oxford Worldwide, LLC, Memphis, USA) at xylene:paraffin wax for 60 min at 60°C, then rinsed in pure paraffin wax twice for 1 h for 60°C. Following the last rinse, the samples were embedded in the paraffin wax and left to solidify at 4°C until further processing. Sections (5 µm) were cut using a Leica RM 2125RT manual rotary microtome (Leica Microsystems Inc., Richmond Hill, Canada) and slides were incubated overnight on a slide warmer at 45°C.

The following day, sections were deparaffinized with xylene (two rinses for 5 min each), and rehydrated via a descending series of ethanol washes (100% ethanol twice for 2 min, 95% ethanol for 2 min, 70% ethanol for 2 min, 50% ethanol for 2 min) and finally in distilled water for 20 min. Next, sections were subjected to a heat-induced epitope retrieval (HIER) by immersing slides in a sodium citrate buffer (10 nmol l<sup>-1</sup>, pH 6.0) and heating both slides and solution in a microwave oven for 4 min. The solution and slides were allowed to cool for 20 min,

reheated for 2 min, and left to stand at room temperature (RT) for 15 min. Slides were then washed three times in phosphate-buffered saline (PBS) pH 7.4, 0.4% Kodak Photo-Flo 200 in PBS (PBS/PF, 10 min), 0.05% Triton X-100 in PBS (PBS/TX, 10 min), and 10% antibody dilution buffer (ADB; 10% goat serum, 3% BSA and 0.05% Triton X-100 in PBS) in PBS (PBS/ADB, 10 min). Slides were incubated overnight at RT with a guinea pig polyclonal anti-V<sub>1</sub> (Ab 353-2 against the V<sub>1</sub> complex, identical antibody used in western blot analyses, at 1:5000 dilution in ADB) in combination with a 1:100 mouse polyclonal anti-ATP6V0A1 antibody for V<sub>0</sub> (Abnova, Taipei, Taiwan).

Following overnight primary antibody incubation, slides were washed briefly in distilled water, with sequential washes with PBS/PF, PBS/TX, and PBS/ADB for 10 min each as described above. A goat anti-guinea pig antibody (for V<sub>1</sub> detection) conjugated to AlexaFluor 488 (1:500 in ADB, Jackson ImmunoResearch, Laboratories West Grove, PA, USA) and sheep anti-mouse antibody (for V<sub>0</sub> detection) conjugated to AlexaFluor 594 (1:500 in ADB, Jackson ImmunoResearch Laboratories, West Grove, PA, USA) were applied to visualize the VA complexes. The slides were left to incubate in the secondary antibody for 60 min at RT. For negative controls, slides were processed as described above with primary antibodies omitted. Slides were then washed in distilled water/0.4% PF three times for 1 min each and finally in distilled water for 1 min. Slides were air dried for 30 min and mounted using ProLong™ Gold antifade reagent with DAPI (Life Technologies, Burlington, ON, Canada). Fluorescence images were captured using an Olympus IX81 inverted fluorescent microscope (Olympus Canada, Richmond Hill, ON, Canada).

## cGMP and cAMP Measurements

A competitive cGMP ELISA kit (Cell Signaling Technology, #4360) and cAMP ELISA kit (Cell Signaling Technology, #4339) were used to measure the effect of DH<sub>31</sub>, DH<sub>44</sub> and *Aedae*CAPA-1 on cGMP and cAMP levels in the MTs. Adult MTs were isolated under physiological saline from 50 female *A. aegypti* for each biological replicate (defined as n=1). To prevent cGMP degradation, tubules were incubated first with a phosphodiesterase inhibitor, 0.1 mmol l<sup>-1</sup> zaprinast, for 10 min (Kean et al., 2002) or 0.5 mmol l<sup>-1</sup> 3-isobutyl-1-methylxanthine (IBMX) for 10 min (to prevent cAMP degradation) (Coast et al., 2005) before incubated in one of the experimental treatments, specifically *Aedes* saline, 25 nmol<sup>-1</sup> DH<sub>31</sub>, 10 nmol l<sup>-1</sup> DH<sub>44</sub>, 1 fmol<sup>-1</sup> *Aedae*CAPA-1, 25 nmol<sup>-1</sup> DH<sub>31</sub> + 1 fmol<sup>-1</sup> *Aedae*CAPA-1, or 10 nmol<sup>-1</sup> DH<sub>44</sub> + 1 fmol<sup>-1</sup> *Aedae*CAPA-1 for a further 20 min. After incubation was complete, tissues were stored at -80°C until processing. To measure cGMP and cAMP concentrations, frozen tubule samples were thawed on ice and 125 µL of 1X cell lysis buffer (CLB, #9803) was added to each tube (1 mmol<sup>-1</sup> phenylmethylsulfonyl fluoride (PMSF) was added to 1X CLB fresh each time). Tissue samples were kept on ice for 10 min, sonicated for 10 s (similar conditions as described for NKA/VA activity assay), centrifuged for 3 min at 10,000 rpm, and the supernatant was isolated and kept on ice. Using a commercial 96-well microtitre plate precoated with either a cGMP or cAMP rabbit monoclonal antibody, the cGMP-HRP (or cAMP-HRP) conjugate was added in triplicate wells with 50 µL per well. This was followed by the addition of 50 µL of either tubule samples or cGMP (or cAMP) standards ranging from 100 nmol<sup>-1</sup> to 0.25 nmol<sup>-1</sup>. The plate was covered and incubated at RT for 3 h on a horizontal orbital plate shaker. Following incubation, plate contents were discarded, and wells were washed four times with 200 µL/well of 1X wash buffer. Next, 100 µL of 3,3',5,5'-tetramethylbenzidine (TMB) substrate was added to each well, and the plate

was covered and kept for 10 min at RT. The enzymatic reaction was quenched by adding 100  $\mu\text{L}$  of 2  $\text{mmol}^{-1}$  HCl and absorbance read at 450 nm using a Synergy 2 Multi-Mode Microplate Reader (BioTek, Winooski, VT, USA).

## Statistical analyses

Data was compiled using Microsoft Excel and transferred to Graphpad Prism software v.7 to create figures and conduct all statistical analyses. Data was analyzed accordingly using a one-way or two-way ANOVA and a Bonferroni post-test, or Student's t-test, with differences between treatments considered significant if  $p < 0.05$ .

## 4.4 Results

### Bafilomycin inhibits $\text{DH}_{31}$ - and 5HT-stimulated fluid secretion rate

To determine the appropriate concentration of bafilomycin to test on adult *A. aegypti* MTs, several doses were applied against  $\text{DH}_{31}$ -stimulated tubules (Figure S4-1). Higher doses of bafilomycin ( $10^{-4}$  M and  $10^{-5}$  M) resulted in significant inhibition of fluid secretion rate, with maximal inhibition leading to a five-fold decrease, observed with treatment of  $10^{-5}$  M bafilomycin. Next, to determine whether inhibiting the VA would decrease fluid secretion rate stimulated by other diuretic hormones, including 5HT and  $\text{DH}_{44}$ , the effect of  $10^{-5}$  M bafilomycin on adult tubules stimulated with these diuretics was tested (Figure 4-1). Fluid secretion rates were measured over 30 min under control (stimulated) conditions, and then at 10-min intervals in the presence of bafilomycin. Treatment of MTs with  $10^{-5}$  M bafilomycin against  $\text{DH}_{31}$  led to a decrease in fluid secretion over the treatment interval. Specifically, 30 min after treatment with bafilomycin, fluid secretion rate was significantly reduced by over two-fold to  $0.438 \pm 0.041$   $\text{nL min}^{-1}$ , compared to  $\text{DH}_{31}$  alone,  $0.941 \pm 0.077$   $\text{nL min}^{-1}$  (Figure 4-1A). Similar results were seen

with 5HT-stimulated MTs; however, a decrease in fluid secretion was observed 30 min post-bafilomycin, with a significant inhibition 40 min after treatment ( $0.522 \pm 0.072$  nL min<sup>-1</sup>, 5HT alone vs.  $0.182 \pm 0.045$  nL min<sup>-1</sup>, 5HT + bafilomycin) (Figure 4-1B). Distinct from DH<sub>31</sub> and 5HT-stimulated tubules, DH<sub>44</sub>-stimulated secretion was insensitive to bafilomycin treatment (Figure 4-1C). To confirm whether *Aedae*CAPA-1 and bafilomycin elicit similar effects against DH<sub>31</sub>-stimulated MTs, adult female MTs were treated with either DH<sub>31</sub> alone or in combination with *Aedae*CAPA-1, bafilomycin, or both (Figure 4-1D). MTs treated with either *Aedae*CAPA-1 or bafilomycin resulted in a significant inhibition of DH<sub>31</sub>-stimulated secretion, and similar inhibition was observed when both *Aedae*CAPA-1 and bafilomycin were applied together with no evidence of any additive inhibitory effects (Figure 4-1D).

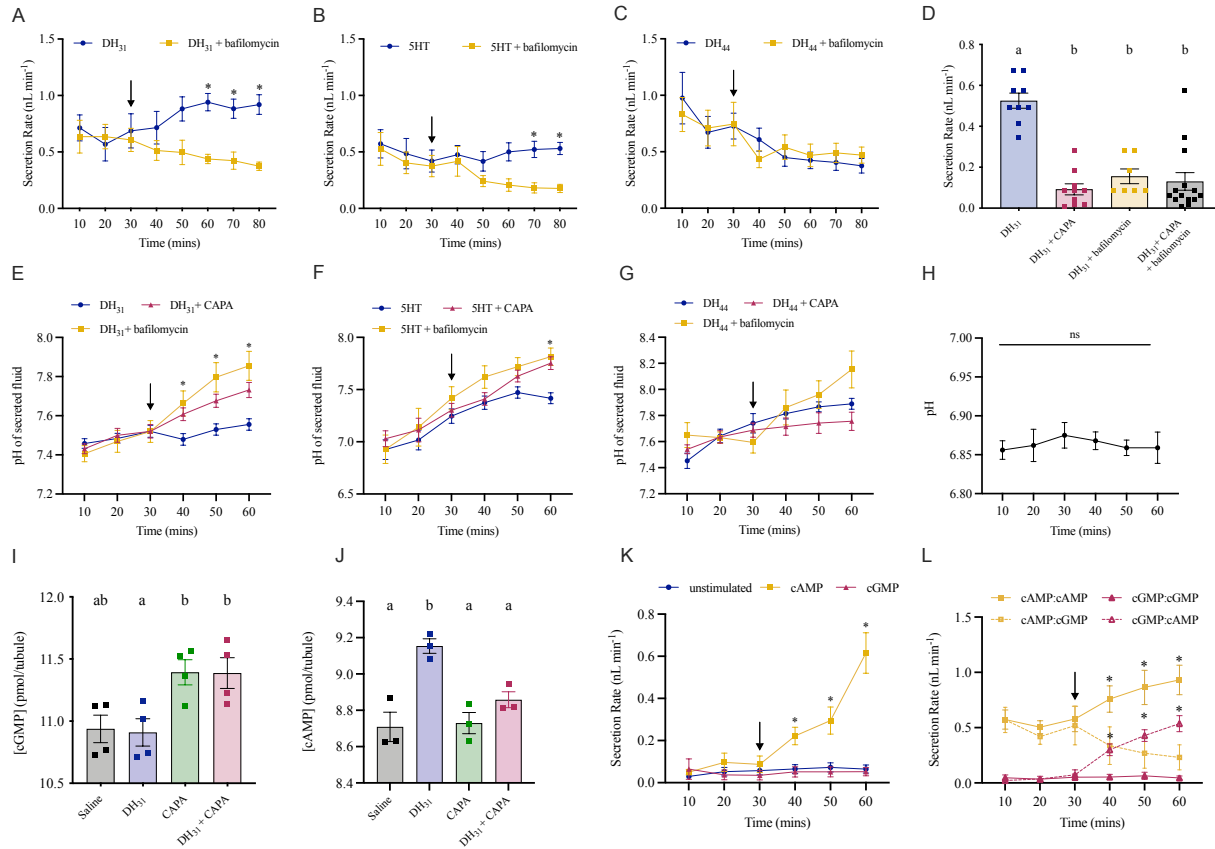


**Figure 4-1. Effect of bafilomycin on fluid secretion rates and pH along with cyclic nucleotide second messengers on adult *A. aegypti* MTs.** Tubules were treated with either (A) DH<sub>31</sub> (B) 5HT or (C) DH<sub>44</sub> and secreted droplets were measured at 10-min intervals for 30 min. Immediately following measurement of the 30-min point fluid droplet (solid arrow), MTs were treated with (A) DH<sub>31</sub> (B) 5HT (C) or DH<sub>44</sub> alone or in combination with *Aedae*CAPA-1 or bafilomycin. (D) MTs were treated with DH<sub>31</sub> alone or in combination with *Aedae*CAPA-1, bafilomycin, or both *Aedae*CAPA-1 and bafilomycin for 60 min. Secreted fluid pH was measured in tubules treated with either (E) DH<sub>31</sub> (F) 5HT or (G) DH<sub>44</sub> before and after addition of *Aedae*CAPA-1, bafilomycin, or both *Aedae*CAPA-1 and bafilomycin along with unstimulated MTs (H). Production of (I) cGMP and (J) cAMP in DH<sub>31</sub>-stimulated MTs treated with *Aedae*CAPA-1. (A-C) Significant differences between bafilomycin-treated and the corresponding time point controls and (E-H) significant differences in secreted fluid pH between both *Aedae*CAPA-1- and bafilomycin-treated and the corresponding time point controls are denoted by an asterisk, as determined by a two-way ANOVA and Bonferroni multiple comparison post-hoc test ( $p < 0.05$ ). Data represent the mean  $\pm$  SEM ( $n = 12-34$ ), ns denotes no statistical significance. (D, I, J) Bars labeled with different letters are significantly different from each other (mean  $\pm$  SEM; one-way ANOVA with Bonferroni multiple comparison,  $p < 0.05$ , (D)  $n = 7-17$  (I, J)  $n = 50$  sets of MTs for all treatments ( $n = 3$  per treatment)). (K) Fluid secretion rates were measured at 10 min intervals initially over a 30 min interval (unstimulated) and then over a second 30 min interval after the addition (solid arrow) of  $10^{-4}$  M cAMP or  $10^{-8}$  M cGMP. Significant differences between cAMP-treated MTs and the corresponding time point controls (or cGMP-treated MTs) are denoted by an asterisk (mean  $\pm$  SEM; two-way ANOVA with

Bonferroni multiple comparison,  $p < 0.05$ ,  $n = 5-6$ ). (L) Significant differences between cAMP-treated MTs and corresponding time point after addition at 30 min (downward arrow) of cGMP are denoted by an asterisk (similar with cGMP alone and cAMP added at 30 min,  $\text{mean} \pm \text{SEM}$ ; one-way ANOVA with Bonferroni multiple comparison,  $p < 0.05$ ,  $n = 5-9$ ).

### ***Aedae*CAPA-1 and bafilomycin alkalizes secreted fluid in DH<sub>31</sub>- and 5HT-stimulated MTs**

The VA pumps protons from the cell into the tubule lumen thus generating an electromotive potential (Beyenbach et al., 2000; Wieczorek et al., 1999b) and providing energy to drive the secretion of cations via Na<sup>+</sup>/H<sup>+</sup> and/or K<sup>+</sup>/H<sup>+</sup> antiporters (Weng et al., 2003). An indirect way to measure whether *Aedae*CAPA-1 and bafilomycin inhibits VA activity involves measuring the pH of the secreted fluid from diuretic-stimulated MTs treated with *Aedae*CAPA-1 or bafilomycin (Figure 4-1E-G). In DH<sub>31</sub>-stimulated MTs treated with *Aedae*CAPA-1, there was an immediate significantly higher pH in the secreted fluid (7.479±0.030) at 40 min relative to control, increasing up to 7.73±0.038 at 60 min (Figure 4-1E). Similarly, pH levels in DH<sub>31</sub>-stimulated MTs treated with bafilomycin were significantly higher (7.66±0.064) relative to control at 40 min, increasing up to 7.855±0.074 at 60 min. Comparable to DH<sub>31</sub>, addition of *Aedae*CAPA-1 or bafilomycin significantly increased the pH of secreted fluid from 5HT-stimulated MTs to 7.75±0.061 and 7.82±0.083 respectively, at the 60 min mark (Figure 4-1F). In contrast, unlike the effects observed with DH<sub>31</sub>- and 5HT-stimulated MTs, *Aedae*CAPA-1 or bafilomycin did not alter the pH of the secreted fluid in DH<sub>44</sub>-stimulated MTs (Figure 4-1G). The pH increased from 7.4 to 7.9 during the 30-min DH<sub>44</sub> incubation; however, pH did not change following the addition of *Aedae*CAPA-1 or bafilomycin. Separately, we conducted measurements in unstimulated tubules to verify pH in these small droplets did not drift over a time frame consistent with our above experiments. Unstimulated MTs were allowed to secrete, the droplets isolated, and their pH was subsequently measured over the course of 60 min. Over this incubation period, no change was observed in the pH of secreted droplets from unstimulated MTs (Figure 4-1H), upholding the notion that the alkalization of secreted fluid observed following *Aedae*CAPA-1 (or bafilomycin) treatment of DH<sub>31</sub>- and 5HT-stimulated MTs is a

result of VA inhibition. Additionally, unstimulated MTs treated with either *Aedae*CAPA-1 or bafilomycin resulted in no significant changes in either secretion rate (Figure S4-2A) or pH (Figure S4-2B).

### ***Aedae*CAPA-1 increases cGMP and decreases cAMP levels in DH<sub>31</sub>-treated MTs**

To further clarify the CAPA signalling pathway involving the second messengers, cGMP and cAMP, we sought to determine changes in levels of these cyclic nucleotides in MTs incubated in DH<sub>31</sub> alone or combined with *Aedae*CAPA-1. Treatment of MTs with DH<sub>31</sub> alone had basal levels of cGMP,  $10.91 \pm 0.109$  pmol<sup>-1</sup>/tubule, comparable to saline treated MTs. Treatment of MTs with *Aedae*CAPA-1 resulted in a significant increase in cGMP levels compared to DH<sub>31</sub>- incubated tubules, increasing to  $11.39 \pm 0.101$  pmol<sup>-1</sup>/tubule (Figure 4-1I). Similar results were observed with MTs treated with both DH<sub>31</sub> + *Aedae*CAPA-1, with significantly increased cGMP levels of  $11.39 \pm 0.123$  pmol<sup>-1</sup>/tubule (Figure 4-1I) compared to MTs treated with DH<sub>31</sub> alone. In contrast, treatment of MTs with DH<sub>31</sub> alone led to significantly higher levels of cAMP,  $9.153 \pm 0.039$  pmol<sup>-1</sup>/tubule, while baseline levels of this second messenger were observed in saline, DH<sub>31</sub> + *Aedae*CAPA-1, and *Aedae*CAPA-1 treated tubules (Figure 4-1J). To further confirm the stimulatory role of cAMP and inhibitory role of cGMP, tubules were treated with either cyclic nucleotide alone, and secretion rates were measured (Figure 4-1K). Unstimulated fluid secretion rates were measured over the first 30 min, and then at 10-min intervals with either cAMP or cGMP. Treatment of MTs with  $10^{-4}$  M cAMP led to a significant increase over the treatment interval, with fluid secretion rates increasing to  $0.615 \pm 0.096$  nL min<sup>-1</sup> at 60 min, compared to  $10^{-8}$  M cGMP ( $0.052 \pm 0.091$  nL min<sup>-1</sup>) and unstimulated ( $0.065 \pm 0.091$  nL min<sup>-1</sup>) (Figure 4-1K). Finally, to establish whether these cyclic

nucleotide second messengers elicit antagonistic control of the MTs in adult *A. aegypti*, tubules were treated initially with cAMP over the first 30 min and then cGMP was added in the presence of cAMP for a subsequent 30 min (Figure 4-1L). Similarly, we also tested the opposite treatment regime where MTs were treated initially with cGMP and subsequently with cAMP added along with cGMP. Treatment of cAMP-stimulated MTs with  $10^{-8}$  M cGMP led to a significant decrease (~4-fold) over the treatment interval, with secretion rates decreasing to  $0.231 \pm 0.113$  nL min<sup>-1</sup> at 60 min, compared to  $10^{-4}$  M cAMP alone ( $0.931 \pm 0.134$  nL min<sup>-1</sup>). In contrast, cGMP-incubated tubules treated with  $10^{-4}$  M cAMP led to a significant increase (~10-fold) in secretion rate ( $0.537 \pm 0.072$  nL min<sup>-1</sup>) compared to MTs treated with  $10^{-8}$  M cGMP alone ( $0.045 \pm 0.018$  nL min<sup>-1</sup>).

Parallel studies examining cAMP levels were measured in DH<sub>44</sub>-incubated MTs. Treatment of MTs with DH<sub>44</sub> alone had high levels of cAMP,  $9.115 \pm 0.061$  pmol<sup>-1</sup>/tubule, compared to saline treated MTs,  $8.709 \pm 0.081$  pmol<sup>-1</sup>/tubule (Figure S4-3A). Levels of cAMP remained unchanged in tubules treated with both DH<sub>44</sub> + *Aedae*CAPA-1,  $8.954 \pm 0.108$  pmol<sup>-1</sup>/tubule. To further resolve the cAMP signalling pathway downstream of DH<sub>31</sub> and DH<sub>44</sub> stimulated diuresis, a PKA inhibitor (KT5720) was tested against diuretic-stimulated MTs. KT5720 abolished the stimulatory effect of DH<sub>31</sub>, whereas secretion by DH<sub>44</sub>-treated MTs remained unchanged (Figure S4-3B).

### ***Aedae*CAPA-1 decreases VA activity in DH<sub>31</sub>-stimulated MTs through the NOS/cGMP/PKG pathway**

In *Aedes* MTs, 50-60% of the total ATPase activity can be attributed to a bafilomycin- and nitrate-sensitive component that reflects the activity of the VA pump (Weng et al., 2003). The remaining ATPase activity may be due to nucleotide cyclases, protein kinases, myosin,

DNA helicases, and other ATP-consuming processes such as the NKA (Weng et al., 2003). As such, to determine whether CAPA inhibits VA and/or NKA function, female diuretic-stimulated MTs were challenged with *Aedae*CAPA-1 to measure the resultant NKA and VA activity. As expected, given its role as the natriuretic diuretic hormone, adult female MTs treated with DH<sub>31</sub> resulted in a significant (> two-fold) increase of VA activity, 0.0329±0.0007 μmoles ADP/μg protein/hour, compared to saline controls, 0.0151±0.0021 μmoles ADP/μg protein/hour (Figure 4-2A). Importantly, MTs incubated with both DH<sub>31</sub> and *Aedae*CAPA-1 had significantly lower VA activity, resulting in activity levels indistinguishable from saline controls. In contrast, neither 5HT nor DH<sub>44</sub> influenced VA activity (p>0.05) when compared with saline controls, while co-treatment with *Aedae*CAPA-1 also resulted in indistinguishable VA activity. Similar VA activity levels were observed between 5HT and DH<sub>44</sub> (0.0255±0.0078 and 0.0208±0.0042 μmoles ADP/μg protein/hour) and with co-application of *Aedae*CAPA-1 (0.0150±0.0036 and 0.0154±0.0070 μmoles ADP/μg protein/hour). Unlike changes observed in VA activity following treatment with DH<sub>31</sub>, diuretic-stimulation or *Aedae*CAPA-1 treatment did not perturb NKA activity, with levels similar to that of unstimulated MTs (Figure 4-2B).

To confirm the actions of CAPA are mediated through the NOS/cGMP/PKG pathway, pharmacological blockers, including inhibitors of NOS (L-NAME) and PKG (KT5823), were tested against DH<sub>31</sub>-stimulated MTs treated with either *Aedae*CAPA-1 or cGMP (Figure 4-2C). Application of L-NAME or KT5823 abolished the inhibitory effect of *Aedae*CAPA-1, resulting in high levels of VA activity, 0.02671±0.0025 and 0.03653±0.0051 μmoles ADP/μg protein/hour respectively, compared to MTs treated with DH<sub>31</sub> + *Aedae*CAPA-1. As expected, treatment of DH<sub>31</sub>-stimulated MTs with cGMP resulted in a significant decrease in VA activity, 0.006±0.0026

$\mu$ moles ADP/ $\mu$ g protein/hour, similar to *Aedae*CAPA-1-treated MTs, while co-treatment with KT5823 abolished the inhibitory effect of cGMP, resulting in an increase in VA activity.

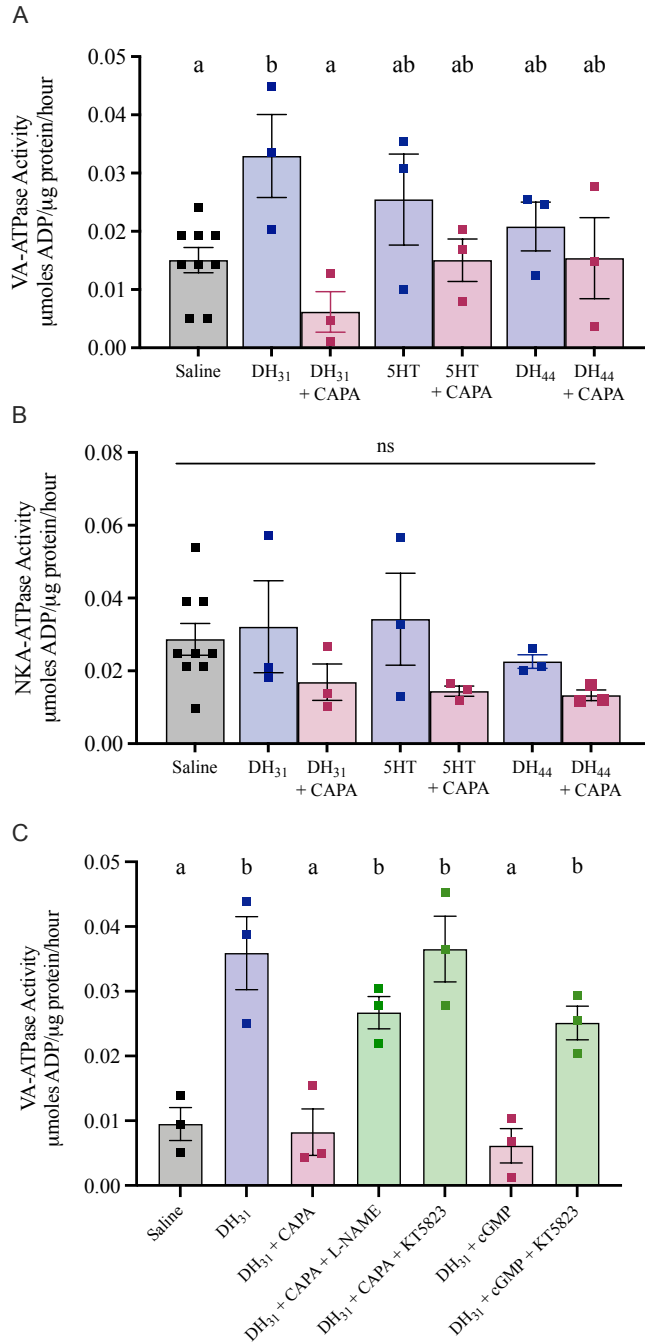


**Figure 4-2. Effect of *AedaeCAPA-1* and NOS/PKG inhibitors on VA and NKA activity in diuretic stimulated *A. aegypti* MTs.** MTs were incubated in *Aedes* saline, diuretics (DH<sub>31</sub>, 5HT, and DH<sub>44</sub>) alone or in combination with *AedaeCAPA-1* for 30 min before collection to measure (A) VA and (B) NKA activity. (C) MTs were treated with pharmacological blockers, NOS inhibitor (L-NAME) and PKG inhibitor (KT5823) in combination with either *AedaeCAPA-1* or cGMP. Bars labeled with different letters are significantly different from each other (mean±SEM; one-way ANOVA with Bonferroni multiple comparison, p<0.05). ns denotes no statistical significance. For each treatment, 50 sets of MTs were collected with n=3 biological replicates per treatment.

### ***Aedae*CAPA-1 leads to VA holoenzyme dissociation in DH<sub>31</sub>-treated MTs**

The reversible dissociation of the V<sub>1</sub> complex from the V<sub>o</sub> membrane-integrated complex is a well-known mechanism for regulating VA transport activity (Dames et al., 2006; Quinlan and O'Donnell, 1998; Rein et al., 2008; Wieczorek et al., 1999b; Zimmermann et al., 2003). To determine whether *Aedae*CAPA-1 influences VA complex dissociation, membrane and cytosolic protein fractions were isolated from DH<sub>31</sub> and DH<sub>31</sub> + *Aedae*CAPA-1 incubated MTs, and a polyclonal V<sub>1</sub> antibody (Weng et al., 2003) was used to measure protein abundance. First, membrane and cytosolic protein isolation was verified with specific cytosolic (beta-tubulin) and membrane (AQP1) markers (Figure S4-4). Western blot analysis revealed three protein bands, with calculated molecular masses of 74 kDa, 56 kDa, and 32 kDa (Tiburcy et al., 2013; Weng et al., 2003) (Figure S4-5). The V<sub>1</sub> complex is composed of eight subunits (A-H), which includes the A (~74kDa) and B subunit (~56Da) that are arranged in a ring forming the globular headpiece for ATP binding and hydrolysis (Wieczorek et al., 1999b). Additionally, studies have suggested that subunit D (~32kDa) alongside subunit F constitute the central rotational stalk of the V<sub>1</sub> complex (Harvey et al., 1998). There was no difference in abundance observed for the A subunit (74 kDa band) in either membrane or cytosolic fractions between saline and DH<sub>31</sub> incubated treatments whereas DH<sub>31</sub> + *Aedae*CAPA-1 incubated MTs had increased A subunit (74 kDa band) protein abundance in cytosolic fractions compared to saline treatment (Figure 3-3A) and decreased abundance in the membrane fraction compared to MTs treated solely with DH<sub>31</sub> (Figure 4-3B). Similarly, the V<sub>1</sub> complex B subunit abundance (56 kDa band) was similar in all treatments within the cytosolic protein fraction (Figure 4-3C) whereas DH<sub>31</sub> + *Aedae*CAPA-1 incubated MTs had significantly lower abundance in membrane fractions compared to MTs treated with DH<sub>31</sub> alone (Figure 4-3D). Finally, there was no difference in abundance of the V<sub>1</sub>

complex subunit D (32 kDa band) between saline and DH<sub>31</sub> treated MTs in neither cytosolic or membrane fractions. However, as observed for the A and B subunit bands (74 and 56 kDa band, respectively) DH<sub>31</sub> + *Aedae*CAPA-1 incubated MTs showed a significant increase in the D subunit in cytosolic fractions compared to saline treated MTs (Figure 4-3E) and a decrease in its abundance in membrane fraction compared to MTs treated with DH<sub>31</sub> alone (Figure 4-3F). In summary, all three of the V1 complex immunoreactive bands corresponding to subunits A, B and D (74, 56 and 32 kDa, respectively) showed significantly higher abundance in cytosolic protein fractions and lower abundance in membrane fractions in DH<sub>31</sub> + *Aedae*CAPA-1 incubated MTs.

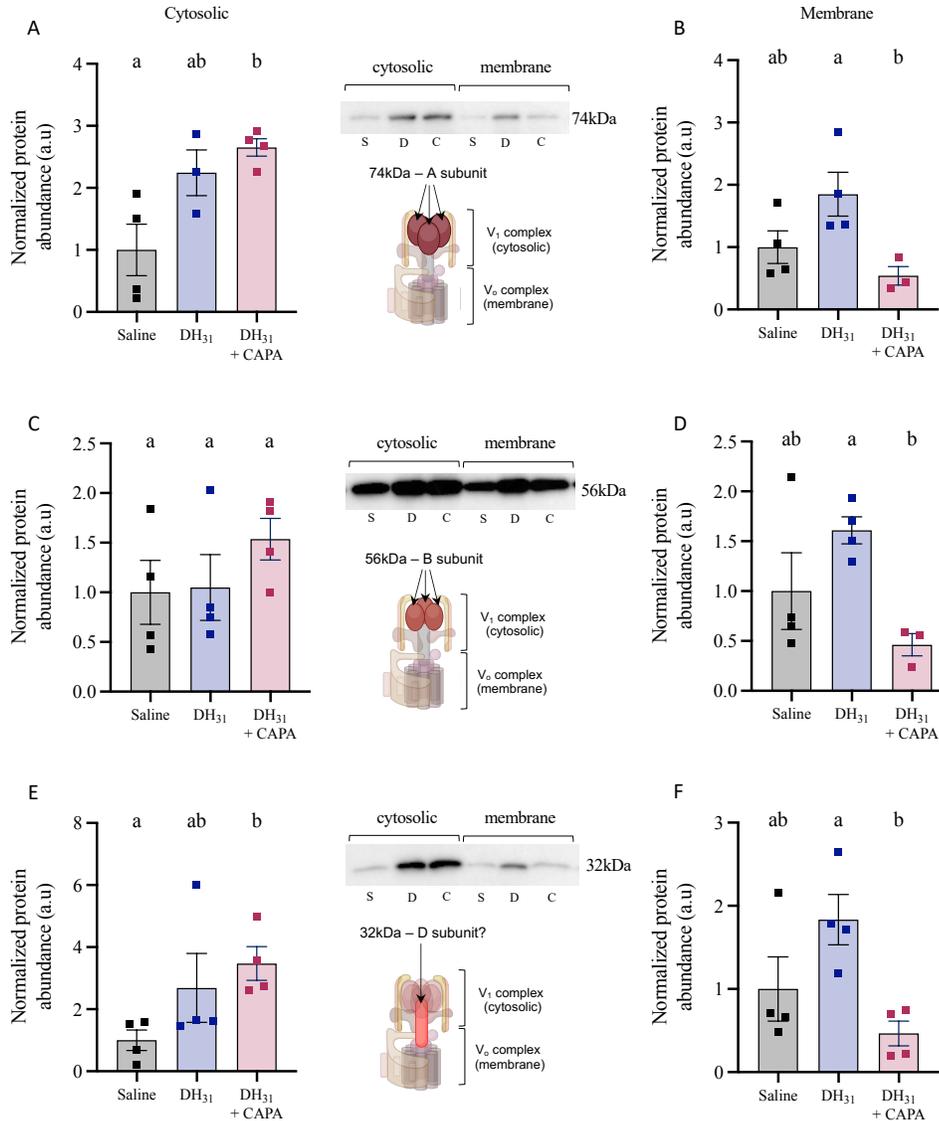


**Figure 4-3. Membrane and cytosolic protein abundance of the V<sub>1</sub> complex in MTs of *A. aegypti*.** The MTs (n=40–50) were incubated in *Aedes* saline, DH<sub>31</sub>, or DH<sub>31</sub> + *Aedae*CAPA-1 for one hour before collection. Protein abundance was measured in the (A) 74 kDa band, A subunit (B) 56 kDa band, B subunit and (C) 32 kDa band, suggested D subunit of the V<sub>1</sub> complex. Individual band densities were normalized to total protein using Coomassie staining, and graphed relative to saline-treated controls. Abbreviations: saline (S), DH<sub>31</sub> (D), and DH<sub>31</sub> + CAPA (C). Bars labeled with different letters are significantly different from each other (mean±SEM; one-way ANOVA with Bonferroni multiple comparison, p<0.05, n=3–4 replicates).

To visualize this potential endocrine-mediated reorganization of the VA holoenzyme in this simple epithelium, we immunolocalized the membrane-integrated  $V_o$  and cytosolic  $V_1$  complex in the female *A. aegypti* MTs. Transverse sections of saline-incubated (control) MTs demonstrated moderate enrichment of  $V_o$  (Figure 4-4A, red), and  $V_1$  (Figure 4-4B, green) complexes in the apical membrane of principal cells (Figure 4-4C, S4-6A-D). Comparatively,  $DH_{31}$ -incubated MTs revealed intense localization of the  $V_o$  (Figure 4-4D, red), and  $V_1$  (Figure 4-4E, green) complexes within principal cells, where  $V_1$  staining was strictly co-localized with  $V_o$  staining on the apical membrane (Figure 4-4F, Figure S4-6E-H). Interestingly, although  $V_o$  immunolocalization was restricted to the apical membrane,  $V_1$  immunoreactivity was observed in both the apical membrane and cytosolic region in  $DH_{31}$  + *Aedae*CAPA-1 co-treated MTs (Figure 4-4G-I, Figure S4-6I-T). Immunostaining was absent in control preparations probed with only secondary antibodies (not shown) confirming the specific detection of the VA complexes with each primary antibody.

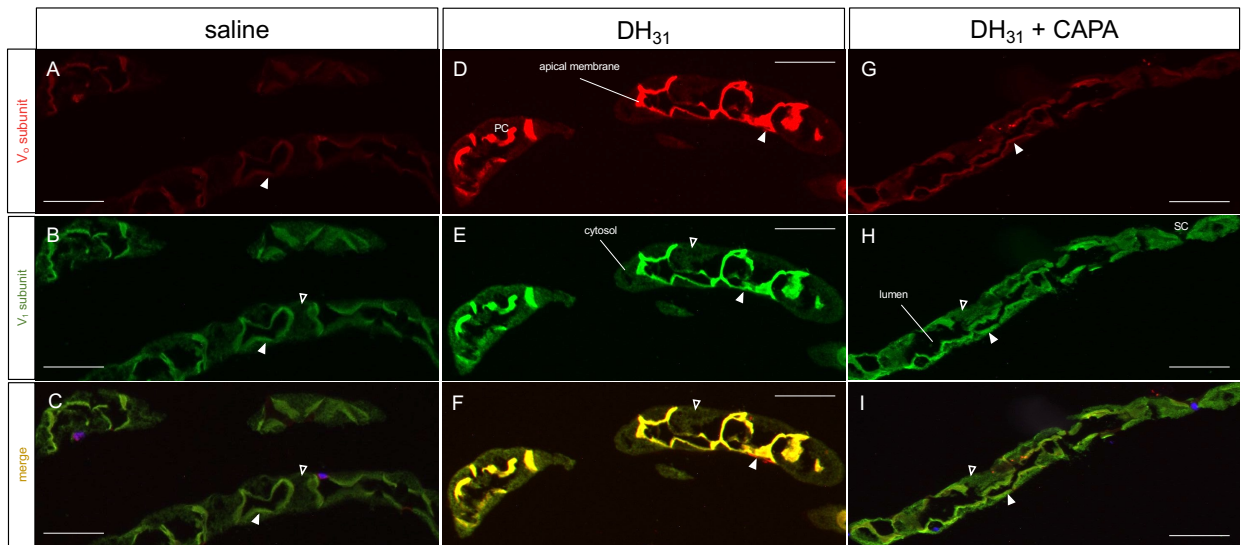


**Figure 4-4. Immunolocalization of the  $V_0$  and  $V_1$  complexes in transverse sections of stimulated *A. aegypti* MTs.** Representative paraffin-embedded sections of *A. aegypti* MTs incubated in either (A-C) *Aedes* saline alone, (D-F)  $DH_{31}$  and (G-I)  $DH_{31}$  + *Aedae*CAPA-1 for 30 min. Panels (A,D,G) show  $V_0$  staining (red), (B,E,H) show  $V_1$  staining (green), and panels (C,F,I) show merged images with staining highly colocalized in  $DH_{31}$  treatment but less evident in saline and *Aedae*CAPA-1 added treatments. Solid white arrows denote apical VA staining, and empty arrows indicate cytosolic VA staining. Where visible in sections, DAPI nuclear staining is shown in blue. Scale bar 100  $\mu$ m, n=4 biological replicates, (SC = stellate cell).

To investigate this endocrine-mediated phenomenon *in vivo*, we immunolocalized the membrane-integrated  $V_o$  and cytosolic  $V_1$  complex in blood fed females at different time points. Whole body sections of non-blood fed similarly aged females (control) demonstrated moderate enrichment of both  $V_o$  (Figure 4-5A, red), and  $V_1$  (Figure 4-4B, green) in the MTs, with minimal co-localization (Figure 4-5C), resembling saline-incubated MTs. Interestingly, blood fed female MTs revealed strong co-localization of the  $V_o$  and  $V_1$  complexes at 10 min (Figure 4-5D-F) and 30 min (Figure 4-5G-I) post-bloodmeal, whereas  $V_1$  immunoreactivity was more dispersed in both the apical membrane and cytosolic area in MTs 3 hrs post-bloodmeal (Figure 4-5J-L), comparable to non-blood fed females.

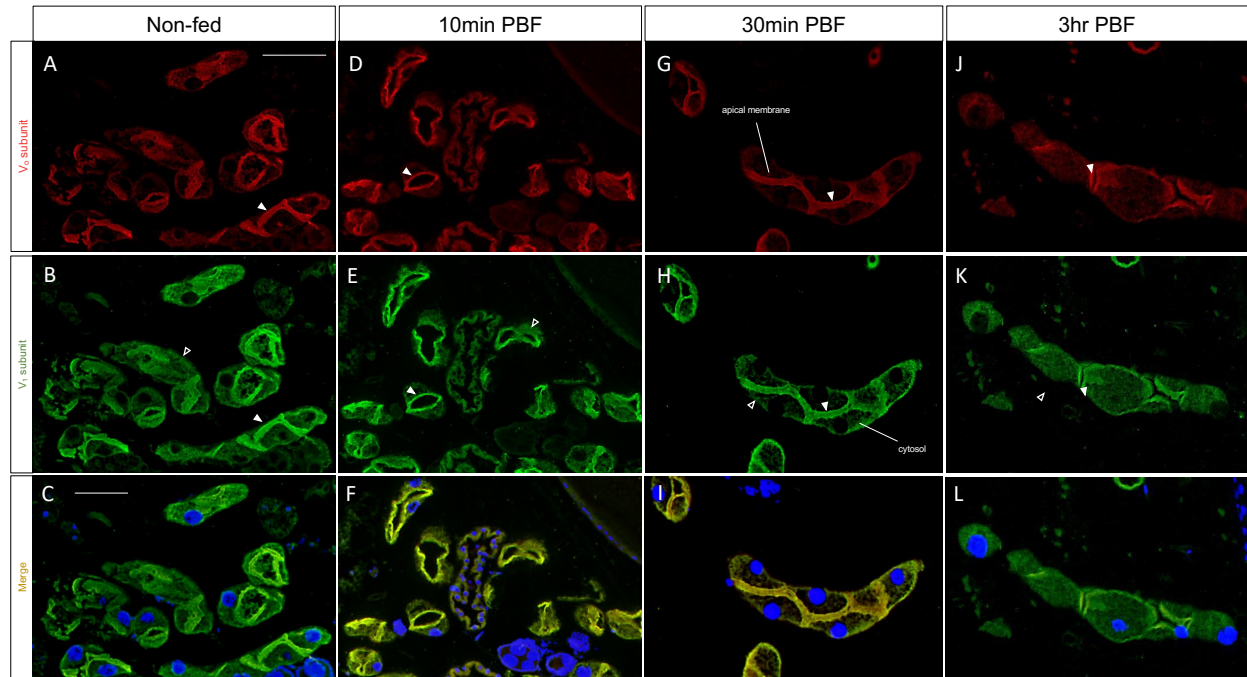


**Figure 4-5. Immunolocalization of the  $V_0$  and  $V_1$  complexes in blood fed *A. aegypti* females.** Representative paraffin-embedded sections of whole-body non-blood fed females (A-C), blood fed females isolated (D-F) 10 min (G-I) 30 min and (J-L) 3 hr post-bloodmeal. Panels (A,D,G,J) show  $V_0$  staining (red), (B,E,H,K)  $V_1$  staining (green), and panels (C,F,I,L) show merged immunoreactive staining. DAPI nuclear staining is shown in blue. Scale bar 100  $\mu$ m, n=4 biological replicates.

## 4.5 Discussion

The MTs of the *Aedes* mosquito are the main organs responsible for the secretion of water and solutes, thereby contributing towards hydromineral homeostasis of the animal (Beyenbach and Piermarini, 2011). Active ion transport in *A. aegypti* MTs is accomplished mainly by the V-ATPases (VA) densely localized in the apical brush-border membrane of principal cells, that energize the apical and basolateral membrane as well as the paracellular pathway, allowing for transepithelial secretion of NaCl, KCl, and other solutes (Beyenbach, 2001). In animal cells, V-ATPase molecules in the plasma membrane, especially on the apical membrane of epithelial cells, contribute to extracellular acidification or alkalization, intracellular pH homeostasis, or energize the plasma membrane for secondary active transport (Nelson and Harvey, 1999; Nishi and Forgac, 2002). In insect MTs, the VA plays a major role in fluid secretion, thus serving as a primary target for both diuretic and, as this study demonstrates, anti-diuretic hormonal regulation of the insect ‘renal’ tubules. Although the structure and function of the VA has been elucidated in some detail (Beyenbach et al., 2000; Beyenbach et al., 2010; Dames et al., 2006; Kane, 1995; Voss et al., 2007; Weng et al., 2003; Wiczorek et al., 1999b), the regulation of the proton pump remains unclear. Of the various regulatory mechanisms for VA activity, the most studied is the reversible dissociation of the cytosolic  $V_1$  complex from the membrane-integrated  $V_o$  complex, first established in the midgut of the tobacco hornworm, *Manduca sexta* and yeast, *Saccharomyces cerevisiae* (Kane, 1995; Sumner et al., 1995). In the present study, the activity and regulation of the VA was investigated under both diuretic and anti-diuretic hormone control of the adult female *A. aegypti* MTs. Notably, the current results advance our knowledge of the anti-diuretic control of the *A. aegypti* MTs, revealing a cellular mechanism for CAPA inhibition of the MTs by targeting the VA to block fluid secretion

stimulated by select diuretic factors. This includes inhibition of the DH<sub>31</sub>-related mosquito natriuretic peptide, which is critical for the post-haematophagy diuresis that eliminates excess water and sodium originating from the bloodmeal-derived plasma.

In insects, water excretion is tightly regulated to maintain homeostasis of ions and water (Beyenbach, 2003; Coast, 2007; O'Donnell and Spring, 2000). Female *A. aegypti* engorge a salt- and water-rich bloodmeal to obtain the necessary nutrients and proteins for their eggs (Beyenbach, 2003), with about 40% of the ingested water eliminated in the first hour post-feeding (Williams et al., 1983). The high rates of water excretion along with the high rates of primary urine production post-bloodmeal suggest a highly coordinated and defined hormonal regulation of the signalling processes and downstream cellular targets for ion and water transport (Jagge and Pietrantonio, 2008). In *Aedes* MTs, fluid secretion increases at least three-fold after stimulation with mosquito natriuretic peptide (identified as DH<sub>31</sub>), via cAMP as a second messenger (Beyenbach, 2003), activating PKA, which subsequently activates V-ATPase-driven cation transport processes (Dames et al., 2006; Tiburcy et al., 2013; Zimmermann et al., 2003). Herein we show that DH<sub>31</sub>-stimulated secretion is inhibited by bafilomycin, thought to block the proton channel of the VA (Zhang et al., 1994). Moreover, the addition of either bafilomycin or *Aedae*CAPA-1 caused alkalization of the secreted fluid, indicating inhibition of the VA, which may lead to constrained entry of cations across the apical membrane through a proposed alkali cation/proton antiporter (Wieczorek, 1992; Wieczoreks et al., 1991). Thus, since bafilomycin inhibits DH<sub>31</sub>-stimulated secretion, this supports the VA as a target in the inhibition of fluid secretion. Consequently, the driving force for ion movement and osmotically-obliged water is reduced, but select Na<sup>+</sup> channels and cotransporters remain unaffected in the presence of *Aedae*CAPA-1, as observed by the unchanged natriuretic effect of DH<sub>31</sub> despite reduced

secretion rates in response to *Aedae*CAPA-1 (Chapter 2; Sajadi et al., 2018). Similar results were seen in 5HT-stimulated secretion, albeit a partial inhibition. An earlier study demonstrated that  $\text{Ca}^{2+}$ -mediated diuresis does not require the assembly and activation of the VA (Quinlan et al., 1997; Tiburcy et al., 2013). The cAMP effect on the VA is implemented by protein kinase A (PKA), with inhibitors of PKA abolishing hormone-induced assembly and activation of the VA (Rein et al., 2008). Although the endogenous 5HT receptor expressed within the *A. aegypti* MTs necessary for diuretic activity remains elusive, in the kissing bug, *Rhodnius prolixus*, both cAMP and  $\text{Ca}^{2+}$  have been shown to initiate diuresis in response to 5HT (Gioino et al., 2014), which could explain the partial inhibitory response of *Aedae*CAPA-1 inhibition on 5HT-stimulated tubules as  $\text{Ca}^{2+}$ -mediated diuresis is independent of the VA (Tiburcy et al., 2013). Notably, the anticipated 5HT type 2 receptor subtype expressed in the principal cells of the MTs is predicted to couple through a Gq/11 signalling mechanism (Chapter 1; Sajadi and Paluzzi, 2021) and likely excludes the type 7 Gs-coupled receptor localized to tracheolar cells associated with the MTs (Lee and Pietrantonio, 2003; Pietrantonio et al., 2001) as well as the type 1 Gi-coupled receptor localized to principal cells in larval stage mosquitoes (Petrova and Moffett, 2016).

Interestingly,  $\text{DH}_{44}$ -mediated stimulation was observed to be independent of the VA, as bafilomycin had no effect on the secretion rate or pH of the secreted fluid following application of this CRF-related diuretic peptide. Previous studies have noted that low nanomolar concentrations of a  $\text{DH}_{44}$ -related peptide were linked to the stimulation of the paracellular pathway only (Clark et al., 1998), mediating this action through intracellular  $\text{Ca}^{2+}$  as a second messenger (Clark et al., 1998). In contrast, high nanomolar concentrations of a  $\text{DH}_{44}$ -related peptide were shown to influence both paracellular and transcellular transport, increasing intracellular  $\text{Ca}^{2+}$  and cAMP (Clark et al., 1998). Although haemolymph concentrations of

diuretic peptides have yet to be determined in mosquitoes, DH<sub>31</sub> is immediately released into circulation post-bloodmeal, stimulating rapid secretion of Na<sup>+</sup> and excess water (Coast et al., 2005; Williams et al., 1983). In contrast, DH<sub>44</sub>-stimulated diuresis in *A. aegypti* involves non-selective transport of Na<sup>+</sup> and K<sup>+</sup> cations (Chapter 2; Sajadi et al., 2018), which supports a delayed release of this diuretic hormone post-feeding to maintain production (albeit reduced) of primary urine whilst conserving Na<sup>+</sup> ions.

In unstimulated adult female *Aedes* MTs isolated *in vitro*, the VA exhibits variable rates of enzyme activity, consistent with highly variable rates of secretion, as found also in various other insect species (Dow et al., 1994; Petzel et al., 1985; Petzel et al., 1999). The VA is the main energizer in MTs as 60% of total ATPase activity can be linked to the VA (Weng et al., 2003), whereas the NKA, with around 28% of ATPase activity, also plays a role in membrane energization, denoting a more important role in the function of MTs than was previously assumed (Beyenbach, 2001; Beyenbach and Piermarini, 2011; Patrick et al., 2006; Tiburcy et al., 2013). Here we show a significant two-fold increase in VA activity in MTs treated with DH<sub>31</sub> compared to the unstimulated MTs, with no change in VA activity in 5HT and DH<sub>44</sub>-treated MTs. Notably, *Aedae*CAPA-1 treatment blocked the DH<sub>31</sub>-driven increase in VA activity, which corroborates the reduced fluid secretion rate and alkalization of the secreted fluid. Additionally, we sought to establish the importance of the NOS/cGMP/PKG pathway in the inhibitory actions of *Aedae*CAPA-1 on VA association. In stimulated MTs treated with *Aedae*CAPA-1 along with NOS inhibitor, L-NAME, or PKG inhibitor, KT5823, the inhibitory activity of *Aedae*CAPA-1 and its second messenger cGMP was abolished, resulting in elevated VA activity as a result of DH<sub>31</sub> treatment. The present study examined the effects of *Aedae*CAPA-1 on DH<sub>31</sub>-stimulated VA activation for the first time in insects. Stimulation of DH<sub>31</sub> causes an increase in cAMP

production, which activates  $\text{Na}^+$  channels and the  $\text{Na}^+/\text{K}^+/\text{2Cl}^-$  cotransporter in the basolateral membrane (Petzel et al., 1987) and up-regulates VA activity (as shown herein and previously) critical for increased fluid secretion (Karas et al., 2005). The  $\text{DH}_{31}$  receptor (*AegGPRCAL1*) is expressed in a distal-proximal gradient in the MTs, with greater expression in principal cells where the VA in the apical membrane is highly expressed (Kwon et al., 2012; Patrick et al., 2006). The co-localization of the  $\text{DH}_{31}$  receptor, VA, and cation exchangers (Kang'ethe et al., 2007; Piermarini et al., 2009; Pullikuth et al., 2006) in the distal segment of the MTs, along with the CAPA receptor (Chapter 3; Sajadi et al., 2020), collectively supports the major roles  $\text{DH}_{31}$  and CAPA play in post-prandial diuresis and anti-diuresis, respectively. In contrast to the marked changes in VA activity in response to diuretic and anti-diuretic hormones, NKA activity remained unchanged in response to treatments conducted herein. Further studies should examine the potential role of the NKA in diuretic and anti-diuretic processes.

The reversible dissociation of the  $V_1$  and  $V_o$  complexes is currently thought as a universal regulatory mechanism of V-ATPases, appearing to be widely conserved from yeast to animal cells (Dames et al., 2006; Merzendorfer et al., 1999; Weng et al., 2003; Zimmermann et al., 2003). Although previously shown with cAMP (Karas et al., 2005), it remained unclear whether other second messengers (eg.  $\text{Ca}^{2+}$ , cGMP, and nitric oxide) affect the assembly/disassembly of the  $V_1V_o$  complexes in insect MTs. In this study, VA protein abundance in membrane and cytosolic fractions of MTs was confirmed by western blot analyses. The 56 kDa band represents the B subunit (Novak et al., 1992), while the 74 kDa and 32 kDa bands are suggested to be the A and D subunits, respectively, of the  $V_1$  complex (Wieczorek et al., 1999a). The higher abundance of these  $V_1$  complex protein subunits in the cytosolic fraction and lower abundance in membrane fraction in *Aedae*CAPA-1-treated MTs provides novel evidence of hormonally regulated  $V_1$

dissociation from the holoenzyme in *A. aegypti* MTs. This was further confirmed with V<sub>1</sub> staining found both in the apical membrane and cytosol of the MTs treated with DH<sub>31</sub> and *Aedae*CAPA-1 in contrast to the strict co-localization of the V<sub>1</sub> and V<sub>o</sub> complex in the apical membrane of MTs treated with DH<sub>31</sub> alone. In unstimulated *A. aegypti* MTs, 40-73% of the V<sub>1</sub> subunits were found to be membrane associated, with reassembly of the V<sub>1</sub>V<sub>o</sub> complex observed upon stimulation with cAMP analogues (Tiburcy et al., 2013). Although studies have revealed that hormonal regulation can activate the assembly of the holoenzyme, the signalling mechanisms achieving this control are unclear. In this study, the data provides evidence of VA assembly in DH<sub>31</sub>-treated MTs, with V<sub>1</sub> complex protein subunit enrichment found in the membrane fractions, confirming the crucial role of the VA in DH<sub>31</sub>-stimulated secretion. Studies in *A. aegypti* have demonstrated the involvement of PKA in the activation and assembly of the VA upon natriuretic hormone (i.e. DH<sub>31</sub>) stimulation and indicate the phosphorylation of the VA subunits by PKA in the MTs (Tiburcy et al., 2013). These studies indicate a regulatory role of PKA in VA assembly and its activation that may be independent or in addition to phosphorylation (Tiburcy et al., 2013). In line with these earlier observations, the current results indicate PKA is critical for DH<sub>31</sub>-stimulated fluid secretion by MTs whereas DH<sub>44</sub>-stimulated diuresis was found to be PKA-independent.

Together, these results indicate that *Aedae*CAPA-1 binding to its cognate receptor in principal cells of the MTs (Chapter 3; Sajadi et al., 2020) targets the NOS/cGMP/PKG pathway (Chapter 3; Sajadi et al., 2020), to inhibit DH<sub>31</sub>-mediated elevation of cAMP (Coast et al., 2005; Petzel et al., 1987), which blocks PKA-activated VA association and prevents protons from being pumped across the apical membrane, resulting in a more alkaline lumen. Our study provides novel evidence that the anti-diuretic activity of CAPA is mediated through the

dissociation of the VA holoenzyme involving the removal of the  $V_1$  complex from the apical membrane, hindering luminal flux of protons that in turn starves cation/ $H^+$  exchange, which ultimately reduces fluid secretion (Figure 4-6). In *R. prolixus* MTs, the physiological roles of cGMP and cAMP were examined (Quinlan and O'Donnell, 1998) suggesting cGMP inhibits fluid secretion by activating a phosphodiesterase (PDE) that degrades cAMP elevated following 5HT and diuretic hormone stimulation of MTs. Indeed, the current results demonstrated the addition of cAMP reversed the inhibitory effects of cGMP, while the addition of cGMP reduced the stimulatory response of cAMP, supporting that these two cyclic nucleotides facilitate two opposing physiological roles in the MTs of adult *A. aegypti*. The data herein reveals cGMP levels increase in MTs treated with CAPA alone or in combination with  $DH_{31}$  while cAMP levels decrease in MTs treated with CAPA in combination with  $DH_{31}$  compared to tubules stimulated with  $DH_{31}$  alone, which upholds the roles of cAMP and cGMP in diuretic and anti-diuretic signalling pathways, respectively. Interestingly, mid-nanomolar concentrations of  $DH_{44}$  also led to increased levels of cAMP, with levels unchanging in response to *Aedae*CAPA-1, raising doubt regarding the involvement of a PDE. Treatment of a PKA inhibitor, KT5720, abolished  $DH_{31}$ -stimulated secretion but had no effect on  $DH_{44}$ -mediated stimulation. It is well established that the effects of cAMP are mediated by activation of cAMP-dependent protein kinase (PKA), a major cAMP target, followed by phosphorylation of target proteins (Seino and Shibasaki, 2005). More recently, in *D. melanogaster* MTs, two distinct cAMP pathways have been elucidated to sustain fluid secretion; a PKA-dependent pathway, shown to regulate basal fluid secretion in principal cells; and a PKA-independent pathway, specifically a stimulatory principal EPAC (exchange proteins directly activated by cAMP) pathway, stimulating fluid

secretion above basal levels (Efetova et al., 2013). Future studies should examine the potential DH<sub>44</sub>-stimulated PKA-independent pathway leading to secretion in *A. aegypti* MTs.

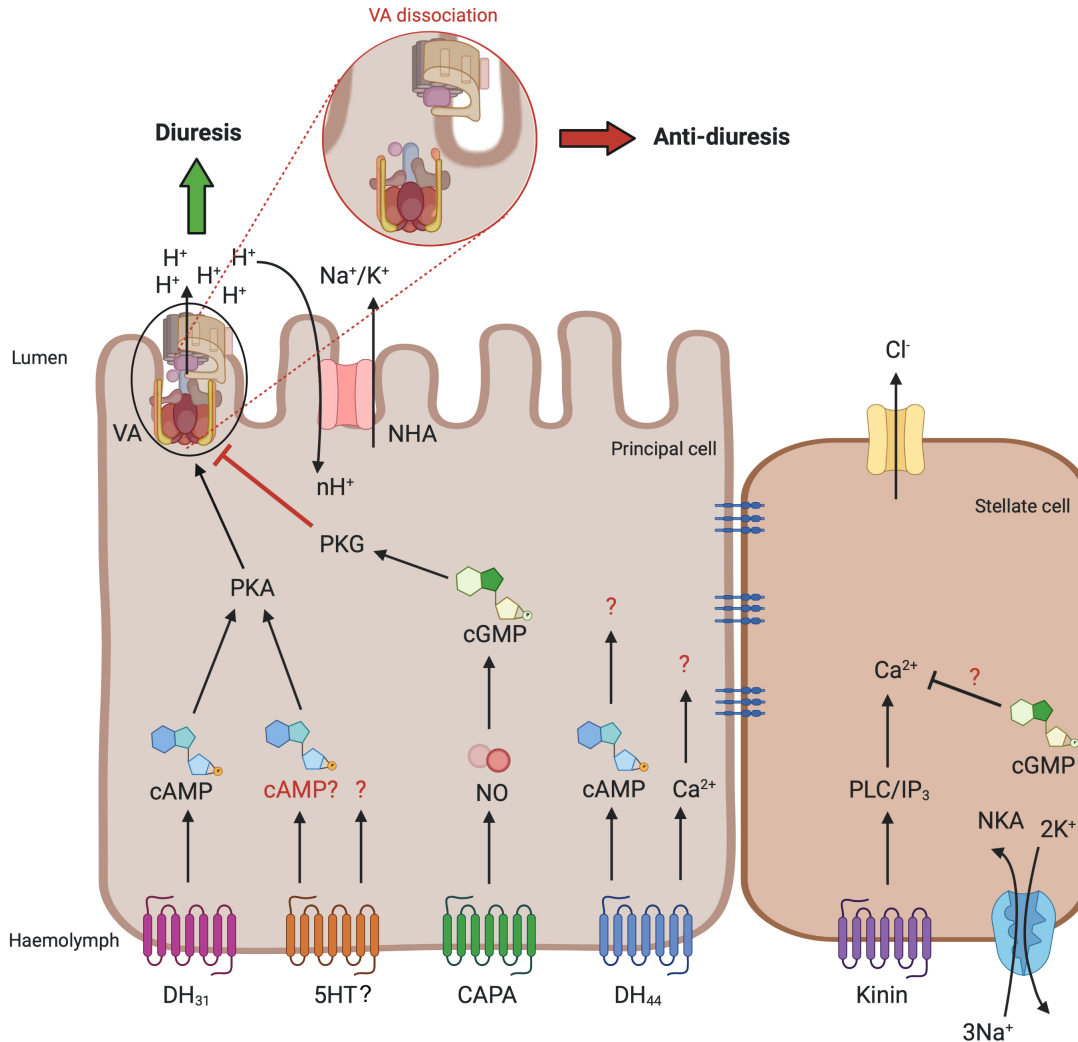


**Figure 4-6. Schematic diagram summarizing the signalling pathway of diuretic and anti-diuretic control of adult *A. aegypti* MTs.** The principal cells in *A. aegypti* MTs are responsible for the transport of Na<sup>+</sup> and K<sup>+</sup> cations via secondary active transport, energized by the V-type H<sup>+</sup>-ATPase (VA), localized in the brush border of the apical membrane. The movement of protons creates a gradient, driving the exchange of Na<sup>+</sup> and K<sup>+</sup> through cation/H<sup>+</sup> antiporters (NHA). Neurohormone receptors for DH<sub>31</sub>, 5HT, DH<sub>44</sub>, and CAPA are localized to the basolateral membrane of the principal cells, while the kinin receptor is localized exclusively in the stellate cells. The current results together with previous data indicates that DH<sub>31</sub> stimulates diuresis through activation and assembly of the VA in the apical membrane, with no effect on the Na<sup>+</sup>/K<sup>+</sup>-ATPase (NKA). The anti-diuretic effect of *Aedae*CAPA-1, facilitated by the NOS/cGMP/PKG pathway, causes V<sub>1</sub> dissociation from the membrane, hindering activity, and thus reducing fluid secretion. The biogenic amine, 5HT, has also been shown to stimulate activation of the VA, however, to a lesser extent. DH<sub>44</sub>-related peptide receptor activation increases Ca<sup>2+</sup> and cAMP, but its action was found to be independent of PKA and VA. Lastly, it was shown earlier that cGMP inhibits kinin-stimulated diuresis, suggesting an additional anti-diuretic factor may exist that acts specifically on stellate cells.

In summary, our study highlights a novel target in the anti-diuretic signalling pathway of adult female *A. aegypti* MTs, emphasizing the intricate and precise regulatory mechanism of anti-diuresis. Although a plethora of studies have investigated the process of hydromineral balance in terrestrial insects from a diuretic perspective (Beyenbach, 2003; Beyenbach et al., 1993; Coast et al., 2005; Paluzzi et al., 2012; Terhzaz et al., 2012; Veenstra, 1988), these current findings advance our understanding of anti-diuretic hormone control while providing further evidence of a previously elusive endocrine regulatory mechanism of the VA in mosquitoes (Figure 4-6). Given that many terrestrial insects are recognized as agricultural pests or disease vectors, further investigating the complex regulation of their ionic and osmotic balance may aid in lessening their burden on human health and prosperity through development of improved management strategies that, at least in part, impede their neuroendocrine control of hydromineral homeostasis.

#### 4.6 References

- Beyenbach, K. W.** (2001). Energizing epithelial transport with the vacuolar H<sup>+</sup>-ATPase. *News Physiol. Sci.* **16**, 145–151.
- Beyenbach, K. W.** (2003). Transport mechanisms of diuresis in Malpighian tubules of insects. *J. Exp. Biol.* **206**, 3845–3856.
- Beyenbach, K. W., and Piermarini, P. M.** (2011). Transcellular and paracellular pathways of transepithelial fluid secretion in Malpighian (renal) tubules of the yellow fever mosquito *Aedes aegypti*. *Acta. Physiol. (Oxf.)* **202**, 387–407.
- Beyenbach, K. W., and Wieczorek, H.** (2006). The V-type H<sup>+</sup> ATPase: molecular structure and function, physiological roles and regulation. *J. Exp. Biol.* **209**, 577–589.
- Beyenbach, K. W., Oviedo, A., and Aneshansley, D. J.** (1993). Malpighian tubules of *Aedes aegypti*: five tubules, one function. *J. Insect Physiol.* **39**, 639–648.
- Beyenbach, K. W., Pannabecker, T. L., and Nagel, W.** (2000). Central role of the apical membrane H<sup>+</sup>-ATPase in electrogenesis and epithelial transport in Malpighian tubules. *J. Exp. Biol.* **203**, 1459–1468.
- Beyenbach, K. W., Skaer, H., and Dow, J. A. T.** (2010). The developmental, molecular, and transport biology of Malpighian tubules. *Annu. Rev. of Entomol.* **55**, 351–374.
- Butler, T. A. J., Paul, J. W., Chan, E. C., Smith, R., and Tolosa, J. M.** (2019). Misleading westerns: common quantification mistakes in western blot densitometry and proposed corrective measures. *Biomed. Res. Int.* doi: 10.1155/2019/5214821.
- Cady, C., and Hagedorn, H. H.** (1999). Effects of putative diuretic factors on intracellular second messenger levels in the Malpighian tubules of *Aedes aegypti*. *J. Insect Physiol.* **45**, 327–337.

- Chasiotis, H., and Kelly, S. P.** (2008). Occludin immunolocalization and protein expression in goldfish. *J. Exp. Biol.* **211**, 1524–1534.
- Clark, T. M., and Bradley, T. J.** (1997). Malpighian tubules of larval *Aedes aegypti* are hormonally stimulated by 5-hydroxytryptamine in response to increased salinity. *Arch. Insect Biochem. Physiol.* **34**, 123–141.
- Clark, T. M., and Bradley, T. J.** (1998). Additive effects of 5-HT and diuretic peptide on *Aedes* Malpighian tubule fluid secretion. *Comp. Biochem. Physiol. - A Mol. Integr. Physiol.* **119**, 599–605.
- Clark, T. M., Hayes, T. K., and Beyenbach, K. W.** (1998). Dose-dependent effects of CRF-like diuretic peptide on transcellular and paracellular transport pathways. *Am. J. Physiol. Renal Physiol.* **274**, F834–F840
- Clark, T. M., Hayes, T. K., Holman, G.M., Beyenbach, K. W.** (1998). The concentration-dependence of CRF-like diuretic peptide: mechanisms of action. *J. Exp. Biol.* **201**, 1753–1762.
- Coast, G.** (2007). The endocrine control of salt balance in insects. *Gen. Comp. Endocrinol.* **152**, 332–338.
- Coast, G. M., and Garside, C. S.** (2005). Neuropeptide control of fluid balance in insects. *Ann. N. Y. Acad. Sci.* **1040**, 1–8.
- Coast, G. M., Garside, C. S., Webster, S. G., Schegg, K. M., and Schooley, D. A.** (2005). Mosquito natriuretic peptide identified as a calcitonin-like diuretic hormone in *Anopheles gambiae* (Giles). *J. Exp. Biol.* **208**, 3281–3291.
- Dames, P., Zimmermann, B., Schmidt, R., Rein, J., Voss, M., Schewe, B., Walz, B., and Baumann, O.** (2006). cAMP regulates plasma membrane vacuolar-type H<sup>+</sup>-ATPase

- assembly and activity in blowfly salivary glands. *Proc. Natl. Acad. Sci. USA* **103**, 3926–3931.
- Davies, S. A., Cabrero, P., Povsic, M., Johnston, N. R., Terhzaz, S., and Dow, J. A. T.** (2012). Signaling by *Drosophila* capa neuropeptides. *Gen. Comp. Endocrinol.* **188**, 60–66.
- Dow, J. A., Maddrell, S. H., Görtz, A., Skaer, N. J., Brogan, S., and Kaiser, K.** (1994). The Malpighian tubules of *Drosophila melanogaster*: a novel phenotype for studies of fluid secretion and its control. *J. Exp. Biol.* **197**, 421–428.
- Dschida, W. J. A., and Bowman, B. J.** (1995). The vacuolar ATPase: sulfite stabilization and the mechanism of nitrate inactivation. *J. Biol. Chem.* **270**, 1557–1563.
- Durant, A. C., and Donini, A.** (2020). Ammonium transporter expression in sperm of the disease vector *Aedes aegypti* mosquito influences male fertility. *Proc. Natl. Acad. Sci. USA* **117**, 29712–29719.
- Efetova, M., Petereit, L., Rosiewicz, K., Overend, G., Haußig, F., Hovemann, B. T., Cabrero, P., Dow, J. A. T., and Schwärzel, M.** (2013). Separate roles of PKA and EPAC in renal function unraveled by the optogenetic control of cAMP levels in vivo. *J. Cell Sci.* **126**, 778–788.
- Fosang, A. J., and Colbran, R. J.** (2015). Transparency is the key to quality. *J. Biol. Chem.* **290**, 29692–29694.
- Gioino, P., Murray, B. G., and Ianowski, J. P.** (2014). Serotonin triggers cAMP and PKA-mediated intracellular calcium waves in Malpighian tubules of *Rhodnius prolixus*. *Am. J. Physiol. Regul. Integr. Comp. Physiol.* **307**, R828–R836.

- Harvey, W. R., Maddrell, S. H. P., Telfer, W. H., and Wieczorek, H.** (1998). H<sup>+</sup> V-ATPases energize animal plasma membranes for secretion and absorption of ions and fluids. *Am. Zool.* **38**, 426–441.
- Hine, R. M., Rouhier, M. F., Park, S. T., Qi, Z., Piermarini, P. M., and Beyenbach, K. W.** (2014). The excretion of NaCl and KCl loads in mosquitoes. 1. control data. *Am. J. Physiol. Regul. Integr. Comp. Physiol.* **307**, R837–R849.
- Ionescu, A., and Donini, A.** (2012). *Aedes* CAPA-PVK-1 displays diuretic and dose dependent antidiuretic potential in the larval mosquito *Aedes aegypti* (Liverpool). *J. Insect Physiol.* **58**, 1299–1306.
- Jagge, C. L., and Pietrantonio, P. V.** (2008). Diuretic hormone 44 receptor in Malpighian tubules of the mosquito *Aedes aegypti*: evidence for transcriptional regulation paralleling urination. *Insect Mol. Biol.* **17**, 413–426.
- Jonusaite, S., Kelly, S. P., and Donini, A.** (2011). The physiological response of larval *Chironomus riparius* (Meigen) to abrupt brackish water exposure. *J. Comp. Physiol. B* **181**, 343–352.
- Jurenka, R.** (2015). The PRXamide neuropeptide signalling system - conserved in animals. *Adv. Insect Physiol.* **49**, 123–170.
- Kane, P. M.** (1995). Disassembly and reassembly of the yeast vacuolar H<sup>+</sup>-ATPase in vivo. *J. Biol. Chem.* **270**, 17025–17032.
- Kang'ethe, W., Aimanova, K. G., Pullikuth, A. K., and Gill, S. S.** (2007). NHE8 mediates amiloride-sensitive Na<sup>+</sup>/H<sup>+</sup> exchange across mosquito Malpighian tubules and catalyzes Na<sup>+</sup> and K<sup>+</sup> transport in reconstituted proteoliposomes. *Am. J. Physiol. Renal Physiol.* **292**, 1501–1512.

- Karas, K., Brauer, P., and Petzel, D.** (2005). Actin redistribution in mosquito Malpighian tubules after a blood meal and cyclic AMP stimulation. *J. Insect Physiol.* **51**, 1041–1054.
- Kean, L., Cazenave, W., Costes, L., Broderick, K. E., Graham, S., Pollock, V. P., Davies, S. A., Veenstra, J. A., and Dow, J. A. T.** (2002). Two nitridergic peptides are encoded by the gene capability in *Drosophila melanogaster*. *Am. J. Physiol. Regul. Integr. Comp. Physiol.* **282**, R1297–R1307.
- Kwon, H., Lu, H. L., Longnecker, M. T., and Pietrantonio, P. V.** (2012). Role in diuresis of a calcitonin receptor (GPCAL1) expressed in a distal-proximal gradient in renal organs of the mosquito *Aedes aegypti* (L.). *PLoS One* **7**, e50374.
- Lee, D. W., and Pietrantonio, P. V.** (2003). In vitro expression and pharmacology of the 5-HT<sub>7</sub>-like receptor present in the mosquito *Aedes aegypti* tracheolar cells and hindgut-associated nerves. *Insect Mol. Biol.* **12**, 561–569.
- Lee, H. R., Zandawala, M., Lange, A. B., and Orchard, I.** (2016). Isolation and characterization of the corticotropin-releasing factor-related diuretic hormone receptor in *Rhodnius prolixus*. *Cell Signal.* **28**, 1152–1162.
- Li, Y., Piermarini, P. M., Esquivel, C. J., Drumm, H. E., Schilkey, F. D., and Hansen, I. A.** (2017). RNA-Seq comparison of larval and adult Malpighian tubules of the yellow fever mosquito *Aedes aegypti* reveals life stage-specific changes in renal function. *Front. Physiol.* **8**, 1–13.
- Lu, H. L., Kersch, C., and Pietrantonio, P. V.** (2011). The kinin receptor is expressed in the Malpighian tubule stellate cells in the mosquito *Aedes aegypti* (L.): a new model needed to explain ion transport? *Insect Biochem. Mol. Biol.* **41**, 135–140.

- MacMillan, H. A., Nazal, B., Wali, S., Yerushalm, G. Y., Misyura, L., Donini, A., and Paluzzi, J. P.** (2018). Anti-diuretic activity of a CAPA neuropeptide can compromise *Drosophila* chill tolerance. *J. Exp. Biol.* **221**, doi: 10.1242/jeb.185884.
- McCormick, S. D.** (1993). Methods for nonlethal gill biopsy and measurement of Na<sup>+</sup>, K<sup>+</sup>-ATPase activity. *Can. J. Fish. Aqua. Sci.* **50**, 656–658.
- Merzendorfer, H., Huss, M., Schmid, R., Harvey, W. R., and Wieczorek, H.** (1999). A novel insect V-ATPase subunit M9.7 is glycosylated extensively. *J. Biol. Chem.* **274**, 17372–17378.
- Misyura, L., Guardian, E. G., Durant, A. C., and Donini, A.** (2020). A comparison of aquaporin expression in mosquito larvae (*Aedes aegypti*) that develop in hypo-osmotic freshwater and iso-osmotic brackish water. *PLoS One* **15**, e0234892.
- Nelson, N., and Harvey, W. R.** (1999). Vacuolar and plasma membrane proton-adenosinetriphosphatases. *Physiol. Rev.* **79**, 361–385.
- Nishi, T., and Forgac, M.** (2002). The vacuolar (H<sup>+</sup>)-ATPases - nature's most versatile proton pumps. *Nat. Rev. Mol. Cell Biol.* **3**, 94–103.
- Novak, F. J. S., Gräf, R., Waring, R. B., Wolfersberger, M. G., Wieczorek, H., and Harvey, W. R.** (1992). Primary structure of V-ATPase subunit B from *Manduca sexta* midgut. *BBA - Gene Struct. Expr.* **1132**, 67–71.
- O'Donnell, M. J., and Spring, J. H.** (2000). Modes of control of insect Malpighian tubules: synergism, antagonism, cooperation and autonomous regulation. *J. Insect Physiol.* **46**, 107–117.

- Paluzzi, J. P., Naikhwah, W. and O'Donnell, M. J.** (2012). Natriuresis and diuretic hormone synergism in *R. prolixus* upper Malpighian tubules is inhibited by the anti-diuretic hormone, *RhoprCAPA-α2*. *J. Insect Physiol.* **58**, 534–542.
- Pan, Y. X., Gu, H. H., Xu, J., and Dean, G. E.** (1993). *Saccharomyces cerevisiae* expression of exogenous vacuolar ATPase subunits B. *BBA – Biomembr.* **1151**, 175–185.
- Patrick, M. L., Aimanova, K., Sanders, H. R., and Gill, S. S.** (2006). P-type Na<sup>+</sup>/K<sup>+</sup>-ATPase and V-type H<sup>+</sup>-ATPase expression patterns in the osmoregulatory organs of larval and adult mosquito *Aedes aegypti*. *J. Exp. Biol.* **209**, 4638–4651.
- Petrova, A., and Moffett, D. F.** (2016). Comprehensive immunolocalization studies of a putative serotonin receptor from the alimentary canal of *Aedes aegypti* larvae suggest its diverse roles in digestion and homeostasis. *PLoS One* **11**, e0146587.
- Petzel, D. H., Hagedorn, H. H., and Beyenbach, K. W.** (1985). Preliminary isolation of mosquito natriuretic factor. *Am. J. Physiol. Regul. Integr. Comp. Physiol.* **249**, R379–R386.
- Petzel, D. H., Berg, M. M., and Beyenbach, K. W.** (1987). Hormone-controlled cAMP-mediated fluid secretion in yellow-fever mosquito. *Am. J. Physiol. Regul. Integr. Comp. Physiol.* **253**, R701–R711.
- Petzel, D. H., Pirotte, P. T., and van Kerkhove, E.** (1999). Intracellular and luminal pH measurements of Malpighian tubules of the mosquito *Aedes aegypti*: the effects of cAMP. *J. Insect Physiol.* **45**, 973–982.
- Piermarini, P. M., Weihrauch, D., Meyer, H., Huss, M., and Beyenbach, K. W.** (2009). NHE8 is an intracellular cation/H<sup>+</sup> exchanger in renal tubules of the yellow fever mosquito *Aedes aegypti*. *Am. J. Physiol. - Renal Physiol.* **296**, 730–750.

- Pietrantonio, P. V., Jagge, C., and McDowell, C.** (2001). Cloning and expression analysis of a 5HT7-like serotonin receptor cDNA from mosquito *Aedes aegypti* female excretory and respiratory systems. *Insect Mol. Biol.* **10**, 357–369.
- Pullikuth, A. K., Aimanova, K., Kang’ethe, W., Sanders, H. R., and Gill, S. S.** (2006). Molecular characterization of sodium/proton exchanger 3 (NHE3) from the yellow fever vector, *Aedes aegypti*. *J. Exp. Biol.* **209**, 3529–3544.
- Quinlan, M. C., and O’Donnell, M. J.** (1998). Anti-diuresis in the blood-feeding insect *Rhodnius prolixus* Stål: antagonistic actions of cAMP and cGMP and the role of organic acid transport. *J. Insect Physiol.* **44**, 561–568.
- Quinlan, M. C., Tublitz, N. J., and O’Donnell, M. J.** (1997). Anti-diuresis in the blood-feeding insect *Rhodnius prolixus* Stål: the peptide CAP(2b) and cyclic GMP inhibit Malpighian tubule fluid secretion. *J. Exp. Biol.* **200**, 2363–2367.
- Rein, J., Voss, M., Blenau, W., Walz, B., and Baumann, O.** (2008). Hormone-induced assembly and activation of V-ATPase in blowfly salivary glands is mediated by protein kinase A. *Am. J. Physiol. Cell Physiol.* **294**, C56–C65.
- Rheault, M. R., and O’Donnell, M. J.** (2004). Organic cation transport by Malpighian tubules of *Drosophila melanogaster*: application of two novel electrophysiological methods. *J. Exp. Biol.* **207**, 2173–2184.
- Rocco, D. A., Kim, D. H., and Paluzzi, J. P.** (2017). Immunohistochemical mapping and transcript expression of the GPA2/GPB5 receptor in tissues of the adult mosquito, *Aedes aegypti*. *Cell Tissue Res.* **369**, 313–330.
- Rodan, A. R., Baum, M., and Huang, C. L.** (2012). The *Drosophila* NKCC Ncc69 is required for normal renal tubule function. *Am. J. Physiol. Cell Physiol.* **303**, C883–C894.

- Sajadi, F., Curcuruto, C., Al Dhaheri, A., and Paluzzi, J. P.** (2018). Anti-diuretic action of a CAPA neuropeptide against a subset of diuretic hormones in the disease vector, *Aedes aegypti*. *J. Exp. Biol.* **221**.
- Sajadi F., Lajevardi, A., Donini, A., and Paluzzi, J. P.** (2021). Studying the activity of neuropeptides and other regulators of the excretory system in the adult mosquito. *J. Vis. Exp.* **174**, doi: 10.3791/61849.
- Sajadi, F., Uyuklu, A., Paputsis, C., Lajevardi, A., Wahedi, A., Ber, L. T., Matei, A., and Paluzzi, J. P.** (2020). CAPA neuropeptides and their receptor form an anti-diuretic hormone signaling system in the human disease vector, *Aedes aegypti*. *Sci. Rep.* **10**. <https://doi.org/10.1038/s41598-020-58731-y>.
- Seino, S., and Shibasaki, T.** (2005). PKA-dependent and PKA-independent pathways for cAMP-regulated exocytosis. *Physiol. Rev.* **85**, 1303–1342.
- Sumner, J. P., Dow, J. A. T., Earley, F. G. P., Klein, U., Jager, D., and Wiczorek, H.** (1995). Regulation of plasma membrane V-ATPase activity by dissociation of peripheral subunits. *J. Biol. Chem.* **270**, 5649–5653.
- Te Brugge, V., Paluzzi, J. P., Schooley, D. A., and Orchard, I.** (2011). Identification of the elusive peptidergic diuretic hormone in the blood-feeding bug *Rhodnius prolixus*: a CRF-related peptide. *J. Exp. Biol.* **214**, 371–381.
- Terhzaz, S., Cabrero, P., Robben, J. H., Radford, J. C., Hudson, B. D., Milligan, G., Dow, J. A. T., and Davies, S. A.** (2012). Mechanism and function of *Drosophila* capa GPCR: a desiccation stress-responsive receptor with functional homology to human neuromedinu receptor. *PLoS One* **7**, e29897.

- Tiburcy, F., Beyenbach, K. W., and Wiczorek, H.** (2013). Protein kinase A-dependent and – independent activation of the V-ATPase in Malpighian tubules of *Aedes aegypti*. *J. Exp. Biol.* **216**, 881–891.
- Vanderveken, M., and O'Donnell, M. J.** (2014). Effects of diuretic hormone 31, *drosokinin*, and allatostatin A on transepithelial K<sup>+</sup> transport and contraction frequency in the midgut and hindgut of larval *Drosophila melanogaster*. *Arch. Insect Biochem. Physiol.* **85**, 76–93.
- Veenstra, J. A.** (1988). Effects of 5-hydroxytryptamine on the Malpighian tubules of *Aedes-aegypti*. *J. Insect Physiol.* **34**, 299–304.
- Voss, M., Vitavska, O., Walz, B., Wiczorek, H., and Baumann, O.** (2007). Stimulus-induced phosphorylation of vacuolar H<sup>+</sup>-ATPase by protein kinase A. *J. Biol. Chem.* **282**, 33735–33742.
- Weng, X. H., Huss, M., Wiczorek, H., and Beyenbach, K. W.** (2003). The V-type H<sup>+</sup>-ATPase in Malpighian tubules of *Aedes aegypti*: localization and activity. *J. Exp. Biol.* **206**, 2211–2219.
- Wiczorek, H.** (1992). The insect V-ATPase, a plasma membrane proton pump energizing secondary active transport: molecular analysis of electrogenic potassium transport in the tobacco hornworm midgut. *J. Exp. Biol.* **172**, 335–343.
- Wiczorek, H., Grüber, G., Harvey, W. R., Huss, M., and Merzendorfer, H.** (1999a). The plasma membrane H<sup>+</sup>-V-ATPase from tobacco hornworm midgut. *J. Bioenerg. Biomemb.* **31**, 67–74.
- Wiczorek, H., Brown, D., Grinstein, S., Ehrenfeld, J., and Harvey, W. R.** (1999b). Animal plasma membrane energization by proton-motive V-ATPases. *BioEssays* **21**, 637–648.

- Wieczorek, H., Beyenbach, K. W., Huss, M., and Vitavska, O.** (2009). Vacuolar-type proton pumps in insect epithelia. *J. Exp. Biol.* **212**, 1611–1619.
- Wieczorek, H., Putzenlechner, M., and Klein, U.** (1991). A vacuolar-type proton pump energizes  $K^+/H^+$  antiport in an animal plasma membrane. *J. Biol. Chem.* **266**, 15340–15347.
- Williams, J. C., Hagedorn, H. H., and Beyenbach, K. W.** (1983). Dynamic changes in flow rate and composition of urine during the post-bloodmeal diuresis in *Aedes aegypti* (L.). *J. Comp. Physiol.* **153**, 257–265.
- Zhang, J., Feng, Y., and Forgac, M.** (1994). Proton conduction and bafilomycin binding by the  $V_0$  domain of the coated vesicle V-ATPase. *J. Biol. Chem.* **269**, 23518–23523.
- Zimmermann, B., Dames, P., Walz, B., and Baumann, O.** (2003). Distribution and serotonin-induced activation of vacuolar-type  $H^+$ -ATPase in the salivary glands of the blowfly *Calliphora vicina*. *J. Exp. Biol.* **206**, 1867–1876.

## 4.7 Supplementary Figures

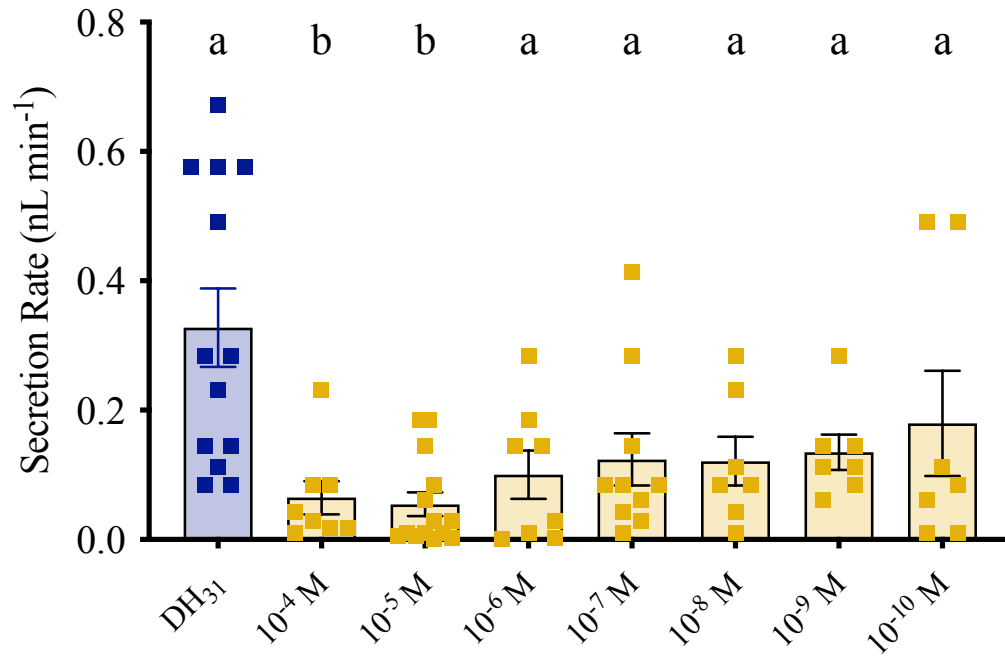


**Figure S4-1. Dose response of bafilomycin on fluid secretion rates of DH<sub>31</sub>-stimulated MTs *in vitro* isolated from adult female *A. aegypti*.** Doses of 10<sup>-4</sup> M to 10<sup>-10</sup> M bafilomycin were applied to MTs together with DH<sub>31</sub> for 60 min. Bars labeled with different letters are significantly different from each other (mean±SEM; one-way ANOVA with Bonferroni multiple comparison, p<0.05, n=7–13).

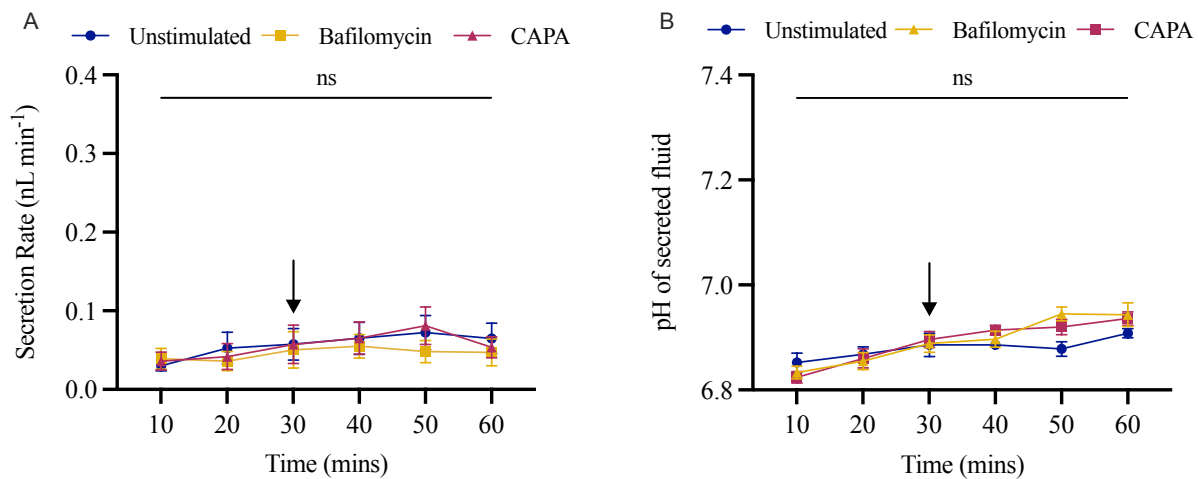


**Figure S4-2. Effect of bafilomycin and *Aedae*CAPA-1 on the secretion rate and pH of the secreted fluid by unstimulated MTs *in vitro* from adult female *A. aegypti*.** (A) Fluid secretion rates were measured at 10 min intervals over a 30 min control period and then after the addition (solid arrow) of  $10^{-5}$  M bafilomycin (yellow),  $1 \text{ fmol l}^{-1}$  *Aedae*CAPA-1 (purple), or unstimulated alone (blue). (B) The pH of the secreted droplets was measured at 10-min intervals for 60 min using an ion-selective microelectrode. No significant differences were observed in the measurements (mean $\pm$ SEM; two-way ANOVA with Bonferroni multiple comparison,  $p < 0.05$ ,  $n = 5-8$ ); ns denotes no statistical significance.

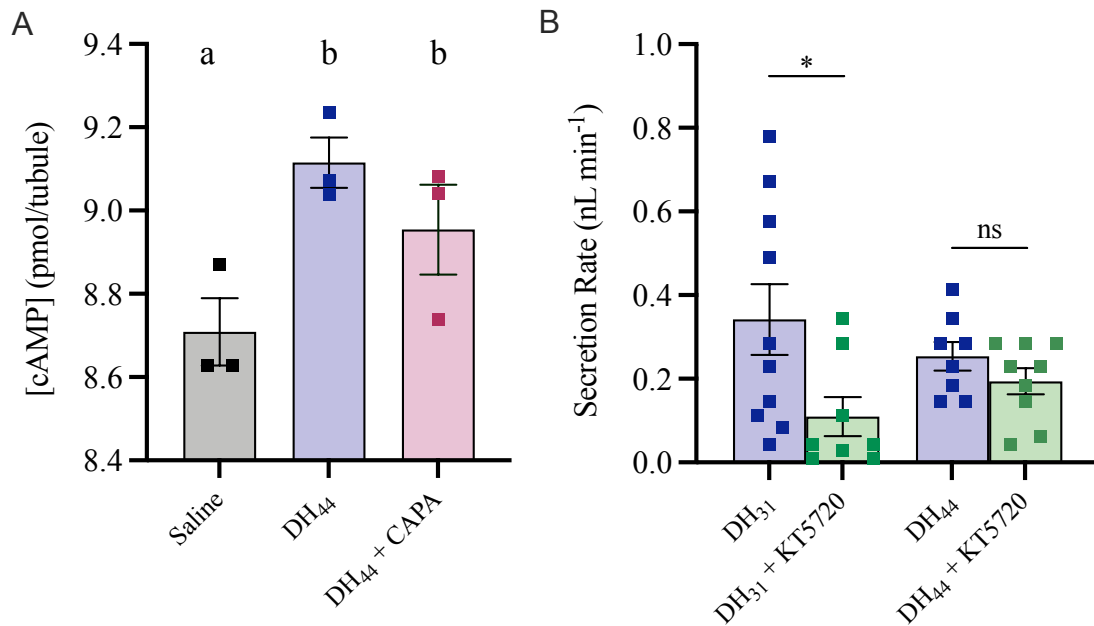


**Figure S4-3. Intracellular levels of cAMP in DH<sub>44</sub>-treated *A. aegypti* MTs.** (A) To monitor activity of *Aedae*CAPA-1 on cAMP levels in DH<sub>44</sub>-stimulated *A. aegypti* MTs, tubules were incubated in IBMX for 10 min prior to the following treatments: *Aedes* saline, DH<sub>44</sub> alone, or in combination with *Aedae*CAPA-1 for 20 min before collection. Bars labeled with different letters are significantly different from each other (mean±SEM; one-way ANOVA with Bonferroni multiple comparison,  $p < 0.05$ ). For each treatment, 50 sets of MTs were isolated and combined ( $n = 3$  biological replicates per treatment). (B) Female MTs were treated with either DH<sub>31</sub> or DH<sub>44</sub> alone or in combination with the PKA inhibitor, KT5720 for 60 min to measure fluid secretion rate. Significant differences are denoted by an asterisk (mean±SEM; one-way ANOVA with Bonferroni multiple comparison,  $p < 0.05$ ,  $n = 8-10$ ).

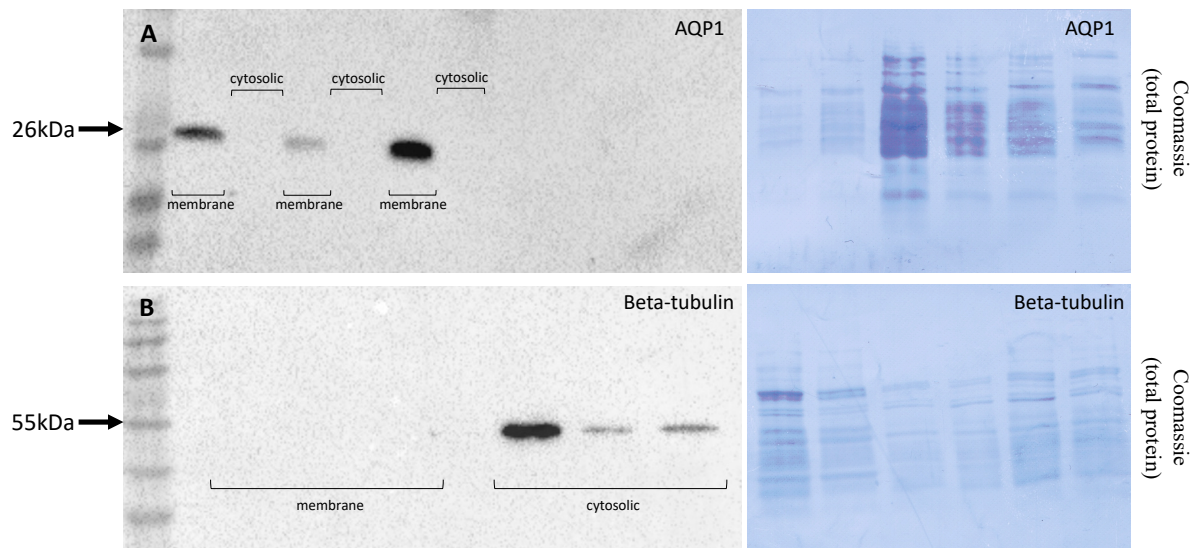


**Figure S4-4. Representative western blot of membrane and cytosolic protein fraction isolation validated using established membrane (aquaporin-1 in *A. aegypti* MTs) and cytosolic (beta-tubulin) protein markers.** (A) Aquaporin-1 (AQP1) detection shown in membrane fractions of *Aedes* saline-incubated MTs at 26 kDa, and (B) beta-tubulin in cytosolic fractions of *Aedes* saline-incubated MTs at 55 kDa (n=40–50 MTs per replicate, n=3 biological replicates). Protein abundance was normalized to total protein (Coomassie) used as a loading control.

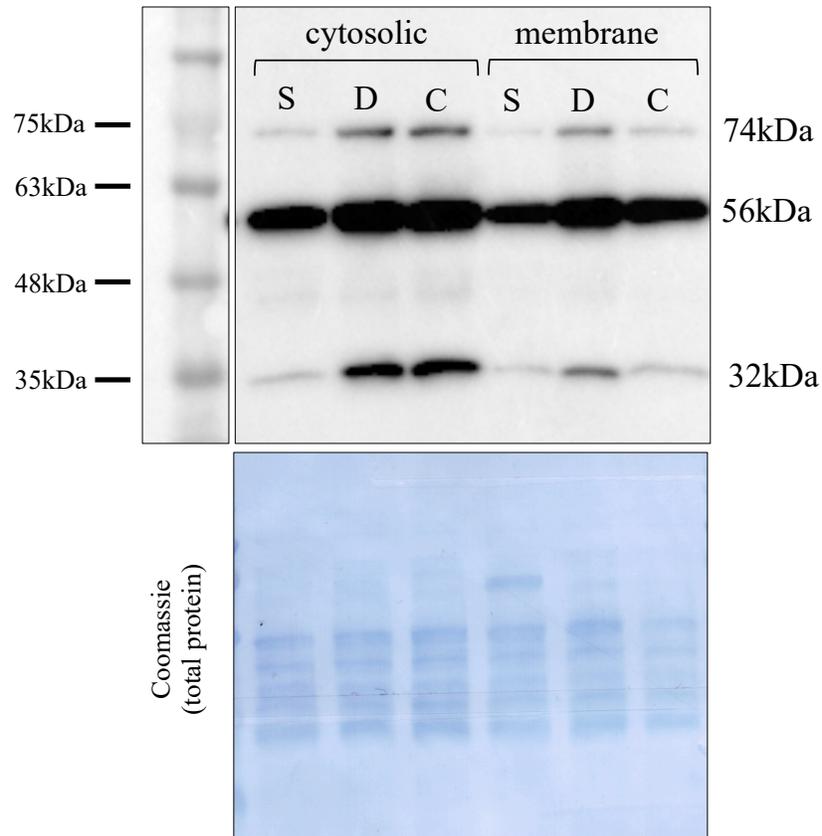


**Figure S4-5. Representative western blot image of membrane and cytosolic protein abundance of the V<sub>1</sub> complex in *A. aegypti* MTs.** The MTs (n=40–50) were incubated in *Aedes* saline alone, DH<sub>31</sub>, or DH<sub>31</sub> + *Aedae*CAPA-1 for one hour before collection. Western blot analysis revealed three protein bands, with calculated molecular masses of 74 kDa, 56 kDa, and 32 kDa (S = *Aedes* saline, D = DH<sub>31</sub>, C = DH<sub>31</sub> + *Aedae*CAPA-1). Protein abundance was normalized to total protein (Coomassie, shown in the lower panel), used as a loading control.

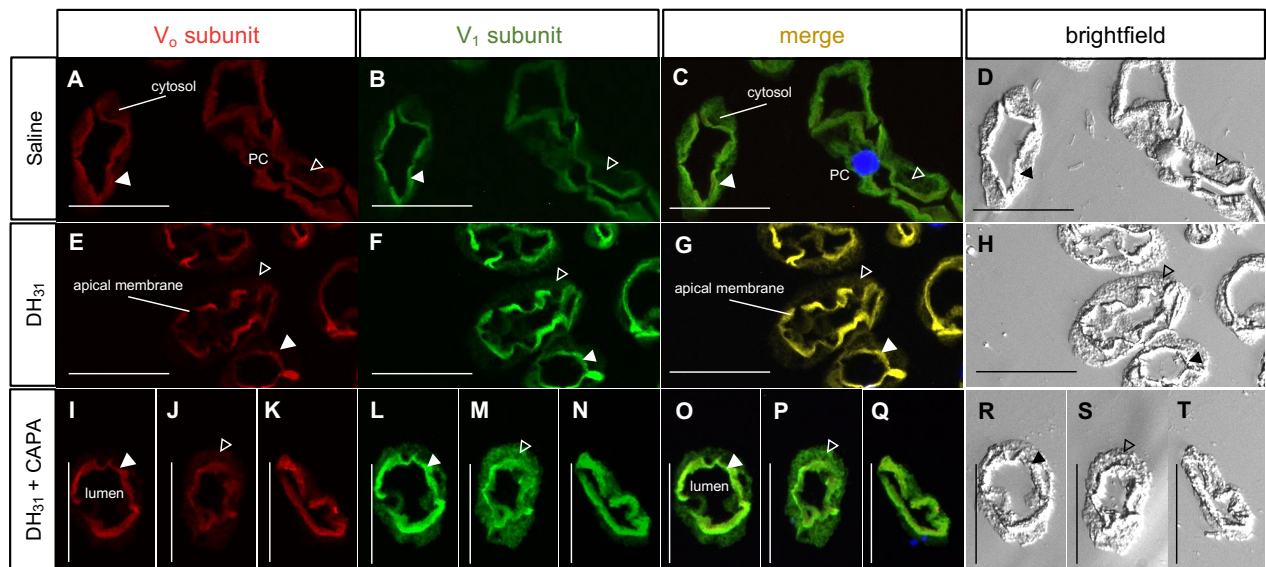


**Figure S4-6. Immunolocalization of the  $V_0$  and  $V_1$  complexes in cross sections of stimulated *A. aegypti* MTs.** Representative paraffin-embedded sections of *A. aegypti* MTs incubated in either (A-D) *Aedes* saline, (E-H) DH<sub>31</sub> and (I-T) DH<sub>31</sub> + *Aedae*CAPA-1. Panels (A,E,I-K) show membrane-integrated  $V_0$  immunoreactive staining (red), (B,F,L-N) demonstrate  $V_1$  immunoreactive staining (green), (C,G,O-Q) show merged images of  $V_0$  and  $V_1$  staining, while (D,H,R-T) show brightfield images. Solid white arrowheads denote apical VA staining, and empty arrowheads mark cytosolic VA staining. DAPI nuclear staining is shown in blue. Scale bar 100  $\mu$ m, n=3–4 biological replicates (PC = principal cell).

## **Chapter Five**

### **Dynamics of DH<sub>31</sub> and CAPA neuropeptide release and activity post-bloodmeal in the female mosquito, *A. aegypti***

This chapter has not yet been submitted for publication.

## 5.1 Summary

Female *Aedes aegypti* secrete urine rapidly and copiously post-bloodmeal ingestion, with diuresis beginning immediately even while still feeding on the vertebrate host to enable removal of excess salts and water. This post-prandial diuresis occurs in three phases; peak phase, post-peak phase, and late phase, which are achieved by the combined actions of multiple hormones, including diuretic and anti-diuretic factors. Calcitonin-like diuretic hormone 31 (DH<sub>31</sub>) is believed to be released post-bloodmeal to stimulate diuresis and natriuresis through its actions on the DH<sub>31</sub> receptor, *Aedae*DH<sub>31</sub>-R, that has previously been localized to the Malpighian ‘renal’ tubules (MTs). In contrast, the anti-diuretic neurohormone, CAPA, inhibits secretion by MTs stimulated by select diuretic hormones, including DH<sub>31</sub>. While both DH<sub>31</sub> and CAPA are critical in achieving post-prandial diuresis and anti-diuresis, respectively, the exact timing of release and haemolymph levels of these peptides remain unknown. Herein, using heterologously expressed *A. aegypti* DH<sub>31</sub> and CAPA receptors, we investigated the titres of both peptides in the haemolymph of females at different time points after blood feeding. Since the functional deorphanization of *Aedae*DH<sub>31</sub>-R has not been previously reported, a heterologous receptor assay was used to characterize ligand specificity and revealed the receptor was highly selective to mosquito DH<sub>31</sub>. Haemolymph extracts were then tested in the heterologous assay indicating levels of DH<sub>31</sub> in the haemolymph increase immediately post-bloodmeal, with levels remaining elevated for 15 minutes, and peaking at 5 minutes. We also tested the activity of haemolymph extracts using an *in vitro* bioassay, whereby female MTs were treated with haemolymph samples to measure secretion rate. Haemolymph samples collected between 0 and 5 minutes post-bloodmeal resulted in stimulation of fluid secretion, coinciding with DH<sub>31</sub> release into the female haemolymph validated by the heterologous receptor assay. Comparatively, haemolymph CAPA

levels steadily increase 15 minutes post-blood feeding, with levels peaking at 30 minutes. These results suggest that DH<sub>31</sub> is released immediately post-bloodmeal and, along with CAPA peptides, have a coordinative action on the MTs to maintain haemolymph homeostasis through regulation of primary urine secretion.

## 5.2 Introduction

Female *A. aegypti* mosquitoes ingest bloodmeals equivalent to more than twice their body mass which presents an enormous payload to the flying animal, making them more susceptible to predation (Roitberg et al., 2003). The bloodmeal, imbibed with each reproductive cycle, serves as a source of protein, nutrients, and vitamins for egg development (Beyenbach and Petzel, 1987), but also contains considerable amounts of unwanted salts and water that threaten haemolymph homeostasis (Beyenbach, 2003). To counter this challenge, a rapid natriuresis and diuresis commences before the bloodmeal is completed, with almost half the imbibed plasma volume and salt excreted within 1-2 hours of feeding (Williams et al., 1983). In female *A. aegypti*, post-prandial diuresis is observed in three phases: peak phase (within 10 min of feeding), post-peak phase (10–50 min), and late phase (50–120 min), with significant water eliminated during the peak phase (Williams et al., 1983). During these three post-prandial phases, ion composition in the urine varies, with greatest natriuresis ( $\text{Na}^+$  secretion) occurring during the peak phase (Beyenbach, 2003), and kaliuresis ( $\text{K}^+$  secretion) delayed until post-peak and late phases. The varied pattern of water and salt loss indicates that multiple regulatory mechanisms act simultaneously during post-prandial diuresis (Williams et al., 1983).

Endocrine control of this post-prandial diuresis is regulated by the actions of both diuretic and anti-diuretic hormones, including calcitonin-like diuretic hormone 31 ( $\text{DH}_{31}$ ) (Coast et al., 2005; Kwon et al., 2012; Chapters 2-4; Sajadi et al., 2018; Sajadi et al., 2020), corticotropin-releasing factor (CRF)-like diuretic hormone 44 ( $\text{DH}_{44}$ ) (Clark and Bradley, 1996; Clark et al., 1998a; Clark et al., 1998b; Jagge and Pietrantonio, 2008; Chapters 2 and 4; Sajadi et al., 2018), insect kinins (Lu et al., 2011; Schepel et al., 2010; Veenstra, 1994; Chapter 2; Sajadi et al., 2018), biogenic amines such as 5-hydroxytryptamine (serotonin, 5HT) (Ionescu and Donini,

2012; Veenstra, 1988; Chapters 2-4; Sajadi et al., 2018; Sajadi et al., 2020), and CAPA neuropeptides (Ionescu and Donini, 2012; Pollock et al., 2004; Chapters 2-4; Sajadi et al., 2018; Sajadi et al., 2020). These endocrine messengers act on cognate receptors in the renal organs, the Malpighian tubules (MTs), to stimulate ion and water transport for primary urine production (Beyenbach, 2003). In the *Aedes* mosquito, MTs are comprised of two cell types forming a simple epithelium; mitochondria-rich principal cells, which facilitate active cation ( $\text{Na}^+$  and  $\text{K}^+$ ) transport from the haemolymph into the tubule lumen, and thin stellate cells that aid in the transepithelial secretion of  $\text{Cl}^-$  (Beyenbach, 2003; Patrick et al., 2006). Post-bloodmeal, excess fluid and ions ( $\text{Na}^+$ ,  $\text{K}^+$ , and  $\text{Cl}^-$ ) are transported from the haemolymph into the lumen of the MTs, secreting high rates of urine (Beyenbach, 2003; Lu et al., 2011). Transport is achieved by channels and cotransporters in the principal and stellate cells, driven by the V-type  $\text{H}^+$ -ATPase (VA) (Beyenbach, 2003; Patrick et al., 2006; Wiczorek et al., 1991; Chapter 4) expressed in the apical brush border membrane of principal cells (Weng et al., 2003). The initial stimulus for this diuresis and natriuresis post-blood feeding is mosquito natriuretic peptide (MNP), which is released into the haemolymph when the female takes a bloodmeal (Beyenbach and Petzel, 1987). The calcitonin-like hormone,  $\text{DH}_{31}$ , was identified as the MNP in the mosquitoes *A. aegypti* and *Anopheles gambiae* (Coast et al., 2005), activating transepithelial secretion of  $\text{Na}^+$  in the MTs via the second messenger, cyclic AMP (cAMP) (Beyenbach, 2003). Upon release from the CNS,  $\text{DH}_{31}$  binds to a G-protein coupled receptor (GPCR) expressed in select principal cells in a distal-proximal gradient (Kwon et al., 2012), increasing cAMP production (Beyenbach and Petzel, 1987), upregulating VA function and assembly, to ultimately increase fluid secretion (Karas et al., 2005; Chapter 4).

In adult female *A. aegypti* MTs, CAPA neuropeptides elicit an anti-diuretic role, with CAPA-1 shown to inhibit secretion by MTs stimulated by select diuretic factors, DH<sub>31</sub> and 5HT (Chapter 2; Sajadi et al., 2018). Recent studies have reported that CAPA peptides bind to GPCRs localized exclusively to the principal cells (Chapter 3; Sajadi et al., 2020), eliciting their actions through the nitric oxide synthase (NOS)/ cyclic GMP (cGMP)/ protein kinase G (PKG) pathway (Ionescu and Donini, 2012; Pollock et al., 2004; Terhzaz et al., 2012; Chapter 3; Sajadi et al., 2020), targeting the VA and promoting VA holoenzyme dissociation (see Chapter 4).

While haemolymph levels of DH<sub>31</sub> and CAPA have yet to be determined, studies suggest the DH<sub>31</sub> peptide is immediately released into circulation post-bloodmeal, allowing for the rapid secretion of Na<sup>+</sup> and excess water (Coast et al., 2005). The *A. aegypti* DH<sub>31</sub> receptor is a member of the class B (secretin) GPCR family and is localized in select principal cells where the V-ATPases in the apical membrane and proton/cation exchangers in the basolateral membranes are highly expressed, which points towards compartmentalization of hormone signalling to achieve high levels of fluid secretion (Kwon et al., 2012). In the present study, the *A. aegypti* DH<sub>31</sub> and CAPA receptors identified previously (Kwon et al., 2012; Sajadi et al., 2020) were heterologously expressed to determine the circulating titres of DH<sub>31</sub> and CAPA peptides in the haemolymph of blood fed females helping to elucidate the timing of release of diuretic and anti-diuretic peptides in the adult female mosquito. Using this approach, we found that DH<sub>31</sub> is released into the female haemolymph almost instantaneously, peaking at about 5 minutes post-bloodmeal, with levels declining in the haemolymph after 15 and 30 minutes. In contrast, CAPA neuropeptides were found to rise steadily in the haemolymph after 15 minutes post-feeding, peaking at 30 minutes post-bloodmeal. This rise in both DH<sub>31</sub> and CAPA levels correspond with the immediate and short-lived peak phase of diuresis after a female ingests a bloodmeal, further

uncovering the precise regulatory mechanisms in the female mosquito acting to prevent disturbances to their haemolymph hydromineral balance and contributing to the success of the infamous blood feeding insect and disease vector.

### **5.3 Materials and Methods**

#### **Animals**

*Aedes aegypti* (Liverpool) eggs were collected from an established laboratory colony, and hatched in double-distilled water in an incubator at 26°C on a 12:12 hour light:dark cycle. Larvae were fed a solution of 2% (w/v) brewer's yeast, 2% (w/v) Argentine beef liver powder (NOW foods, Bloomington, IL, USA), and adults were provided with a 10% sucrose solution *ad libidum*. Colony upkeep involved routinely feeding adult females with sheep's blood in Alsever's solution weekly (Cedarlane Laboratories Ltd., Burlington, ON, Canada) using an artificial feeding system described previously (Rocco et al., 2017). All experiments were performed on four to seven-day old females that were either sucrose-fed or blood-fed as specified.

#### **Haemolymph collection**

To collect haemolymph samples, adult *A. aegypti* female mosquitoes were placed in two treatment conditions; 1) non-blood-fed females provided 10% sucrose solution *ad libidum* and 2) blood-fed females provided a bloodmeal (also provided 10% sucrose solution *ad libidum*). Females in the blood-fed condition were fed to repletion and subsequently isolated after 0, 2, 5, 10, 15, 30, 60, 90 and 120 min post-bloodmeal (0 min corresponds to the time immediately post-bloodmeal). Each female mosquito (either blood fed or sucrose-fed) was carefully opened within

a 70  $\mu$ L droplet of 1X nuclease-free Dulbecco's phosphate-buffered saline (DPBS; Wisent Corp., St. Bruno, QC, Canada) at the segmental line between the last two abdominal segments and haemolymph was allowed to diffuse into droplet, all while ensuring no organs or blood-filled midguts ruptured. The surgically opened females were incubated in the DPBS droplet for 10 min, and haemolymph DPBS mixture was subsequently collected and stored at  $-20^{\circ}\text{C}$ .

### **Preparation of mammalian expression constructs**

Gene-specific primers were designed to amplify the open reading frame of the *AedaeDH<sub>31</sub>* receptor based on a previously published sequence (Genbank Accession Numbers: AAGE02017873) (Kwon et al., 2012) including a forward primer possessing the consensus Kozak translation initiation sequence (Paluzzi et al., 2010) at the 5' end of the start codon (*AedaeDH<sub>31</sub>-R* forward primer: GCCACCATGACATCCTCAAACGAC; *AedaeDH<sub>31</sub>-R* reverse primer: TCTAGACGCTGGCGTACTCTTTTAG). The amplified PCR product was purified using a Monarch PCR purification kit (New England Biolabs, Whitby, ON, Canada) and reamplified using modified primers containing restriction sites *Sall* and *XbaI* at 5' and 3' ends, respectively. Products were A-tailed and cloned into pGEM-T Easy vector (Promega, Madison, WI, USA) and then transformed into high efficiency competent *E. coli* cells (New England Biolabs, Whitby, ON, Canada). Purified plasmid DNA miniprep was confirmed by Sanger sequencing (The Centre for Applied Genomics, Sick Kids, Toronto, ON, Canada) to verify base pair accuracy. The receptor construct (DH<sub>31</sub>-R) was excised using standard restriction enzyme digestion and subcloned into the mammalian expression vector, pBudCE4.1 G $\alpha$ 15 (Life Technologies, Burlington, ON, Canada). Plasmid DNA was purified from overnight bacterial cultures using the Monarch Plasmid Miniprep Kit (New England Biolabs, Whitby, ON, Canada)

following manufacturer guidelines. Previously cloned *A. aegypti* CAPA receptor inserted into pcDNA3.1<sup>+</sup> (Chapter 3; Sajadi et al., 2020) was also used for transfection of mammalian cells to quantify timing and release of CAPA neuropeptides (both CAPA-1 and CAPA-2) along with DH<sub>31</sub>.

### **Heterologous receptor functional activation bioluminescence assay**

Functional activation of the *Aedae*DH<sub>31</sub>-R and *Aedae*CAPA-R was assayed using a previously established cell culture system involving a recombinant Chinese hamster ovary (CHO)-K1 cell line stably expressing aequorin (Paluzzi et al., 2012; Wahedi and Paluzzi, 2018). Cells were grown and maintained in Dulbecco's modified eagles medium:nutrient F12 (DMEM:F12; 1:1) media containing 10% heat-inactivated fetal bovine serum (FBS; Wisent, St. Bruno, QC, Canada), 1x antimycotic-antibiotic, and 200 µg/mL Geneticin. Mammalian cell lines were transiently transfected with pBudCE4.1 *Ga*15 expression vector possessing *Aedae*DH<sub>31</sub>-R or with pcDNA3.1<sup>+</sup> expression vector possessing *Aedae*CAPA-R using Lipofectamine LTX and Plus Reagent transfection system (Invitrogen, Burlington, ON, Canada) following a 3:1:1 transfection reagent (µL): Plus reagent (µL): plasmid DNA (µg) as described previously (Wahedi and Paluzzi, 2018). To confirm successful transfection, a separate flask of cells was simultaneously transfected with enhanced green fluorescent protein (EGFP), which also acts as negative control for the bioluminescence assay as it used the same vector backbone but lacking a receptor insert. Approximately 48 h post-transfection, cells were dislodged from the culture flasks using 5 mmol l<sup>-1</sup> ethylenediaminetetraacetic acid (EDTA; Life Technologies, Burlington, ON, Canada) in DPBS and cells were resuspended in BSA medium (DMEM-F12 media containing 0.1% bovine serum albumin, 1X antimycotic-antibiotic) at a concentration of 10<sup>6</sup>-10<sup>7</sup>

cells/mL. Coelenterazine *h* (Promega, Madison, WI, USA) was added to the cells to a final concentration of 5  $\mu$ M and incubated for 3 hours in the dark at room temperature on a stirrer set at 200 rpm. Subsequently, the cell suspension was diluted 10-fold in BSA medium and incubated for an additional hour at room temperature. To measure *in vivo* circulating levels of DH<sub>31</sub> in female mosquitoes, collected haemolymph samples were loaded into 96-well luminescence plates (Greiner Bio-One, Germany), and cells expressing either *Aedae*DH<sub>31</sub>-R, *Aedae*CAPA-R or EGFP (control) were loaded into each well with an automatic injector unit and luminescence was measured for 20 seconds using a Synergy 2 Multi-Mode Microplate Reader (BioTek, Winooski, VT, USA). To confirm receptor specificity, serial dilutions of peptide ligands (purity >90%, Genscript, Piscataway, NJ, USA) were prepared in BSA medium and loaded into quadruplicates in 96-well luminescence plates. A list of peptides used in this study is found in Table 5-1. Negative controls were carried out using BSA medium alone while 5  $\mu$ M ATP was used as a positive control, which activates endogenously expressed purinoceptors (Iredale and Hill, 1993; Michel et al., 1998). Experimental sample luminescent responses were normalized to ATP-induced maximal luminescent responses and neuropeptide concentration levels in the haemolymph were determined through non-linear regression analysis in GraphPad Prism 9.1 (GraphPad Software, San Diego, CA, USA).

### **Fluid secretion assay on individually isolated MTs**

In order to determine fluid secretion rates, modified Ramsay assays were performed as described previously (Sajadi et al., 2021; Chapters 2-4; Sajadi et al., 2018; Sajadi et al., 2020). Female adults (four-seven day old) were dissected under physiological *Aedes* saline adapted from (Petzel et al., 1987) that contained (in mmol<sup>-1</sup>): 150 NaCl, 25 HEPES, 3.4 KCl, 7.5 NaOH,

1.8 NaHCO<sub>3</sub>, 1 MgSO<sub>4</sub>, 1.7 CaCl<sub>2</sub>, and 5 glucose, and titrated to pH 7.1. Individual MTs were removed and placed in a Sylgard-lined Petri dish containing 20 µL bathing droplets (1:1 mixture of Schneider's Insect Medium (Sigma-Aldrich, Oakville, ON, Canada): *Aedes* saline), immersed in hydrated mineral oil to prevent evaporation. The proximal end of each tubule was wrapped around a Minutien pin to allow for fluid secretion measurements. Dose response analysis for *Aedae*DH<sub>31</sub> was determined by using dosages ranging from 10<sup>-5</sup> to 10<sup>-12</sup> mol l<sup>-1</sup> *Aedae*DH<sub>31</sub> against unstimulated MTs. To investigate the effects of haemolymph solutions collected on fluid secretion rate, haemolymph collected from both non-blood fed and blood fed females were used against unstimulated MTs and allowed to incubate for 60 min before measurement. To test *in vitro* application of *Aedae*DH<sub>31</sub> and *Aedae*CAPA-1, dosages of 25 nmol l<sup>-1</sup> and 1 fmol l<sup>-1</sup> were used, respectively (Chapters 2-4; Sajadi et al., 2018; Sajadi et al., 2020).

### **Statistical analyses**

Data was compiled using Microsoft Excel and transferred to Graphpad Prism software v.9 to create figures and conduct all statistical analyses. Data was analyzed accordingly using a one-way ANOVA and the appropriate post-hoc test as indicated in the figure captions, with differences between treatments considered significant if p<0.05.

## **5.4 Results**

### **Functional characterization of *Aedae*DH<sub>31</sub>-R**

A heterologous receptor functional assay involving CHO-K1 cells stably expressing a bioluminescent calcium sensor, aequorin (Paluzzi et al., 2012; Wahedi and Paluzzi, 2018), was used to functionally characterize the cloned *Aedes* DH<sub>31</sub> receptor (*Aedae*DH<sub>31</sub>-R). Our results

confirm the specificity of the *Aedae*DH<sub>31</sub>-R for the *Aedae*DH<sub>31</sub> peptide alone (EC<sub>50</sub>=28.45 nM) as demonstrated by the dose-dependent luminescent response (Figure 5-1A). The activity of other endogenous neuropeptides tested, including corticotropin-releasing factor (CRF)-like peptide (DH<sub>44</sub>), displayed no detectable activity over background luminescence levels (Figure 5-1B, Table 5-1). No luminescence signals above background were obtained in CHO-K1-aeq cells transfected with EGFP (data not shown) to any peptide used in this study, confirming the calcium-based luminescence response observed was a result of the DH<sub>31</sub> neuropeptide binding and activating the heterologously expressed *A. aegypti* DH<sub>31</sub> receptor.

**Table 5-1. Name and structure of insect neuropeptides used in the heterologous functional assay testing *Aedae*DH<sub>31</sub>-R and summary of activities in eliciting a luminescent response.**

Peptide Family (Name)	Peptide Sequence	EC <sub>50</sub> on DH <sub>31</sub> -R
Diuretic hormone 31 (DH <sub>31</sub> )	TVDFGLSRGYSGAQEAKHRMAMAVA NFAGGP-NH <sub>2</sub>	28.45 nM
<i>Rhodnius prolixus</i> corticotropin-releasing factor-like (CRF) peptide (DH <sub>44</sub> )	MQRPQGPSLSVANPIEVLRSRLLLEIAR RRMKEQDASRVSKNRQYLQIQI-NH <sub>2</sub>	NA
CAPA (CAPA1)	GPTVGLFAFPRV -NH <sub>2</sub>	NA
Pyrokinin-1 (PK1)	AGNSGANSGMWFPGPRL-NH <sub>2</sub>	NA
Corazonin (CRZ)	pQTFQYSRGWTN-NH <sub>2</sub>	NA
Adipokinetic corazonin-related peptide (ACP)	pQVTFSRDWNA-NH <sub>2</sub>	NA
Adipokinetic hormone 1 (AKH1)	pQLTFTPSW-NH <sub>2</sub>	NA
Culex depolarizing peptide (CDP)	NPFHSWG-NH <sub>2</sub>	NA
CNMamide (CNMa)	YMSLCHFCLCNM-NH <sub>2</sub>	NA
RYamide1 (RYa-1)	PVFFVASRY-NH <sub>2</sub>	NA
CCHamide1 (CCHa1)	KGGCLSYGHSCWGGH-NH <sub>2</sub>	NA
CCHamide2 (CCHa2)	GCAAFGHACYGGH-NH <sub>2</sub>	NA

No activity (NA) denotes peptides with no detectable activity when tested with titres up to a maximum of 10 µM.

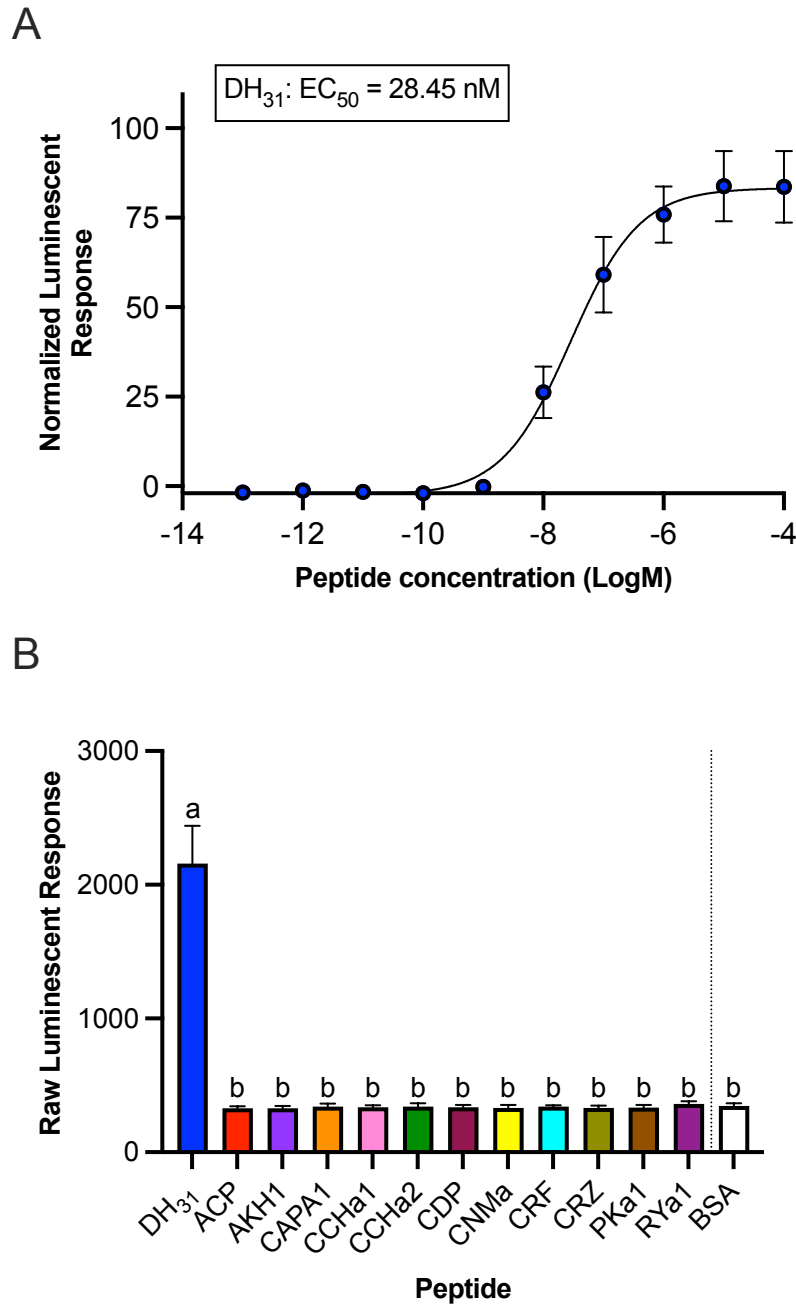


**Figure 5-1. Functional heterologous receptor assay of CHO-K1 cells expressing the *A. aegypti* DH<sub>31</sub> receptor.** (A) Normalized dose-response curve after the addition of  $10^{-13}$  –  $10^{-4}$  M doses of *Aedes*DH<sub>31</sub> peptide. Luminescence was normalized to the BSA control and plotted relative to the maximal response ( $10^{-4}$  M). The EC<sub>50</sub> for *Aedae*DH<sub>31</sub> is 28.45 nM. (B) Raw luminescent response following addition of  $10^{-6}$  M dose of representative neuropeptides belonging to several insect peptide families. For peptide sequence information, see Table 5-1. Different letters denote bars that are significantly different from one another as determined by a one-way ANOVA and Tukey’s multiple comparison post-hoc test ( $p < 0.01$ ). Data represent the mean  $\pm$  SEM ( $n=3$ ).

### ***Aedae*DH<sub>31</sub> levels rise in female haemolymph post-bloodmeal**

To examine the timing of release of DH<sub>31</sub> in the *Aedes* mosquito, females were allowed to blood feed, and their haemolymph was subsequently collected after 0, 2, 5, 10, 15, 30, 60, and 120 min post-blood feeding. Using a heterologous receptor assay, we expressed the *Aedae*DH<sub>31</sub>-R and its activation was monitored following treatment with collected haemolymph samples, which allowed us to determine the circulating DH<sub>31</sub> titres in the haemolymph. Relative to non-blood-fed females, haemolymph samples collected from mosquitoes immediately after ingesting a bloodmeal caused a significant increase in the luminescent response (~24-fold increase) (Figure 5-2A). Maximal luminescence response was observed in haemolymph samples taken 5 min post-blood feeding, with levels slowly dropping at 10 and 15 min post-bloodmeal. Normalized luminescent responses were interpolated from a dose-response curve established using synthesized DH<sub>31</sub> so that endogenous DH<sub>31</sub> concentrations could be determined (Figure 5-2B). Immediately post-blood feeding, DH<sub>31</sub> levels in the female mosquito rise to (Log-9.450)  $0.354 \pm 0.030$  nM compared to (Log-9.603)  $0.249 \pm 0.016$  nM in non-blood-fed females. Levels of DH<sub>31</sub> peak at 5 min at (Log-9.305)  $0.495 \pm 0.038$  nM and slowly start to decrease at 10 and 15 mins ( $0.390 \pm 0.056$  nM, Log-9.409 and  $0.360 \pm 0.026$  nM, Log-9.444) respectively. After 15 mins, DH<sub>31</sub> levels plateau from 60 – 120 min, with levels slightly above non-blood fed females. No luminescence signals were obtained in PBS samples alone. Due to the selective specificity of the *Aedae*DH<sub>31</sub>-R to DH<sub>31</sub>, this indicates that the luminescent response observed when *Aedae*DH<sub>31</sub>-R was exposed to the haemolymph samples was a result of receptor activation by the endogenous DH<sub>31</sub> peptide.

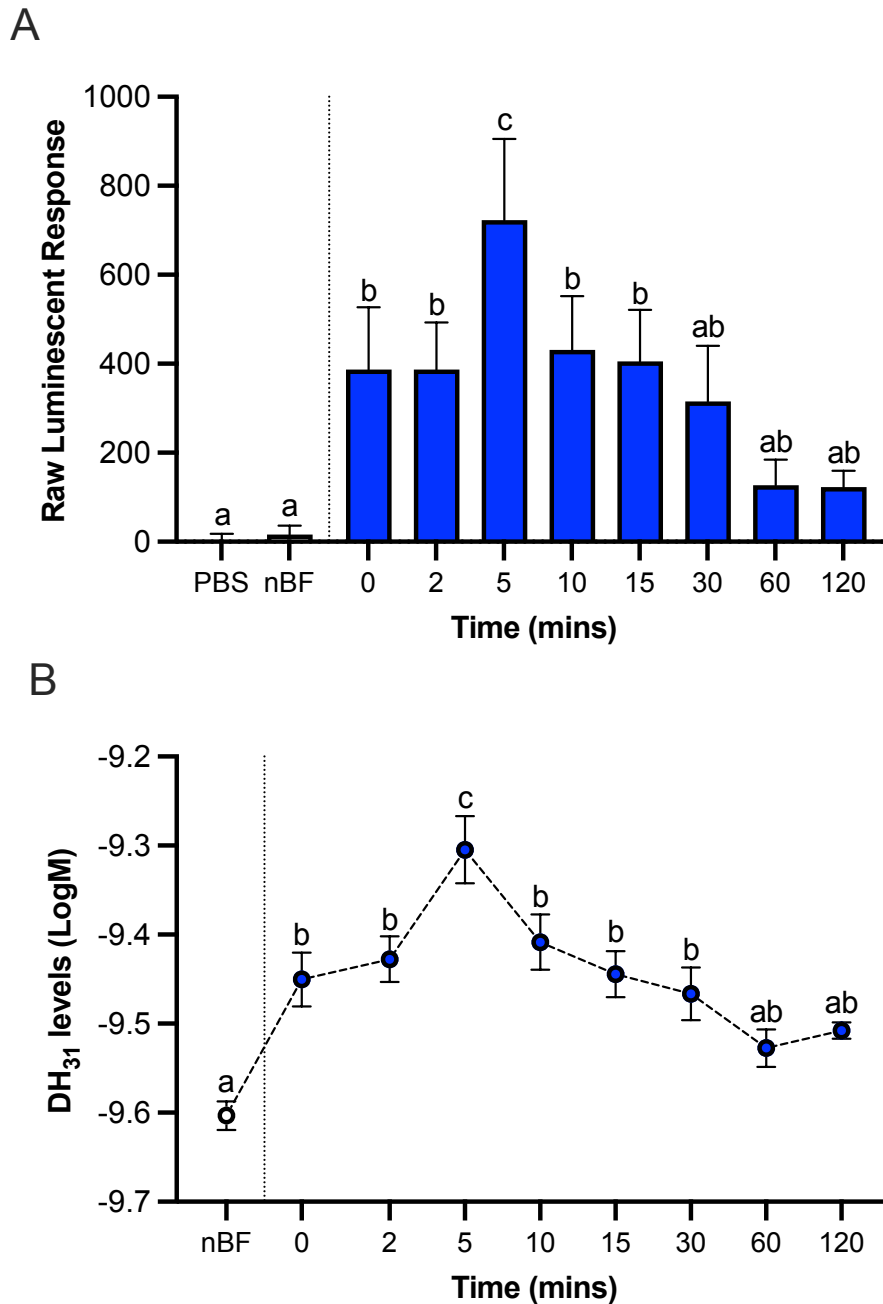


**Figure 5-2. *Aeda*DH<sub>31</sub> titres in blood fed haemolymphs of female *A. aegypti*.** (A) Raw luminescent response of DH<sub>31</sub> levels in collected blood fed female haemolymphs. Females were blood fed and their haemolymph was collected after 0, 2, 5, 10, 15, 30, 60, and 120 min post-feeding and compared to non-blood fed (sugar-fed only) females and PBS. (B) Normalized concentrations of DH<sub>31</sub> in female *A. aegypti* haemolymph following a bloodmeal. (nBF = non-blood fed). Different letters denote bars that are significantly different from one another as determined by a one-way ANOVA and Tukey's multiple comparison post-hoc test ( $p < 0.05$ ). Data represent the mean  $\pm$  SEM ( $n = 10-15$ ).

### ***AedaeDH*<sub>31</sub> involved in stimulating rapid diuresis post-bloodmeal**

To determine the *in vitro* potency of *AedaeDH*<sub>31</sub> on isolated adult *A. aegypti* MTs, a wide range of dosages were applied against unstimulated tubules (Figure 5-3A). Application of synthesized *AedaeDH*<sub>31</sub> at doses ranging from  $10^{-5}$  M to  $10^{-7}$  M to unstimulated adult tubules of *A. aegypti* resulted in a significant dose-dependent stimulation of basal rates of fluid secretion with a half maximal response in the low- to mid-nanomolar range ( $EC_{50} = 13.30$  nM). Doses of  $10^{-9}$  M to  $10^{-12}$  M had no effect on unstimulated tubules, with fluid secretion rates similar to unstimulated control levels. Maximal secretion rates were seen at  $10^{-6}$  M ( $0.549 \pm 0.082$  nL min<sup>-1</sup>) with rates dropping to  $0.040 \pm 0.012$  nL min<sup>-1</sup> at  $10^{-12}$  M. To test whether the collected haemolymph samples would also stimulate fluid secretion, and thereby correlate quantified values of *AedaeDH*<sub>31</sub> with total diuretic activity of the haemolymph samples, 2  $\mu$ L of each sample was applied to 18  $\mu$ L saline:Schneider's medium droplets in which MTs were allowed to incubate for 60 min (Figure 5-3B). Haemolymph sample collected immediately post-blood feeding (0 min) caused a significant increase in fluid secretion ( $0.197 \pm 0.024$  nL min<sup>-1</sup>) representing a four-fold increase in the secretion rate, in comparison to activity from non-blood fed haemolymph samples ( $0.048 \pm 0.016$  nL min<sup>-1</sup>). High secretion rates were also observed for MTs treated with haemolymph samples collected after 2 and 5 min post-feeding ( $0.203 \pm 0.024$  nL min<sup>-1</sup> and  $0.174 \pm 0.027$  nL min<sup>-1</sup>), respectively. Interestingly, haemolymph samples collected 10 – 30 min post-blood feeding caused a moderate stimulation in fluid secretion, whereas 60 to 120 min post-feeding resulted in secretion rates comparable to non-blood fed females and MTs treated with *AedaeDH*<sub>31</sub> in combination with *AedaeCAPA*-1. Tubules treated with PBS alone did not result in stimulation of fluid secretion rates.

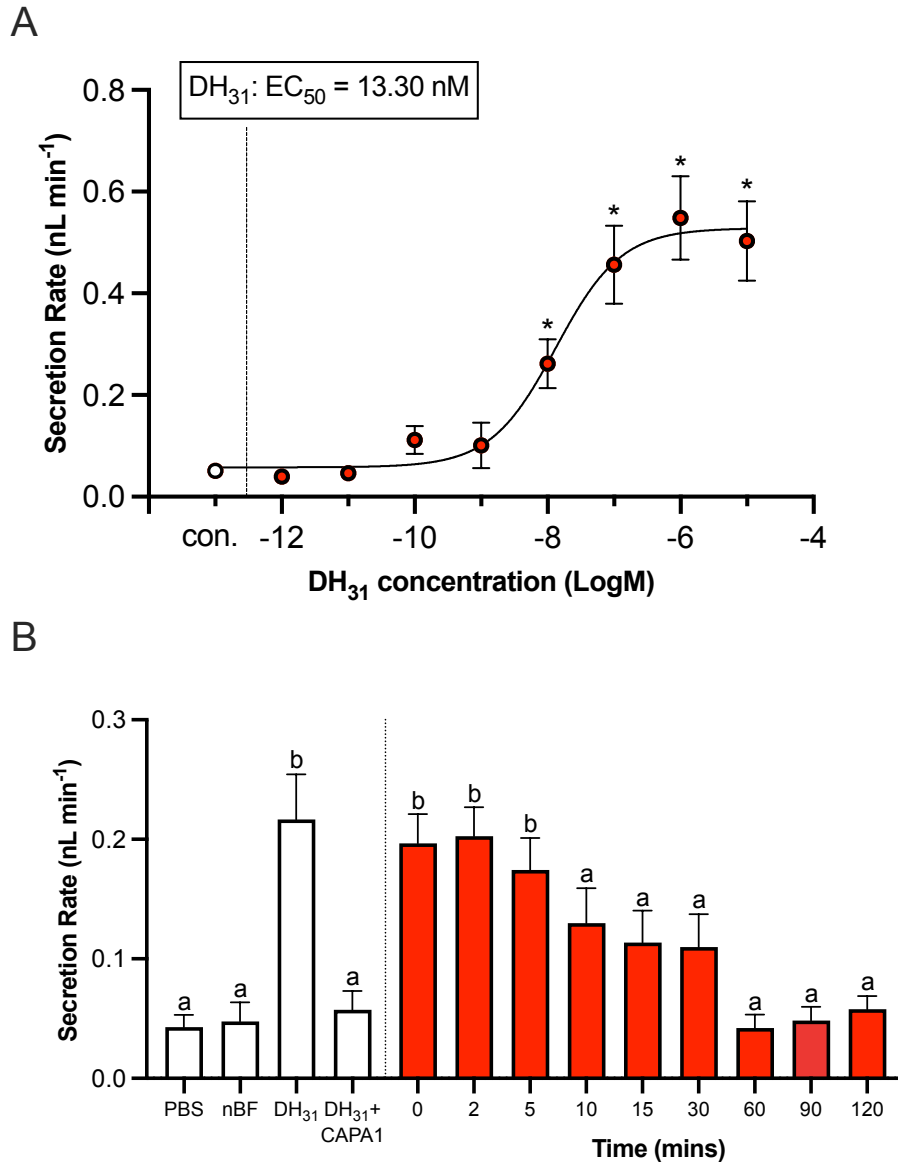


**Figure 5-3. Fluid secretion rates by MTs of adult female *A. aegypti* treated with different doses of *AedaeDH*<sub>31</sub> and haemolymph extracts collected after blood feeding.** (A) Dose-response of *AedaeDH*<sub>31</sub> on unstimulated MTs *in vitro*. Dosages of 10<sup>-5</sup> M to 10<sup>-12</sup> M *AedaeDH*<sub>31</sub> were applied to MTs for 60 min. The EC<sub>50</sub> for *AedaeDH*<sub>31</sub> is 13.30 nM. Significant differences between unstimulated controls and *AedaeDH*<sub>31</sub>-treated MTs are denoted by an asterisk (\*) (mean±SEM; one-way ANOVA with Bonferroni multiple comparison, p<0.05, n=6–12). Error bars for doses 10<sup>-11</sup> M and 10<sup>-12</sup> M are shorter than the size of the symbol, thus not visible. (B) Fluid secretion rates of MTs treated with haemolymph samples from blood fed females after 0, 2, 5, 10, 15, 30, 60, 90, and 120 min post-feeding. MTs were also treated with PBS, nBF haemolymph samples, 25 nM *AedaeDH*<sub>31</sub> and 25 nM *AedaeDH*<sub>31</sub> + 1 fM *AedaeCAPA*-1 (nBF = non-blood fed). Different letters denote bars that are significantly different from one another as determined by a one-way ANOVA and Tukey's multiple comparison post-hoc test (p<0.05). Data represent the mean±SEM (n=7–15).

### **CAPA peptides involved in inhibiting DH<sub>31</sub>-stimulated rapid diuresis post-bloodmeal**

In order to elucidate the timing and release of CAPA neuropeptides, CHO-K1 cells were transfected with the previously characterized anti-diuretic hormone receptor, *Aedae*CAPA-R (see Chapter 3; Sajadi et al., 2020). The receptor was activated by the *Aedae*CAPA-1 peptide ( $EC_{50}=1.83$  nM), as demonstrated by the dose-dependent luminescent response (Figure 5-4A). Haemolymph samples collected from females at 0, 5, 10, 15, 30, 60, 90, and 120 min post-feeding were tested for presence of CAPA peptides (both CAPA-1 and CAPA-2) using the heterologous assay (Figure 5-4B). Haemolymph samples collected at 0, 5, and 10 min post-feeding resulted in a similar luminescent response as observed with haemolymph samples collected from non-blood fed females. Maximal luminescence response was observed in haemolymph samples collected 30 min post-blood feeding (~3-fold increase), with levels steadily dropping from 60 to 120 min post-feeding. Normalized luminescent responses were interpolated from the dose-response curve and CAPA concentrations were determined (Figure 5-4C). During non-blood fed conditions, haemolymph CAPA levels in females are at  $10.96\pm 0.007$  pM (Log-10.96). While CAPA titres steadily rise between 10 and 15 minutes post-blood feeding, levels peak at 30 min  $12.59\pm 0.012$  pM (Log-10.90). After 30 minutes, CAPA levels plateau from 60 to 120 min, with levels returning back to titres observed in non-blood fed females. No luminescence signals were obtained in PBS samples, indicating the luminescent response observed when *Aedae*CAPA-R was exposed to the haemolymph samples was a result of the activation of the receptor by the endogenous CAPA peptides.

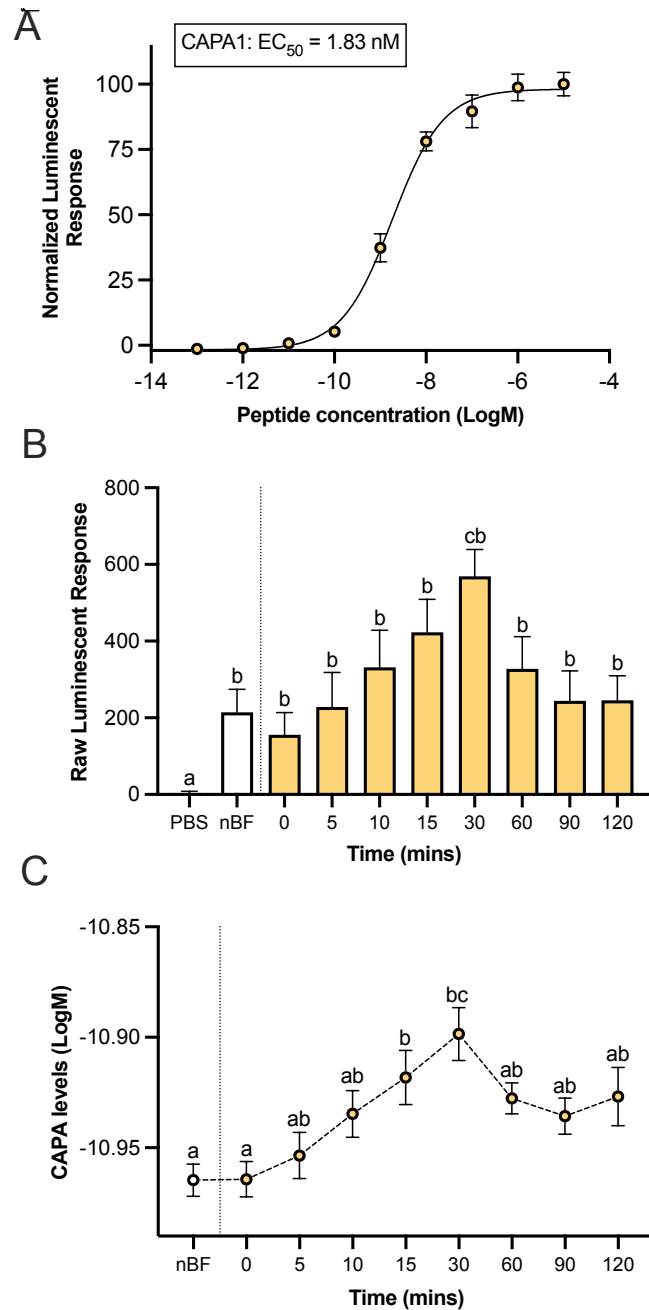


**Figure 5-4. CAPA peptide titres in haemolymph of blood fed female *A. aegypti*.** (A) Normalized dose-response curve after the addition of  $10^{-13}$  –  $10^{-5}$  M doses of *Aedes*CAPA-1 peptide (EC<sub>50</sub> = 1.83 nM). Luminescence was normalized to ATP and plotted relative to the maximal response ( $10^{-5}$  M). (B) Raw luminescent response depicting CAPA peptide levels in haemolymph collected from blood fed females (see methods for details). (C) Measured concentrations of CAPA in female *A. aegypti* haemolymph following a bloodmeal. (nBF = non-blood fed; PBS = diluent without any haemolymph sample). Different letters denote bars that are significantly different from one another as determined by a one-way ANOVA and Tukey's multiple comparison post-hoc test ( $p < 0.05$ ). Data represent the mean  $\pm$  SEM ( $n = 10$ – $15$ ).

## 5.5 Discussion

In female *A. aegypti*, the evolution of blood feeding behaviour and adaptation required precisely coordinating several physiological processes including digestion, excretion, and oogenesis (Klowden, 2013). While blood feeding is necessary for egg development, providing a source of nutrients, vitamins, and proteins (Beyenbach, 2003; Beyenbach and Petzel, 1987), females ingest more than ten times their haemolymph volume in blood, thus imposing an osmoregulatory challenge (Kersch and Pietrantonio, 2011). Consequently, females retain essential proteins from the bloodmeal in the midgut while excess water and ions are excreted from the body by the actions of the MTs and hindgut, the latter of which is the main reabsorptive organ (Beyenbach, 2003; Williams et al., 1983). This rapid diuresis that ensues can result in the elimination of 40% of the ingested plasma volume within the first hour after the bloodmeal (Williams et al., 1983). As a result, this process requires rigorous control of the excretory system to ensure proper removal of excess ions and fluid from the body (Adams, 1999), and subsequently, modulation to this regulation to avoid excessive elimination. While numerous hormones function in regulating diuresis after a bloodmeal, the mosquito natriuretic peptide, DH<sub>31</sub>, is of particular interest because of its dual diuretic and natriuretic roles (Coast et al., 2005; Kwon et al., 2012; see Chapter 2; Sajadi et al., 2018). In mosquitoes, previous studies have shown that rapid fluid secretion during the peak phase of diuresis is driven by the action of the natriuretic hormone, DH<sub>31</sub>, acting through cAMP to drive secretion of Na<sup>+</sup> across the tubule membrane (Beyenbach, 2003; Coast et al., 2005). Recent reports have identified a selective anti-diuretic hormone, CAPA, shown to inhibit DH<sub>31</sub>-stimulated secretion through a NOS/cGMP/PKG pathway by targeting V-ATPase activity (Chapters 2-4; Sajadi et al., 2018; Sajadi et al., 2020). While the actions of both DH<sub>31</sub> and CAPA have been elucidated in the

female *A. aegypti* mosquito, the precise timing of release and haemolymph levels of these neuropeptides remain unknown. The present paper sought to measure the titres of DH<sub>31</sub> and CAPA peptides in the haemolymph of blood fed females to determine their timing of release, which helps to better understand their roles and actions in relation to blood feeding in female *A. aegypti*.

Based on review of current evidence in the literature, direct data confirming this receptor is specifically activated exclusively by the mosquito natriuretic DH<sub>31</sub> is lacking but was nonetheless assumed based on homology when the DH<sub>31</sub> receptor was molecularly identified earlier (Kwon et al., 2012). Therefore, using a heterologous receptor assay, we determined the functional activation of *Aedae*DH<sub>31</sub>-R, testing various peptidergic ligands. Our findings reveal that the receptor is specific and activated only by its ligand DH<sub>31</sub>, whereas other tested insect neuropeptides failed to activate *Aedae*DH<sub>31</sub>-R. Insect calcitonin-like (CT) /diuretic hormone (DH) receptors belong to the family of secretin-like (family B) GPCRs (Hewes and Taghert, 2001) and the first insect CT/DH receptor was functionally characterized in the fruit fly, *Drosophila melanogaster* (Johnson et al., 2005). CT-like receptors have also been reported in other insects based on genome or protein database searches (see Caers et al., 2012), while relatively few have been functionally confirmed using heterologous receptor assays, including the kissing bug *Rhodnius prolixus* (Zandawala et al., 2013) and the silkworm *Bombyx mori* (Iga and Kataoka, 2015). Herein, we have functionally validated that *Aedae*DH<sub>31</sub> activates the *Aedae*DH<sub>31</sub>-R. Similar binding specificity of DH<sub>31</sub> receptor has been observed previously in *B. mori* with EC<sub>50</sub> values reported at 24.2 nmol l<sup>-1</sup> (Iga and Kataoka, 2015) and 116 nmol l<sup>-1</sup> in *D. melanogaster* (Johnson et al., 2005), consistent with the nanomolar ranges observed in the current study on *Aedae*DH<sub>31</sub>-R in *A. aegypti*. Additionally, previous research in the

aforementioned insects have observed that  $DH_{31}$  receptors are not activated by other insect neuropeptides (Johnson et al., 2005), indicating strict specificity for their natural peptidergic ligands as also observed herein.

Studies have established that post-blood feeding, diuretic hormones induce fluid secretion within 2 minutes (Petzel et al., 1987), with secretion rates varying depending on bloodmeal size and hormone concentration (Nijhout and Carrow, 1978). Maximum rates of diuresis occur within 10-12 minutes of a bloodmeal, with excretion rates of 40 nL/min (Williams et al., 1983; Wheelock et al., 1988) allowing for 40% of the water content of the bloodmeal to be excreted within 2 hours of feeding. Kwon et al., (2012) showed that the *Aedae* $DH_{31}$ -R regulates immediate fluid secretion from MTs treated with *Aedae* $DH_{31}$ , which correlated with high excretion rates *in vivo* from whole females post-bloodmeal. Both *in vitro* application of *Aedae* $DH_{31}$  and providing a female with a full blood meal resulted in an increase in fluid secretion within 5 minutes (Kwon et al., 2012). Thus, consistent with these previous observations, we determined that *Aedae* $DH_{31}$  is released immediately post-blood feeding into the female haemolymph, with levels peaking at 5 minutes at ~0.495 nM and slowly returning to basal levels by 15-30 minutes equivalent to titres in non-blood fed female mosquitoes. In the principal cells of the MTs, the haemolymph to lumen osmotic gradient is energized by the VA, driving the transepithelial secretion of  $Na^+$  and  $K^+$  through coupling with a proton/cation antiporter (Beyenbach, 2003). Further ion transport is driven from the haemolymph through various ion channels and cotransporters (Beyenbach, 2012; Coast, 2007; O'Connor and Beyenbach, 2001; Patrick et al., 2006; Wiczorek, 1992). The resulting electrochemical gradient, which is lumen positive, drives  $Cl^-$  and osmotically-obliged water from the haemolymph to the

lumen of the MTs, thus generating primary urine (Beyenbach, 2003; Beyenbach and Wieczorek, 2006).

In *A. aegypti* MTs, fluid secretion increases approximately three-fold after stimulation with *Aedae*DH<sub>31</sub> (Coast et al., 2005; Chapter 2; Sajadi et al., 2018), via cAMP as a second messenger (Beyenbach, 2003), activating Na<sup>+</sup> channels and the Na<sup>+</sup>:K<sup>+</sup>:2Cl<sup>-</sup> co-transporter in the basolateral membrane of principal cells, subsequently activating protein kinase A (PKA), and upregulating VA activity and VA-driven cation transport processes (Dames et al., 2006; Tiburcy et al., 2013; Zimmermann et al., 2003; Chapter 4). Among the diuretic hormones studied in *A. aegypti*, *Aedae*DH<sub>31</sub> is the only reported natriuretic hormone (Coast, 2009; Coast et al., 2005; see Chapter 2; Sajadi et al., 2018). Additionally, *Aedae*DH<sub>31</sub>-R expression is found in a distal-proximal gradient, with greatest colocalization with the VA and exchangers in principal cells of the secretory distal regions of the MTs (Kwon et al., 2012; Patrick et al., 2006). The colocalization of the *Aedae*DH<sub>31</sub>-R, VA, and cation/proton exchangers (Kang'ethe et al., 2007; Piermarini et al., 2009; Pullikuth et al., 2006) in the secreting distal regions can explain the rapid transport of ions (mainly Na<sup>+</sup>), and water in response to *Aedae*DH<sub>31</sub> (Kwon et al., 2012) immediately post-bloodmeal. This natriuretic process is critical given that mammalian blood is 55% plasma and 45% cells by volume, with a plasma-rich NaCl and a K<sup>+</sup>-rich cytoplasm (Blaustein et al., 2012; Dow 1986). The current findings provide greater insight into the time course of release of the natriuretic DH<sub>31</sub> peptide into the female haemolymph following blood feeding. Increased hormone titres of DH<sub>31</sub> are critical to ensure secretion of the Na<sup>+</sup>-rich plasma portion of the bloodmeal that lasts for at least the first 45 min after blood feeding (Williams et al., 1983). This timing of decreased natriuresis coincides with the observations that DH<sub>31</sub> hormone levels, while increase rapidly and peaking at 5 min after blood-feeding, begin

decreasing thereafter with levels at 30 min after blood-feeding being no different from non-blood fed mosquitoes. Thus, after the presumed cessation of DH<sub>31</sub> release and once the bulk of the Na<sup>+</sup>-rich plasma portion of the blood meal has been secreted, other diuretics such as kinin-like peptides and DH<sub>44</sub>, which are not natriuretic (see Chapter 2, Coast et al., 2005; Sajadi et al., 2018; Pannabecker et al., 1993), can be released to continue diuresis as the nutritive component of the bloodmeal (i.e. cells) is processed. Of relevance to this dynamic regulation, the female mosquito begins to digest the bloodmeal in two phases; early phase commences one to three hours post-bloodmeal, while late phase digestion begins 8-36 hours post-bloodmeal (Felix et al., 1991), which can prompt the release of the kaliuretic hormones, such as 5HT (see Chapter 2; Sajadi et al., 2018), to secrete a K<sup>+</sup>-rich urine to eliminate the excess levels of this cation following lysis of the imbibed blood cells.

The current study also found that MTs stimulated with haemolymph samples showed the greatest secretory activity when treated with samples collected 5 minutes post-bloodmeal, with lower activity observed when tubules were treated with samples collected 10-30 minutes post-blood feeding. While the increase in fluid secretion mimics the immediate release of DH<sub>31</sub> into the haemolymph, it may also suggest the actions of additional diuretic factors such as 5HT, DH<sub>44</sub> or kinin-like peptides released prior to or at the same time as DH<sub>31</sub>. This possibility is supported by the observation that peak secretory activity were already observed in haemolymph samples collected 2 minutes post-bloodmeal, whereas levels of DH<sub>31</sub> in the haemolymph peaked at 5 minutes post-blood feeding as determined using the heterologous assay involving the *Aedae*DH<sub>31</sub>-R. The decrease in fluid secretion observed shortly after 5 minutes may be due to the release of another factor into the haemolymph, initiating a feedback mechanism to inhibit cAMP signalling (Cabrero et al., 2002). Additionally, a few studies have noted that the involvement of

G protein-coupled receptor kinases (GRKs) and beta-arrestins can result in the desensitization and internalization of the *Aedae*DH<sub>31</sub>-R (Padilla et al., 2007; Reiter and Lefkowitz, 2006). While it was previously assumed that diuresis in blood feeding insects was terminated by reducing the concentration of diuretic hormones circulating in the haemolymph, (Maddrell, 1964), later research raised the notion that the termination of diuresis may involve the release and actions of an anti-diuretic hormone, CAPA (Paluzzi and Orchard, 2006; Quinlan and O'Donnell, 1998; Quinlan et al., 1997).

Here, this study sought to determine whether CAPA neuropeptides are released post-blood feeding and may (in part) be responsible for the decreased fluid secretion subsequent to the now established peak titres of *Aedae*DH<sub>31</sub> observed at 5 minutes post-blood feeding. CAPA peptides were shown to steadily increase post-bloodmeal, with highest levels quantified at 30 minutes after feeding. Levels of CAPA decreased thereafter, with levels steadily returning to baseline titres by 60 minutes after the blood meal. Taken together, this may suggest a combined action of increased release of CAPA peptides together with reduction in DH<sub>31</sub> release into the female haemolymph which may be the cause of the decreased secretion rate observed 5 minutes after blood feeding. Thus, this may coordinate the transition between the different phases of post-blood feeding diuresis reported in the *A. aegypti* mosquito (Williams et al., 1983). The early peak phase is dominated by diuretic hormones including *Aedae*DH<sub>31</sub>, which we have quantified and found increases significantly after blood-feeding peaking at 5 min. Comparatively, the post-peak phase of diuresis still involves pronounced rates of fluid secretion but is marked as a transitional stage where the excretory system switches from handling the bulk of the NaCl-rich plasma to the KCl-rich waste derived from nutritive cellular portion of the blood meal occurring during the post-peak phase of the diuresis (Williams et al., 1983). Moreover, our results support that other

diuretics are likely active in the early stages of the peak phase of diuresis since significantly elevated fluid secretion rate (~ four-fold over unstimulated rates) was evident in MTs treated with haemolymph extracts collected immediately following blood feeding. This is to be expected, given the well-documented evidence of synergistic actions (and, at minimum, additive effects) of diuretic hormones. In *R. prolixus*, application of diuretic hormones, 5HT and *Rhopr*DH, produces a synergistic effect, with a fluid secretion rate nearly four-fold greater than that expected if effects were additive (Paluzzi et al., 2012). Interestingly, while *Rhopr*CAPA- $\alpha$ 2 did not influence *Rhopr*DH-stimulated secretion, addition of *Rhopr*CAPA- $\alpha$ 2 together with both diuretic hormones abolished the synergism observed (Paluzzi et al., 2012). Similarly, in the cockroach, *Diploptera punctata*, MTs treated simultaneously with the peptides DH<sub>31</sub> and CRF-like DH (DH<sub>46</sub>) show an increase in fluid secretion rates greater than the sum of the individual responses to these agonists (Furuya et al., 2000). While no studies have examined potential additive or synergistic effects in the *Aedes* MTs, our results support the release of other diuretics in addition to DH<sub>31</sub>, which results in a greater combined fluid secretion rate. Together, DH<sub>31</sub> plays an important role in fluid transport of mosquito excretory organs including both the MTs and hindgut, where it has been shown to increase hindgut contract frequency (Kwon and Pietrantonio, 2013). These results suggest that DH<sub>31</sub> released post-bloodmeal has a direct and coordinative action on the excretory system, by which DH<sub>31</sub>-R signalling stimulates MT primary urine secretion and hindgut contraction resulting in rapid post-feeding fluid excretion. Thus, the release of CAPA 30 minutes post-blood meal ensures the activity of DH<sub>31</sub> on the MTs is abolished, while allowing the effects on the hindgut to continue excreting a reduced Na<sup>+</sup>-rich urine.

In the *Aedes* mosquito, CAPA peptides have been shown to demonstrate anti-diuretic effects, in both larval and adult stages (Ionescu and Donini, 2012; Pollock et al., 2004; see Chapters 2-4; Sajadi et al., 2018; Sajadi et al., 2020). Recent reports in the adult female *A. aegypti* have indicated that *Aedae*CAPA-1 binds to its cognate receptor, which is highly expressed in principal cells of the MTs, targeting the NOS/cGMP/PKG pathway (see Chapter 3, Sajadi et al., 2020), to inhibit DH<sub>31</sub>-mediated elevation of cAMP (Coast et al., 2005; Petzel et al., 1987; Chapter 4). Further studies suggested this inhibition is mediated through the inactivation of the VA holoenzyme, involving the dissociation of the V<sub>1</sub> complex from the membrane-integrated apical V<sub>o</sub> complex, hindering luminal flux of protons required for cation/proton exchange, which ultimately reduces tubule fluid secretion (see Chapter 4). In *D. melanogaster*, CAPA peptides have been broadly reported to act as diuretic hormones on MTs isolated *in vitro* at higher doses (Terhzaz et al., 2012; Davies et al., 2013; Kean et al., 2002) and particularly anti-diuretic at lower (femtomolar to picomolar) concentrations (MacMillan et al., 2018), which was consistent in both larval (Ionescu and Donini, 2012) and adult (see Chapters 2-4, Sajadi et al., 2018; Sajadi et al., 2020) *Aedes* mosquitoes. Further testing in *D. melanogaster* to quantify CAPA levels in the haemolymph using a CAPA peptide-specific ELISA indicated that resting titres in *Drosophila* are below 25 fmol l<sup>-1</sup> (MacMillan et al., 2018). Consistent with earlier observations, these results suggest that circulating levels of CAPA peptides can be found at picomolar concentrations, which has been previously shown to inhibit DH<sub>31</sub>-mediated secretion (see Chapter 2, Sajadi et al., 2018). CAPA neuropeptides are secreted and released within a pair of ventral neurosecretory cells located in each abdominal ganglia of the ventral nerve cord, with axonal projections exiting each ganglia releasing the peptide into the haemolymph (Chapter 3; Sajadi et al., 2020). Consequently, due to the close proximity of the abdominal ganglia (CAPA

release sites) and MTs (CAPA target sites), large fluctuations in haemolymph levels may not be necessary to elicit its actions. Fluctuations in hormonal titres following a stimulus have been investigated in various insect haemolymphs, including *R. prolixus* where haemolymph levels of diuretic *Rhopr*-CRF/DH was shown to increase significantly to 5 nM one-hour post-feeding, confirming its role as a true diuretic hormone (Lee et al., 2016). In *Schistocerca gregaria* (Audsley et al., 2006), levels of the ion transport peptide-like (ITP-L) peptide was shown to increase more than four-fold in fed male locusts to 41.5 nM, in comparison to starved locusts. The functionally analogous hormone vasopressin (AVP) or antidiuretic hormone (ADH) in humans also play a major role in controlling body water homeostasis, where plasma ADH rises from 2 to 4 pg/mL with a 2% decrease of in total body water, demonstrating the change in hormonal release upon an increase in plasma osmolarity (Schrier et al., 1979). Thus, consistent with previous studies, our results support the release of DH<sub>31</sub> into the haemolymph post-bloodmeal (stimulus), acting as a true diuretic and natriuretic hormone in female *A. aegypti*.

The female *A. aegypti* mosquito ingests a bloodmeal for the purpose of gaining proteins and other nutrients essential for egg production (Beyenbach, 2003; Beyenbach and Petzel, 1987; Christophers, 1960). However, the bloodmeal also contains large amounts of unwanted salts and water which poses a threat to the haemolymph homeostasis (Beyenbach, 2003) and reduces the manoeuvrability and flight speed of the mosquito (Roitberg et al., 2003). While considerable studies have examined the roles of diuretic and anti-diuretic hormones post-blood feeding, here we functionally characterized the *Aedae*DH<sub>31</sub>-R in the *A. aegypti* mosquito and provided novel evidence demonstrating both DH<sub>31</sub> and CAPA peptides are dynamically released in the haemolymph post-bloodmeal. Based on the heterologous functional receptor assay and *in vitro* fluid secretion assays on isolated MTs, DH<sub>31</sub> in the haemolymph was found in the nanomolar

range and is released immediately post-bloodmeal by two-fold to stimulate fluid secretion and reduce the  $\text{Na}^+$  load from the blood plasma. Accompanying  $\text{DH}_{31}$ , we also provide evidence of the anti-diuretic hormone, CAPA, released 15-30 minutes post-bloodmeal at picomolar ranges, increasing 25% over basal levels, which together with a cessation in  $\text{DH}_{31}$  release in the haemolymph, causes a steady decline in  $\text{DH}_{31}$ -mediated natriuresis that defines the peak phase of diuresis post-blood feeding, thus preventing the excessive loss of  $\text{Na}^+$ . Taken together, these novel findings highlight the physiologically relevant titres of diuretic and anti-diuretic hormones released post-bloodmeal in the mosquito, emphasizing the fine-tuning of the excretory system to maintain haemolymph homeostasis through multiple regulatory factors (i.e. hormones), which possibly contributes in the evolutionary success of blood feeding.

## 5.6 References

- Adams, T. S.** (1999). Hematophagy and hormone release. *Ann. Entomol. Soc. Am.* **92**, 1–13.
- Audsley, N., Meredith, J., and Phillips, J. E.** (2006). Haemolymph levels of *Schistocerca gregaria* ion transport peptide and ion transport-like peptide. *Physiol. Entomol.* **31**, 154–163.
- Beyenbach, K. W.** (2003). Transport mechanisms of diuresis in Malpighian tubules of insects. *J. Exp. Biol.* **206**, 3845–3856.
- Beyenbach, K. W.** (2012). A dynamic paracellular pathway serves diuresis in mosquito Malpighian tubules. *Ann. N Y Acad. Sci.* **1258**, 166–176.
- Beyenbach, K., and Petzel, D.** (1987). Diuresis in mosquitoes: role of a natriuretic factor. *Physiology* **2**, 171–175.
- Beyenbach, K. W., and Wieczorek, H.** (2006). The V-type H<sup>+</sup> ATPase: molecular structure and function, physiological roles and regulation. *J. Exp. Biol.* **209**, 577–589.
- Blaustein, M. P., Leenen, F. H. H., Chen, L., Golovina, V. A., Hamlyn, J. M., Pallone, T. L., Van Huysse, J. W., Zhang, J., and Wier, W. G.** (2012). How NaCl raises blood pressure: a new paradigm for the pathogenesis of salt-dependent hypertension. *Am. J. Physiol. Heart Circ. Physiol.* **302**, H1031–H1049.
- Cabrero, P., Radford, J. C., Broderick, K. E., Costes, L., Veenstra, J. A., Spana, E. P., Davies, S. A., and Dow, J. A. T.** (2002). The Dh gene of *Drosophila melanogaster* encodes a diuretic peptide that acts through cyclic AMP. *J. Exp. Biol.* **205**, 3799–3807.
- Caers, J. Peeters, L., Jansen, T., De Haes, W., Gade, G., Schoofs, L.** (2012). Structure-activity studies of *Drosophila* adipokinetic (AKH) by a cellular expression system of dipteran AKH receptors. *Gen. Comp. Endocrinol.* **77**, 332–337.

- Clark, T. M., and Bradley, T. J.** (1996). Stimulation of Malpighian tubules from larval *Aedes aegypti* by secretagogues. *J. Insect Physiol.* **42**, 593–602.
- Clark, T. M., Hayes, T. K., Holman, G. M., and Beyenbach, K. W.** (1998a). The concentration-dependence of CRF-like diuretic peptide: mechanisms of action. *J. Exp. Biol.* **201**, 1753–1762.
- Clark, T. M., Hayes, T. K., and Beyenbach, K. W.** (1998b). Dose-dependent effects of CRF-like diuretic peptide on transcellular and paracellular transport pathways. *Am. J. Physiol.* **274**, F834–F840.
- Coast, G.** (2007). The endocrine control of salt balance in insects. *Gen. Comp. Endocrinol.* **152**, 332–338.
- Coast, G. M.** (2009). Neuroendocrine control of ionic homeostasis in blood-sucking insects. *J. Exp. Biol.* **212**, 378–386.
- Coast, G. M., Garside, C. S., Webster, S. G., Schegg, K. M., and Schooley, D. A.** (2005). Mosquito natriuretic peptide identified as a calcitonin-like diuretic hormone in *Anopheles gambiae* (Giles). *J. Exp. Biol.* **208**, 3281–3291.
- Dames, P., Zimmermann, B., Schmidt, R., Rein, J., Voss, M., Schewe, B., Walz, B., and Baumann, O.** (2006). cAMP regulates plasma membrane vacuolar-type H<sup>+</sup>-ATPase assembly and activity in blowfly salivary glands. *Proc. Natl. Acad. Sci. U S A* **103**, 3926–3931.
- Davies, S. A., Cabrero, P., Povsic, M., Johnston, N. R., Terhzaz, S., and Dow, J. A. T.** (2013). Signaling by *Drosophila capa* neuropeptides. *Gen. Comp. Endocrinol.* **188**, 60–66.

- Felix, C. R., Betschart, B., Billingsley, P. F., Freyvogel, T. A.** (1991). Post-feeding induction of trypsin in the midgut of *Aedes aegypti* L. (Diptera, Culicidae) is separable into 2 cellular phases. *Insect Biochem.* **21**, 197–203.
- Furuya, K., Milchak, R. J., Schegg, K. M., Zhang, J., Tobe, S. S., Coast, G. M., and Schooley, D. A.** (2000). Cockroach diuretic hormones: characterization of a calcitonin-like peptide in insect. *Proc. Natl. Acad. Sci. U S A* **97**, 6469–6474.
- Hewes, R. S., and Taghert, P. H.** (2001). Neuropeptides and neuropeptide receptors in the *Drosophila melanogaster* genome. *Genome Res.* **11**, 1126–1142.
- Iga, M., and Kataoka, H.** (2015). Identification and characterization of the diuretic hormone 31 receptor in the silkworm *Bombyx mori*. *Biosci. Biotechnol. Biochem.* **79**, 1305–1307.
- Ionescu, A., and Donini, A.** (2012). *Aedes*CAPA-PVK-1 displays diuretic and dose dependent antidiuretic potential in the larval mosquito *Aedes aegypti* (Liverpool). *J. Insect Physiol.* **58**, 1299–1306.
- Iredale, P. A., and Hill, S. J.** (1993). Increases in intracellular calcium via activation of an endogenous P2-purinoceptor in cultured CHO-K1 cells. *Br. J. Pharmacol.* **110**, 1305–1310.
- Jagge, C. L., and Pietrantonio, P. V.** (2008). Diuretic hormone 44 receptor in Malpighian tubules of the mosquito *Aedes aegypti*: evidence for transcriptional regulation paralleling urination. *Insect Mol. Biol.* **17**, 413–426.
- Johnson, E. C., Shafer, O. T., Trigg, J. S., Park, J., Schooley, D. A., Dow, J. A., and Taghert, P. H.** (2005). A novel diuretic hormone receptor in *Drosophila*: evidence for conservation of CGRP signaling. *J. Exp. Biol.* **208**, 1239–1246.
- Kang'ethe, W., Aimanova, K. G., Pullikuth, A. K., and Gill, S. S.** (2007). NHE8 mediates amiloride-sensitive  $\text{Na}^+/\text{H}^+$  exchange across mosquito Malpighian tubules and catalyzes  $\text{Na}^+$

- and K<sup>+</sup> transport in reconstituted proteoliposomes. *Am. J. Physiol. Renal Physiol.* **292**, 1501–1512.
- Karas, K., Brauer, P., and Petzel, D.** (2005). Actin redistribution in mosquito Malpighian tubules after a blood meal and cyclic AMP stimulation. *J. Insect Physiol.* **51**, 1041–1054.
- Kean, L., Cazenave, W., Costes, L., Broderick, K. E., Graham, S., Pollock, V. P., Davies, S. A., Veenstra, J. A., and Dow, J. A. T.** (2002). Two nitridergic peptides are encoded by the gene capability in *Drosophila melanogaster*. *Am. J. Physiol. Regul. Integr. Comp. Physiol.* **282**, R1297–R1307.
- Kersch, C. N., and Pietrantonio, P. V.** (2011). Mosquito *Aedes aegypti* (L.) leucokinin receptor is critical for *in vivo* fluid excretion post blood feeding. *FEBS Letters* **585**. doi: 10.1016/j.febslet.2011.10.001
- Klowden, M. J.** (2013). *Physiological Systems in Insects: Third Edition*. Amsterdam: Elsevier.
- Kwon, H., Lu, H. L., Longnecker, M. T., and Pietrantonio, P. V.** (2012). Role in diuresis of a calcitonin receptor (GPCRAL1) expressed in a distal-proximal gradient in renal organs of the mosquito *Aedes aegypti* (L.). *PLoS One* **7**, e50374.
- Lee, H-R., Zandawala, M., Lange, A. B., Orchard, I.** (2016). Isolation and characterization of the corticotropin-releasing factor-related diuretic hormone receptor in *Rhodnius prolixus*. *Cell. Sig.* **28**, 1152–1162.
- Lu, H. L., Kersch, C., and Pietrantonio, P. V.** (2011). The kinin receptor is expressed in the Malpighian tubule stellate cells in the mosquito *Aedes aegypti* (L.): a new model needed to explain ion transport? *Insect Biochem. Mol. Biol.* **41**, 135–140.

- MacMillan, H. A., Nazal, B., Wali, S., Yerushalm, G. Y., Misyura, L., Donini, A., and Paluzzi, J. P.** (2018). Anti-diuretic activity of a CAPA neuropeptide can compromise *Drosophila* chill tolerance. *J. Exp. Biol.* **221**, doi: 10.1242/jeb.185884.
- Maddrell, S. H. P.** (1964). Excretion in the blood-sucking bug, *Rhodnius Prolixus* Stål: II. the normal course of diuresis and the effect of temperature. *J. Exp. Biol.* **41**, 163–176.
- Michel, A. D., Chessell, I. P., Hibell, A. D., Simon, J., and Humphrey, P. P. A.** (1998). Identification and characterization of an endogenous P2X<sub>7</sub> (P2Z) receptor in CHO-K1 cells. *Br. J. Pharmacol.* **125**, 1194–1201.
- Nijhout, H. F., and Carrow, G. M.** (1978). Diuresis after a bloodmeal in female *Anopheles freeborni*. *J. Insect Physiol.* **24**, 293–298.
- O'Connor, K. R., and Beyenbach, K. W.** (2001). Chloride channels in apical membrane patches of stellate cells of Malpighian tubules of *Aedes aegypti*. *J. Exp. Biol.* **204**, 367–378.
- Padilla, B. E., Cottrell, G. S., Roosterman, D., Pikios, S., Muller, L., Steinhoff, M., and Bunnett, N. W.** (2007). Endothelin-converting enzyme-1 regulates endosomal sorting of calcitonin receptor-like receptor and beta-arrestins. *J. Cell Biol.* **179**, 981–97.
- Paluzzi, J. P., Naikhwah, W., and O'Donnell, M. J.** (2012). Natriuresis and diuretic hormone synergism in *R. prolixus* upper Malpighian tubules is inhibited by the anti-diuretic hormone, *RhoprCAPA-α2*. *J. Insect Physiol.* **58**, 534–542.
- Paluzzi, J. P., and Orchard, I.** (2006). Distribution, activity and evidence for the release of an anti-diuretic peptide in the kissing bug *Rhodnius prolixus*. *J. Exp. Biol.* **209**, 907–915.
- Paluzzi, J. P., Park, Y., Nachman, R. J., and Orchard, I.** (2010). Isolation, expression analysis, and functional characterization of the first antidiuretic hormone receptor in insects. *Proc. Natl. Acad. Sci. U S A* **107**, 10290–10295.

- Paluzzi, J. P., Young, P., Defferrari, M. S., Orchard, I., Carlini, C. R., and O'Donnell, M. J.** (2012). Investigation of the potential involvement of eicosanoid metabolites in anti-diuretic hormone signaling in *Rhodnius prolixus*. *Peptides (N.Y.)* **34**, 127–134.
- Pannabecker, T. L., Hayes, T. K., and Beyenbach, K. W.** (1993). Regulation of epithelial shunt conductance by the peptide leucokinin. *J. Membr. Biol.* **132**, 63–76.
- Patrick, M. L., Aimanova, K., Sanders, H. R., and Gill, S. S.** (2006). P-type Na<sup>+</sup>/K<sup>+</sup>-ATPase and V-type H<sup>+</sup>-ATPase expression patterns in the osmoregulatory organs of larval and adult mosquito *Aedes aegypti*. *J. Exp. Biol.* **209**, 4638–4651.
- Petzel, D. H., Berg, M. M., and Beyenbach, K. W.** (1987). Hormone-controlled cAMP-mediated fluid secretion in yellow-fever mosquito. *Am. J. Physiol. Regul. Integr. Comp. Physiol.* **253**, R701–R711.
- Piermarini, P. M., Weihrauch, D., Meyer, H., Huss, M., and Beyenbach, K. W.** (2009). NHE8 is an intracellular cation/H<sup>+</sup> exchanger in renal tubules of the yellow fever mosquito *Aedes aegypti*. *Am. J. Physiol. Renal Physiol.* **296**, 730–750.
- Pollock, V. P., McGettigan, J., Cabrero, P., Maudlin, I. M., Dow, J. A. T., and Davies, S. A.** (2004). Conservation of capa peptide-induced nitric oxide signalling in Diptera. *J. Exp. Biol.* **207**, 4135–4145.
- Pullikuth, A. K., Aimanova, K., Kang'ethe, W., Sanders, H. R., and Gill, S. S.** (2006). Molecular characterization of sodium/proton exchanger 3 (NHE3) from the yellow fever vector, *Aedes aegypti*. *J. Exp. Biol.* **209**, 3529–3544.
- Quinlan, M. C., and O'Donnell, M. J.** (1998). Anti-diuresis in the blood-feeding insect *Rhodnius prolixus* Stal: antagonistic actions of cAMP and cGMP and the role of organic acid transport. *J. Insect Physiol.* **44**, 561–568.

- Quinlan, M. C., Tublitz, N. J., and O'Donnell, M. J.** (1997). Anti-diuresis in the blood-feeding insect *Rhodnius prolixus* Stål: the peptide CAP(2b) and cyclic GMP inhibit Malpighian tubule fluid secretion. *J. Exp. Biol.* **200**, 2363–2367.
- Reiter, E., and Lefkowitz, R. J.** (2006). GRKs and beta-arrestins: roles in receptor silencing, trafficking and signaling. *Trends Endocrinol. Metab.* **17**, 159–65.
- Rocco, D. A., Kim, D. H., and Paluzzi, J. P.** (2017). Immunohistochemical mapping and transcript expression of the GPA2/GPB5 receptor in tissues of the adult mosquito, *Aedes aegypti*. *Cell Tissue Res.* **369**, 313–330.
- Roitberg, B. D., Mondor, E. B., and Tyerman, J. G. A.** (2003). Pouncing spider, flying mosquito: blood acquisition increases predation risk in mosquitoes. *Behav. Ecol.* **14**, 736–740.
- Sajadi, F., Curcuruto, C., Al Dhaheri, A., and Paluzzi, J. P.** (2018). Anti-diuretic action of a CAPA neuropeptide against a subset of diuretic hormones in the disease vector, *Aedes aegypti*. *J. Exp. Biol.* **221**.
- Sajadi F., Lajevardi, A., Donini, A., and Paluzzi, J. P. V.** (2021). Studying the activity of neuropeptides and other regulators of the excretory system in the adult mosquito. *J. Vis. Exp.* **174**, doi: 10.3791/61849.
- Sajadi, F., Uyklu, A., Paputsis, C., Lajevardi, A., Wahedi, A., Ber, L.T., Matei, A., and Paluzzi, J. P.** (2020). CAPA neuropeptides and their receptor form an anti-diuretic hormone signaling system in the human disease vector, *Aedes aegypti*. *Scientific Reports* **10**. <https://doi.org/10.1038/s41598-020-58731-y>.
- Schepel, S. A., Fox, A. J., Miyauchi, J. T., Sou, T., Yang, J. D., Lau, K., Blum, A. W., Nicholson, L. K., Tiburcy, F., Nachman, R. J., et al.** (2010). The single kinin receptor

- signals to separate and independent physiological pathways in Malpighian tubules of the yellow fever mosquito. *Am. J. Physiol. Regul. Integr. Comp. Physiol.* **299**, R612–R622.
- Schrier, R. W., Berl, T., and Anderson, R. J.** (1979). Osmotic and nonosmotic control of vasopressin release. *Am. J. Physiol. Ren. Physiol.* **236**, F321–F332.
- Terhzaz, S., Cabrero, P., Robben, J. H., Radford, J. C., Hudson, B. D., Milligan, G., Dow, J. A. T., and Davies, S. A.** (2012). Mechanism and function of *drosophila* capa GPCR: a desiccation stress-responsive receptor with functional homology to human neuromedinu receptor. *PLoS One* **7**, e29897.
- Tiburcy, F., Beyenbach, K. W., and Wieczorek, H.** (2013). Protein kinase A-dependent and-independent activation of the V-ATPase in Malpighian tubules of *Aedes aegypti*. *J. Exp. Biol.* **216**, 881–891.
- Veenstra, J. A.** (1988). Effects of 5-hydroxytryptamine on the Malpighian tubules of *Aedes aegypti*. *J. Insect Physiol.* **34**, 299–304.
- Veenstra, J. A.** (1994). Isolation and Identification of 3 leucokinins from the Mosquito *Aedes aegypti*. *Biochem. Biophys. Res. Commun.* **202**, 715–719.
- Wahedi, A., and Paluzzi, J. P.** (2018). Molecular identification, transcript expression, and functional deorphanization of the adipokinetic hormone/corazonin-related peptide receptor in the disease vector, *Aedes aegypti*. *Sci. Rep.* **8**, 2146.
- Weng, X. H., Huss, M., Wieczorek, H., and Beyenbach, K. W.** (2003). The V-type H<sup>+</sup>-ATPase in Malpighian tubules of *Aedes aegypti*: localization and activity. *J. Exp. Biol.* **206**, 2211–2219.

- Wheelock, G. D., Petzel, D. H., Gillet, J. D., Beyenbach, K. W., and Hagedorn, H. H. (1988).** Evidence for hormonal control of diuresis after a blood meal in the mosquito *Aedes aegypti*. *Arch. Insect. Biochem. Physiol. B*, 75–89.
- Wieczorek, H. (1992).** The insect V-ATPase, a plasma membrane proton pump energizing secondary active transport: molecular analysis of electrogenic potassium transport in the tobacco hornworm midgut. *J. Exp. Biol.* **172**, 335–343.
- Wieczorek, H., Putzenlechner, M., and Klein, U. (1991).** A vacuolar-type proton pump energizes K<sup>+</sup>/H<sup>+</sup> antiport in an animal plasma membrane. *J. Biol. Chem.* **266**, 15340–15347.
- Williams, J. C., Hagedorn, H. H., and Beyenbach, K. W. (1983).** Dynamic changes in flow rate and composition of urine during the post-bloodmeal diuresis in *Aedes aegypti* (L.). *J. Comp. Physiol.* **153**, 257–265.
- Zandawala, M., Li, S., Hauser, F., Grimmelikhuijzen, C. J. P., and Orchard, I. (2013).** Isolation and functional characterization of calcitonin-like diuretic hormone receptors in *Rhodnius prolixus*. *PLoS One* **11**, e82466.
- Zimmermann, B., Dames, P., Walz, B., and Baumann, O. (2003).** Distribution and serotonin-induced activation of vacuolar-type H<sup>+</sup>-ATPase in the salivary glands of the blowfly *Calliphora vicina*. *J. Exp. Biol.* **206**, 1867–1876.

## **Chapter Six**

### **Molecular characterization, localization, and physiological roles of ITP and ITP-L in the mosquito, *Aedes aegypti***

This chapter has not yet been submitted for publication.

## 6.1 Summary

The insect ion transport peptide (ITP) and its alternatively spliced variant, ITP-like peptide (ITP-L), belong to the crustacean hyperglycemic hormone family of peptides and are widely conserved among insect species. While limited, studies have characterized the ITP/ITP-L signalling system within many insects, and putative functions including regulation of ion and fluid transport, ovarian maturation, and thirst/excretion have been proposed. Herein, I aim to molecularly investigate *Itp* and *Itp-l* expression profiles in the mosquito *Aedes aegypti*, examine peptide immunolocalization and transcript distribution within adult tissues, and elucidate putative physiological roles for these neuropeptides. Transcript expression profiles of both *AedaeItp* and *AedaeItp-l* reveal enrichment in adults, with *AedaeItp* expressed in the brain and *AedaeItp-l* expression predominantly within the abdominal ganglia. Immunohistochemical analysis and fluorescence *in situ* hybridization within the central nervous system reveals expression of *AedaeITP* peptide and its transcript in a number of cells in the brain and in the terminal ganglion. Comparatively, *AedaeITP-L* peptide and transcript was localized solely within the abdominal ganglia of the central nervous system. Interestingly, starvation and blood feeding caused upregulation of *AedaeItp* and *AedaeItp-l* levels in adult mosquitoes, suggesting possible functional roles in ionoregulation and/or feeding. RNAi-mediated knockdown of *AedaeItp* caused an increase in urine excretion, while knockdown of both *AedaeItp* and *AedaeItp-l* reduced blood feeding and egg-laying in females while reducing egg viability, suggesting roles in reproductive physiology and behaviour. Altogether, this study identifies *AedaeITP* and *AedaeITP-L* as key pleiotropic hormones, regulating various critical physiological processes in the disease vector, *A. aegypti*.

## 6.2 Introduction

Neuropeptides comprise a large and diverse class of signalling molecules that, together with their receptors, play a significant role in controlling a myriad of behavioural and physiological processes, including reproduction, feeding, development, energy homeostasis, water and ion balance, and more (Coast, 2007; Schoofs et al., 2017; Strand et al., 2016) (Nässel et al., 2019). The crustacean hyperglycemic hormone (CHH) family of peptides are a large neuropeptide superfamily, that includes structurally-related peptides composed of 72 to more than 80 amino acids (Chen et al., 2020), with the addition of three highly conserved intramolecular disulfide bonds (Nagai et al., 2014). Functional roles for the CHH family of peptides are linked to molting, stress responses, reproduction, and homeostatic regulation of energy metabolism (Webster et al., 2012). The insect ion transport peptide (ITP) and its alternatively spliced variant, ITP-like or ITP-long (ITP-L) belong to the CHH family of peptides (Dai et al., 2007; Keller, 1992) and are widely conserved among insect species, including lepidopterans, such as the silkworm *Bombyx mori* (Dai et al., 2007; Endo et al., 2000), and the tobacco hornworm *Manduca sexta* (Drexler et al., 2007). While investigations examining the roles of ITP and ITP-L are limited, studies have suggested functions of both peptides as regulators of ion and fluid transport across the ileum of the desert locust *Schistocerca gregaria* (Audsley et al., 1992) in ecdysis in *M. sexta* (Drexler et al., 2007), in ovarian maturation in the red flower beetle *Tribolium castaneum* (Begum et al., 2009), and thirst/excretion regulation and clock neuron modulation in the fruit fly *Drosophila melanogaster* (Gáliková et al., 2018; Johard et al., 2009).

The insect ITP was originally identified in *S. gregaria* (Audsley et al., 1992; Dai et al., 2007), where it drives chloride-dependent movement of fluid across the ileum, hence suggesting

a role as an anti-diuretic hormone (Audsley et al., 1992; Phillips and Audsley, 1995). Subsequently, Meredith *et al.* identified the complete amino acid sequence of *SchgrITP*, with a 72-residue mature peptide sequence and six cysteine residues proposed to participate in disulphide bridge formation (Meredith et al., 1996). The mature *SchgrITPL* peptide is only four amino acids longer than ITP, containing a unique carboxy-terminus (Dirksen, 2009; Phillips et al., 1998). Studies have revealed that both peptides share a common N-terminal sequence, whereas the C-terminal sequences diverge significantly, thus were predicted to arise from alternative splicing (Meredith et al., 1996). Due to the shared N-terminus between the two peptide precursors, earlier studies proposed that the N-terminus permits the peptides to bind to its receptor (Phillips et al., 1998). ITP is a potent stimulator of ileal short circuit current, whereas ITP-L is devoid of such activity, suggesting an antagonistic role of ITP-L on the putative ITP receptors in locust hindgut (Oehler et al., 2014).

Differential tissue immunolocalization of ITP and ITP-L in *M. sexta* and *B. mori* revealed ITP expression in bilaterally-paired neurosecretory cells in the brain with projections to the retrocerebral complex, whereas ITP-L expression was seen in peripheral neurosecretory cells and neurons of the ventral ganglia (Dai et al., 2007). Further investigations confirmed ITP localization exclusively to the central nervous system, and ITP-L to the central nervous system and peripheral tissues (Dirksen et al., 2008; Meredith et al., 1996; Yu et al., 2016), suggesting differential functional roles for the alternatively spliced peptides. In 2007, Dai *et al.* were the first to identify a conserved ITP gene (*Itp*) in the mosquito, *Aedes aegypti*, which by alternative splicing, encodes for *AedaeITP-L*; a longer peptide isoform with an unblocked C-terminus, and *AedaeITP*; a shorter peptide with an amidated C-terminus. To date, the expression pattern, tissue distribution, and putative physiological function of either ITP or ITP-L has not been determined

in *A. aegypti*. Herein, this study set out to characterize the tissue-specific expression and localization, and elucidate a physiological role of *AedaeITP* and *AedaeITP-L* in the *A. aegypti* mosquito. Using a combination of molecular and physiological techniques, *AedaeITP* and *AedaeITP-L* was characterized in the adult stage mosquito, with expression and localization of *AedaeITP* in the brain and the terminal ganglion while *AedaeITP-L* was detected in the abdominal ganglia of the ventral nerve cord. Furthermore, using RNA interference (RNAi), the current results provide novel evidence that *AedaeITP* and *AedaeITP-L* play essential roles in ionoregulation, reproductive physiology and mating behaviour in the *Aedes* mosquito. Overall, these findings greatly advance our understanding of the ITP and ITP-L neuropeptides in mosquitoes and provide novel directions for future research to unravel neuropeptidergic signalling in the disease-vector, *A. aegypti*.

### **6.3 Materials and Methods**

#### **Animals**

*Aedes aegypti* eggs (Liverpool strain) were collected from an established laboratory colony as described previously (Rocco et al., 2017; Chapters 2-5; Sajadi et al., 2018; Sajadi et al., 2020) and hatched in double-distilled water in an incubator at 26°C on a 12:12 hour light:dark cycle. Larvae were fed a solution of 2% (w/v) brewer's yeast and 2% (w/v) Argentine beef liver powder (NOW foods, Bloomingdale, IL, USA). For colony upkeep, female mosquitoes were fed sheep's blood in Alsever's solution (Cedarlane Laboratories Ltd., Burlington, ON, Canada) using an artificial feeding system (Rocco et al., 2017). Adults were provided with 10% sucrose solution *ad libidum*.

### **Tissue/organ dissections, RNA extraction, and cDNA synthesis**

One- and four-day old adult female (n=30) and male (n=40) *A. aegypti* were briefly anaesthetized with CO<sub>2</sub> and submerged in Dulbecco's phosphate buffered saline (DPBS; Wisent Corporation, St. Bruno, QC, Canada), and the following body segments and/or tissues/organs were dissected and isolated: head, thorax, midgut, Malpighian tubules (MTs), hindgut, reproductive tissues (ovaries, testes, and accessory reproductive tissues) and carcass (remaining cuticle, musculature, fat body, and abdominal ganglia). Whole adult RNA was obtained by collecting one- and four-day old adult female (n=10) and male (n=11) mosquitoes. For the starvation assay, whole adult male (n=6-7) and females (n=5-6) were isolated 24 h or 48 h post treatment. To confirm knockdown efficiency following dsRNA treatment, whole adult male (n=5-6) and females (n=5) were isolated four-, six-, and eight-days post injection. Whole adult and organ samples were stored in a 1:1 mixture of RNA protection buffer:nuclease-free H<sub>2</sub>O at -20°C until further processing. Samples were then thawed at room temperature and total RNA was isolated using the Monarch Total RNA Miniprep Kit following manufacturers protocol with an on-column DNase treatment to remove genomic DNA (New England Biolabs, Whitby, ON, Canada). Purified total RNA samples were subsequently aliquoted onto a Take3 micro-volume plate and quantified on a Synergy Multi-Mode Microplate Reader (BioTek, Winooski, VT, USA). To determine *AedaeItp* and *AedaeItp-l* transcript levels, cDNA was synthesized from 500 ng (developmental expression profile), 80 ng (spatial expression profile), and 250 ng (starvation assay and dsRNA injections) total RNA using the iScript™ Reverse Transcription Supermix for RT-qPCR (Bio-Rad, Mississauga, ON, Canada) following manufacturers protocol, including a ten-fold dilution of cDNA following synthesis.

## RT- quantitative PCR

To measure expression profiles for *AedaeItp* and *AedaeItp-l*, transcript abundance was quantified on a StepOnePlus™ Real Time PCR system (Applied Biosystems, Carlsbad, CA, USA) using PowerUP™ SYBR® Green Master Mix (Applied Biosystems, Carlsbad, CA, USA). Cycling conditions were as follows: 1) UDG activation 50°C for 2 min, 2) 95°C for 2 min, and 3) 40 cycles of i) 95°C for 15 seconds and ii) 60°C for 1 minute. Gene-specific primers for *AedaeItp* and *AedaeItp-l* were designed over multiple exons (see Table 6-S1 for list of primers) based on a previously reported mRNA sequence (Genbank Accession Numbers: (*Itp*) AY950503 and (*Itp-l*) AY950506) (Dai et al., 2007). To ensure specificity for each individual peptide-specific transcript, reverse primers for *AedaeItp* (nucleotides 418-438) and *AedaeItp-l* (nucleotides 418-428) were designed over transcript-specific exon-exon boundaries that, in the case of *AedaeItp-l*, includes exon 3 since this exon is absent in *AedaeItp* (Figure 6-S1). Relative expression levels were determined using the  $\Delta\Delta C_T$  method (Livak and Schmittgen, 2001) and normalized to the geometric mean of *rp49* and *rps18* reference genes, which were previously determined as optimal endogenous controls (Paluzzi et al., 2014). Developmental expression profiles consisted of an average of 5-6 biological replicates that each included triplicate technical replicates for each target gene. Spatial expression profiles consisted of an average of 3-4 biological replicates. The starvation assay and dsRNA knockdown consisted of an average of 4 and 3 biological replicates, respectively. Primer specificity for target mRNA was assessed by conducting no reverse-transcriptase and no-template controls along with performing standard curves to calculate primer efficiencies.

## Immunohistochemistry

To examine *Aedae*ITP and *Aedae*ITP-L immunoreactivity in the central nervous system, whole one- and four- day old adult male and female *A. aegypti* were collected and incubated in 4% paraformaldehyde (PFA) fixative overnight at 4°C. The following day, tissue dissections of the central nervous system consisting of the brain, thoracic ganglia, and the abdominal ganglia, were performed in DPBS. Tissues were then incubated on a rocker for 1 h at RT in 4% Triton X-100 (Sigma Aldrich, Oakville, ON, Canada), 10% normal sheep serum (NSS) (v/v) and 2% BSA (w/v) prepared in DPBS, followed by three 15 min washes in DPBS. After the last wash, the DPBS was removed and substituted with a preincubated 1:1000 dilution of primary antiserum solution (0.4% Triton-X- 100, 2% NSS (v/v), and 2% BSA (w/v)) in DPBS (prepared the day before use and incubated at 4°C to reduce non-specific binding) on a rocker for 96 h at 4°C. A custom-synthesized primary antiserum solution was raised in rabbit against a synthetic peptide (SSFFDIECKGQFNKA) antigen corresponding to a 15-amino acid region of *Aedae*ITP and *Aedae*ITP-L (nucleotides 154-198 on common exon 2, amino acids 1-15 of the shared N-terminal sequence), thus targeting both *Aedae*ITP and *Aedae*ITP-L (Biomatik, Kitchener, ON, Canada). Following incubation, tissues were washed with DPBS four times on a rocker over the course of an hour and subsequently incubated overnight at 4°C with a goat anti-rabbit Alexa Fluor® 568 IgG (H+L) secondary antibody (Molecular Probes, Life Technologies, Eugene, OR, USA) diluted 1:200 in 10% NSS made up in DPBS and protected from light. The following day, tissues were washed three times with DPBS for 15 min each. As a negative control, the anti-*Aedae*ITP/ITP-L primary antiserum was preincubated with 10 µM antigen (SSFFDIECKGQFNKA) overnight prior to use. Additionally, tissues were also incubated with a no-primary control (0.4% Triton-X-100, 2% NSS (v/v), and 2% BSA (w/v) prepared in DPBS).

Tissues were mounted on cover slips with mounting media comprised of DPBS with 50% glycerol containing 4 µg/mL 4'6-diamidino-2-phenylindole dihydrochloride (DAPI) and were visualized on a Zeiss LSM 800 confocal laser microscope (Carl Zeiss, Jena, Germany) and processed with the Zeiss LSM Image Browser software or visualized on a Lumen Dynamics XCite™ 120Q Nikon fluorescence microscope (Nikon, Mississauga, ON, Canada).

### **Preparation of digoxigenin-labeled RNA probes and fluorescent *in situ* hybridization**

Localization and distribution of cells expressing the *AedaeItp* and *AedaeItp-l* mRNA within the CNS was determined using fluorescent *in situ* hybridization (FISH) following a similar protocol as previously described (Paluzzi et al., 2008; Sajadi et al., 2020; Chapter 3). To synthesize the sense and antisense probes, *AedaeItp* and *AedaeItp-l* were amplified via PCR using one-day old female head and one-day whole body male cDNA, respectively, as template. Gene-specific primers with the addition of the T7 promoter sequence (5'-TAATACGACTCACTATAGGG-3') were utilized to add the T7 sequence to the 5' end of the target for sense probe (control) and 3' end of the target for anti-sense probe templates (Table 6-S1). *AedaeItp* primers were designed over common exons 2 and 4, targeting both *AedaeItp* and *AedaeItp-l* transcripts, whereas *AedaeItp-l* primers were designed over the unique exon 3 targeting only *AedaeItp-l* transcript. The amplified target sequences with the T7 promoter additions were then ligated to a pGEM-T-Easy vector (Promega, Madison, WI, USA) and directionally screened and amplified using a combination of a T7 promoter sequence and gene-specific reverse primers. Digoxigenin (DIG)-labeled antisense and sense *AedaeItp* and *AedaeItp-l* probes were generated by *in vitro* transcription, using a T7 RNA Polymerase Mix, 10X Reaction Buffer, and the DIG RNA Labeling Mix, 10X conc. (Roche Applied Science,

Mannheim, Germany), following the manufacturer's protocol. Once DIG-labeled RNA synthesis was complete, template DNA was removed with DNase I (New England Biolabs, Whitby, ON, Canada) and run on a non-denaturing 1% agarose gel to confirm RNA probe integrity. RNA probes were quantified by UV spectroscopy using a Take3 micro-volume plate and measured on a Synergy Multi-Mode Microplate Reader.

The *in-situ* hybridization procedure was modified based on a previously described protocol for the kissing bug, *Rhodnius prolixus*, and *A. aegypti* (Paluzzi et al., 2008; Chapter 3; Sajadi et al., 2020). Tissues/organs were dissected under nuclease-free DPBS and immediately placed into microcentrifuge tubes containing freshly-prepared 4% PFA in DPBS and fixed for 1 h at RT on a rocker. Tissues/organs were subsequently washed five times with 0.1% Tween-20 in DPBS (PBT) and treated with 1% H<sub>2</sub>O<sub>2</sub> (diluted in DPBS) for 20 min at RT to quench endogenous peroxidase activity. Next, tissues/organs were incubated in 4% Triton X-100 in PBT for 1 h at RT to permeabilize the tissues/organs and subsequently washed three times with PBT. A secondary fixation was performed for 20 min in fresh 4% PFA and tissues/organs were then washed with PBT to remove traces of fixative. The tissues/organs were then rinsed with a 1:1 mixture of PBT:RNA hybridization solution (50% formamide, 5 x SSC, 0.1 mg/mL heparin, 0.1 mg/mL sonicated salmon sperm DNA and 0.1% Tween-20), which was then replaced with RT pre-RNA hybridization solution (prepared by denaturing at 80°C for five min and subsequently cooled on ice for five min). Tissues/organs were then incubated at 56°C for 1 h. Labelled RNA probes (sense for control and anti-sense for experimental) were prepared by adding to pre-boiled RNA hybridization (2 ng/μL final concentration) and this mixture was heated at 80°C for 3 min to denature the single-stranded RNA probes and cooled on ice for 5 min. Tissues/organs were incubated overnight in the hybridization solution containing the DIG-labelled probe at 50°C. The

following day, tissues/organs were washed twice with hybridization solution, and subsequently with 3:1, 1:1 and 1:3 (vol/vol) mixtures of hybridization solution:PBT (all pre-warmed to 50°C overnight). Next, tissues/organs were washed with pre-warmed (50°C) PBT and subsequently blocked with PBTB (DPBS, 0.1% Tween-20, 1% Molecular Probes block reagent; Invitrogen, Carlsbad, CA, USA) for 1 h to reduce non-specific staining. Tissues/organs were then incubated with a 1:400 mouse anti-DIG biotin-conjugated antibody (Jackson ImmunoResearch Laboratories, West Grove, PA, USA) in PBTB for 1.5 h on a rocker protected from light, followed by several washes in PBTB over 1 h. Afterward, tissues/organs were incubated with horseradish peroxidase-streptavidin conjugate (Molecular Probes, Eugene, OR, USA) diluted 1:100 in PBTB for 1 h and tissues were washed again in PBTB several times over 1 h. Tissues/organs were then washed twice with PBT and once with DPBS. A tyramide solution was prepared consisting of Alexa Fluor 594 tyramide dye in 1X reaction buffer containing 1X H<sub>2</sub>O<sub>2</sub> following the manufacturer's protocol. After troubleshooting experiments using various incubations times with the tyramide solution, a 6.5 min incubation period provided optimal results with minimal background staining for the brain and ganglia. After the last DPBS was removed, tissues/organs were incubated in the tyramide solution for 6.5 min on a rocker protected from light, after which 100 µL of stop solution was added. The tyramide/stop solution mixture was then removed, and the tissues/organs were washed with DPBS several times over 1 h and stored overnight in DPBS at 4°C and then mounted on cover slips with mounting media. The tissues/organs were visualized on a Zeiss LSM 800 confocal laser microscope and processed with the Zeiss LSM Image Browser software or visualized on a Lumen Dynamics Xcite™ 120Q Nikon fluorescence microscope.

### **Starvation and blood feeding assay**

To examine the potential roles of *AedaeITP* and *AedaeITP-L* in mosquito feeding/starvation, adult males and females were isolated post-emergence and sorted into three treatment conditions: non-fed (no food or water provided), fed (10% sucrose *ad-libitum*), and hydrated (only water provided). The adults were collected after 24 h or 48 h, and mRNA transcript levels of *AedaeItp* and *AedaeItp-l* were examined by RT-qPCR (as described above). To investigate whether a protein-rich meal influences the transcript abundance of *AedaeItp* and *AedaeItp-l*, adult female mosquitoes (five-six day old) were given 20 min to blood feed on sheep's blood in Alsever's solution (Cedarlane Laboratories, Burlington, ON, Canada), and all blood fed females were subsequently isolated after 1, 6, 12 and 24 h post blood meal. Blood fed females were compared to control, similarly aged (five-six day old) females that were provided sucrose *ad libitum*. Post isolation, mRNA transcript levels of *AedaeItp* and *AedaeItp-l* were examined by RT-qPCR (as described above).

### **Preparation and microinjection of *AedaeItp* and *AedaeItp-l* dsRNA**

Gene-specific primers were designed to amplify a region of the *AedaeItp* and *AedaeItp-l* transcripts as a template for double stranded RNA (dsRNA) synthesis (ensuring no overlap with RT-qPCR primers, Table 6-S1). Similar to the gene-specific probes, ds*AedaeItp* primers were designed over common exons 1 and 2, targeting and knocking down both *AedaeItp* and *AedaeItp-l* mRNA, whereas *AedaeItp-l* primers were designed over the unique exon 3 targeting only *AedaeItp-l* transcript. The *AedaeItp* and *AedaeItp-l* target regions were amplified and cloned into pGEM-T-Easy and subsequently subcloned into the L4440 vector, which possesses two T7 promoters, each flanking either side of the multiple cloning site. L4440 was a gift from Andrew

Fire (Addgene plasmid#1654; <http://n2t.net/addgene:1654>; RRID:Addgene\_1654). The *AedaeItp* and *AedaeItp-l* targets were screened with a M13 forward (5'-TGTAACGACGCCAGT-3') and L4440 reverse primer (5'-AGCGAGTCAGTCAGTGAGCGAG-3') and reamplified with a T7 primer serving as a forward and reverse primer. Double stranded RNA was synthesized by *in vitro* transcription using the HiScribe T7 High Yield RNA Synthesis Kit (New England Biolabs, Whitby, ON, Canada) following manufacturers recommendations. The dsRNA was incubated at 75°C for 5 min for denaturation and left at RT for 15 min to allow rehybridization, followed by RNA purification using a Monarch RNA Cleanup Kit following the manufacturer's protocol (New England Biolabs, Whitby, ON, Canada). One-day old male and female adult mosquitoes were briefly anesthetized using CO<sub>2</sub> and injected in the thorax with 1 µg of *AedaeItp*, *AedaeItp-l* or control *Egfp* (enhanced green fluorescent protein) dsRNA using a Nanoject III Programmable Nanoliter Injector (Drummond Scientific, Broomall, PA, USA).

### ***In vivo* urine production assay**

To determine if *AedaeITP* and/or *AedaeITP-L* influences urine output, adult female mosquitoes were injected with 500 nL of a HEPES buffered saline (HBS), consisting of 11.9 mM HEPES, 137 mM NaCl, and 2.7 mM KCl, titrated to a pH of 7.45 and filter sterilized before use. Based on an established protocol (Calkins and Piermarini, 2015), four-day old females were injected and placed into a graduated, packed-cell volume tube (MidSci, St. Louis, MO, USA) for two hours at 28°C with three mosquitoes per tube and excretion volumes were measured. Specifically, following the incubation period, mosquitoes were removed from the tube, which was then centrifuged at 16 000 g for 30 s to allow for the excreted volume to be measured visually under a dissection microscope, via the graduated column at the bottom of the tube.

Treatment females were either four-day old *dsEgfp*, *dsAedaeItp*, *dsAedaeItp-l* females (injected at one-day old), or non-dsRNA injected four-day old female mosquitoes that served as controls.

### **Mating and egg-laying assay**

*A. aegypti* mosquitoes were separated at the pupal stage and individually placed into a 24-well plate to allow adults to emerge. One-day old non-mated male and female adults were then isolated and injected as follows: 1) *dsAedaeItp* or *dsAedaeItp-l* knockdown females mated with virgin males, 2) *dsAedaeItp* or *dsAedaeItp-l* knockdown males mated with virgin females, and 3) *dsAedaeItp* or *dsAedaeItp-l* knockdown females mated with *dsAedaeItp* or *dsAedaeItp-l* males. For 1), *dsAedaeItp* or *dsAedaeItp-l* females were grouped with one-day old virgin males at a 1:2 ratio of female:male per insect box (BugDorm-5 insect box, MegaView Science Co. Taiwan) between 18 and 24 h after dsRNA injection. After four-five days post-mating, knockdown females were provided a bloodmeal. For 2), *dsAedaeItp* or *dsAedaeItp-l* males were mated with two-three-day old virgin females, and females were provided a bloodmeal 48 h post-mating. Lastly, for 3), *dsAedaeItp* or *dsAedaeItp-l* males and females were mated, and females were provided a bloodmeal four-five days post injection. For all blood feeding assays, females were given 20 min to blood feed, and blood fed females were subsequently isolated and weighed individually before being placed in an inverted 25 cm<sup>2</sup> cell culture flask (Corning) containing 3 mL of distilled water (dH<sub>2</sub>O) from larvae rearing containers to attract egg laying, lined with filter paper. Laid eggs were collected after 4 days and were semi-desiccated for 72 h and counted. Females were then removed and weighed before spermathecae were dissected and viewed under a microscope to confirm insemination. Eggs were placed in 40 mL of dH<sub>2</sub>O with 1 mL larval

food (1:1 ratio of 2% brewer's yeast and 2% liver powder), and hatched larvae (if any) were counted after 48 h.

### **Sperm Quantification**

Sperm quantification in the paired seminal vesicles (male sperm storage organs) and testes of male *A. aegypti*, along with the spermathecae (female sperm storage organs) of female *A. aegypti* 4 days post dsRNA injection was performed following previously published protocols (Durant and Donini, 2020; Rocco et al., 2019). The seminal vesicles, testes, and spermathecae were isolated from individual male and female mosquitoes (9-11 mosquitoes per dsRNA mating treatment from 3-4 mating replicates), placed in a 96-well plate with 100  $\mu$ L PBS, and gently torn open using forceps to release spermatozoa. An additional 10  $\mu$ L PBS was used to rinse the forceps and the PBS with spermatozoa was mixed thoroughly using a P100 pipette. Five 1  $\mu$ L droplets of the PBS/spermatozoa mixture were spotted onto a microscope slide (previously treated with poly-L-lysine to promote sperm attachment), allowed to air dry completely, and subsequently fixed with 70% ethanol. Slides were mounted using mounting media comprised of DPBS with 50% glycerol containing 4  $\mu$ g/mL DAPI, and the nuclei of spermatozoa within each 1  $\mu$ L droplet was imaged under 4X magnification using an Olympus IX81 inverted microscope (Olympus Canada, Richmond Hill, ON, Canada). The nuclei of spermatozoa were counted in each 1  $\mu$ L droplet, averaged across all five droplets for each animal, and multiplied by the dilution factor to determine total spermatozoa numbers within the seminal vesicle, testes, and spermatheca.

## Statistical analyses

All graphs were created and statistical analyses performed using GraphPad Prism software. Data was analyzed accordingly using a one-way or two-way ANOVA and the appropriate post-hoc test as indicated in the figure captions, with differences between treatments considered significant if  $p < 0.05$ .

## 6.4 Results

### Tissue/organ-specific expression profile of *AedaeItp* and *AedaeItp-l* transcript

Post-embryonic stages and selected tissues/organs of mosquitoes were examined for *AedaeItp* and *AedaeItp-l* transcript expression and compared between males and females. Developmental expression profiling revealed significant enrichment of *AedaeItp* transcript abundance in adult stage mosquitoes (Figure 6-1A,B), with greatest enrichment in one- and four-day old males. In contrast, *AedaeItp-l* transcript was observed in late pupal and adult stage mosquitoes, including one-day old males and females (Figure 6-1A,C). Transcript abundance of *AedaeItp* was significantly higher compared to *AedaeItp-l* abundance in the adult-stage mosquitoes, with over a three-fold higher abundance of *AedaeItp* transcript compared to *AedaeItp-l*. Additionally, *AedaeItp* transcript abundance was exclusively enriched in the head (Figure 6-1D,H) and brain (Figure 6-1F,J) in both adult male and female mosquitoes. Expression of *AedaeItp-l* transcript expression was observed in the carcass (Figure 6-1E,I) and abdominal ganglia (Figure 6-1G, K) in adult mosquitoes.

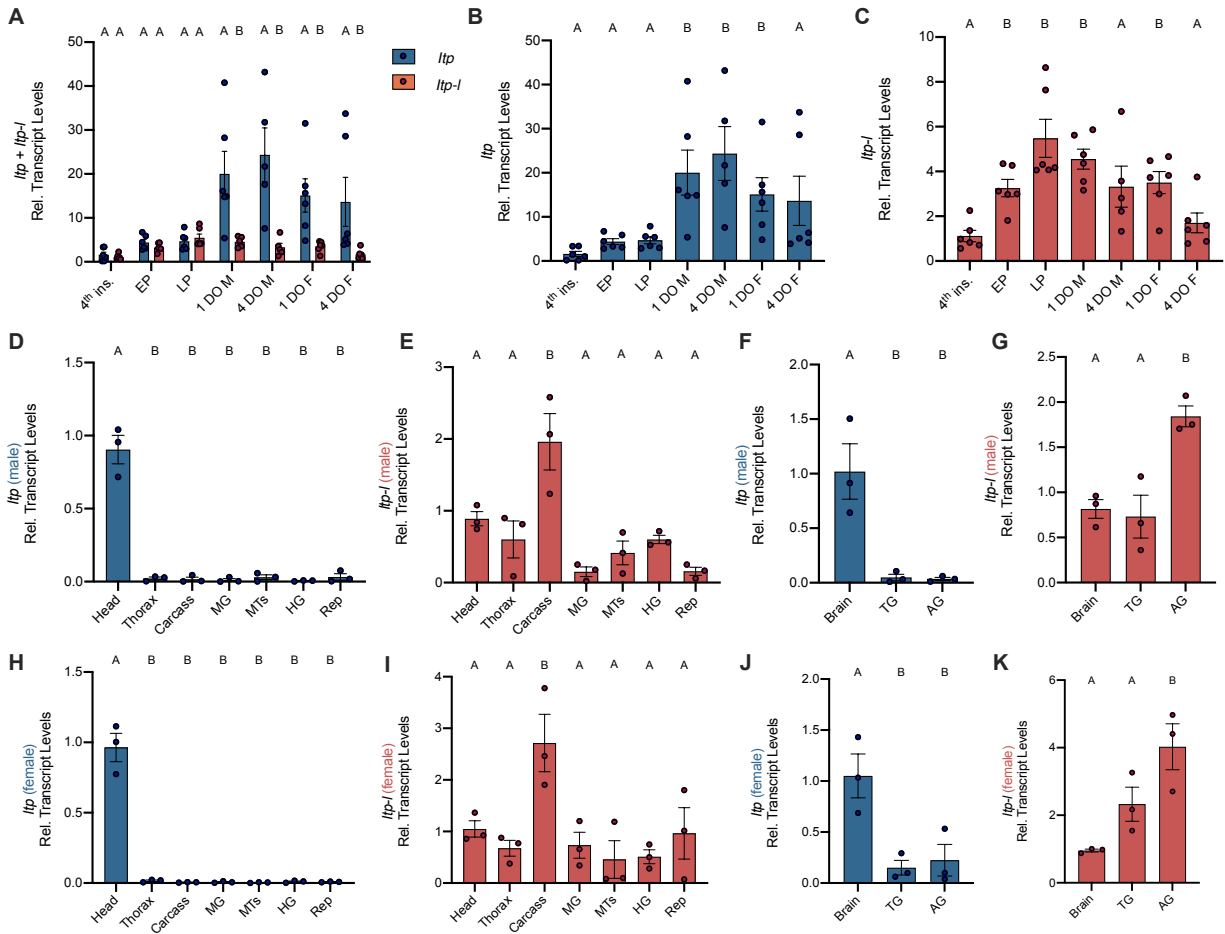


**Figure 6-1. Developmental and spatial transcript expression profile of *AedaeItp* and *AedaeItp-l* in *A. aegypti*.** Expression of *AedaeItp* and *AedaeItp-l* transcript was analyzed in post-embryonic stages (A-C) of the mosquito shown relative to transcript levels in fourth instar larvae. Expression of *AedaeItp* (D,F,H,J) and *AedaeItp-l* (E,G,I,K) transcript levels were analyzed in various tissues/organs from one-day old adult males (D-G) and females (H-K) shown relative to transcript levels in the mosquito head/brain. Abbreviations: 4<sup>th</sup> instar (4<sup>th</sup> ins), early pupa (EP), late pupa (LP), Malpighian tubules (MTs), midgut (MG), hindgut (HG), reproductive tissues/organs (Rep), thoracic ganglia (TG), and abdominal ganglia (AG). Data labeled with different letters are significantly different from fourth instar larvae (mean±SEM; one-way or two-way ANOVA with Bonferroni multiple comparison,  $p < 0.05$ ,  $n = 3-6$  biological replicates).

### ***Aedae*ITP- and *Aedae*ITP-L-like immunoreactivity and transcript localization**

Using whole mount immunohistochemistry, the central nervous system from one-day old male and female mosquitoes revealed *Aedae*ITP- and *Aedae*ITP-L-like immunostaining in three pairs of lateral neurosecretory cells in the medial anterior region of each brain hemisphere with axonal processes projecting anteriorly near an additional single pair of lateral neurosecretory cells (Figure 6-2A-E). A number of varicosities and blebs can be seen peripherally near the axonal projections, suggestive of release sites of these neuropeptides (Figure 6-2A-E). No *Aedae*ITP- or *Aedae*ITP-L-like immunostaining was observed in the thoracic ganglia (not shown). In the abdominal ganglia, *Aedae*ITP- and *Aedae*ITP-L-like staining was observed in a single pair of neurosecretory cells, positioned laterally on either side of each ganglia (abdominal ganglia 2-6) (Figure 6-2F-G). The terminal ganglion (which is a fusion of abdominal ganglia 7 and 8, revealed *Aedae*ITP- and *Aedae*ITP-L-like immunostaining in a single pair of neurosecretory cells located in the anterior region of the ganglion (abdominal ganglia 7) (Figure 6-2H). Similar staining was observed in four-day male and female mosquitoes (not shown). Staining in these cells and projections were absent in control treatments where the antiserum was preabsorbed with ITP antigen and omission of the primary anti-serum (Figure 6-S2).

Assessment of cell specific expression of *A. aegypti* *Itp* and *Itp-l* was accomplished using fluorescence *in situ* hybridization. Gene-specific probes were generated for both *AedaeItp* and *AedaeItp-l* to differentiate ITP and ITP-L immunoreactivity in the CNS. *AedaeItp* antisense primers were designed over common exons 2 and 4 resulting in transcript localization of potentially both *AedaeItp* and/or *AedaeItp-l*, whereas *AedaeItp-l* antisense primers were designed over the unique exon 3 targeting only the *AedaeItp-l* transcript (Figure 6-S1). The CNS, including the brain, thoracic ganglia, and abdominal ganglia were examined for *AedaeItp* and

*AedaeItp-l* transcripts (Figure 6-3). In contrast to the *AedaeItp-* and *Itp-L* like immunolocalization patterns, nervous tissues from one-day old adult male and female mosquitoes revealed fluorescence signals corresponding to *AedaeItp* and/or *AedaeItp-l* mRNA transcript in six to seven pairs of neurosecretory cells in the anterior protocerebrum (Figure 6-3A,B). *AedaeItp* and/or *AedaeItp-l* mRNA transcript was also observed in two pairs of neurosecretory cells in each abdominal ganglia, positioned laterally on either side of the ganglia, similar to *AedaeItp-* and *AedaeItp-L*-like immunolocalization, and an additional neurosecretory cell located medio-posteriorly and ventrally within each ganglia (Figure 6-3D). The *AedaeItp* antisense probe also revealed staining in one lateral pair of neurosecretory cells in the terminal abdominal ganglion (Figure 6-3E). Fluorescence of these cells and the neurosecretory cells in the brain were not observed in control preparations treated with the sense probe (not shown).

*AedaeItp-l* transcript was specifically localized to the abdominal ganglia of one-day old mosquitoes (Figure 6-3F). Similar staining was observed in both male and females, and in four-day old adults (not shown). Findings indicate *AedaeItp-l* transcript in two pairs of neurosecretory cells positioned laterally on either side of each abdominal ganglia and a single pair located medio-posteriorly and ventrally, similar to the cell-specific fluorescence signals observed with the *AedaeItp* antisense probe. Interestingly, no *AedaeItp-l* transcript fluorescence was observed in the brain of the mosquitoes, as observed with the *AedaeItp* antisense probe (Figure 6-3C,D), or in the thoracic ganglia (not shown). In contrast to the *AedaeItp* cell-specific fluorescence signals, *AedaeItp-l* transcript was not observed in the terminal ganglion (Figure 6-3E). No fluorescence signals were observed in the CNS preparations treated with sense probes (not shown).

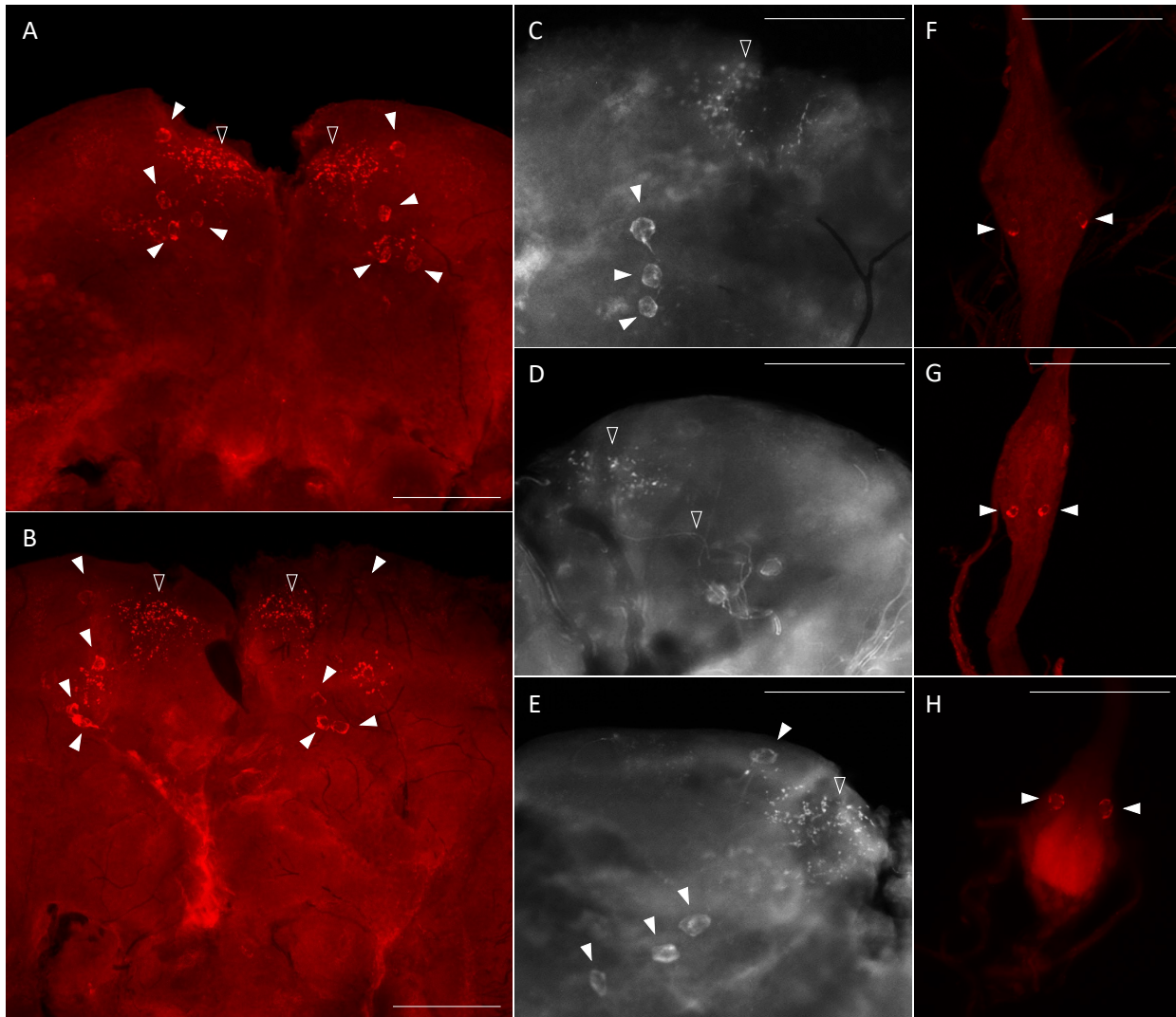


**Figure 6-2. Immunolocalization of *AedaeITP* and *AedaeITP-L* in the central nervous system of the *A. aegypti* mosquito.** *AedaeITP*- and *AedaeITP-L*-like immunoreactivity was examined in (A) male and (B) female brains, in four pairs of neurosecretory cells (indicated by white arrowheads), with axonal processes projecting anteriorly (C-E), towards varicosities and blebs on the periphery of the brain (indicated by empty arrowheads). (F,G) Ventral view of abdominal ganglia showing a single pair of lateral neurosecretory cells and (H) an anterior pair observed in the terminal ganglion. Scale bars: (A-B) 200  $\mu$ M; (C-H) 100  $\mu$ M.

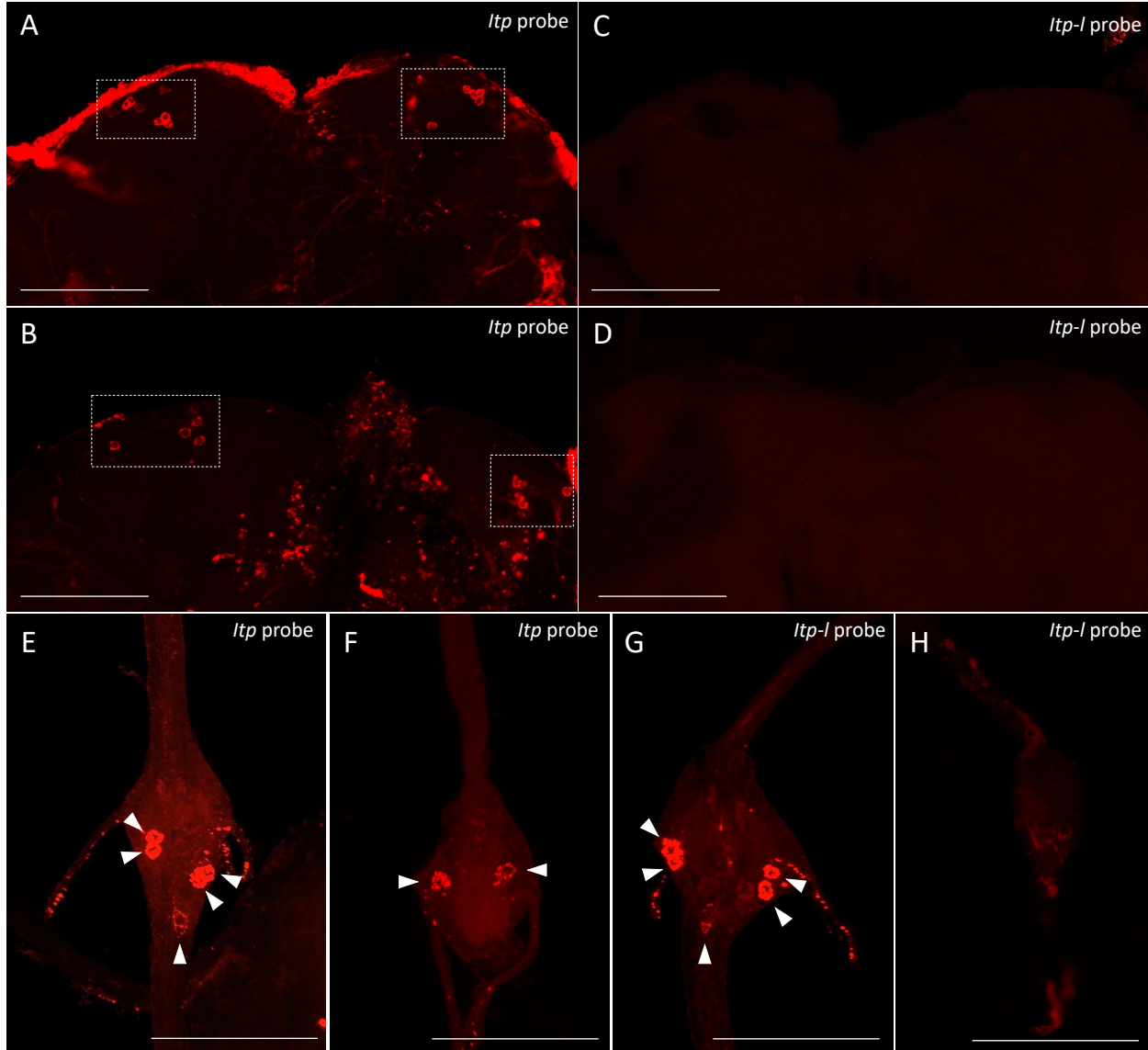


**Figure 6-3. Distribution of *AedaeItp* and *AedaeItp-l* transcript in the central nervous system of the *A. aegypti* mosquito.** *AedaeItp* and *AedaeItp-l* transcript was examined in (A,C) male and (B,D) female brains. (A,B) *AedaeItp* antisense probe revealed six to seven pairs of neurosecretory cells in the brain, while (C,D) *AedaeItp-l* antisense probe showed no staining in the brain. (E) *AedaeItp* antisense probe revealed two pairs of lateral cells and one single medial neurosecretory cell in the abdominal ganglia, and (F) one pair of cells in the terminal ganglion. (G) *AedaeItp-l* antisense probe detected two lateral cells and a single medial cell in the abdominal ganglia, but no cell-specific staining in the terminal ganglion (H). Scale bars: (A-D) 200  $\mu$ M; (E-H) 100  $\mu$ M.

### **Role of *AedaeITP* and *AedaeITP-L* in feeding and starvation**

Post emergence, one-day old adult male and female mosquitoes were placed in either a fed (provided a 10% sucrose meal), non-fed (no food provided), or hydrated (provided a water meal, no sucrose) condition and isolated after 24 or 48 h to examine a potential role of *AedaeITP* and *AedaeITP-L* in feeding and starvation (Figure 6-4A). When adult male and female mosquitoes were placed in the non-fed or hydrated treatment for 24 h, there was no difference in mRNA abundance of either *AedaeItp* or *AedaeItp-l* compared to control fed conditions (Figure 6-4B,D,F,H). However, when the mosquitoes were subjected to these treatments for 48 h, there was a significant enrichment, approximately two-fold, of both *AedaeItp* and *AedaeItp-l* transcript levels in the non-fed condition compared to control fed animals (Figure 6-4C,G,E,I). Next, to determine if *AedaeITP* and/or *AedaeITP-L* may play a role in relation to blood feeding, four to six-day old adult female mosquitoes were provided a bloodmeal to examine whether a protein-rich meal influences the transcript abundance of *AedaeItp* and *AedaeItp-l* (Figure 6-4J). *AedaeItp* mRNA abundance did not change post-blood feeding compared to control, sucrose-fed females (Figure 6-4K). In contrast, *AedaeItp-l* mRNA abundance was significantly increased 6 h post blood-feeding, with modest enrichment 12 and 24 h post-bloodmeal (Figure 6-4L).

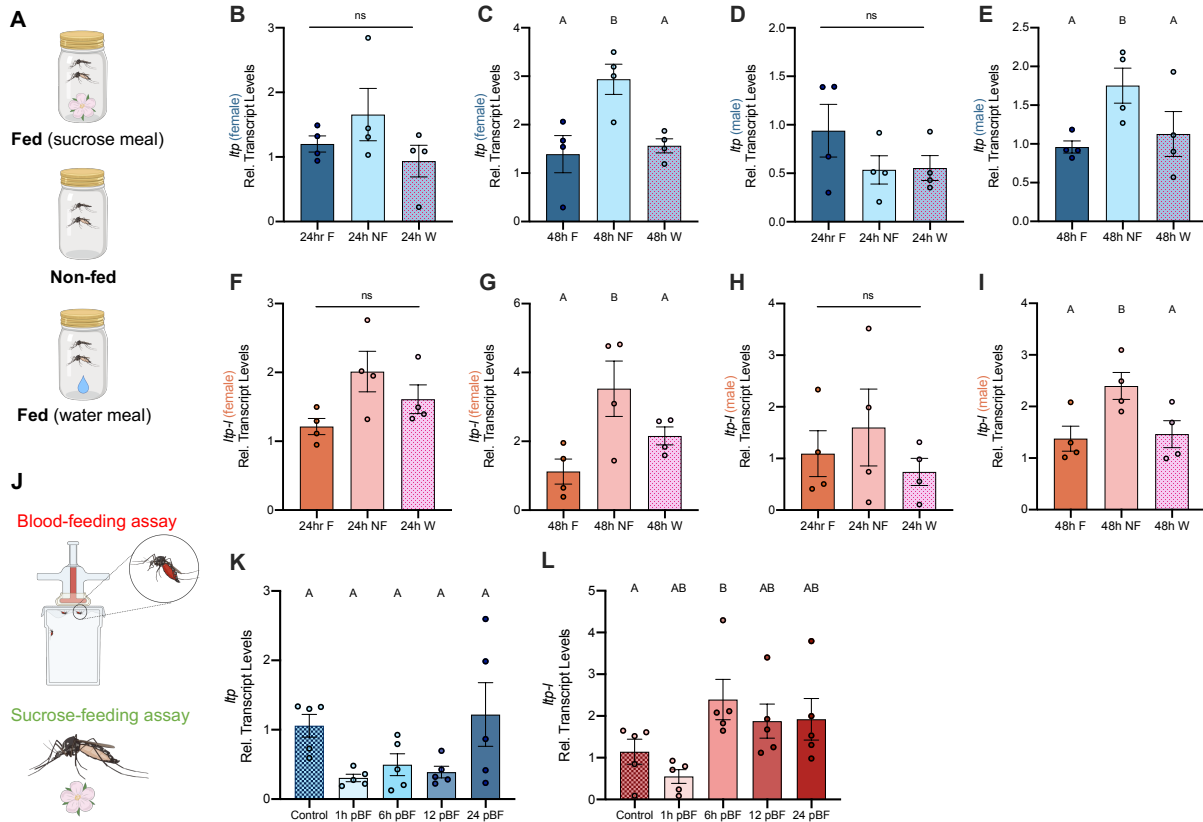


**Figure 6-4. Effect of feeding and starvation on transcript expression levels of *AedaeItp* and *AedaeItp-1* in adult *A. aegypti*.** (A) Post-emergence, adult males were placed in a fed (sucrose meal provided), non-fed (no food provided), and hydrated (water meal provided) condition for 24 h and 48 h, and abundance of (B-E) *AedaeItp* and (F-I) *AedaeItp-1* transcript were analyzed, shown relative to transcript levels in 24 h fed adults. Data labeled with different letters are significantly different from 24 h fed adults. (J) Four to six day old adult females were blood-fed and isolated at 1, 6, 12, and 24 post blood-feeding and (K) *AedaeItp* and (L) *AedaeItp-1* transcript levels were analyzed, shown relative to control, sucrose-fed females. Abbreviations: fed (F), non-fed (NF), water (W) and pBF (post-blood feeding). Data labeled with different letters are significantly different from control, sucrose-fed females (mean±SEM; one-way ANOVA with Bonferroni multiple comparison,  $p < 0.05$ ,  $n = 4-5$  biological replicates).

### **dsRNA knockdown of *AedaeItp* and *AedaeItp-l* in adult *Aedes* mosquitoes**

RNA interference of the *AedaeItp* and *AedaeItp-l* gene was accomplished through dsRNA-injections of one-day old adult male and female mosquitoes (Figure 6-5). Given the conserved exons 1, 2, and 4 between *AedaeItp* and *AedaeItp-l*, the ds*AedaeItp* primers were designed over a common exon 2 resulting in the knockdown of both *AedaeItp* and *AedaeItp-l* transcripts (Figure 6-5A). However, ds*AedaeItp-l* primers were designed over the unique exon 3 allowing knockdown of only the *AedaeItp-l* transcript. Relative to control ds*Egfp*-injected mosquitoes, *AedaeItp* and *AedaeItp-l* transcripts were significantly reduced by ~75% in four-day old male (Figure 6-5B) and female (Figure 6-5C) mosquitoes injected with ds*AedaeItp*. Comparatively, ds*AedaeItp-l* treatment resulted in a significant decrease in *AedaeItp-l* transcript abundance by ~80% in males (Figure 6-5B) and ~60% in females (Figure 6-5C) in four-day old adults, whereas *AedaeItp* transcript abundance remained unaffected. A similar trend was observed in six-day old females following ds*AedaeItp* and ds*AedaeItp-l* injection (Figure 6-5F), while *AedaeItp* and *AedaeItp-l* transcript restored to normal levels within six and eight days post-injection in males (Figure 6-5E,G), and eight days post-injection in females (Figure 6-5H). To confirm injection alone does not influence *AedaeItp* and *AedaeItp-l* transcript levels, four days post-ds*Egfp* injected animals were compared to four-day old non-injected mosquitoes (Figure 6-5D), with no significant changes in *AedaeItp* and *AedaeItp-l* transcript abundance in ds*Egfp*-injected males and females compared to non-injected mosquitoes.

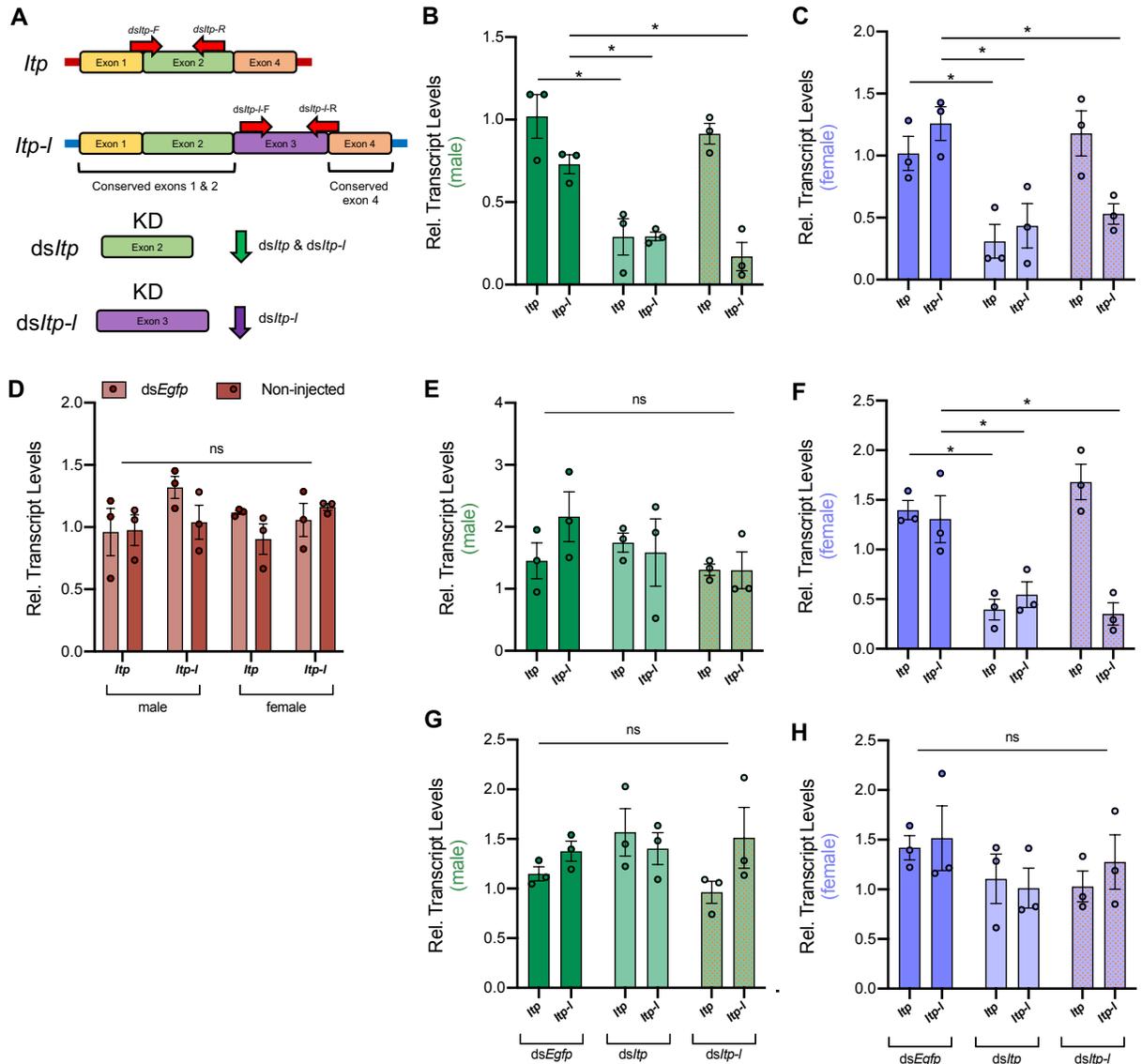


**Figure 6-5. *Aedaeltip* and *Aedaeltip-l* knockdown efficiency in adult *A. aegypti*.** (A) *dsAedaeltip* primers were designed over a common exon 2 resulting in the knockdown of both *Aedaeltip* and *Aedaeltip-l* transcripts, whereas *dsAedaeltip-l* primers were designed over a unique exon 3 targeting only the *Aedaeltip-l* transcript. One day old adult male (B,E,I) and female (C,F,H) mosquitoes were injected with *dsAedaeltip*, *dsAedaeltip-l* or control *dsEgfp* (D) and collected four (B,C) six (E,F) and eight (G,H) days post-injection to determine knockdown efficiency. Transcript levels are shown relative to control *dsEgfp* mosquitoes. (D) *dsEgfp*-injected animals compared to non-injected animals. Data shown as mean $\pm$ SEM; one-way ANOVA with Bonferroni multiple comparison, \* denotes significant knockdown,  $p < 0.05$ ,  $n = 3$  biological replicates (ns denotes no statistical significance).

### **dsRNA knockdown confirms *AedaeITP* and *AedaeITP-L* immunolocalization**

To further confirm ds*AedaeItp*- and *AedaeItp-l* knockdown and differentiate between *AedaeITP* and *AedaeITP-L* immunolocalization, both peptide and transcript expression in the CNS were examined in mosquitoes four-days post-dsRNA injection. Wholemounds of ds*AedaeItp*-injected male and female mosquitoes showed no *AedaeITP*- and *AedaeITP-L*-like immunostaining in the brain (Figures 6-6A,B), abdominal ganglia (Figure 6-6C), and in the terminal ganglion (Figure 6-6D). In contrast, ds*AedaeItp-l*-injected mosquitoes did not exhibit changes to immunostaining in the brain (Figure 6-6E,F), with similar staining as described above (Figure 6-2A,B), and in control ds*Egfp*-injected mosquitoes (Figure 6-S3A,B). However, as expected, knockdown of *AedaeItp-l* resulted in abolished staining of neurosecretory cells in the abdominal ganglia (Figure 6-6G), and interestingly, no effect on immunostaining in the terminal ganglion (Figure 6-6H), with a single pair of cells as observed in control ds*Egfp*-injected mosquitoes (Figure 6-S3C,D).

Similar to the *AedaeITP*- and *AedaeITP-L*-like immunolocalization pattern in knockdown animals, wholemounts of nervous tissue revealed no fluorescence signals corresponding to *AedaeItp* and *AedaeItp-l* transcript in ds*AedaeItp*-injected males and females (Figure 6-7). No cell-specific staining was observed in the brain (Figure 6-7A,B), abdominal ganglia (Figure 6-7E), nor the terminal ganglion (Figure 6-7F) with preparations treated with the *AedaeItp* antisense probe. As expected, ds*AedaeItp-l*-injected male and female showed no fluorescence signals in the brain (Figure 6-6C,D) and in the terminal ganglion (Figure 6-6H) with the *AedaeITP-L* antisense probe. However, as expected, staining in the abdominal ganglia was also abolished in the ds*AedaeItp-l*-injected mosquitoes (Figure 6-6G).

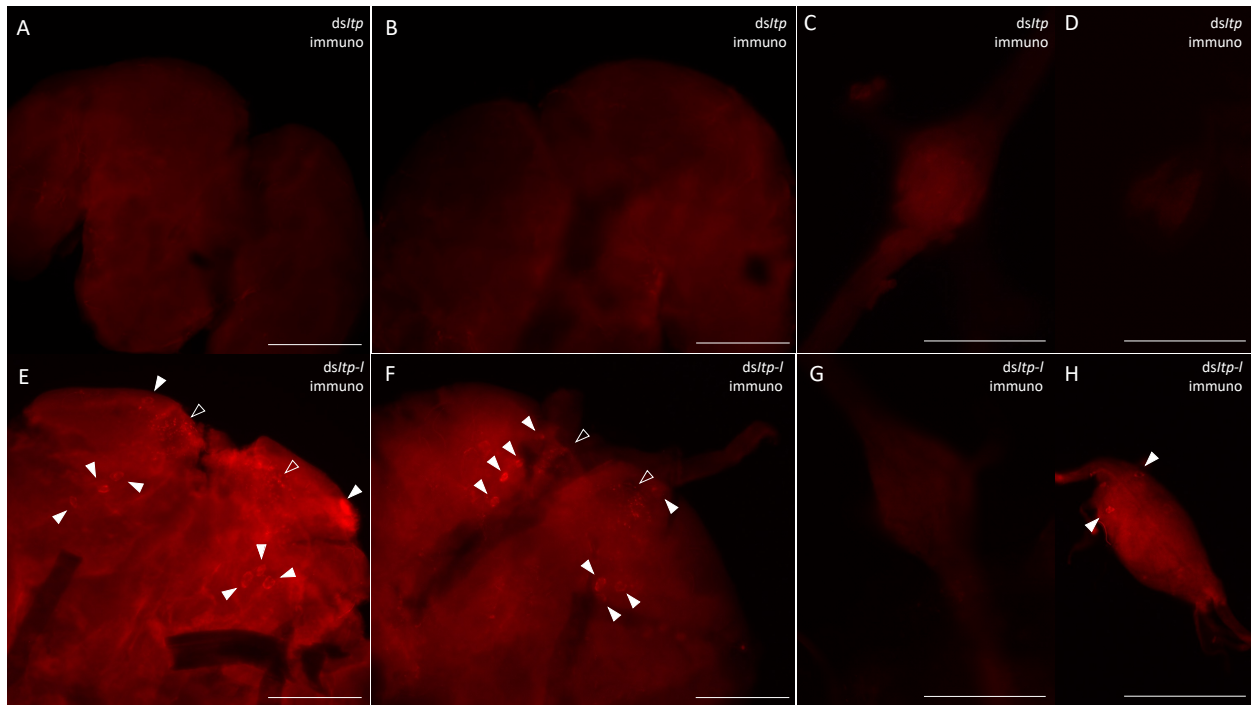


**Figure 6-6. Immunolocalization of *AedaeITP* and *AedaeITP-L* in the central nervous system of adult *A. aegypti* mosquitoes following *dsAedaeItp* and *dsAedaeItp-l* injection.** *AedaeITP*- and *AedaeITP-L*-like immunoreactivity is abolished in (A) *dsAedaeItp*-injected male and (B) female brain, (C) abdominal ganglia and (D) terminal ganglion. (E) *dsAedaeItp-l* treated male and (F) female brain reveal immunoreactivity in four pairs of neurosecretory cells (indicated by white arrowheads), with axonal processes emanating anteriorly towards release sites (indicated by empty arrowheads). (G) No immunostaining was observed in the abdominal ganglia following *dsAedaeItp-l* treatment whereas (H) one pair of lateral anterior cells were observed in the terminal ganglion. Scale bars: (A,B,E,F) 200  $\mu$ M; (C,D,G,H) 100  $\mu$ M.

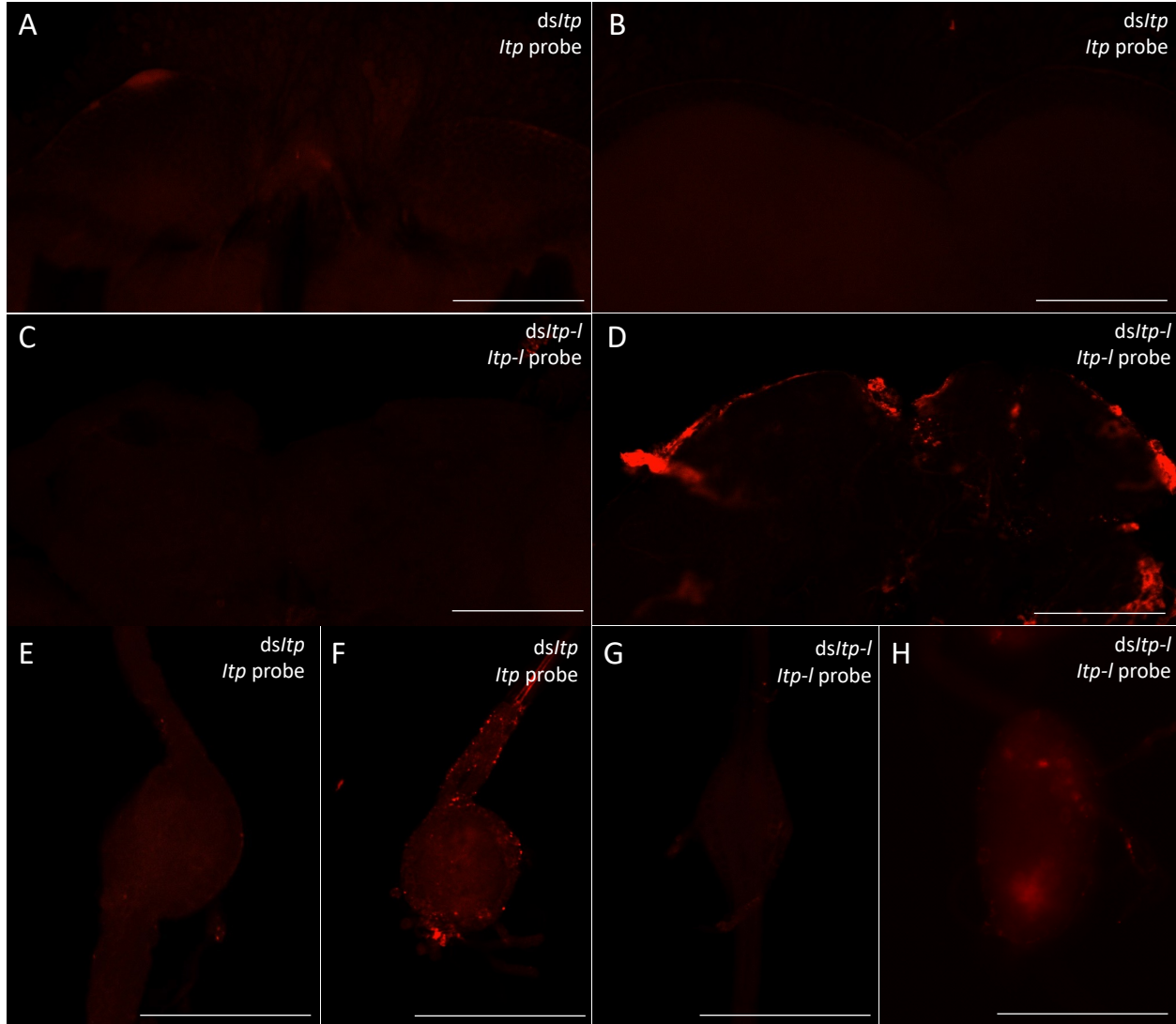


**Figure 6-7. Distribution of *AedaeItp* and *AedaeItp-l* transcript in the central nervous system of adult *A. aegypti* mosquitoes after *dsAedaeItp* and *dsAedaeItp-l* injection.** *dsAedaeItp*-injected and *dsAedaeItp-l*-injected (A,C) male and (B,D) female mosquitoes reveal no cell-specific fluorescence staining in the brain, (E,G) abdominal ganglia and (F,H) in the terminal ganglion. Scale bars: (A-D) 200  $\mu$ M; (E-H) 100  $\mu$ M.

### ***AedaeItp* knockdown influences urine output in adult females**

To determine if *AedaeItp* and/or *AedaeItp-L* influences ionoregulation and urine excretion, we volume loaded ds*AedaeItp* and ds*AedaeItp-l* injected females with saline and measured their urine output over two hours post volume loading. Four-day old HBS-injected females excreted a volume of  $429.5 \pm 53.49$  nL of urine, which was significantly higher compared to control four-day old non-HBS injected females ( $106.8 \pm 15.39$  nL) (Figure 6-8). Notably, ds*Egfp* treated females excreted a similar volume of urine ( $391.6 \pm 61.03$  nL) compared to HBS-injected females. In contrast, ds*AedaeItp* mosquitoes injected with HBS secreted a significantly higher amount of urine,  $972.7 \pm 70.18$  nL, approximately 2.5-fold higher compared to ds*Egfp*-injected females. Interestingly, no significant change in urine output was observed in ds*AedaeItp-l* females injected with HBS ( $604.2 \pm 78.87$  nL), compared to HBS loaded control (non-dsRNA injected) and ds*Egfp*-injected females.

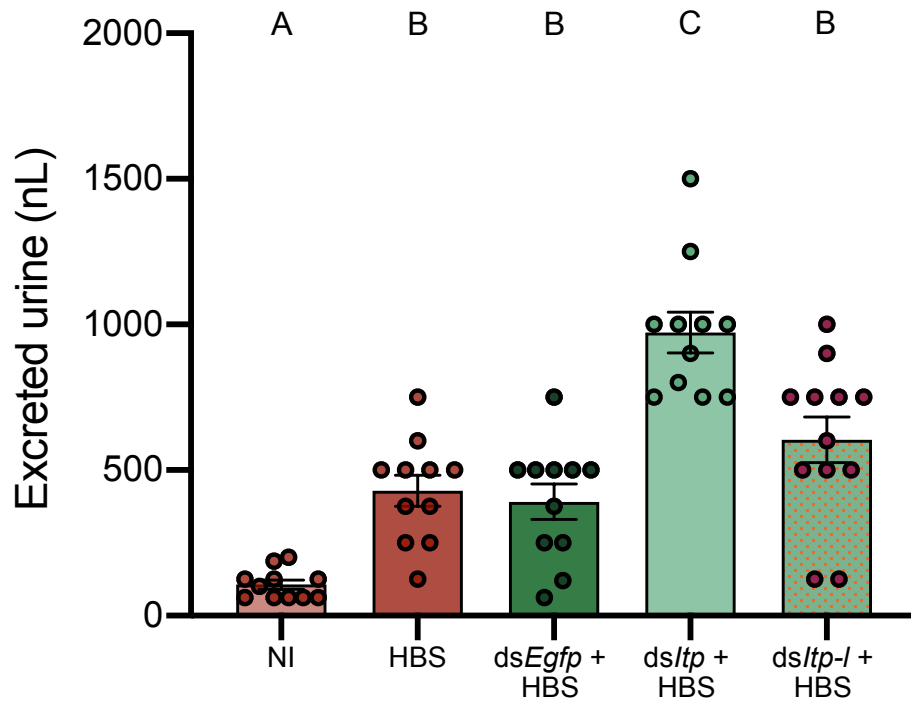


**Figure 6-8. Effect of *AedaeItp* and *AedaeItp-1* knockdown on urine excretion in adult female *A. aegypti*.** Four-day old females were injected with 500 nL of a HEPES buffered saline (HBS) and allowed to excrete for 2 h. Data labeled with different letters are significantly different from control, ds*Egfp* adults (mean±SEM; one-way ANOVA with Bonferroni multiple comparison,  $p < 0.05$ ,  $n = 11-12$ ).

### ***AedaeItp* and *AedaeItp-l* knockdown influences male and female reproductive success**

To assess the roles of *AedaeItp* and *AedaeItp-L* in reproductive behaviour and physiology, dsRNA-injected virgin mosquitoes were placed into one of the following mating combinations: 1a) ds*AedaeItp* or 1b) ds*AedaeItp-l* females mated with control, non-dsRNA males, 2a) ds*AedaeItp* or 2b) ds*AedaeItp-l* males mated with control, non-dsRNA females, and 3a) ds*AedaeItp* or 3b) ds*AedaeItp-l* females mated with ds*AedaeItp* and ds*AedaeItp-l* males. When ds*AedaeItp* females were mated with normal males, there was a significant reduction in the incidence of blood feeding (Figure 6-9A), reduced bloodmeal engorged by the blood fed female (Figure 6-9B), reduction in the number of eggs laid (Figure 6-9C), and overall reduction in the percentage of larvae hatching per female (Figure 6-9D) was observed. More specifically, there was a ~90% reduction in preference for blood feeding by ds*AedaeItp* females and ~75% reduction in ds*AedaeItp-l* females (Figure 6-9A). ds*AedaeItp-l* females oviposited a similar number of eggs and had a comparable percentage of hatched larvae as control ds*Egfp*-females (Figure 6-9C,D). Similar trends were observed in ds*AedaeItp* and ds*AedaeItp-l* males mated with normal females, with significantly reduced number of eggs oviposited (Figure 6-9G), as well as a reduced percentage of viable eggs and larvae hatching per female in ds*AedaeItp-l* animals (Figure 6-9H) was observed. ds*AedaeItp* and ds*AedaeItp-l* males mated with normal females did not influence female preference for blood feeding (Figure 6-9E). Interestingly, ds*AedaeItp* and ds*AedaeItp-l* females mated with ds*AedaeItp* and ds*AedaeItp-l* males almost completely abolished the preference for blood feeding (Figure 6-9I), with almost no eggs laid by the female (Figure 6-9K), and complete absence of larval hatching (Figure 6-9K). No significant changes were observed in the weight of blood fed females immediately post-feeding and subsequently post-egg laying (4 days post-feeding) (Figure 6-9F,J). It should be noted that reduced preference

for blood feeding limited the number of blood fed females used for subsequent studies. Mated males and females injected with control *dsEgfp* had similar preference for blood-feeding, weight of blood-fed females, produced similar number of eggs and comparable larval hatching as non-injected females (Figure 6-S4).

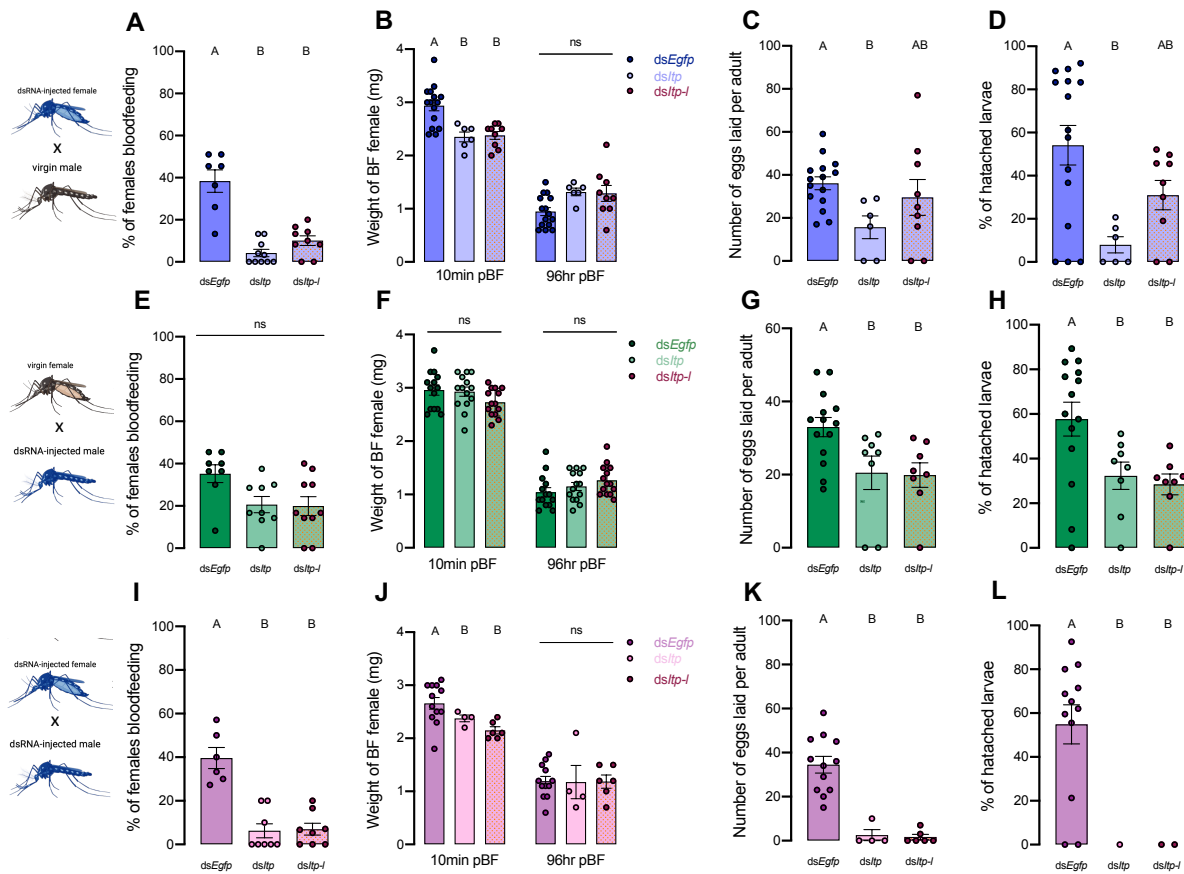


**Figure 6-9. Effect of *AedaeItp* and *AedaeItp-l* knockdown on blood-feeding, egg laying, and larval hatching (egg viability) in adult *A. aegypti*.** (A-D) *dsAedaeItp* or *dsAedaeItp-l* females mated with normal males, (E-H) *dsAedaeItp* or *dsAedaeItp-l* males mated with normal females, and (I-L) *dsAedaeItp* or *dsAedaeItp-l* females mated with *dsAedaeItp* or *dsAedaeItp-l* males. The effect of *dsAedaeItp* or *dsAedaeItp-l* knockdown was tested on (A,E,I) preference for blood feeding, (B,F,J) weight of blood fed female before and after egg collection, (C,G,K) number of eggs oviposited, and (D,H,L) percentage of larval hatching. Data labeled with different letters are significantly different from control, *dsEgfp* adults (mean±SEM; one-way ANOVA with Bonferroni multiple comparison,  $p < 0.05$ , (A,E,I,  $n = 6-11$  mating replicates, each point represents individual replicate values) (B-D,F-H,J,K,  $n = 1-15$ , each point represents data from individual females), (ns denotes no statistical significance).

### ***AedaeItp* and *AedaeItp-l* knockdown reduces spermatozoa count**

In light of the results above, it supports the notion that knockdown of *AedaeItp* and *AedaeItp-l* may have a distinct role in male reproductive biology separate from their effects on females since pairings between normal females and knockdown males revealed females had normal preference for blood-feeding and as well as bloodmeal weight; however, oviposition rates by females and larval hatching rates were significantly reduced. Considering the overall reduced preference for blood feeding in *dsAedaeItp* and *dsAedaeItp-l* females, we speculated that *AedaeITP* and *AedaeITP-L* proteins play an essential role in spermatozoa production and release. Sperm was collected separately from the testes and seminal vesicles of four-day old *dsAedaeItp*- and *dsAedaeItp-l*-injected males (from all three mating conditions described above) and spermathecae of four-day old *dsAedaeItp*- and *AedaeItp-l*-injected females (again, from all three mating conditions noted above), and the quantity of mature spermatozoa was compared to *dsEgfp*-injected animals (Figure 6-10A,B). For spermatozoa collected from the seminal vesicles, *dsAedaeItp*- and *dsAedaeItp-l*-injected females mated with normal males produced similar mature spermatozoa counts compared to control *dsEgfp* animals (Figure 6-10C, Figure 6-S5B,E). Interestingly, knockdown resulted in significant reductions in the number of spermatozoa in the seminal vesicle, from both *dsAedaeItp*- and *dsAedaeItp-l*-injected males mated with control females and when mated with *dsAedaeItp*- and *dsAedaeItp-l* females (Figure 6-10C, Figure 6-S5C,D,F,G). Similar trends were observed for the number of spermatozoa collected directly from the male testes (Figure 6-S6). Comparatively, *AedaeItp*- and *AedaeItp-l* knockdown resulted in an ~85% reduction in mature spermatozoa counts in the spermatheca in all three mating conditions (Figure 6-10C, Figure 6-S5H-N). Animals injected with *dsEgfp* resulted in similar

number of spermatozoa in the testes, seminal vesicles, and spermathecae compared to non-injected animals (Figure 6-S7).



## 6.5 Discussion

ITP and ITP-L belong to the CHH family of neuropeptides and have been functionally characterized in many insect species (Begum et al., 2009; Dircksen et al., 2008; Drexler et al., 2007; Gálíková et al., 2018; Nagai et al., 2014; Sun et al., 2020; Webster et al., 2012; Yu et al., 2016). However, while limited studies have examined ITP signalling pathways in insects, ITP/ITP-L receptors have generally not been identified and characterized thus far, except for in the domestic silk moth *B. mori* (Nagai et al., 2014). In the present study, the *A. aegypti* ITP and ITP-L peptides along with their corresponding transcripts have been localized, confirming the distribution of these peptides in neurosecretory cells and processes within the mosquito central nervous system. Additionally, prospective physiological functions have been investigated for *AedaeITP* and *AedaeITP-L* including roles in feeding, urine output, and reproductive success of adult male and female mosquitoes. This is the first report that examines the distribution, localization, and physiological function of the ITP/ITP-L signalling system in *A. aegypti* mosquitoes.

### **Distribution pattern of *AedaeITP* and *AedaeITP-L* in the CNS**

Expression profiles of transcripts encoding *A. aegypti* ITP and ITP-L were measured to reveal potential functional or sex-specific roles for these peptides. Examination of the developmental and tissue-specific expression profile revealed enrichment of *AedaeItp* and *AedaeItp-l* in both one- and four-day old male and females, with significant enrichment of *AedaeItp* in the brain and *AedaeItp-l* in the abdominal ganglia. The expression of ITP and ITP-L in the central and peripheral nervous system has been examined in numerous insects (Dircksen et al., 2008; Meredith et al., 1996; Yu et al., 2016). While *Itp* mRNA expression has been detected

only in the nervous system, evidence has suggested *Itp-l* expression in peripheral tissues as well. In *T. castaneum*, *Itp-l* transcript expression was found to be highly expressed in the midgut (Begum et al., 2009), and in the Malpighian tubules and hindgut in *S. gregaria* (Meredith et al., 1996).

Previous studies in *M. sexta* revealed that *MasITP* and *MasITPL* are differentially expressed in mainly nonoverlapping populations of central and peripheral neurons (which includes neuronal projections from the CNS) in the nervous system (Dai et al., 2007). RT-PCR, immunohistochemistry, and *in situ* hybridization studies indicated expression of *MasITP* exclusively in the brain to two neuron types; in type Ia<sub>2</sub> neurosecretory cells, with axonal projections to the retrocerebral complex (Copenhaver and Truman, 1986; Homberg et al., 1991; Zitnan et al., 1995; Zitnan and Adams, 2005) and in small neurons adjacent to type Ia<sub>2</sub> cells, established as interneurons, as their projections remain within the protocerebrum (Dai et al., 2007). Thus, in the *M. sexta*, it is suggested that ITP is released as a neurohormone from type Ia<sub>2</sub> cells into the haemolymph, whereas ITP produced in the small interneurons may serve transmitter or modulatory functions in the brain (Dai et al., 2007). Similarly in *S. gregaria*, ITP is believed to be synthesized in the neurosecretory cells of the pars intercerebralis of the brain where it is then transported for storage and eventual release in the corpora cardiaca (Meredith et al., 1996). The existence of ITP-L transcripts was first reported in *S. gregaria* (Macins et al., 1999), while the mature peptide was identified by Dai *et al.*, (2007) demonstrating ITP-L transcript and peptide distribution in the central and peripheral nervous system of insects, including *B. mori*, *M. sexta*, and the grasshopper, *Schistocerca americana*. Relatively weak ITP-L immunoreactivity was observed in the brain type Ia<sub>2</sub> cells but was found to be completely absent in axons and terminals within the retrocerebral complex (Dai et al., 2007). ITP-L peptides

are abundant in the ventral ganglia, flight muscle, MTs, and ileal tissues, indicating a possible distinctive function from ITP (Meredith et al., 1996; Phillips and Audsley, 1995).

Through RNAi-mediated knockdown, we confirmed *AedaeITP* immunoreactivity in four pairs of neurosecretory cells in the anterior region of the protocerebrum and in a single pair of lateral neurosecretory cells in the terminal ganglion. In contrast, *AedaeITP-L* immunoreactivity was observed in one pair of lateral neurosecretory cells in each abdominal ganglia of the ventral nerve cord. Cell-specific *AedaeITP* transcript localization revealed six to seven clusters of cells in the anterior protocerebrum and in a pair of lateral neurosecretory cells in the terminal ganglion, while *AedaeITP-L* transcript was localized only to the abdominal ganglia, with no staining in the brain, thus corroborating the RT-qPCR results of enriched *AedaeItp* expression in the brain, and *AedaeItp-l* in the abdominal ganglia. In general, expression patterns of *AedaeItp* and *AedaeItp-l* were similar to those described in *M. sexta*, *T. castaneum*, *B. mori*, and *D. melanogaster* (Begum et al., 2009; Dai et al., 2007; Dirksen, 2009; Dirksen et al., 2008). In *T. castaneum*, *Itp* expression was in five pairs of brain cells on the dorsal side of the protocerebral hemispheres and in a pair of cells in the abdominal terminal ganglion (Begum et al., 2009). Similarly, ITP expression was observed in four pairs of brain cells in *D. melanogaster*. While still inconclusive, previous immunohistochemical studies in other insects allude to protocerebral cells with projections to the corpora cardiaca and allata, and the cells in the terminal abdominal ganglion may have projections to the hindgut (Dirksen et al., 2008) and possibly to reproductive organs (Begum et al., 2009), which can hint to novel functions for the ITP/ITP-L signalling system. Given the immunoreactivity and transcript expression of *AedaeITP* in the terminal ganglion, this can suggest iono-regulatory roles in the hindgut, acting possibly as an anti-diuretic

hormone to increase water or ion reabsorption, similar to effects seen in the desert locust (Audsley et al., 1992).

### **Role of ITP and ITP-L in feeding and urine excretion**

The challenges of osmotic and ionic regulation vary between distinct environmental conditions that might be faced by the adult mosquito. In desiccating environments, insects must safeguard water balance and reduce the rate of water loss (Terhzaz et al., 2012). The current findings reveal an increase in both *AedaeItp* and *AedaeItp-l* transcript levels after 48 hours with no food and water in both adult male and female mosquitoes. These findings are similar to studies in *Drosophila*, where ITP was linked as a natural component of desiccation and osmotic stress responses, since both stressors triggered an increase in *Itp* expression, while ITP knockdown reduced survival under desiccation and osmotic stress (Gáliková et al., 2018). *DrosoITP* plays roles in hunger, thirst, and excretion in *Drosophila* suggesting that ITP-regulated changes to physiology and behaviour represent critical insect responses to cope with reduction in body water (Gáliková et al., 2018).

The discovery of the first anti-diuretic hormone mediating its effects on the insect hindgut was described by Audsley *et al.*, (1992) when ITP was purified from the corpora cardiaca of the locust, *S. gregaria*. A conserved *Itp* gene was later uncovered in the genome of the mosquito, *A. aegypti*, raising the prospect for a similar role in maintaining iono- and osmo-regulation (Dai et al., 2007). *A. aegypti* mosquitoes utilize a specialized excretory system comprised of the Malpighian ‘renal’ tubules (MTs) and the hindgut (Coast, 2007), functioning to counter disturbances to their haemolymph. The MTs, which are functional analogs of vertebrate kidneys, are responsible for the formation of primary urine (Coast, 2007), driven by the V-type

H<sup>+</sup>-ATPase (Wieczorek, 1992) that permits transport of Na<sup>+</sup> and K<sup>+</sup> cations across the membrane (Beyenbach, 2003) via a putative H<sup>+</sup>/cation exchanger (Wieczorek et al., 2009). The MTs are hormonally regulated by various diuretic factors, which in *A. aegypti* includes the biogenic amine 5-hydroxytryptamine (5HT) (Clark and Bradley, 1998; Veenstra, 1988), DH<sub>31</sub> (Coast et al., 2005), DH<sub>44</sub> (Clark et al., 1998; Clark et al., 1998), and kinin-like peptides (Lu et al., 2011; Pietrantonio et al., 2005). The primary urine then enters the hindgut, where it is further modified through secretory and reabsorptive processes. Here, we show that *Itp* knockdown increases excretion of urine, with *Itp-l* knockdown showing no influence, suggesting an anti-diuretic role for *AedaeITP*. Thus, it is likely that *AedaeITP* promotes water reabsorption in the hindgut similar to previous studies in *S. gregaria*. *SchgrITP* was found to stimulate chloride-dependent water reabsorption specifically in the ileum of the locust, promoting an increase in Na<sup>+</sup>, K<sup>+</sup> and Cl<sup>-</sup> transport (Audsley et al., 1992; Audsley et al., 2013). Interestingly, while *SchgrITP* promotes a reabsorptive role on ileal tissue, ITP-L did not display any stimulatory effect, instead inhibiting the stimulatory effect of synthetic ITP (Ring et al., 1998). A key step to understanding the ITP and ITP-L actions in the *Aedes* mosquito is to identify the unknown *A. aegypti* ITP receptor. The first presumed receptors for ITP and ITPL were characterized in the silkworm *Bombyx mori* (Nagai et al., 2014). Specifically, Nagai *et al.*, (2014) identified three *B. mori* orphan GPCRs as receptors for ITP and ITP-L, that all responded to recombinant ITP, with elevating levels of intracellular cGMP upon receptor binding (Nagai et al., 2014), which support the suggested ITP's mode of action on ileal ion transport involving this second messenger in *S. gregaria* (Audsley et al., 2013). In the locust, *SchgrITP* is proposed to bind to two different receptors, a G-protein coupled receptor and a membrane bound guanylate cyclase, on the ileal basolateral membrane, increasing both cyclic GMP (cGMP) and cyclic AMP (cAMP) levels, to regulate ion

and fluid transport (Audsley et al., 1992). cGMP stimulates  $\text{Cl}^-$  reabsorption and  $\text{H}^+$  secretion across the ileum, whereas cAMP stimulates  $\text{Na}^+$ ,  $\text{K}^+$ , and  $\text{Cl}^-$  reabsorption (Audsley et al., 1992). To further understand how these second messengers interact to regulate the physiological actions of *SchgrITP* on the ileum will require the ITP receptor(s) to be characterized.

### **Role of ITP and ITP-L in reproductive behaviour and success**

Female *A. aegypti* are day-biting mosquitoes, taking a single or multiple bloodmeals to obtain vitamins, nutrients, proteins, and minerals for egg development (Beyenbach, 2003). *AedaeItp-l* transcript levels were shown to increase 6 hours post-blood feeding, while *AedaeItp* levels remained unchanged. To elucidate whether the ITP and ITP-L signalling might be involved in reproduction, RNA interference was utilized to knockdown expression of *Itp* and *Itp-l* in adult *A. aegypti*. Overall, *AedaeItp* and *AedaeItp-l* knockdown female mosquitoes had a lower preference for blood feeding, laid fewer eggs, and had a reduced percentage of successful larvae hatching. In *T. castaneum*, ITP and ITP-L is required throughout all life stages and are essential for reproduction and offspring survival (Begum et al., 2009). Knockdown of both ITP and ITP-L resulted in dramatic decreases in egg numbers and in survival of eggs, with reduced ovaries that lack mature ovarioles in the ITPL knockdown females (Begum et al., 2009). In contrast, ITP knockdown females had fully developed ovaries, however showed reduced oviposition rates and offspring survival. It was suggested that these developmental defects in *T. castaneum* could be caused by a hormonal imbalance in ovarian development, or indirectly caused by mating deficiencies, preventing exposure to male ejaculatory products essential for completion of ovarian development (Begum et al., 2009).

In light of finding that *AedaeItp* and *Itp-l* knockdown resulted in fewer eggs laid by females mated with knockdown males, we predicted that transfer of sperm or sperm storage may be targeted. The regulation and entry of sperm into, protection within, and release from the storage organs (seminal vesicle in males, and spermathecae in females) requires both male and female-derived molecules (Avila et al., 2010; Avila et al., 2015; Schnakenberg et al., 2011). In male mosquitoes, spermatogenesis occurs in the paired testes, allowing for mature sperm cells, spermatozoa, to be synthesized (Rocco et al., 2017; Rocco et al., 2019) and transported to the seminal vesicles via the vas deferens (Clements, 2000; Oliva et al., 2014; Rocco and Paluzzi, 2016). During mating, male *A. aegypti* deposit sperm from the seminal vesicles into the female reproductive tract starting from the bursa and later stored in the spermathecae for long-term storage (Camargo et al., 2020; Degner and Harrington, 2016). Herein, the results revealed lower spermatozoa counts in testes and seminal vesicles of males with *Itp* and *Itp-l* knockdown. Thus, this data not only shows that *AedaeITP/ITP-L* knockdown reduces the incidence of blood feeding by females, but also that knockdown reduces the number of spermatozoa in male seminal vesicles and in the spermathecae of females, which ultimately results in fewer eggs laid and reduced larval hatching. It remains to be investigated exactly what role *AedaeITP* and *ITP-L* play in male and female reproduction or in blood feeding behaviour. However, given the already established roles of these neuropeptides in *T. castaneum* reproduction (Begum et al., 2009), it is possible that *AedaeITP* and *ITP-L* are similarly involved in regulation of male or female reproductive biology or mating behaviour, influencing successful mating and transfer of spermatozoa into the female *A. aegypti*. Recent evidence suggests *ITP* and *ITP-L* as multifunctional neuropeptides involved in metabolism, regulation of water and ion homeostasis, cuticle expansion and melanisation, and reproduction (Dirksen 2009; Yu et al., 2016; Gálíková

et al., 2018; Begum et al., 2009). The role in reproduction has been supported by ITPL expression in the *B. mori* male reproductive system with innervations of the accessory glands, the seminal vesicles, and the ejaculatory ducts (Klöcklerova, et al., 2023), all organs critical for successful mating and reproduction. ITPL expression has also been found in the seminal fluid of the brown plant hopper, *Nilaparvata lugens* (Yu et al., 2016), which is transferred to females during mating. Future research examining the signalling mechanism of *Aedae*ITP and ITP-L can allow for more detailed studies to unravel the actions of these neuropeptides in mosquito reproductive biology.

ITP and ITP-L peptides are highly homologous to the crustacean CHH peptides, which has been linked to molting, energy metabolism, immune defence, reproduction, and homeostatic regulation of osmotic and other stress responses (Sonobe et al., 2001; Webster et al., 2012). In insects, ITP stimulates fluid reabsorption and Cl<sup>-</sup>, Na<sup>+</sup>, and K<sup>+</sup> transport, while inhibiting secretion of H<sup>+</sup> in the ileum (Audsley et al., 1992; Meredith et al., 1996). In *Drosophila*, ITP plays an essential role in development and locomotion (Gáliková et al., 2018; Johard et al., 2009), and water homeostasis by protecting the fly from water loss by increasing thirst, reducing excretion rate, and promoting ingestion of water (Gáliková et al., 2018). Studies have also shown functions of ITP during ecdysis in *M. sexta* (Drexler et al., 2007), while ITP-L has been linked to ovarian maturation in *T. castaneum* (Begum et al., 2009) and wing expansion and cuticle melanism in *N. lugens* (Yu et al., 2016). Differences in the structure and cellular distribution patterns of ITP and ITP-L peptides suggest they may serve different biological functions. The results of this study expand upon our knowledge of ITP and ITP-L in insects, providing transcript expression profiles, insight into their cell-specific distribution, and reveal novel physiological roles for these neuropeptides in the *A. aegypti* mosquito. These findings also

contribute towards our understanding of *A. aegypti* reproductive biology, which is of great medical importance given the propensity of feeding on human hosts and their role as a disease vector. As such, these neuropeptides appear to function as signals for pleiotropic actions related to successful mosquito mating and reproduction, which could contribute towards development of novel strategies for decreasing vector fitness providing a better means for vector control.

## 6.6 References

- Audsley, N., Mcintosh, C., and Phillips, J. E.** (1992). Actions of ion-transport peptide from locust corpus cardiacum on several hindgut transport processes. *J. Exp. Biol.* **173**, 275–288.
- Audsley, N., Jensen, D., and Schooley, D. A.** (2013). Signal transduction for *Schistocerca gregaria* ion transport peptide is mediated via both cyclic AMP and cyclic GMP. *Peptides (N.Y.)* **41**, 74–80.
- Avila, F. W., Ram, K. R., Bloch Qazi, M. C., and Wolfner, M. F.** (2010). Sex peptide is required for the efficient release of stored sperm in mated *drosophila* females. *Genetics* **186**, 595–600.
- Avila, F. W., Mattei, A. L., and Wolfner, M. F.** (2015). Sex peptide receptor is required for the release of stored sperm by mated *Drosophila melanogaster* females. *J. Insect Physiol.* **76**, 1–6.
- Begum, K., Li, B., Beeman, R. W., and Park, Y.** (2009). Functions of ion transport peptide and ion transport peptide-like in the red flour beetle *Tribolium castaneum*. *Insect Biochem. Mol. Biol.* **39**, 717–725.
- Beyenbach, K. W.** (2003). Transport mechanisms of diuresis in Malpighian tubules of insects. *J. Exp. Biol.* **206**, 3845–3856.
- Calkins, T. L., and Piermarini, P. M.** (2015). Pharmacological and genetic evidence for gap junctions as potential new insecticide targets in the yellow fever mosquito, *Aedes aegypti*. *PloS One* **10**, e0137084.
- Camargo, C., Ahmed-Braimah, Y. H., Amaro, I. A., Harrington, L. C., Wolfner, M. F., and Avila, F. W.** (2020). Mating and blood-feeding induce transcriptome changes in the spermathecae of the yellow fever mosquito *Aedes aegypti*. *Sci. Rep.* **10**, 14899.

- Chen, H-Y., Toullec, J-Y., and Lee, C-Y.** (2020). The crustacean hyperglycemic hormone superfamily: progress made in the past decade. *Front. Endocrinol.* **11**, 578958.
- Clark, T. M., and Bradley, T. J.** (1998). Additive effects of 5-HT and diuretic peptide on *Aedes* Malpighian tubule fluid secretion. *Comp. Biochem. Physiol. Mol. Integr. Physiol.* **119**, 599–605.
- Clark, T. M., Hayes, T. K., and Beyenbach, K. W.** (1998). Dose-dependent effects of CRF-like diuretic peptide on transcellular and paracellular transport pathways. *Am. J. Physiol.* **274**, F834–F840.
- Clark, T. M., Hayes, T. K., Holman, G.M., Beyenbach, K. W.** (1998). The concentration-dependence of CRF-like diuretic peptide: mechanisms of action. *J. Exp. Biol.* **201**, 1753–1762.
- Coast, G.** (2007). The endocrine control of salt balance in insects. *Gen. Comp. Endocrinol.* **152**, 332–338.
- Coast, G. M., Garside, C. S., Webster, S. G., Schegg, K. M., and Schooley, D. A.** (2005). Mosquito natriuretic peptide identified as a calcitonin-like diuretic hormone in *Anopheles gambiae* (Giles). *J. Exp. Biol.* **208**, 3281–3291.
- Copenhaver, P. F., and Truman, J. W.** (1986). Metamorphosis of the cerebral neuroendocrine system in the moth *Manduca sexta*. *J. Comp. Neurol.* **249**, 186–204.
- Dai, L., Zitnan, D., and Adams, M. E.** (2007). Strategic expression of ion transport peptide gene products in central and peripheral neurons of insects. *J. Comp. Neurol.* **500**, 353–367.
- Degner, E. C., and Harrington, L. C.** (2016). A mosquito sperm's journey from male ejaculate to egg: mechanisms, molecules, and methods for exploration. *Mol. Reprod. Dev.* **83**, 897–911.

- Dircksen, H.** (2009). Insect ion transport peptides are derived from alternatively spliced genes and differentially expressed in the central and peripheral nervous system. *J. Exp. Biol.* **212**, 401–412.
- Dircksen, H., Tesfai, L. K., Albus, C., and Nässel, D. R.** (2008). Ion transport peptide splice forms in central and peripheral neurons throughout postembryogenesis of *Drosophila melanogaster*. *J. Comp. Neurol.* **509**, 23–41.
- Drexler, A. L., Harris, C. C., dela Pena, M. G., Asuncion-Uchi, M., Chung, S., Webster, S., and Fuse, M.** (2007). Molecular characterization and cell-specific expression of an ion transport peptide in the tobacco hornworm, *Manduca sexta*. *Cell Tissue Res.* **329**, 391–408.
- Durant, A. C., and Donini, A.** (2020). Ammonium transporter expression in sperm of the disease vector *Aedes aegypti* mosquito influences male fertility. *Proc. Natl. Acad. Sci. USA* **117**, 29712–29719.
- Endo, H., Nagasawa, H., and Watanabe, T.** (2000). Isolation of a cDNA encoding a CHH-family peptide from the silkworm *Bombyx mori*. *Insect Biochem. Mol. Biol.* **30**, 355–361.
- Gáliková, M., Dircksen, H., and Nässel, D. R.** (2018). The thirsty fly: ion transport peptide (ITP) is a novel endocrine regulator of water homeostasis in *Drosophila*. *PloS Genet.* **14**, e1007618.
- Homberg, U., Davis, N. T., and Hildebrand, J. G.** (1991). Peptide-immunocytochemistry of neurosecretory cells in the brain and retrocerebral complex of the sphinx moth *Manduca sexta*. *J. Comp. Neurol.* **303**, 35–52.
- Johard, H. A. D., Yoishii, T., Dircksen, H., Cusumano, P., Rouyer, F., Helfrich-Förster, C., and Nässel, D. R.** (2009). Peptidergic clock neurons in *Drosophila*: ion transport peptide

- and short neuropeptide F in subsets of dorsal and ventral lateral neurons. *J. Comp. Neurol.* **516**, 59–73.
- Keller, R.** (1992). Crustacean neuropeptides: structures, functions and comparative aspects. *Experientia* **48**, 439–448.
- Klöcklerova, V., Gálíková, Z., Roller, L., and Zitnan, D.** (2023). Differential expression of ITP and ITPL indicate multiple functions in the silkworm *Bombyx mori*. *Cell Tissue Res.* 10.1007/s00441-023-03752-y.
- Livak, K. J., and Schmittgen, T. D.** (2001). Analysis of relative gene expression data using real-time quantitative PCR and the 2(-delta delta C(T)) method. *Methods* **25**, 402–408.
- Lu, H. L., Kersch, C., and Pietrantonio, P. V.** (2011). The kinin receptor is expressed in the Malpighian tubule stellate cells in the mosquito *Aedes aegypti* (L.): a new model needed to explain ion transport? *Insect Biochem. Mol. Biol.* **41**, 135–140.
- Macins, A., Meredith, J., Zhao, Y., Brock, H. W., and Phillips, J. E.** (1999). Occurrence of ion transport peptide (ITP) and ion transport-like peptide (ITP-L) in orthopteroids. *Arch. Insect Biochem. Physiol.* **40**, 107–118.
- Meredith, J., Ring, M., Macins, A., Marschall, J., Cheng, N. N., Theilmann, D., Brock, H. W., and Phillips, J. E.** (1996). Locust ion transport peptide (ITP): primary structure, cDNA and expression in a baculovirus system. *J. Exp. Biol.* **199**, 1053–1061.
- Nagai, C., Mabashi-Asazuma, H., Nagasawa, H., and Nagata, S.** (2014). Identification and characterization of receptors for ion transport peptide (ITP) and ITP-like (ITPL) in the silkworm *Bombyx mori*. *J. Biol. Chem.* **289**, 32166–32177.

- Nässel, D. R., Pauls, D., and Huetteroth, W.** (2019). Neuropeptides in modulation of *Drosophila* behavior: how to get a grip on their pleiotropic actions. *Curr. Opin. Insect Sci.* **36**, 1–8.
- Oehler, E., Watrin, L., Larre, P., Leparc-Goffart, I., Lastäre, S., Valour, F., Baudouin, L., Mallet, H. P., Musso, D., and Ghawche, F.** (2014). Zika virus infection complicated by guillain-barré syndrome case report, French Polynesia, December 2013. *Eurosurveillance* **19**, 51–58.
- Oliva, C. F., Damiens, D., and Benedict, M. Q.** (2014). Male reproductive biology of *Aedes* mosquitoes. *Acta. Trop.* **132**, S12–S19.
- Paluzzi, J. P., Russell, W. K., Nachman, R. J., and Orchard, I.** (2008). Isolation, cloning, and expression mapping of a gene encoding an antidiuretic hormone and other CAPA-related peptides in the disease vector, *Rhodnius prolixus*. *Endocrinology* **149**, 4638–4646.
- Phillips, J. E., and Audsley, N.** (1995). Neuropeptide control of ion and fluid transport across locust hindgut. *Integr. Comp. Biol.* **35**, 503–514.
- Phillips, J. E., Meredith, J., Auosley, N., Richardson, N., Macins, A., and Ring, M.** (1998). Locust ion transport peptide (ITP): a putative hormone controlling water and ionic balance in terrestrial insects. *Am. Zool.* **38**, 461–470.
- Pietrantonio, P. V., Jagge, C., Taneja-Bageshwar, S., Nachman, R. J., and Barhoumi, R.** (2005). The mosquito *Aedes aegypti* (L.) leucokinin receptor is a multiligand receptor for the three *Aedes* kinins. *Insect Mol. Biol.* **14**, 55–67.
- Ring, M., Meredith, J., Wiens, C., Macins, A., Brock, H. W., Phillips, J. E., and Theilmann, D. A.** (1998). Expression of *Schistocerca gregaria* ion transport peptide (ITP) and its

- homologue (ITP-L) in a baculovirus/insect cell system. *Insect Biochem. Mol. Biol.* **28**, 51–58.
- Rocco, D. A., and Paluzzi, J. P.** (2016). Functional role of the heterodimeric glycoprotein hormone, GPA2/GPB5, and its receptor, LGR1: an invertebrate perspective. *Gen. Comp. Endocrinol.* **234**, 20–27.
- Rocco, D. A., Kim, D. H., and Paluzzi, J. P.** (2017). Immunohistochemical mapping and transcript expression of the GPA2/GPB5 receptor in tissues of the adult mosquito, *Aedes aegypti*. *Cell Tissue Res.* **369**, 313–330.
- Rocco, D. A., Garcia, A. S. G., Scudeler, E. L., dos Santos, D. C., Nóbrega, R. H., and Paluzzi, J. P.** (2019). Glycoprotein hormone receptor knockdown leads to reduced reproductive success in male *Aedes aegypti*. *Front. Physiol.* **10**, 266.
- Sajadi, F., Curcuruto, C., Al Dhaheri, A., and Paluzzi, J. P.** (2018). Anti-diuretic action of a CAPA neuropeptide against a subset of diuretic hormones in the disease vector, *Aedes aegypti*. *J. Exp. Biol.* **221**.
- Sajadi, F., Uyuklu, A., Paputsis, C., Lajevardi, A., Wahedi, A., Ber, L. T., Matei, A., Paluzzi, J. P.** (2020). CAPA neuropeptides and their receptor form an anti-diuretic hormone signaling system in the human disease vector, *Aedes aegypti*. *Sci. Rep.* **10**, <https://doi.org/10.1038/s41598-020-58731-y>.
- Schnakenberg, S. L., Matias, W. R., and Siegal, M. L.** (2011). Sperm-storage defects and live birth in *Drosophila* females lacking spermathecal secretory cells. *PLoS Biol.* **9**, e1001192.
- Schoofs, L., De Loof, A., and Van Hiel, M. B.** (2017). Neuropeptides as regulators of behavior in insects. *Annu. Rev. Entomol.* **62**, 35–52.

- Sonobe, H., Nishimura, T., Sonobe, M., Nakatsuji, T., Yanagihara, R., Kawakami, T., and Aimoto, S.** (2001). The molt-inhibiting hormone in the American crayfish *Procambarus clarkii*: its chemical synthesis and biological activity. *Gen. Comp. Endocrinol.* **121**, 196–204.
- Strand, M. R., Brown, M. R. and Vogel, K. J.** (2016). Mosquito peptide hormones: diversity, production, and function. *Adv. Insect Physiol.* **51**, 145–188.
- Sun, L., Zhang, Z., Zhang, R., Yu, Y., Yang, F., and Tan, A.** (2020). Molecular disruption of ion transport peptide receptor results in impaired water homeostasis and developmental defects in *Bombyx mori*. *Front. Physiol.* **11**, 424.
- Terhzaz, S., Cabrero, P., Robben, J. H., Radford, J. C., Hudson, B. D., Milligan, G., Dow, J. A. T., and Davies, S. A.** (2012). Mechanism and function of *drosophila* capa GPCR: A desiccation stress-responsive receptor with functional homology to human neuromedinu receptor. *PLoS One* **7**, e29897.
- Veenstra, J. A.** (1988). Effects of 5-hydroxytryptamine on the Malpighian tubules of *Aedes aegypti*. *J. Insect Physiol.* **34**, 299–304.
- Webster, S. G., Keller, R., and Dirksen, H.** (2012). The CHH-superfamily of multifunctional peptide hormones controlling crustacean metabolism, osmoregulation, moulting, and reproduction. *Gen. Comp. Endocrinol.* **175**, 217–233.
- Wieczorek, H.** (1992). The insect V-ATPase, a plasma membrane proton pump energizing secondary active transport: molecular analysis of electrogenic potassium transport in the tobacco hornworm midgut. *J. Exp. Biol.* **172**, 335–343.
- Wieczorek, H., Beyenbach, K. W., Huss, M., and Vitavska, O.** (2009). Vacuolar-type proton pumps in insect epithelia. *J. Exp. Biol.* **212**, 1611–1619.

**Yu, B., Li, D. T., Wang, S. L., Xu, H. J., Bao, Y. Y., and Zhang, C. X.** (2016). Ion transport peptide (ITP) regulates wing expansion and cuticle melanism in the brown planthopper, *Nilaparvata lugens*. *Insect Mol. Biol.* **25**, 778–787.

**Žitňan, D., Kingan, T. G., Kramer, S. J., and Beckage, N. E.** (1995). Accumulation of neuropeptides in the cerebral neurosecretory system of *Manduca sexta* larvae parasitized by the braconid wasp *Cotesia congregata*. *J. Comp. Neurol.* **356**, 83–100.

## 6.7 Supplementary Tables and Figures

**Table 6-S1: Gene-specific primer information used for amplification of *A. aegypti* *Itp* and *Itp-l* for RT-qPCR analysis, FISH probe synthesis and dsRNA synthesis.**

Oligo Name	Sequence (5' – 3')	Function	Product size
<i>Itp</i> & <i>Itp-l</i> qPCR F2	AATCGCACTGGTACCTCTGG	qPCR amplification of <i>Itp</i> & <i>Itp-l</i>	195bp ( <i>Itp</i> & <i>Itp-l</i> )
<i>Itp</i> qPCR R2	CCAAAACAGCCCTCTTTGCAG	qPCR amplification of <i>Itp</i>	
<i>Itp-l</i> qPCR R2	GTGAAGCACGACTTTTTGCAG	qPCR amplification of <i>Itp-l</i>	
<i>Itp</i> fish F	ATGTGTTCCCCGCAACTTAGCG	Initial amplification of <i>Itp</i> target for FISH	327bp
<i>Itp</i> fish R	TTACTTCTTCCCCAACATTT	Initial amplification of <i>Itp</i> target for FISH	
<i>Itp</i> fish F + T7	TAATACGACTCACTATAGGG/ ATGTGTTCCCCGCAACTTAGCG	Addition of T7 promoter sequence to <i>Itp</i> FISH target	
<i>Itp</i> fish R + T7	TAATACGACTCACTATAGGG/ TTACTTCTTCCCCAACATTT	Addition of T7 promoter sequence to <i>Itp</i> FISH target	
<i>Itp-l</i> fish F	CTTCACGACAGACTACTTCC	Initial amplification of <i>Itp-l</i> target for FISH	668bp
<i>Itp-l</i> fish R	CGTTCAAAGAATAAGCAATGG	Initial amplification of <i>Itp-l</i> target for FISH	
<i>Itp-l</i> fish F + T7	TAATACGACTCACTATAGGG/ CTTCACGACAGACTACTTCC	Addition of T7 promoter sequence to <i>Itp-l</i> FISH target	
<i>Itp-l</i> fish R + T7	TAATACGACTCACTATAGGG/ CGTTCAAAGAATAAGCAATGG	Addition of T7 promoter sequence to <i>Itp-l</i> FISH target	
<i>Itp</i> dsRNA F	GACTGAATCAAATATGTGTTCCCG	Amplification of ds <i>Itp</i> target	201bp
<i>Itp</i> dsRNA R	AACAACGAGTAGCAGTCTTCG	Amplification of ds <i>Itp</i> target	
<i>Itp-l</i> dsRNA F	CCAAACACGTTATAAGCAGCC	Amplification of ds <i>Itp-l</i> target	486bp
<i>Itp-l</i> dsRNA R	ACGTCAAGATTTCGGATGG	Amplification of ds <i>Itp-l</i> target	
<i>Egfp</i> dsRNA F	ACTCGTGACCACCCTGACCTACG	Amplification of ds <i>Egfp</i> target	324bp
<i>Egfp</i> dsRNA R	AGATCTTGAAGTTCACCTTGATGCC	Amplification of ds <i>Egfp</i> target	

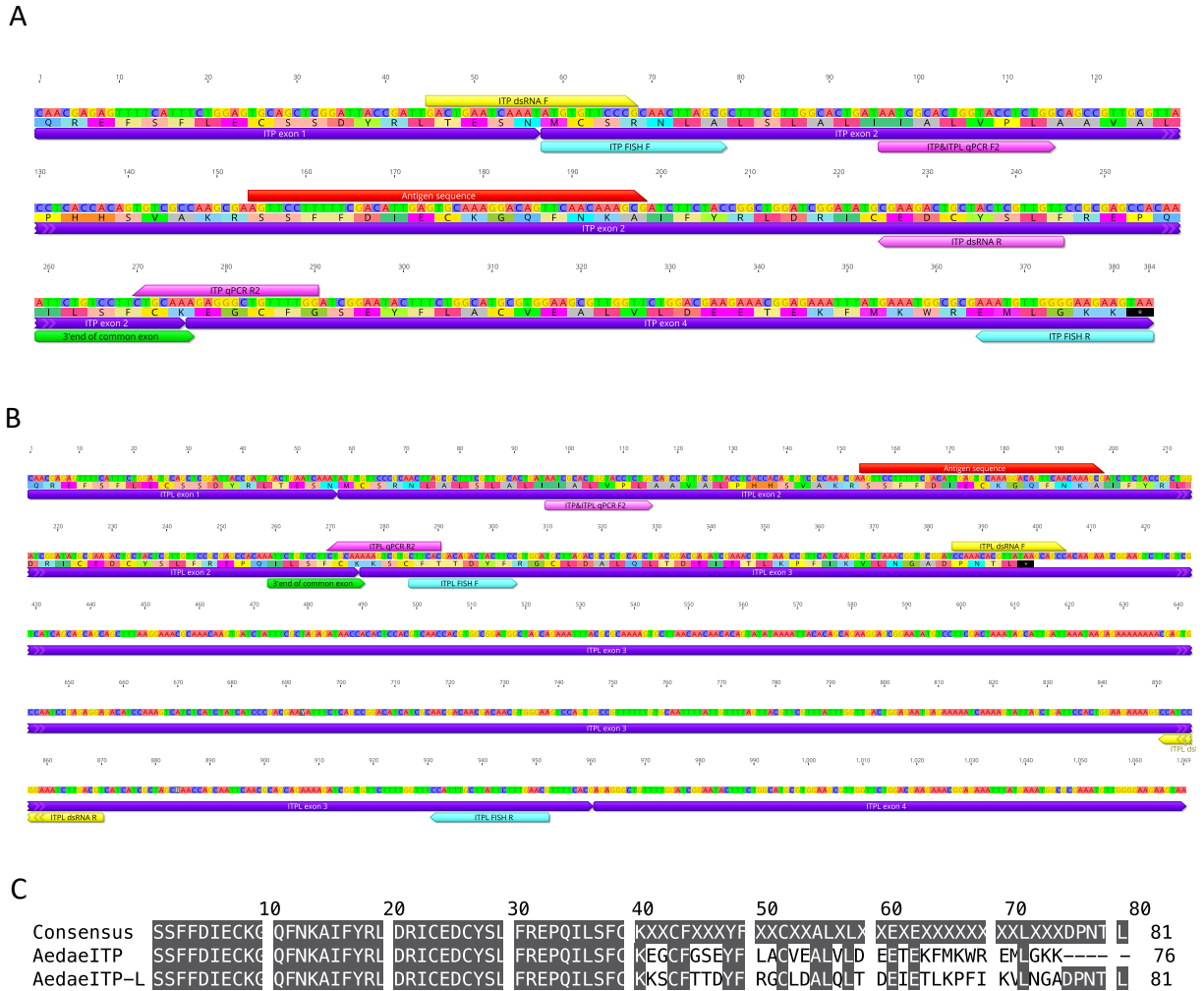


**Figure 6-S1. Primer sets mapped to *A. aegypti* *Itp* and *Itp-l* transcripts, and sequence alignment of *AedaeITP* and *AedaeITP-L* deduced peptides. (A) The *Itp* transcript coding sequence spans three exons, and (B) *Itp-l* spans four exons, denoted in purple. Targets for dsRNA synthesis included regions bracketed by primers shown in yellow, primers utilized for generation of the FISH probe template shown in blue, and qPCR analysis shown in pink. Amino acid region encoding the antigen target sequence of custom *AedaeITP*/*ITP-L* primary antisera is shown in red. The 3' end of common exon for *Itp* and *Itp-l* is shown in green. Top letters indicate nucleotides (positions of which are denoted by numbers above). Second panel of letter indicates the translated sequence. (C) Aligned amino acid sequences of *ITP* and *ITP-L* from *A. aegypti*, *ITP* (Genbank: AY950503), and *ITP-L* (Genbank: AY950506). Highlighting of residues indicates % identity with grey denoting 100% sequence identity.**

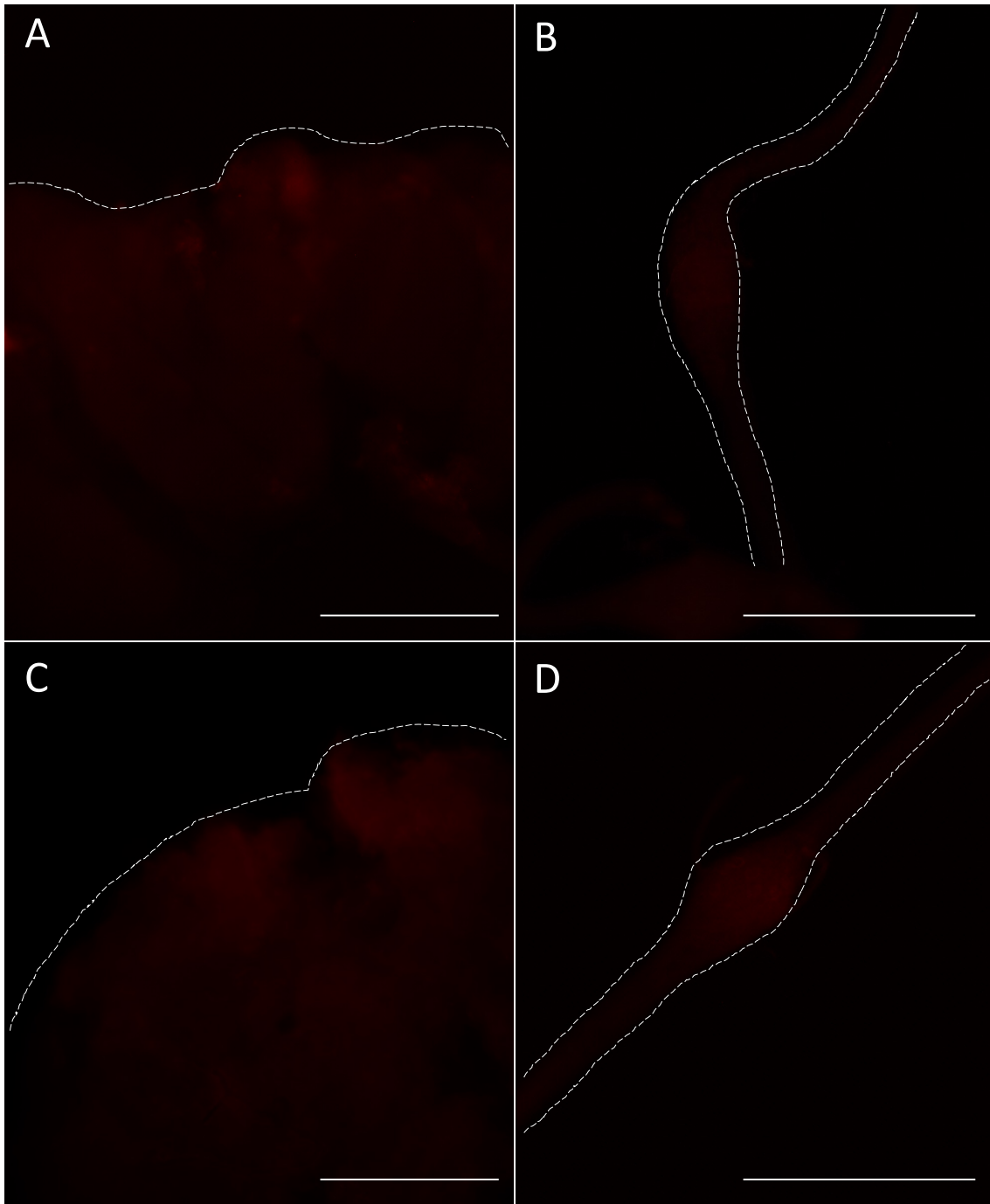


**Figure 6-S2. *Aedae*ITP and *Aedae*ITP-L preabsorbed controls and no primary controls.** Central nervous system tissues were incubated in either (A,B) anti-*Aedae*ITP/ITP-L primary antiserum preincubated with 10  $\mu$ M antigen or (C,D) no primary control. No staining was observed in the nervous tissues including the brain (A,C) or abdominal ganglia (B,D). Scale bars: (A,C) 200  $\mu$ M; (B,D) 100  $\mu$ M.

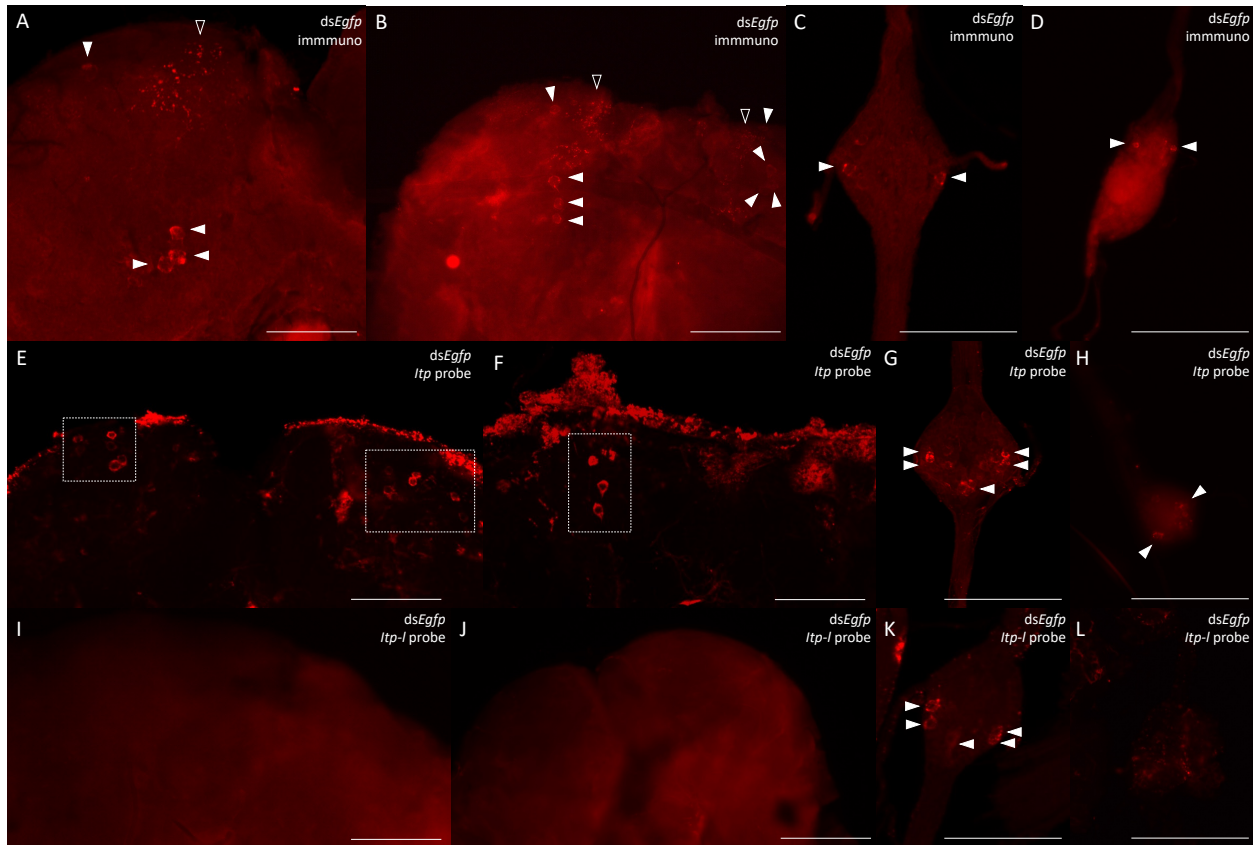


**Figure 6-S3. Immunolocalization and distribution of both *AedaeITP* and *AedaeITP-L* peptide and transcript in the central nervous system of adult *dsEgfp A. aegypti* mosquitoes.** *dsEgfp*-injected (A) male and (B) females reveals immunostaining in four pairs of neurosecretory cells (indicated by white arrowheads), with processes projecting anteriorly towards varicosities and blebs on the periphery of the brain (indicated by empty arrowheads). (C) Ventral view of abdominal ganglia and (D) terminal ganglion showing a single pair of lateral neurosecretory cells. Cell-specific distribution of *AedaeItp* and *AedaeItp-l* transcript in *dsEgfp*-injected (E) male and (F) female brain reveal six to seven pairs of cells in the anterior protocerebrum (G) two lateral pairs of cells, and a single medio-posterior cell in the abdominal ganglia, and (H) two lateral pairs of cells in the terminal ganglion with *AedaeItp* antisense probe. *AedaeItp-l* antisense probe showed no staining in *dsEgfp*-injected (I) male and (J) female brain (L) terminal ganglion and (K) two lateral pairs of cells, and a single medio-posterior cell in the abdominal ganglia. Scale bars: (A,B,E,F,I,J) 200  $\mu$ M; (C,D,G,H,K,L) 100  $\mu$ M.

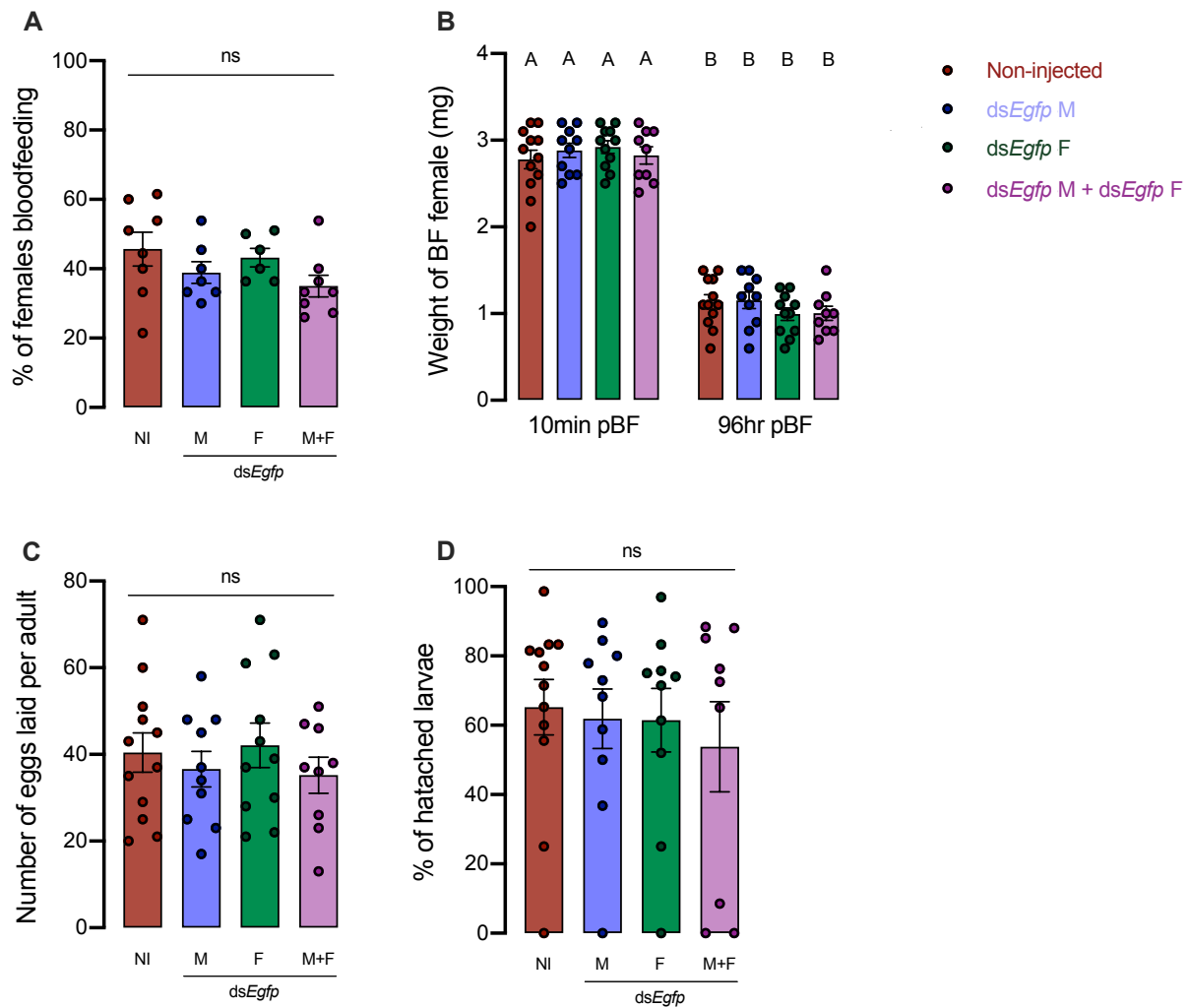


**Figure 6-S4. Effect of control *dsEgfp* on blood-feeding, egg laying, and larval hatching (egg viability) in comparison to non-injected adult *A. aegypti*.** The effect of control *dsEgfp* knockdown was tested on (A) preference for blood-feeding, (B) weight of blood-fed female before and after egg-laying, (C) number of eggs laid, and (D) percentage of larval hatching. Abbreviations: male (M) and female (F). Data labeled with different letters are significantly different from non-injected adults (mean±SEM; one-way ANOVA with Bonferroni multiple comparison,  $p < 0.05$ ,  $n = 6-12$  mating replicates, each point represents individual replicate values), (ns denotes no statistical significance).

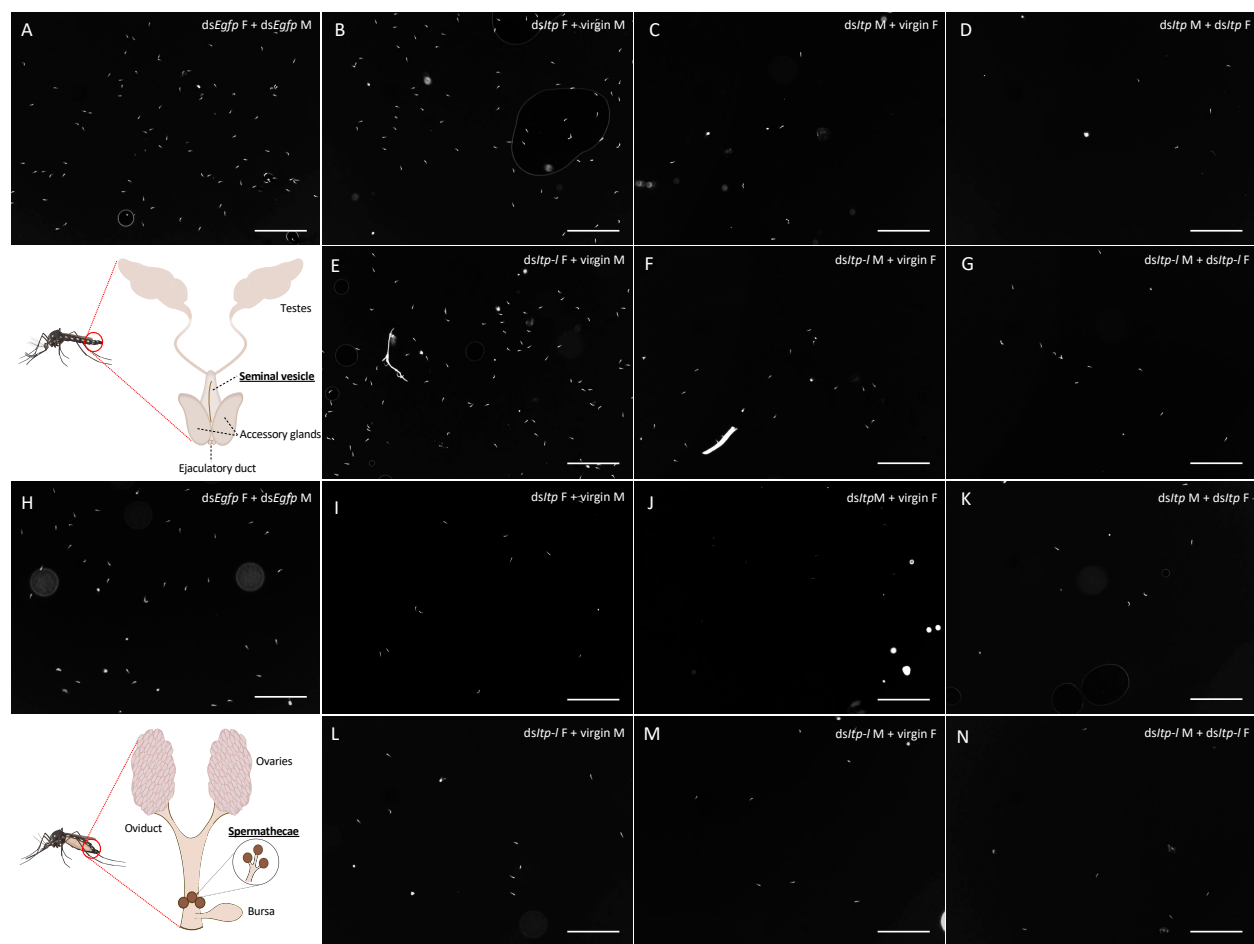


**Figure 6-S5. Representative images of immunofluorescent nuclei of total spermatozoa in the male seminal vesicle and female spermathecae of adult *A. aegypti* following RNAi (dsRNA)-mediated knockdown of *AedaeItp* or *AedaeItp-I*.** Images of immunofluorescent nuclei (DAPI) from fixed spermatozoa in 1  $\mu$ l droplet of DPBS with sperm from the seminal vesicle (A-G) and spermatheca (H-N) of ds*AedaeItp* or ds*AedaeItp-I* injected animals from different mating treatments. Abbreviations: male (M) and female (F). Scale bar: 200  $\mu$ m.

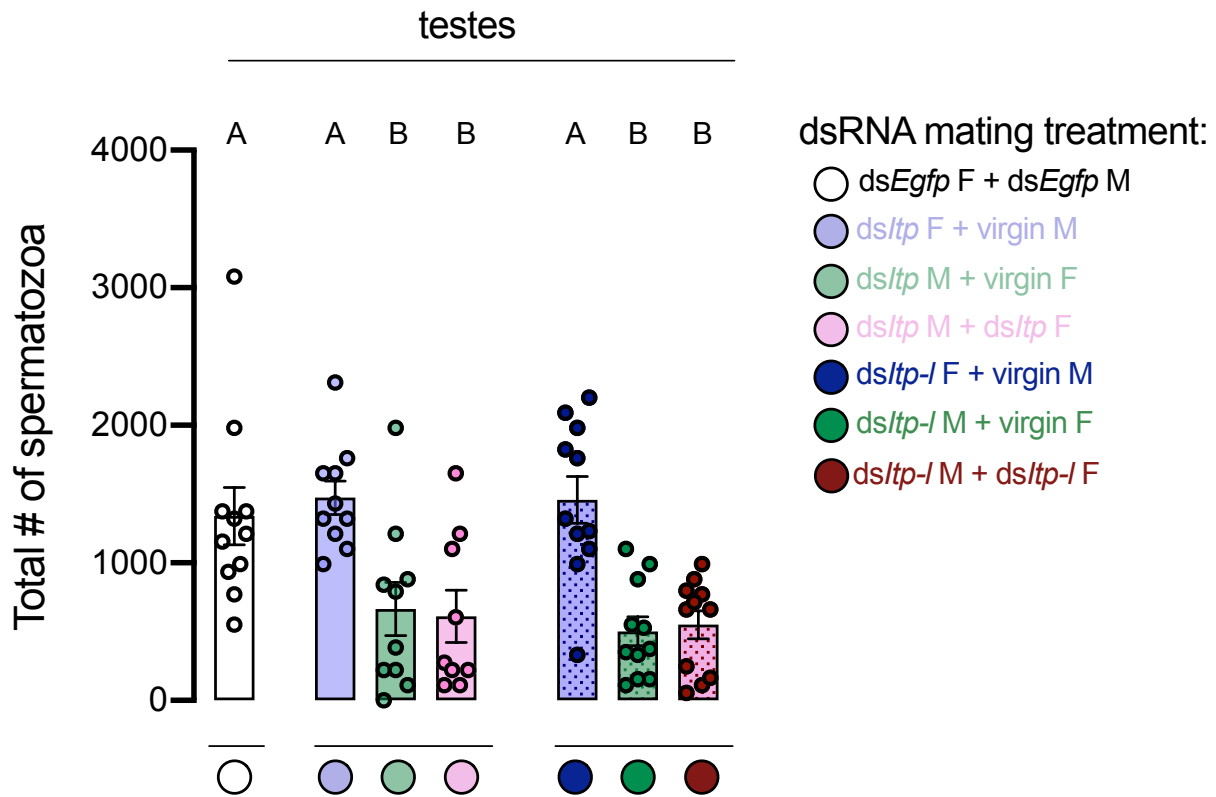


**Figure 6-S6. Total spermatozoa in the testes of adult male *A. aegypti* following RNAi (dsRNA)-mediated knockdown of *AedaeItp* or *AedaeItp-l*.** Number of spermatozoa within the testes of adults four-days post ds*AedaeItp* or ds*AedaeItp-l* injection. Abbreviations: male (M) and female (F). Data labeled with different letters are significantly different from control, ds*Egfp* adults (mean±SEM; one-way ANOVA with Bonferroni multiple comparison,  $p < 0.05$ ,  $n = 9-11$  mating replicates, each point represents individual replicate values).

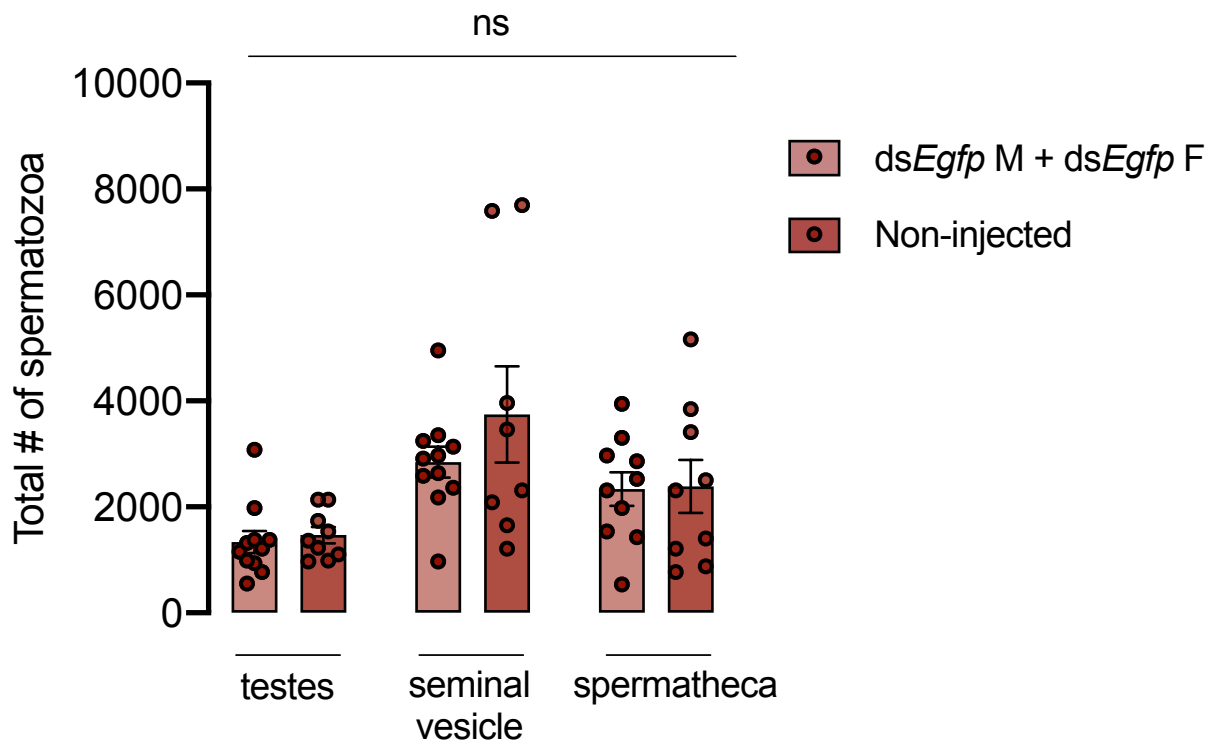


**Figure 6-S7. Total spermatozoa in the male testes and seminal vesicle and female spermathecae of adult *A. aegypti* following *dsEgfp* injection.** Number of spermatozoa per adult four-days post *dsEgfp* injection and non-injected four-day old adults (mean± SEM; one-way ANOVA with Bonferroni multiple comparison,  $p < 0.05$ ,  $n = 8-11$  mating replicates, each point represents individual replicate values), (ns denotes no statistical significance).

## **Chapter Seven**

### **Conclusions and future directions**

## 7.1 Summary

At the beginning of this research, relatively little was known about the anti-diuretic signalling mechanism and downstream cellular targets in the adult *Aedes aegypti* mosquito. While a plethora of studies have investigated the process of hydromineral balance in terrestrial insects focusing on diuretic regulation (Beyenbach, 2003; Beyenbach et al., 1993; Coast et al., 2005; Paluzzi et al., 2012; Terhzaz et al., 2012; Veenstra, 1988), several gaps existed in our understanding of anti-diuretic hormone control. Studies in blood feeding insects, including *Aedes* mosquitoes (Ionescu and Donini, 2012) and *Rhodnius prolixus* (Paluzzi and Orchard, 2006; Paluzzi et al., 2012) introduced CAPA peptides as anti-diuretic hormones involved in inhibiting diuretic-stimulated diuresis, but little was known of the exact mechanism and cellular effectors targeted in CAPA-mediated inhibition in adult female mosquitoes. Further investigating the precise regulatory mechanisms of diuresis and anti-diuresis offered an avenue of research to better understand the neuroendocrine control of hydromineral balance of the female *A. aegypti*, a potent disease vector. The collection of studies presented in this dissertation expands on the knowledge of neuropeptide regulation of mosquito physiology, providing a more profound understanding of the diuretic/anti-diuretic signalling system in the adult disease vector, *A. aegypti* mosquito. A summary of the major findings related to the aims and objectives outlined in the introductory chapter of this dissertation are described below.

### 7.1.1 An anti-diuretic role for CAPA neuropeptides against select diuretic factors

In larval *Aedes* Malpighian ‘renal’ tubules (MTs), CAPA peptides were previously shown to elicit an anti-diuretic role against 5HT-stimulated MTs by activating the nitric oxide synthase (NOS)/ cyclic GMP (cGMP)/ protein kinase G (PKG) pathway (Ionescu and Donini, 2012). In adult MTs, a similar approach involving bioassays, electrophysiology and immunohistochemistry was utilized to establish the role of CAPA peptides (Chapter 1; Sajadi and Paluzzi, 2021; Chapter 2; Sajadi et al., 2018), elucidate the signalling mechanism (Chapter 3; Sajadi et al., 2020), and identify the downstream cellular targets (Chapter 4). The neuropeptide *Aedae*CAPA-1 was found to elicit a selective anti-diuretic role, inhibiting calcitonin-like diuretic hormone 31 (DH<sub>31</sub>)- and 5-hydroxytryptamine (5HT)-stimulated secretion, whilst having no effect on other diuretic factors, including kinin-related peptides and corticotropin-releasing factor-like (CRF) diuretic-related hormones (DH<sub>44</sub>) (Chapter 2; Sajadi et al., 2018). Interestingly, despite the strong anti-diuretic role of *Aedae*CAPA-1, the relative proportions of cations transported remained unaffected, thus maintaining the natriuretic activity of DH<sub>31</sub> and kaliuretic activity of 5HT (Chapter 2; Sajadi et al., 2018). Even more surprising was the observation that although *Aedae*CAPA-1 exhibited no influence on kinin-stimulated secretion, application of cGMP resulted in an inhibition of kinin-mediated secretion (Chapter 2; Sajadi et al., 2018), corroborating with previous reports of cGMP inhibiting depolarization induced in kinin-stimulated MTs (Ruka et al., 2013). This supports the potential of an additional anti-diuretic hormone targeting stellate cells in the MTs or the existence of gap junctions linking the signalling between principal and stellate cells (Beyenbach and Piermarini, 2011). Looking further into the signalling mechanism involved, pharmacological inhibition of NOS and PKG abolished the anti-diuretic activity of *Aedae*CAPA-1-mediated inhibition of DH<sub>31</sub>-stimulated

MTs, while only PKG inhibition mitigated the effects of *Aedae*CAPA-1 in 5HT-stimulated secretion (Chapter 3; Sajadi et al., 2020), indicating that some differences in signalling associated with different diuretic hormones may occur.

A closer investigation into the *Aedae*CAPA-1 signalling cascade and critical role of the V-type H<sup>+</sup>-ATPase (VA) in fluid secretion led to the hypothesis that the VA serves as a primary target for both diuretic and anti-diuretic hormonal regulation of the insect MTs (Chapter 4). VA inhibition reduced 5HT- and DH<sub>31</sub>-stimulated secretion, causing alkalinization of the secreted fluid (Chapter 4), with no effect observed in DH<sub>44</sub>-stimulated MTs (Chapter 4). Importantly, activity of the VA was increased in DH<sub>31</sub>-treated tubules in line with role of this hormone as a potent natriuretic diuretic hormone (Coast et al., 2005; Chapter 2; Sajadi et al., 2018). In contrast, augmented VA activity was abolished in *Aedae*CAPA-1-treated tubules as further evidenced by inhibition of the NOS/cGMP/PKG pathway (Chapter 4). Based on earlier findings in the tobacco hornworm, *Manduca sexta* (Sumner et al., 1995) and yeast, *Saccharomyces cerevisiae* (Kane, 1995), the mechanism of VA regulation was examined, specifically involving the reversible disassembly of the V<sub>1</sub> complex from the holoenzyme (Weng et al., 2003). Higher V<sub>1</sub> protein abundance and apical localization was observed in membrane fractions of DH<sub>31</sub>-treated MTs, whereas in *Aedae*CAPA-1-treated MTs, increased V<sub>1</sub> protein abundance was observed in cytosolic fractions where dispersed immunoreactivity was observed suggesting VA holoenzyme disassociation (Chapter 4). Taken together, these findings reveal a major target in hormone-mediated regulation of MTs, presenting the first reported evidence of anti-diuretic hormone control of the VA in insect tubules. CAPA peptides have been shown to inhibit MTs in *Manduca sexta* (Quinlan et al., 1997), *Tenebrio molitor* (Eigenheer et al., 2002; Eigenheer et al., 2003), *R. prolixus* (Paluzzi and Orchard, 2006; Paluzzi et al., 2012), *D. melanogaster* (Rodan et

al., 2012; MacMillan et al., 2018), and *A. aegypti* (Ionescu and Donini, 2012), and stimulate MTs in *D. melanogaster* (Terhzaz et al., 2012), *Bombyx mori* (Halberg et al., 2015), *Vespula vulgaris* (Halberg et al., 2015), *Gryllus assimilis* (Halberg et al., 2015), and *A. aegypti* (Pollock et al., 2004). Evidently, species-specific and dose-dependent effects of CAPA neuropeptides have been reported in various insect species, suggesting the physiological effects of receptor activation are subject to diversification (Halberg et al., 2015). Indeed, these findings contradict the fellow dipteran, *D. melanogaster*, and establish a true anti-diuretic signalling system in adult female *A. aegypti* mosquito.

### **7.1.2 Diuretic and anti-diuretic signalling systems: importance of neuropeptides and their cognate receptors**

Findings in this research demonstrate the importance of distinct receptor signalling systems in eliciting diuretic and anti-diuretic control in the female mosquito. Characterization of the *Aedes* CAPA receptor confirmed high specificity to mosquito CAPA neuropeptides (Chapter 3; Sajadi et al., 2020), while receptor knockdown abolished CAPA-induced anti-diuretic control of DH<sub>31</sub>-stimulated MTs (Chapter 3; Sajadi et al., 2020). Remarkably, CAPA neuropeptides, which are produced within a pair of neurosecretory cells in each abdominal ganglia (Chapter 3; Sajadi et al., 2020), are released into the female haemolymph 15-30 minutes post-blood feeding (Chapter 5), bind to its cognate receptor localized exclusively to the principal cells in the MTs (Chapter 3; Sajadi et al., 2020), to hinder DH<sub>31</sub>-mediated secretion (Chapters 2-5; Sajadi et al., 2018; Sajadi et al., 2020). On the other hand, *Aedae*DH<sub>31</sub>-R, which was earlier molecularly characterized and localized to the principal cells of the MTs (Kwon et al., 2012), was confirmed to be selective to mosquito DH<sub>31</sub> (Chapter 5). This study utilized the heterologously expressed *Aedae*DH<sub>31</sub>-R demonstrating DH<sub>31</sub> release into the female haemolymph immediately post-

bloodmeal, with highest levels observed at 5 minutes, and a decline in titres at 15-30 minutes post-feeding (Chapter 5). This immediate high release of DH<sub>31</sub> into the haemolymph is an impressive feat as it correlates with the large water and salt volume ingested during a bloodmeal (Beyenbach, 2003), thus, necessary for eliminating these elements via rapid natriuresis which is observed during peak phases of diuresis (10-15 minutes post-feeding) (Williams et al., 1983). Further evidence of *in vivo* release of DH<sub>31</sub> and CAPA neuropeptides comes from the findings that VA holoenzyme assembly and V<sub>1</sub> protein membrane localization is observed between 10 to 30 min post-blood feeding, with VA disassembly occurring by 60 mins, coinciding with the timing release of both DH<sub>31</sub> and CAPA neuropeptides as determined through this research (Chapter 4). Collectively, these findings further uncover the complex regulatory mechanisms occurring after a female ingests a bloodmeal, allowing them to confront the threat to their haemolymph homeostasis, which contributes towards their successful adaptation of blood feeding.

### **7.1.3 Characterization and novel roles for ITP and ITP-L neuropeptides in *A. aegypti***

In insects, the ion transport peptide (ITP) and ITP-like or ITP-long (ITP-L) are implicated in fundamental processes such as anti-diuretic control of the locust hindgut, ovarian maturation in *Tribolium castaneum*, and in thirst/excretion and clock neuron modulation in *D. melanogaster* (Begum et al., 2009; Drexler et al., 2007; Gálíková et al., 2018; Johard et al., 2009). In *A. aegypti*, *AedaeITP* is expressed in the brain of both adult male and female mosquitoes, with *AedaeItp* transcript synthesized in a cluster of six to seven pairs of cells in the anterior region of the brain and stored and released within four pairs of neurosecretory cells in the anterior and medial regions of the brain of the brain (Chapter 6). In contrast, *AedaeITP-L* is expressed in the

abdominal ganglia, specifically to a pair of medial neurosecretory cells (protein) and two pairs and a single neurosecretory cell (transcript) in each ganglia, apart from the terminal ganglion where *AedaeITP* is expressed (Chapter 6). Similar expression patterns were observed in other species, including *T. castaneum* with *Itp* expression in five pairs of brain cells and a pair of cells in the abdominal terminal ganglion (Begum et al., 2009). In *D. melanogaster*, ITP expression was observed in four pairs of brain cells (Dirksen et al., 2008), whereas relatively weak to absent ITP-L staining is observed in the brain, with higher expression and abundance in the ventral ganglia and peripheral tissues of the locust (Meredith et al., 1996; Phillips and Audsley, 1995). Remarkably, this research identified several novel roles for *AedaeITP* and *AedaeITP-L* in *A. aegypti*. Firstly, this research showed ITP and/or ITP-L may function in feeding/starvation since transcript levels of both *AedaeItp* and *AedaeItp-l* increase after 48 hours of starvation and water deprivation in adult mosquitoes, while only *AedaeItp-l* transcript abundance increases in blood fed females, specifically 6 hours post-feeding. Secondly, ITP and ITP-L may also participate in anti-diuretic control of ionoregulation since RNAi-mediated knockdown of *AedaeItp* results in greater urine excretion rates. Thirdly, this research also revealed that ITP and/or ITP-L may modulate reproductive behaviour and success, as *AedaeItp* and *AedaeItp-l* knockdown animals resulted in reduced preference for blood feeding (females only), reduced egg-laying and larval hatching (Chapter 6). Additionally, this is the first instance that ITP and ITP-L has been implicated in regulation or storage of sperm within the spermathecae and/or seminal vesicle in insects. In addition to *A. aegypti*, studies in other insect taxa have established roles of ITP and ITP-L in reproduction, including suggested roles in ovarian development in *T. castaneum* (Begum et al., 2009), successful mating and reproduction in *Bombyx mori* (Klößlerova, et al., 2023), and in sperm transfer in *Nilaparvata lugens* (Yu et al., 2016). These

findings suggest a more complex function of these neuropeptides in regulating mosquito reproduction, evidenced by lower spermatozoa count in *AedaeItp* and *AedaeItp-l* knockdown male testes and seminal vesicles and in female spermathecae (Chapter 6). Oogenesis (process of egg development) in female mosquitoes is coordinated by several well-characterized endocrine signalling pathways including ecdysteroids, juvenile hormone, ovary ecdysteroidogenic hormone, and insulin-like peptides (Raikhel and Lea 1990; Brown and Cao, 2001; Raikhel et al., 2005; Gulia-Nuss et al., 2012, 2015; Dhara et al., 2013; Hansen et al., 2014). In contrast, endocrine control of spermatogenesis (process of sperm development) is not well understood. While a recent study has implicated a glycoprotein hormone, GPA2/GPB5 (Rocco et al., 2019), in male reproductive-related processes, hormonal regulation of successful mating and transfer of sperm remain unexplored. These findings implicate ITP and ITP-L as additional regulators in successful reproductive mating and behaviour in both male and female mosquitoes. Regulation of *A. aegypti* reproductive biology remains an understudied avenue, and while the functional roles of *AedaeITP* and *AedaeITP-L* remain in their infancy, these findings provide novel insights into the neuropeptidergic regulation of male and female reproduction.

## 7.2 Future Directions

In the past few decades, there has been major advances in our understanding of neuroendocrine control of insect diuresis and transepithelial transport, transforming previous notions of anti-diuretic control in Malpighian tubules. The present studies provided important insight into the signalling mechanisms and transporters involved post-blood feeding, a critical process leading to transmission of several viruses (Jentes et al., 2011; Leparac-Goffart et al., 2014; Oehler et al., 2014; Simmons et al., 2012) (Figure 7-1). This work has also characterized

the first anti-diuretic receptor signalling system in the *Aedes* mosquito, revealing the importance of both diuretic and anti-diuretic hormone release in the female mosquito. Additionally, this dissertation provides insight into the *Aedes* ITP and ITP-L peptides providing a molecular characterization, immunolocalization and distribution within the nervous system, as well as evidence for putative physiological functions including novel roles in mosquito reproductive biology.

To completely understand the regulation of the VA in CAPA-mediated inhibition, identification of the specific regulation initiating disassembly of the holoenzyme is necessary. The VA plays an essential role in cell function in both vertebrates and invertebrates (Harvey et al., 1998), and while the reversible assembly/disassembly of the VA holoenzyme has been studied, it remains unclear what mechanism initiates the disassembly of the  $V_1$  complex from the holoenzyme (Dschida and Bowman, 1995; Weng et al., 2003), and what VA subunit is targeted in this disassembly. Upon dissociation of the  $V_1$  complex, subunit C is released from the complex (Gräf et al., 1996; Kane, 1995; Merzendorfer et al., 1999; Vitavska et al., 2003), suggesting a central role in holoenzyme assembly/disassembly. Subunit C binds to subunits E and G of the  $V_1$  complex, and to subunit a of the  $V_o$  complex, bridging the two complexes together (Inoue and Forgac, 2005) and serving as a good candidate for modulating VA stability. In yeast, the cAMP/PKA pathway is proposed to be involved in the reversible dissociation of the VA; however, it is still unknown on whether an active PKA enhances the reassembly or prevents dissociation of the VA (Wieczorek et al., 2009). Additionally, future research should examine the involvement of a PKA-dependent or -independent pathway leading to the activation and inactivation of the VA in the insect MTs. Considerable studies have established PKA as a major cAMP target (Seino and Shibasaki, 2005), however, our results revealed a PKA-dependent

secretory pathway for DH<sub>31</sub> and PKA-independent for DH<sub>44</sub>. While both peptides elicit stimulatory actions through cAMP, future studies should focus on investigating distinct cAMP pathways involving PKA to provide more insight on the precise regulatory action of the VA.

While this research has laid the groundwork for putative functions in the *Aedes* mosquito, it is of great interest to identify and characterize the *A. aegypti* ITP and ITP-L receptor. Continued work in this area would provide a more comprehensive understanding of the roles of *AedaeITP* and *AedaeITP-L* through detecting receptor expression to uncover additional targets of ITP and ITP-L action. The first presumed ITP and ITPL receptors were characterized in *B. mori*, with elevating levels of intracellular cGMP upon binding of recombinant ITP (Nagai et al., 2014). More broadly, future studies should investigate the existence of multiple receptors for ITP and ITP-L activation, given the clear evidence of differential expression and functional roles of both peptides. Several functions have been suggested for ITP and ITP-L peptides in insects, including roles in ionoregulation (Audsley et al., 1992; Dirksen et al., 2008; Drexler et al., 2007; Nagai et al., 2014; Webster et al., 2012; Yu et al., 2016), development and locomotion (Gáliková et al., 2018; Johard et al., 2009), and ovarian maturation (Begum et al., 2009). Finally, while novel putative roles for ITP and ITP-L have been linked to mosquito reproduction, further research needs to examine the exact mechanisms of *AedaeITP* and *AedaeITP-L* action in blood feeding behaviour, in the regulation of mating along with the storage and transfer of spermatozoa in both male and female *A. aegypti* mosquitoes. Future studies examining ITP and ITP-L signalling may provide important insights into these neuropeptides in relation to mosquito reproductive biology.

In summary, the results presented in this dissertation unravel the importance of diuretic (DH<sub>31</sub>, 5HT, DH<sub>44</sub>, and kinin-like peptides) and anti-diuretic hormones (CAPA) on *A. aegypti*

MTs regulating iono- and osmoregulation. Challenges to haemolymph homeostasis as a consequence of ingesting bloodmeals initiates the release of the natriuretic hormone (DH<sub>31</sub>) from the nervous system to eliminate the excess salts and water. Once a large portion of the water and NaCl load has been dealt with by the excretory organs, the current study revealed that anti-diuretic CAPA neuropeptides are released acting to hinder the actions of DH<sub>31</sub> through the NOS/cGMP/PKG pathway and targeting the V-type H<sup>+</sup>-ATPase. Moreover, the alternatively spliced peptides, ITP and ITP-L that in other species have been identified as critical regulators of the insect excretory system, have been linked to a variety of physiological processes including feeding/starvation, urine excretion, and possibly the maintenance, transfer, and storage of spermatozoa during mating and ultimately successful egg fertilization. Collectively, these observations raise the notion that the *A. aegypti* mosquito ITP and ITP-L have pleiotropic roles as observed for these neuropeptides in other insects.

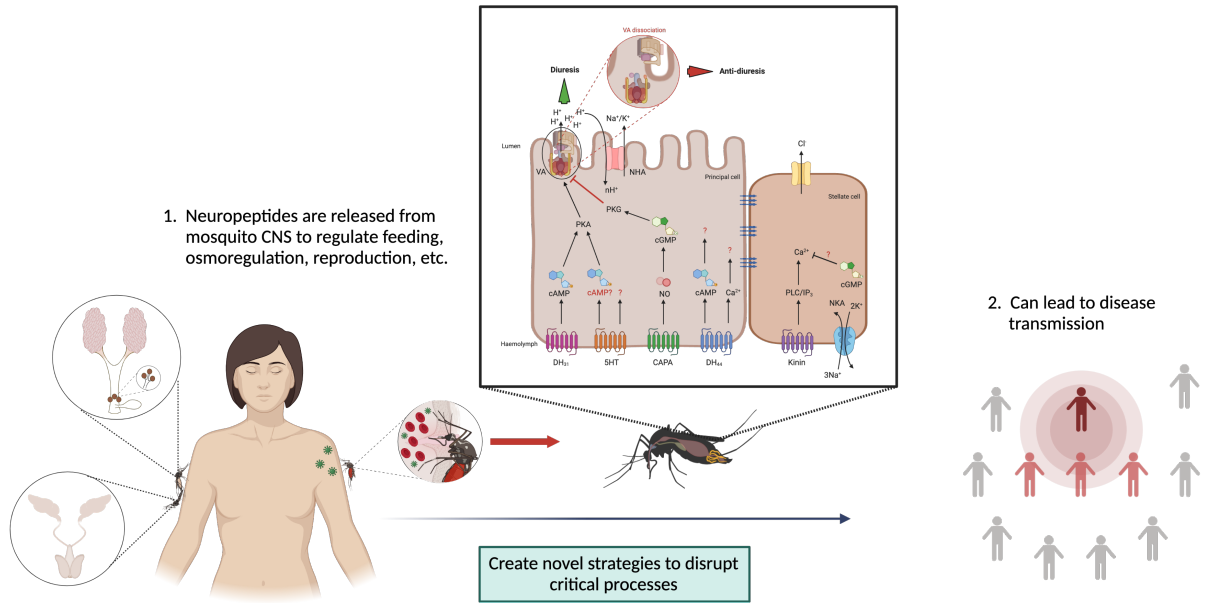


**Figure 7-1. Summary of research findings and overall impact to global society.** Findings of this research highlight the (1) importance of neuropeptides and their receptors in regulating critical physiological processes, including blood-feeding, osmoregulation, and reproduction. Post-blood feeding, diuretic and anti-diuretic factors are released into the female haemolymph, coupling through various signaling mechanisms to challenge the osmotic stress from the hypo-osmotic bloodmeal. Female mosquitoes obtain essential proteins and nutrients required for egg production, allowing them to oviposit 3-4 days post-bloodmeal. (2) These critical physiological events ultimately allow for the successful breeding and disease transmission of the *A. aegypti* vector.

### 7.3 References

- Audsley, N., Mcintosh, C., and Phillips, J. E.** (1992). Actions of ion-transport peptide from locust corpus cardiacum on several hindgut transport processes. *J. Exp. Biol.* **173**, 275–288.
- Begum, K., Li, B., Beeman, R. W., and Park, Y.** (2009). Functions of ion transport peptide and ion transport peptide-like in the red flour beetle *Tribolium castaneum*. *Insect Biochem. Mol. Biol.* **39**, 717–725.
- Beyenbach, K. W.** (2003). Transport mechanisms of diuresis in Malpighian tubules of insects. *J. Exp. Biol.* **206**, 3845–3856.
- Beyenbach, K. W., Oviedo, A., and Aneshansley, D. J.** (1993). Malpighian tubules of *Aedes aegypti*: five tubules, one function. *J. Insect Physiol.* **39**, 639–648.
- Beyenbach, K. W., and Piermarini, P. M.** (2011). Molecular physiology of Malpighian tubules. *Acta. Physiol.* **202**, 387–407.
- Brown, M. R., and Cao, C.** (2001). Distribution of ovary ecdysteroidogenic hormone I in the nervous system and gut of mosquitoes. *J. Insect Sci.* **3**, doi: 10.1672/1536-2442(2001)001.
- Coast, G. M., Garside, C. S., Webster, S. G., Schegg, K. M., and Schooley, D. A.** (2005). Mosquito natriuretic peptide identified as a calcitonin-like diuretic hormone in *Anopheles gambiae* (Giles). *J. Exp. Biol.* **208**, 3281–3291.
- Dhara, A., Eum, J. H., Robertson, A., Gulia-Nuss, M., Vogel, K. J., Clark, K. D., Graf, R., Brown, M. R., and Strand, M. R.** (2013). Ovary ecdysteroidogenic hormone functions independently of the insulin receptor in the yellow fever mosquito, *Aedes aegypti*. *Insect Biochem. Mol. Biol.* **43**, 1100–1108.

- Dircksen, H., Tesfai, L. K., Albus, C., and Nässel, D. R.** (2008). Ion transport peptide splice forms in central and peripheral neurons throughout postembryogenesis of *Drosophila melanogaster*. *J. Comp. Neurol.* **509**, 23–41.
- Drexler, A. L., Harris, C. C., dela Pena, M. G., Asuncion-Uchi, M., Chung, S., Webster, S., and Fuse, M.** (2007). Molecular characterization and cell-specific expression of an ion transport peptide in the tobacco hornworm, *Manduca sexta*. *Cell Tissue Res.* **329**, 391–408.
- Dschida, W. J. A., and Bowman, B. J.** (1995). The vacuolar ATPase: sulfite stabilization and the mechanism of nitrate inactivation. *J. Biol. Chem.* **270**, 1557–1563.
- Eigenheer, R. A., Nicolson, S. W., Schegg, K. M., Hul, J. J., and Schooley, D. A.** (2002). Identification of a potent antidiuretic factor acting on beetle Malpighian tubules. *Proc. Natl. Acad. Sci. USA* **99**, 84–89.
- Eigenheer, R. A., Wiehart, U. M., Nicolson, S. W., Schoofs, L., Schegg, K. M., Hull, J. J., and Schooley, D. A.** (2003). Isolation, identification and localization of a second beetle antidiuretic peptide. *Peptides.* **24**, 27–34.
- Gáliková, M., Dircksen, H., and Nässel, D. R.** (2018). The thirsty fly: ion transport peptide (ITP) is a novel endocrine regulator of water homeostasis in *Drosophila*. *PLoS Genet.* **14**, e1007618.
- Gräf, R., Harvey, W. R., and Wiczorek, H.** (1996). Purification and properties of a cytosolic V1-ATPase. *J. Biol. Chem.* **271**, 20908–20913.
- Gulia-Nuss, M., Elliot, A., Brown, M. R., and Strand, M. R.** (2015). Multiple factors contribute to anautogenous reproduction by the mosquito *Aedes aegypti*. *J. Insect Physiol.* **82**, 8–16, doi: 10.1016/j.jinsphys.2015.08.001.

- Gulia-Nuss, M., Eum, J-H., Strand, M. R., and Brown, M. R.** (2012). Ovary ecdysteroidogenic hormone activates egg maturation in the mosquito *Georgescraigius atropalpus* after adult eclosion or a bloodmeal. *J. Exp. Biol.* **215**, 3758–3767.
- Halberg, K. A., Terhzaz, S., Cabrero, P., Davies, S. A., and Dow, J. A. T.** (2015). Tracing the evolutionary origins of insect renal function. *Nat. Commun.* **6**, 6800.
- Hansen, I. A., Attardo, G. M., Rodriguez, S. D., and Drake, L. L.** (2014). Four-way regulation of mosquito yolk protein precursor genes by juvenile hormone-, ecdysone-, nutrient-, and insulin-like peptide signalling pathways. *Front Physiol.* **5**, 1–8.
- Harvey, W. R., Maddrell, S. H. P., Telfer, W. H., and Wieczorek, H.** (1998). H<sup>+</sup> V-ATPases energize animal plasma membranes for secretion and absorption of ions and fluids. *Am. Zool.* **38**, 426–441.
- Inoue, T., and Forgac, M.** (2005). Cysteine-mediated cross-linking indicates that subunit C of the V-ATPase is in close proximity to subunits E and G of the V1 domain and subunit a of the V0 domain. *J. Biol. Chem.* **280**, 27896–27903.
- Ionescu, A., and Donini, A.** (2012). *Aedes*CAPA-PVK-1 displays diuretic and dose dependent antidiuretic potential in the larval mosquito *Aedes aegypti* (Liverpool). *J. Insect Physiol.* **58**, 1299–1306.
- Jentes, E. S., Pomerol, G., Gershman, M. D., Hill, D. R., Lemarchand, J., Lewis, R. F., Staples, J. E., Tomori, O., Wilder-Smith, A., and Monath, T. P.** (2011). The revised global yellow fever risk map and recommendations for vaccination, 2010: consensus of the informal WHO working group on geographic risk for yellow fever. *Lancet Infect. Dis.* **11**, 622–632.

- Johard, H. A. D., Yoishii, T., Dircksen, H., Cusumano, P., Rouyer, F., Helfrich-Förster, C., and Nässel, D. R.** (2009). Peptidergic clock neurons in *Drosophila*: ion transport peptide and short neuropeptide F in subsets of dorsal and ventral lateral neurons. *J. Comp. Neurol.* **516**, 59–73.
- Kane, P. M.** (1995). Disassembly and reassembly of the yeast vacuolar H<sup>+</sup>-ATPase in vivo. *J. Biol. Chem.* **270**, 17025–17032.
- Klöcklerova, V., Gáliková, Z., Roller, L., and Zitnan, D.** (2023). Differential expression of ITP and ITPL indicate multiple functions in the silkworm *Bombyx mori*. *Cell Tissue Res.* 10.1007/s00441-023-03752-y.
- Leparc-Goffart, I., Nougairede, A., Cassadou, S., Prat, C., and de Lamballerie, X.** (2014). Chikungunya in the Americas. *The Lancet* **383**, 514.
- MacMillan, H. A., Nazal, B., Wali, S., Yerushalm, G. Y., Misyura, L., Donini, A., and Paluzzi, J. P.** (2018). Anti-diuretic activity of a CAPA neuropeptide can compromise *Drosophila* chill tolerance. *J. Exp. Biol.* **221**, doi: 10.1242/jeb.185884.
- Merzendorfer, H., Huss, M., Schmid, R., Harvey, W. R., and Wiczorek, H.** (1999). A novel insect V-ATPase subunit M9.7 is glycosylated extensively. *J. Biol. Chem.* **274**, 17372–17378.
- Nagai, C., Mabashi-Asazuma, H., Nagasawa, H., and Nagata, S.** (2014). Identification and characterization of receptors for ion transport peptide (ITP) and ITP-like (ITPL) in the silkworm *Bombyx mori*. *J. Biol. Chem.* **289**, 32166–32177.
- Oehler, E., Watrin, L., Larre, P., Leparc-Goffart, I., Lastère, S., Valour, F., Baudouin, L., Mallet, H. P., Musso, D., and Ghawche, F.** (2014). Zika virus infection complicated by

- guillain-barré syndrome case report, French Polynesia, December 2013. *Eurosurveillance* **19**, 51–58.
- Paluzzi, J. P., and Orchard, I.** (2006). Distribution, activity and evidence for the release of an anti-diuretic peptide in the kissing bug *Rhodnius prolixus*. *J. Exp. Biol.* **209**, 907–915.
- Paluzzi, J. P., Naikhwah, W., and O'Donnell, M. J.** (2012). Natriuresis and diuretic hormone synergism in *R. prolixus* upper Malpighian tubules is inhibited by the anti-diuretic hormone, *RhoprCAPA- $\alpha$ 2*. *J. Insect Physiol.* **58**, 534–542.
- Pollock, V. P., McGettigan, J., Cabrero, P., Maudlin, I. M., Dow, J. A. T., and Davies, S. A.** (2004). Conservation of capa peptide-induced nitric oxide signalling in Diptera. *J. Exp. Biol.* **207**, 4135–4145.
- Quinlan, M. C., Tublitz, N. J., and O'Donnell, M. J.** (1997). Anti-diuresis in the blood-feeding insect *Rhodnius prolixus* Stål: the peptide CAP(2b) and cyclic GMP inhibit Malpighian tubule fluid secretion. *J. Exp. Biol.* **200**, 2363–2367.
- Raikhel, A. S., and Lea, A. O.** (1990). Juvenile hormone controls previtellogenic proliferation of ribosomal RNA in the mosquito fat body. *Gen. Comp. Endocrinol.* **77**, 423–434.
- Raikhel, A. S. S., Brown, M. R. R., and Belles, X.** (2005). Hormonal control of reproductive processes. *Comp. Mol. Insect Sci.* 433–491,
- Rocco, D. A., Garcia, A. S. G., Scudeler, E. L., dos Santos, D. C., Nóbrega, R. H., and Paluzzi, J. P.** (2019). Glycoprotein hormone receptor knockdown leads to reduced reproductive success in male *Aedes aegypti*. *Front. Physiol.* **10**, 266.
- Rodan, A. R., Baum, M., and Huang, C. L.** (2012). The *Drosophila* NKCC Ncc69 is required for normal renal tubule function. *Am. J. Physiol.* **303**, C883–C894.

- Ruka, K. A., Miller, A. P., and Blumenthal, E. M.** (2013). Inhibition of diuretic stimulation of an insect secretory epithelium by a cGMP-dependent protein kinase. *Am. J. Physiol. Renal Physiol.* **304**, F1210–F1216.
- Sajadi, F., Curcuruto, C., Al Dhaheri, A, and Paluzzi, J. P.** (2018). Anti-diuretic action of a CAPA neuropeptide against a subset of diuretic hormones in the disease vector, *Aedes aegypti*. *J. Exp. Biol.* **221**.
- Sajadi F., Lajevardi, A., Donini, A. and Paluzzi, J. P. V.** (2021). Studying the activity of neuropeptides and other regulators of the excretory system in the adult mosquito. *J. Vis. Exp.* **174**, doi: 10.3791/61849.
- Sajadi, F., Uyuklu, A., Paputsis, C., Lajevardi, A., Wahedi, A., Ber, L.T., Matei, A., and Paluzzi, J. P.** (2020). CAPA neuropeptides and their receptor form an anti-diuretic hormone signaling system in the human disease vector, *Aedes aegypti*. *Sci. Rep.* **10**. <https://doi.org/10.1038/s41598-020-58731-y>.
- Seino, S., and Shibasaki, T.** (2005). PKA-dependent and PKA-independent pathways for cAMP-regulated exocytosis. *Physiol. Rev.* **85**, 1303–1342.
- Simmons, C. P., Farrar, J. J., Van Vinh Chau, N., and Wills, B.** (2012). Current concepts: Dengue. *New Eng. J. Med.* **366**, 1423–1432.
- Sumner, J. P., Dow, J. A. T., Earley, F. G. P., Klein, U., Jager, D., and Wieczorek, H.** (1995). Regulation of plasma membrane V-ATPase activity by dissociation of peripheral subunits. *J. Biol. Chem.* **270**, 5649–5653.
- Terhzaz, S., Cabrero, P., Robben, J. H., Radford, J. C., Hudson, B. D., Milligan, G., Dow, J. A. T., and Davies, S. A.** (2012). Mechanism and function of *drosophila* capa GPCR: A

desiccation stress-responsive receptor with functional homology to human neuromedinu receptor. *PLoS One* **7**, e29897.

**Veenstra, J. A.** (1988). Effects of 5-hydroxytryptamine on the Malpighian tubules of *Aedes aegypti*. *J. Insect Physiol.* **34**, 299–304.

**Vitavska, O., Wiczorek, H., and Merzendorfer, H.** (2003). A novel role for subunit C in mediating binding of the H<sup>+</sup>-V-ATPase to the actin cytoskeleton. *J. Biol. Chem.* **278**, 18499–18505.

**Webster, S. G., Keller, R., and Dirksen, H.** (2012). The CHH-superfamily of multifunctional peptide hormones controlling crustacean metabolism, osmoregulation, moulting, and reproduction. *Gen. Comp. Endocrinol.* **175**, 217–233.

**Weng, X. H., Huss, M., Wiczorek, H., and Beyenbach, K. W.** (2003). The V-type H<sup>+</sup>-ATPase in Malpighian tubules of *Aedes aegypti*: localization and activity. *J. Exp. Biol.* **206**, 2211–2219.

**Wiczorek, H., Beyenbach, K. W., Huss, M., and Vitavska, O.** (2009). Vacuolar-type proton pumps in insect epithelia. *J. Exp. Biol.* **212**, 1611–1619.

**Williams, J. C., Hagedorn, H. H., and Beyenbach, K. W.** (1983). Dynamic changes in flow rate and composition of urine during the post-bloodmeal diuresis in *Aedes aegypti* (L.). *J. Comp. Physiol.* **153**, 257–265.

**Yu, B., Li, D. T., Wang, S. L., Xu, H. J., Bao, Y. Y., and Zhang, C. X.** (2016). Ion transport peptide (ITP) regulates wing expansion and cuticle melanism in the brown planthopper, *Nilaparvata lugens*. *Insect Mol. Biol.* **25**, 778–787.